Global Translational Medicine

ACCSCIENCE PUBLISHING

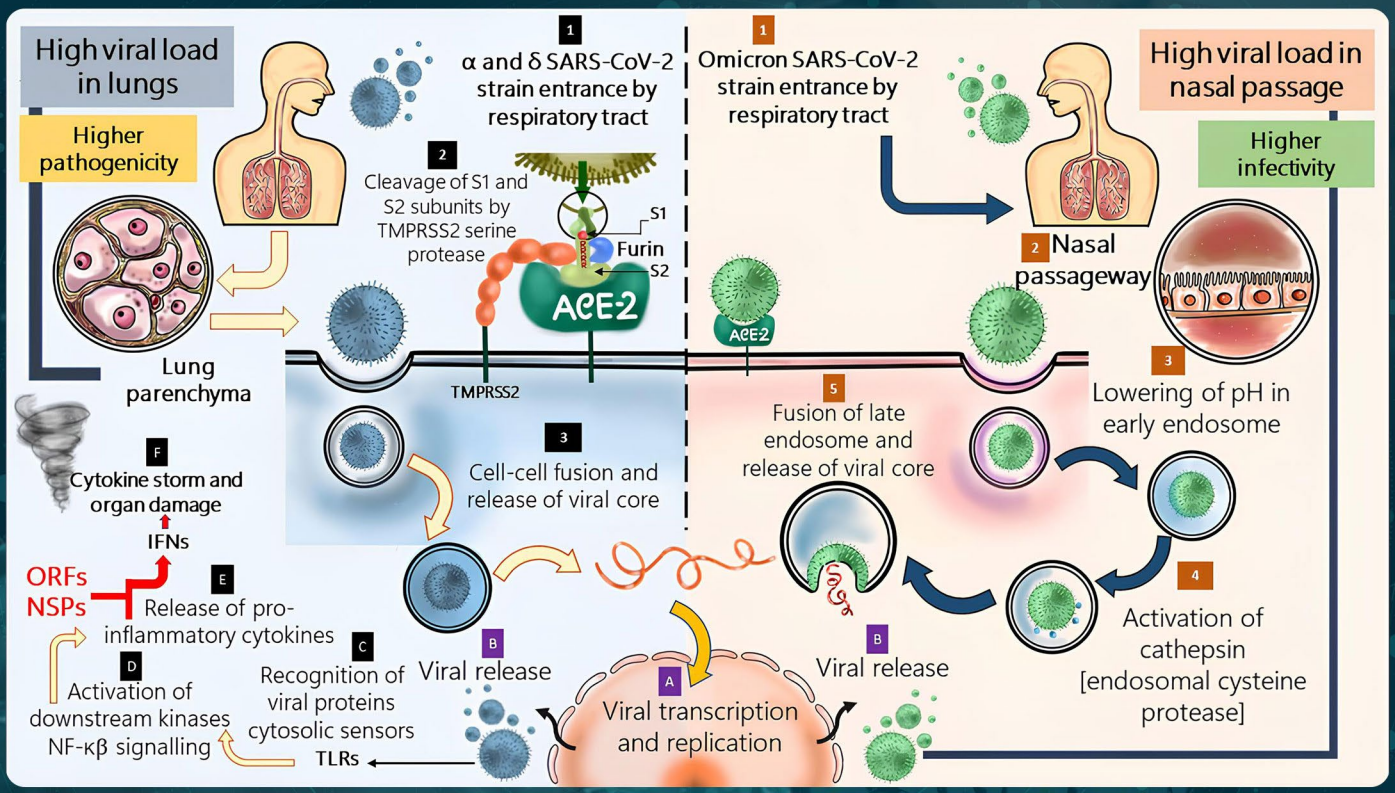

Comparative analysis of immune responses in humans infected with Alpha, Delta, and Omicron strains of SARS-CoV-2

ISSN: 3060-8600 (Print)
ISSN: 2811-0021 (Online)
Volume 3 · Issue 1
March 2024

Global Translational Medicine

Print ISSN: 3060-8600
Online ISSN: 2811-0021

Global Translational Medicine is a quarterly journal that focuses on medicine, biological sciences, and biomaterials engineering. *Global Translational Medicine* provides a platform to fill the gaps in preclinical and inter-disciplinary research, to promote clinical translation of scientific research results, and to contribute to the conception of new and improved preventive measures as well as diagnostic and therapeutic techniques of diseases.

About the Publisher

AccScience Publishing is a publishing company based in Singapore. We publish a range of high-quality, open-access, peer-reviewed journals and books from a broad spectrum of disciplines.

Contact Us

Managing Editor
gtm.office@accscience.sg

AccScience Publishing
8 Burn Road, #15-03 Trivex, Singapore 369977.

Volume 3 • Issue 1 • March 2024
ISSN 3060-8600 (print) ISSN 2811-0021 (online)

GLOBAL TRANSLATIONAL MEDICINE

ACCSCIENCE PUBLISHING

Access Science Without Barriers

GLOBAL TRANSLATIONAL MEDICINE

ISSN: 3060-8600 (print)
ISSN: 2811-0021 (online)

Editorial and Production Credits

Publisher: AccScience Publishing
Managing Editor: Lucille You
Production Editor: Sharmila Velapasamy
Article Layout and Typeset: Sinjore Technologies (India)
Cover Design: ProPub (China)

For all advertising queries, contact gtm.office@accscience.sg.

Supplementary file

Supplementary files of articles can be obtained at https://accscience.com/journal/GTM/3/1.

About the Cover

An abstract illustration of human brain

Disclaimer

AccScience Publishing is not liable to the statements, perspectives, and opinions contained in the publications. The appearance of advertisements in the journal shall not be construed as a warranty, endorsement, or approval of the products or services advertised and/or the safety thereof. AccScience Publishing disclaims responsibility for any injury to persons or property resulting from any ideas or products referred to in the publications or advertisements. AccScience Publishing remains neutral with regard to jurisdictional claims in published maps and institutional affiliations.

Global Translational Medicine

Editorial Board

Early Career Editorial Board

Assistant Editor

*Editorial Board Members as of February 20, 2024

ACCSCIENCE PUBLISHING

Volume 3 | Issue 1 | March 2024 |

Global Translational Medicine

https://accscience.com/journal/gtm

CONTENTS

ACCSCIENCE PUBLISHING

Global Translational Medicine

REVIEW ARTICLE

Challenges and advancements in high-throughput screening strategies for cancer therapeutics

Ruchi Roy[1†*], Sunil Kumar Singh[2†], Nashrah Ahmad[3], and Sweta Misra[1*]

[1]UICentre for Drug Discovery, College of Pharmacy, University of Illinois Chicago, Chicago, Illinois, United States of America

[2]Department of Surgery, University of Illinois Chicago, Illinois, United States of America

[3]Department of Immunology and Microbiology, The Scripps Research Institute, La Jolla, California, United States of America

Abstract

Drug discovery relies on high-throughput screening (HTS) methods incorporating both target- and cell-based assays. This comprehensive review delves into the challenges and benefits associated with these assays within the context of HTS. The strategies for developing screening assays, spanning both primary and secondary screens for target identification, are discussed. Furthermore, we review the methods of identifying the most efficacious drugs through these approaches for the treatment of cancer in detail. While various drugs have been identified for cancer treatment, there remains a pressing need for more relevant phenotypic assays. These assays aim to produce the desired disease phenotype, with a specific emphasis on highlighting targets rather than off-targets. The ultimate goal is to pave the way for innovative drug development strategies that can effectively treat cancer patients, thereby reducing the mortality rate.

Keywords: Target-based screening; Phenotypic-based screening; Targets; Transcriptional reprogramming; High-throughput screening; Cancer therapeutics

†*These authors contributed equally to this work.*

***Corresponding authors:**
Ruchi Roy
(ruchiroy@uic.edu)
Sweta Misra
(sweta16@uic.edu)

Citation: Roy R, Singh SK, Ahmad N, Misra S. Challenges and advancements in high-throughput screening strategies for cancer therapeutics. *Global Transl Med.* 2024;3(1):2448.
https://doi.org/10.36922/gtm.2448

Received: December 15, 2023
Accepted: January 10, 2024
Published Online: March 12, 2024

1. Introduction

The current drug discovery paradigm is highly focused on high-throughput screening (HTS), through which large libraries of compounds are screened against the target of interest to identify suitable and most probable biological or pharmacological targets, aiming for beneficial therapeutic outcomes.[1,2] The lead-identified targets are used as probes to address biological questions in basic research.

At present, combinatorial chemistry and genomics data are extensively employed in HTS within the drug discovery process.[3] HTS often involves robotic systems for rapid testing of large compound libraries against a target or phenotype. It is important to note the distinction between HTS and high-content screening, which emphasizes the simultaneous analysis of multiple cellular features to provide more detailed information on compound effects but at a lower throughput. Target-based screening and phenotypic

screening represent different approaches to HTS, each with its advantages and challenges. These approaches are selected based on the specific goals of the research, the stage of drug discovery, and the available knowledge about the disease and potential drug targets. Target-based screening focuses on identifying compounds that interact with a specific molecular target, such as a protein or enzyme associated with a disease whereas phenotypic screening involves testing compounds based on their ability to induce a desired cellular phenotype without prior knowledge of the target. Target-based screening is commonly used in the early stages of drug discovery to identify lead compounds. This approach typically employs assays involving purified targets, using techniques like fluorescence resonance energy transfer (FRET) or surface plasmon resonance (SPR). Phenotypic screening is often applied later in drug discovery, especially when the molecular basis of a disease is unclear. It utilizes cellular or organismal models and may involve high-content imaging systems, automated microscopy, and other techniques for analyzing complex phenotypes (summarized in Table 1 and Figure 1).

However, testing the large compound libraries for their binding affinity or biological activity with the aim of generating a sufficient number of hits for a drug is a very costly process.[4,5] Recent studies are leaning towards favoring an information-driven strategy over screening a vast number of compounds, aiming to enhance the probability of success. The complexity and cost escalate as we strive to replicate more relevant disease phenotypes. This emphasizes the need for methods that foster an integrated approach to enhance quantity, quality, and cost efficiency. The application of combinatorial chemistry involves screening a diverse array of compounds in one comprehensive sweep, facilitating rapid concurrent screening against specific drug targets. However, the effectiveness of these smart libraries in drug discovery relies heavily on precise knowledge of the druggable target. Genomics plays a crucial role in this context, providing insights into the type of mutation and its burden, which varies depending on the disease and age. For instance, an integrated application of genomic, *in vitro,* and *in vivo* tests was adopted in a case study on a 10-year-old boy with multiple recurrent glioblastoma facing challenges in treatment due to inter

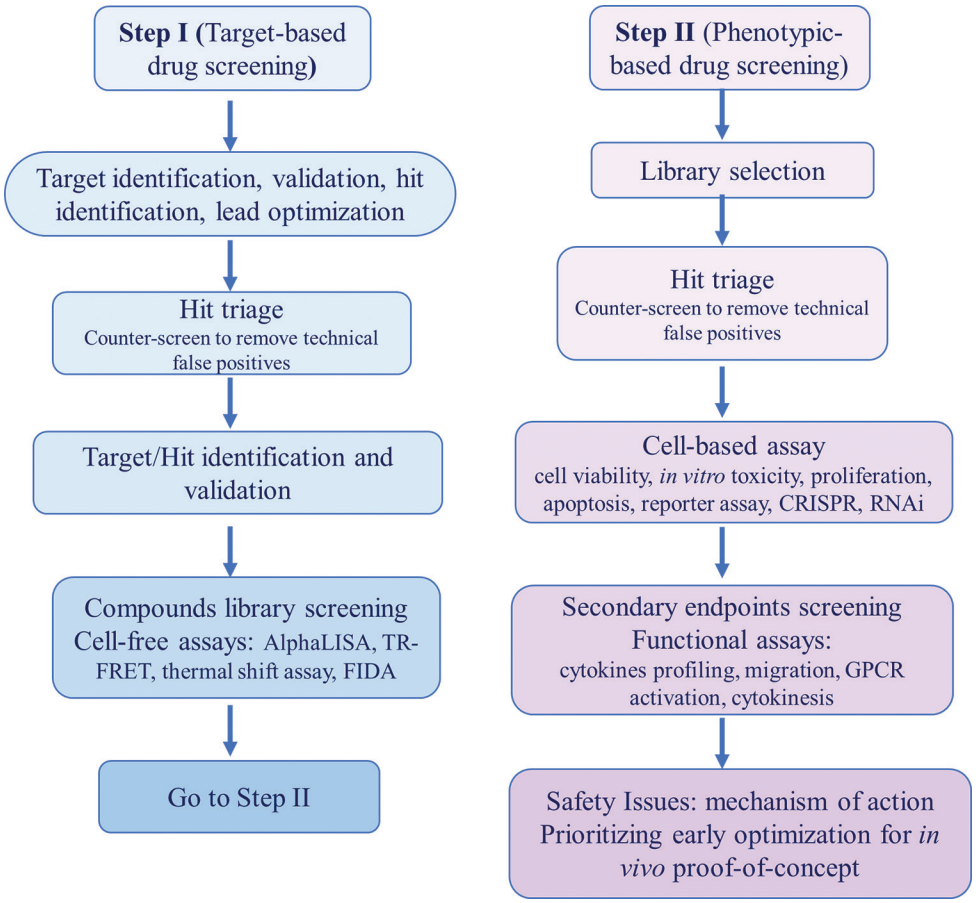

Figure 1. Overview of the drug selection process in high-throughput screening and the workflow of selecting an effective drug.

Table 1. Summary of target- and cell-based assay screening

High-throughput screenings	Strategies	Hallmarks	Techniques involved	Gaps and challenges	Future directions
Target-based screening	• Based on the prior knowledge of drug's mechanism of action such as protein-protein interactions, structural and receptor-mediated protein targets, and regulatory factors • Enhances primary target potency/ efficacy, achieves biochemical selectivity, and demonstrates cell-based activity upon target engagement	• Commonly used in the early stages of drug discovery to identify lead compounds • Involves assessment of enzymatic activity for cell growth, proliferation, differentiation, and metabolism	• Enzyme-based assay: color, fluorescent, luminescence • Proximity assay: fluorescence resonance energy transfer, fluorescence correlation spectroscopy, fluorescence intensity distribution analysis, fluorescence polarization, Alphascreen • Binding-based assay: nuclear magnetic resonance, surface plasmon resonance, differential scanning fluorimetry	• Uncertainty in translation of the molecular drug target to the desired safe clinical outcome or phenotype • Ineffective validation of identified targets, overlooking complex cellular interactions, tumor heterogeneity, and drug resistance	• Integrates technologies like artificial intelligence (AI) and machine learning to facilitate the identification of novel drug targets and the design of more effective compounds • Develops techniques and cellular assays bridging biochemical and phenotypic findings: CETSA, NanoBit (NanoLuc Binary technology), and NanoBRET technology to illustrate protein-protein interactions in cells
Phenotype- based screening	• Based on compounds testing to evaluate their ability to induce a desired cellular phenotype, with-out prior knowledge of a direct molecular target • Biological relevance to the disease • Facilitates to understand the MOA for the disease	• Often applied later in drug discovery, especially when the molecular basis of a disease is unclear • Involves functional assays assessment such as second messenger mobilization (intracellular calcium fluxes or cAMP) after GPCR activation • Primary endpoints, *e.g.,* cell viability and proliferation, are followed by secondary endpoints • Functional assays assessment such as second messenger mobilization (intracellular calcium fluxes or cAMP) after GPCR activation	• Use of target-overexpressing cell lines • Cell-based assay: ATPGlo (luciferase measurement of ATP), CRISPR/cas studies • Imaging-based assays: reporter assays, *e.g.,* TCF/ LEF assay, 3D cultures (organoid preparation)	• Limited ability in identifying precise drug targets, overlooking subtle phenotypic changes or variations in cellular behavior • Readouts (*e.g.,* viability or apoptosis of cancer cell lines) are often not causally related to the disease biology pathway • Doubt on phenotype clinically relevance	• Develop models that mimic disease relevance to study phenotypic endpoints, and build the chain of translatability • Explores 3D cell cultures, 3D cocultures, organoids, organ-on-a-chip systems, and patient-derived models, and high-content screening techniques that better mimic tumor conditions and personalize treatments • Explores animal models, *e.g.,* xenografts • Explores advanced cellular models, *e.g.,* CRISPR/Cas knockout preparations • Develops induced pluripotent stem cell technologies • Explores imaging assay technology

Abbreviations: TCF/LEF: T cell factor/lymphoid enhancer factor family; GPCR: G-protein-coupled receptors.

and intratumoral heterogeneity.[6] Many novel potential drug targets have been identified using the information of genomics. In the pharmaceutical industries, various technologies in terms of assay miniaturization, laboratory automation, and methodologies are utilized to make the whole process cost- and time-effective and enhance its efficacy and selectivity.[7] To improve its efficiency, HTS has been miniaturized to ultra-HTS (uHTS) to enable vigorous testing.[8] Research efforts invested in exploring HTS had led to the development of Viramune (brand name, nevirapine), a non-nucleoside reverse transcriptase inhibitor against HIV.[9] Since 1999, the U.S. Food and Drug Administration (FDA) has approved around 61 first-in-class small molecules for the treatment of cancer, cardiovascular and metabolic disorders, gastrointestinal and infectious diseases.[10,11] Among them, a total of 46 were

evaluated through phenotypic screening (*e.g.*, Azacitidine, Fulvestran, Nelarabine, and Vorinostat) and 17 through target-based screening (*e.g.*, Bortezomib, Gefitinib, Imatinib, Sorafenib, and Sunitinib).

Despite the incorporation of new methodologies, the rate of successful drug screening remains notably low. This is attributed to the molecular heterogeneity underlying disease mechanisms, which varies within and between patients across various disease types.[12-16] These challenges highlight the limitations of contemporary drug discovery strategies. Therefore, "one drug, one target" paradigm is usually followed to reduce unwanted off-target side effects. However, this approach does not take into consideration the complexities of mechanisms, which are in fact very complicated and controlled by various factors inside the cells. Highly potent, single-target treatments may demonstrate weak clinical efficacy when compared to multi-target drugs.[17,18] Nevertheless, most effective drugs are multi-target ligands, and their efficacy is affected by the diverse molecular mechanisms.[19-22] Some examples of multi-target, anti-cancer drugs include lapatinib and duvelisib. Lapatinib is a reversible, ATP-competitive inhibitor of the human epidermal growth factor receptor 2 (HER2) and epidermal growth factor receptor (EGFR) tyrosine kinases.[23] Duvelisib, on the other hand, is a dual inhibitor of PI3K-δ and PI3K-γ. Both drugs have demonstrated promising clinical efficacy in advanced hematologic malignancies.[24]

HTS demands the development of robust assays that provide high signal-to-noise ratios, which can be applied to small volumes as well. Therefore, cell-based *in vitro* assays are more relevant to biological phenotypes in predicting the therapeutic response in a quick and effective manner. Cell-based assays include *in vitro* toxicity assay, RNA interference (RNAi), second messenger, cell proliferation, and reporter assays.[25] Cell-based assays offer several advantages over cell-free biochemical assays in various aspects. They are more cost-effective, closely resemble the clinical physiological state, and provide real selectivity for compounds that can cross the cell membrane to reach target sites.[26-30] Both screening methods have immensely contributed to drug discovery by producing high-quality data (Figure 1, Tables 1 and 2).[31]

Decision of following both phases parallelly or which stream of assays would be performed is dependent on the information available about the disease target and the availability of specific library against that target. Eventually, all primary hit compounds that pass through Step I (primary screening) proceed to Step II for cell-based assays, where *in vitro* pharmacokinetics and pharmacodynamics (bioavailability, solubility, permeability, protein binding, and metabolism) studies are conducted. In this review, we briefly explore screening methods, their challenges, and benefits in HTS. In addition, various recent methodologies are discussed, surrounding topics on developing successful experimental assays, implementation through primary and secondary screens, and target identification. We also discuss the identification of the most efficacious drugs using these approaches, particularly in the context of cancer.

2. Target-based screening

Target-based biochemical assays are based on defined/known molecular targets, which are used to find a lead compound from the library that can efficiently induce/inhibit the target's activity.[32] Target-based screening utilizes genomics information to identify the targets causing disease, which is already available through previous phenotypic studies. Genomic studies also provide functional targets to understand mechanism of action (MOA).[33] Therefore, the target-based approach is simpler, direct, and specific because of prior knowledge of drug's MOA availability, which can be easily utilized to understand the interaction of drug with the target in a relatively easy manner as compared to phenotype-based screening approaches. Various methods have been employed to identify MOA including protein–protein interactions, examination of structural and receptor-mediated protein targets, and regulatory factors. Target-based drug discovery relies on two of the most popular target classes: enzymes and G-protein-coupled receptors (GPCRs). GPCRs, recognized as the largest family of targets for approved drugs, engage in direct interactions with numerous chemical entities, initiating molecular interactions in the extracellular milieu.[34] Another druggable target is ion channels by virtue of its coupling with the plethora of physiological consequences.[35-42]

The hallmark biochemical assays involve the assessment of enzymatic activity for cell growth, proliferation, differentiation, and metabolism. Biochemical assays include enzymatic kinase assays, voltage-gated ion channels, and serine/cysteine proteases FRET, fluorescence correlation spectroscopy, fluorescence intensity distribution analysis, and *in vitro* transcription assays.[43] The main purpose of these assays is to select small molecules from the compound libraries based on their affinity to bind with purified target protein of interest and inhibit or induce enzymatic activity *in vitro* as per the hypothesis being tested.[44] A crucial aspect of kinase assay development is the selection of an appropriate "readout" involving inhibition of ligand-receptor complex formation, reduction of enzymatic activity, or change in cellular phenotype, which further depend on several factors such as the amount of enzymes, the type of cell lines, the type of antibodies, and the reference compounds. Furthermore, these assays must

Table 2. List of targets and compounds/inhibitors against oncogenic pathways

Druggable target	Cancer type	Chemical library source	Compounds	References
P-glycoprotein	Ovarian and breast cancer	Prestwick Chemical Library for Mometasone furoate; National Cancer Institute (NCI) Diversity Set Library for NSC77037 and NSC23925	Mometasone furoate, NSC23925, NSC77037, pimozide, acacetin, and loxapine	131-133, 136-139
			LY335979, R101933, and XR9576	136-139
β-catenin (Wnt signaling)	Colorectal cancer	Two compound series (IWR-1, -2, and IWR-3, -4, -5) from Chen *et al.* [195]~200K compound UTSouthwestern chemical library; The Cancer Research UK Centre for Cancer Therapeutics compound library for CCT031374 analogs preparation	IWP, IWR; XAV939; CCT031374, CCT036477, and CCT7070535	
MEK1	Colon, prostrate, bladder, pancreas cancer cell lines, and athymic nu/nu female mice xenografted with LoVo (colon) human tumor cells	4-phenoxyphenylaniline series (class 1 compounds) prepared by Zhang *et al.*[196] and class 2 series made by Berger *et al.*[197]	Class 1 and Class 2 substituted 4-anilino-3-quinolinecarbonitriles	158
HDAC	Ovarian cancer	Epigenetic drug library purchased from Selleck Chemicals	Trichostatin A (TSA), suberoylanilide hydroxamic acid (SAHA), LBH589, and PXD101	162
KRAS	Colorectal cancer	Primary screen at a single concentration of 2 μg/mL (ChemBridge) or 2 μM (NCI library)	Demethoxyviridin, mithramycin, triphenyl tetrazolium (TPT), sulfinyl cytidine derivative (SC-D)	157
PI3K/PTEN	Colorectal cancer	National Institutes of Health (NIH) Roadmap compound library	N'-[(1-benzyl-1H-indol-3-yl) methylene] benzenesulfonohydrazide (CID1340132)	151
JAK/STAT	Infectious disease and cancer	Chinese National Compound Library	RUS0910-G009	163
EGFR tyrosine kinase	Fibroblasts or human epidermoid carcinoma cells	N/A	PD 153035	198
p53	Colorectal cancer	National Cancer Institute	CP-31398, PRIMA1, and Nutlins	180

be necessarily optimized for various factors, including reagents, readout time-points, buffer conditions, reagent concentrations, timing, stopping, order of addition, plate type, and assay volume.[45]

The fragment-based screening method is one of the most popular approaches for identifying a drug's interaction with a specified target protein of interest, known as a ligand binding assay. In this method, the target of interest must be either isolated and purified for a cell-free system or recombinantly expressed in a cellular system. Subsequently, a library of compounds undergoes screening through various *in vitro* assays to identify selective chemicals capable of modulating the activity of the target proteins. Another approach is measurement of binding activity through nuclear magnetic resonance (NMR) spectroscopy to screen a library of compounds. It is a powerful tool for fragment-based drug discovery to discover high-affinity ligands for target proteins.[46] In 2011, FDA approved the first small-molecule inhibitor, vemurafenib, originating from a fragment-based screen.[47]

Similarly, SPR has been established to provide information on thermodynamic and kinetic aspects of the macromolecule-ligand interaction. SPR helps in the evaluation of molecular interaction between two moieties (either protein–protein, protein–DNA, enzyme–substrate, and protein–drug) while utilizing the advantage of MS. In this case, target of interest or biomolecules are immobilized on the surface of the chip, and the other analytes must pass through a microfluidic system in contact with the chip surface. The kinetics of interaction, *that is*, rate of association and/or dissociation, allosteric effects, as well as Scatchard analysis, and the binding strength, *that is*, affinity, can be measured in the emitted signal.[48] Although NMR, isothermal titration calorimetry (ITC), SPR, and X-ray crystallography are label-free methods and are superior over other methods involving modifications of target protein by adding fluorescence or chemiluminescence labels to facilitate detection, which require more protein for testing and are time-consuming during data analysis.

These approaches, however, have yet to be harmonized with HTS of compound library exceeding 100,000 small molecules. As a result, other advanced techniques are entailed in the HTS to improve the efficiency of label-free methods using spectroscopic techniques, such as label-free matrix-assisted laser desorption/ionization time-of-flight (MALDI-TOF)[49,50] and affinity mass spectrometry (MS),[51] to measure *in vitro* target engagement of small-molecule ligands. A study by Simon *et al.* has demonstrated how using affinity selection (AS)-based sample preparation can be combined with MALDI-TOF to identify orthosteric and allosteric ligands for protein tyrosine phosphatase 1B (PTP1B). In this study, they screened more than 23,000 compounds within 24 h, showing its high compatibility with HTS platform. This method helps to identify multivalent ligands for targeted protein degradation, *for example*, proteolysis-targeting chimeras (PROTACs). Application of AS-MS helps in minimizing the requirement of purification of a stabilized form of the protein target, which poses a great challenge for membrane receptor targets. Another study has shown the importance of affinity MS in screening 20,000 compounds in one pool for a GPCR target.[51] This method provides quantitative measurement of compound binding to the receptor in both the conditions where receptor is either purified or embedded in cell membranes. This approach resulted in the discovery of three new antagonists of the A_{2A} adenosine receptor, *that is*, adenosine, UK-432,097, and NECA (5'-N-ethylcarboxamide adenosine).

Following this robust screening, final lead compounds are evaluated for their pharmacokinetic properties and cellular activity of the protein/enzyme.[52] Usually, target-based screening assays are straightforward and exhibit less variation due to the homogeneous nature of reactions with purified proteins. However, it is crucial to note that the activity of selected compounds in a cellular context or *in vivo* does not always mirror their performance in these assays. The intracellular environment is highly complex, with crosstalk between various signaling pathways, potentially leading to undesired or misleading targets. Factors such as cellular impermeability of the compound or compound metabolism can contribute to undesirable toxic effects. In spite of these challenges, most of the successful drugs results from target-based screening offer new therapeutic options that are precise and personalized to specific mutations or can counter resistance.[53]

Imatinib, a tyrosine kinase inhibitor, was the pioneering cancer therapy that demonstrated targeted specificity against BCR-ABL, c-KIT, and PDGFRA proteins.[54] Beyond its success in treating chronic myeloid leukemia, it has also shown benefits in steroid-refractory chronic graft-versus-host disease due to its activity against PDGFR action. However, resistance issues have emerged involving both Bcr-Abl-dependent and -independent mechanisms. Consequently, new drugs, including dasatinib, nilotinib, bosutinib, and ponatinib, have been developed.[55]

Apart from FDA-approved drugs, several ongoing studies have identified active compounds that are still under preclinical or clinical trials. For example, a natural anticancer compound, cryptotanshinone, is an abietane diterpenoid that functions as an anticancer agent by inhibiting cell proliferation through dual inhibition of pSTAT5 and pSTAT3. This dual inhibition effectively blocks IL-6-mediated STAT3 activation and reverses Bcr-Abl kinase-independent drug resistance in chronic myelogenous leukemia (CML).[56] It has been found that triple-negative breast cancer irrespective of BRCA status can be treated with MLN4924, a selective inhibitor of neddylation enzyme called NEDD8 activation enzyme (NAE1), which targets the neddylation pathway and promotes G2-M arrest and apoptosis in CML cells.[57,58]

2.1. Challenges to target-based screening

Target-based drug discovery is mainly focused on defined drug targets such as a gene, a gene product, or a molecular mechanism that have been identified through genetic analysis or biological studies. In this case, the starting point is a gene product for which small molecule libraries are screened that can modulate its expression, function, or activity. The main drawback to this strategy is the uncertainty about the occupancy of the molecular drug target translation to the desired safe clinical outcome. In general, this strategy is very straightforward and simple, with several well-defined and tractable technical milestones.[59] These limitations may be attributed to an oversimplified assay using recombinant cell lines that may not precisely reflect the relevant phenotype and fail to translate into the clinical outcome. Another challenge is the engagement of drugs with multiple targets rather than a single target, which can diminish the pharmacological value of the drug and may also cause unusual side effects and dysfunctions.

Nonetheless, this strategy is lauded as a fast and cost-effective process, supported by the easily available advanced computational tools used to understand how a drug interacts with its target. Virtual drug screening and *de novo* drug design can improve the outcomes of this strategy. This application can be used to optimize lead compounds by structural modifications to enhance activity or decrease or eliminate adverse side effects.[60]

3. Phenotype-based screening

Despite the continued discovery of therapeutic compounds by means of target-based drug discovery technologies, the recent drug approval list features drugs discovered using cell-based assays, which constitute approximately half of all the high-throughput screens performed.[31,61] Phenotype-based screening offers many advantages over target-based methods due to discovery of multiple protein-level targets or hits and leads in complex biological systems without prior knowledge of a direct molecular target.[31]

In recent years, cell-based assays focused on the modulation of a cellular phenotype in a way that has biological relevance to the disease. These assays identify modulators of a pathway of interest in a more physiological environment that mimics some aspects of disease. This approach increases our understanding of the MOA for the disease, providing an additional layer of information compared to the single-target-based biochemical approach.[62] Multiple endpoints at various levels are determined by primary endpoints and secondary endpoints. Primary endpoints such as cell viability and proliferation are followed by secondary endpoints. Once primary endpoints are successfully determined, functional assays such as second messenger mobilization (intracellular calcium fluxes or cAMP) after GPCR activation,[63,64] reporter gene assays, cell migration, and cytokinesis are performed.[65-67]

A big question that arises is how to determine if a phenotypic drug screen is effective and what defines a good phenotypic drug screen (Figure 2). To answer this, in 2015, Vincent *et al.* coined the phenotypic screening "rule of three" that emphasized on three specific criteria to design the most predictive phenotypic assay.[68] The first rule is the relevance of the assay system to the disease that highlights the importance of physiological relevance in the assay systems. Advancements in *in vitro* preclinical studies can be effectively translated to clinical outcomes by extensively using primary cells and induced pluripotent stem cells (iPSC)-derived cells, which are considered to be more representative of human physiology.[69] In the first HTS study carried out by McNeish *et al.*, murine embryonic stem cell-derived neurons were used to screen around two million compounds in a library for α-amino-3-hydroxyl-5-methyl-4-isoxazolepropionate (AMPA) subtype glutamate receptors.[70] The study demonstrated human translatability by revealing a similar rank order in hit potency. Hence, the phenotypic assays predict more translatability to clinical outcome and help in predicting the clinical therapeutic response to a drug.

The second criterion is the relevance of the stimulus in achieving the production of the desired phenotype. The purpose of stimuli is to target specific signaling pathways related to the disease caused by the imbalance of the crosstalk between signaling pathway. This can be achieved by focusing on the highly disease-relevant biological systems with the same genetic background as depicted by iPSCs.[71-73] In 2012, Lee *et al.* tested a library of 6,912 small-molecule compounds covering a wide range of biologically active and structurally diverse compounds from various commercial sources, including FDA-approved drugs.[73] These compounds were screened for

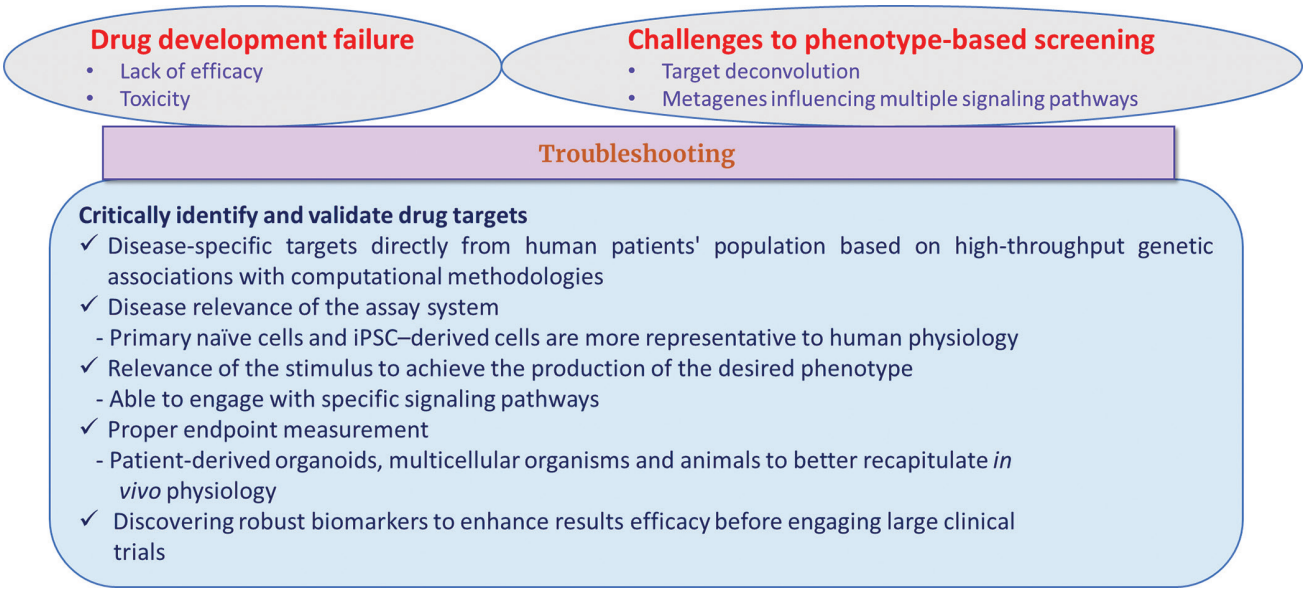

Figure 2. Challenges to drug development and troubleshooting checklist for identifying and validating targets before clinical trials.

their effects on neural crest precursors derived from iPSCs obtained from individuals with familial dysautonomia (FD), a condition resulting from a single point mutation in the I-κ-B kinase complex-associated protein (*IKBKAP*) gene. To effectively screen extensive libraries, defining disease-relevant conditions suitable for HTS is crucial. In this regard, the authors purified FD-iPSC-derived neural crest (FD-NC) precursors using flow cytometry to elucidate why the disease specifically affects the peripheral nervous system. In addition, they focused on selecting a sensitive and disease-relevant readout. To achieve this, the authors developed a qRT-PCR assay in a 384-well format to measure levels of WT-IKBKAP against the 18S internal control. They also determined whether compounds increased both wild-type and mutant (MU) IKBKAP or acted via IKBKAP. The authors identified a potential hit, SKF-86466, capable of rescuing IKBKAP transcription through modulation of intracellular cAMP levels.[73] Another study on cystic fibrosis, which results from mutations in the CF transmembrane conductance regulator (*CFTR*) gene required for an epithelial chloride channel, aimed to correct the processing of F508del-CFTR using small molecules such as VX-809, a CFTR corrector. VX-809 enhances the processing and folding of F508del-CFTR in the endoplasmic reticulum and promotes its trafficking to the cell surface.[72]

If the mechanism and root cause of the disease are not well understood, inflammatory or cytotoxic agents can be used to induce the disease effects to recreate the cellular injury of interest. The last criterion is to determine the assay readout endpoint relevant to the clinical end point. To address this concern, more complex cell models and a range of microphysiological systems that better recapitulate *in vivo* physiological characteristics have emerged. In this regard, patient-derived organoids offer promise for personalized medicine due to their ability to mimic at least some functions of an organ. These organoids can be derived from iPSCs or donor tissue. In extension to this model, whole organism-based screens provide an additional level of physiological relevance beyond cell-based assays. For example, extensive research has been conducted in the pharmaceutical and biotechnology industries by utilizing organisms that can readily adapt to growth, such as yeast and bacteria.[74-78] Following this step, the use of multicellular organisms, such as zebrafish, worms, and plants, becomes crucial because cell-to-cell communication and multi-dimensional tissue organization of these organisms are more relevant to humans'.[78-82] For instance, a large-scale screening of 16,000-compound library identified a compound called persynthamide (psy, 1) that delays S-phase of the cell-cycle and suppresses B-Myb-dependent mitotic defects.[83] These models not only offer a deeper understanding on the developmental process but also help in elucidating the mechanisms of the disease; for instance, chemical genetic analysis using zebrafish embryos has been employed to identify the role of PI3K and ERK in artery/vein specification. This helps determine the cell fate of arteries or veins from angioblasts using GS4898, a known PI3K inhibitor.[84] This study utilized the zebrafish model very effectively in screening small molecules against PI3K inhibitors from the DiverSet E library (Chembridge). Screening was performed in 96-well plates containing embryos in 1- or 2-celled stage and 6-somite stage, which are derived from zebrafish with a mutation (*grlm*^{145}) in *hey2/gridlock* that causes the lack of trunk and tail circulation due to aortic dysmorphogenesis, a model resembling congenital aortic coarctation in humans.

Translational biomarkers can be viewed as clinically relevant endpoint assay readouts that predict efficacy in patients.[85] However, their utility is constrained by the challenge of identifying and validating biomarkers for a range of target hits.[86,87] Most recent advancements in new disciplines such as genomics, proteomics, transcriptomics, metabolomics, bioinformatics, and system biology could impact the understanding of disease due to either loss or gain of function or activation of genes that can be measured by CRISPR technologies.[88,89] Another approach that supports drug discovery is RNAi that helps in hit selection, lead optimization, and development of animal models. For gene editing, CRISPR-Cas9 technology is being used without altering the DNA. Integrated genomic screening approach using CRISPR-Cas9 and RNAi to induce loss of function has been used by Hong *et al.* in a study to identify new potential therapeutic targets in a rare sarcoma.[90] The researchers developed a patient-derived cancer cell line, CLF-PED-015-T, from a patient with a rare undifferentiated sarcoma that holds most of the somatic genetic alterations found in an isolated metastatic lesion. They used other complementary methods such as CRISPR-Cas9 and RNAi-mediated loss-of-function screens to identify CDK4 and XPO1 as druggable cancer targets. A library of small molecules was screened from the Broad Institute Informer Set containing 72 drugs approved by the FDA, 100 clinical candidates, and 268 biologically active chemical probes, to identify antiproliferative effects in the CLF-PED-015-T cell line.

3.1. Challenges to phenotypic screening

Phenotypic screening often suffers from a very potential disadvantage that is target deconvolution, which is an important step for understanding compound MOA. Phenotypic screening provides the identification of multiple off-target proteins or pathways, which might not link to a given biological output. This multiple target identification

can generate a spectrum of other potential associated targets. This process is termed as "target deconvolution" that arises due to possible interaction of small molecules with multiple cellular and/or extracellular targets or non-protein targets.[91,92] However, target deconvolution is not a primary condition or demand for passing any candidate drug from phenotypic screens into late-stage preclinical or even clinical development.[93-95] Advances in the field of chemical proteomics, coupled with *in silico* approaches and genome sequencing, have greatly improved our ability to determine protein targets and underlying hits from phenotypic screens.[96-98] On one hand, a single-target-based approach is more useful to understand MOA of the drug and bridge the link between modulation of target through a MOA, while on the other hand, it could lead to off-target drug activity and toxicity and suggest the need of multi-target therapies to address complex multifactorial disease mechanisms.[99,100]

The second major challenge to phenotypic screening is metagenes influencing multiple signaling pathways. Genome-wide gene expression profiling measures gene activities (expressions) in a given cell for a certain time frame that helps to understand human diseases at the molecular level.[101,102] Molecular targets can be recognized by the consistent pattern of gene expression across large cohorts of human samples, which provide insights in evaluating treatment-related phenotypic changes on the molecular basis. Indeed, distinct tumor subtypes in the same histological environment may present differential responses that can cause remarkable hurdles for drug development and treatment implications.[103] The differential response to therapies may stem from heterogeneous patterns of gene expression known as metagenes. These metagenes influence multiple physiological properties of tumors through various signaling pathways, such as RAS and Myc, regulating the degree of epithelial-to-mesenchymal transition.[104-106] Rising incidences of drug resistance and limited efficacy against complex diseases exacerbate the difficulties of drug discovery. To address these bottlenecks, polypharmacology emerges as an innovative therapeutic strategy in the realm of drug discovery. This approach involves using therapeutic molecules capable of interacting with multiple biomolecular targets.[107] However, the limitation of using this strategy involves toxicological concerns and potential side effects. These complexities in molecular patterns underline the need for more efficient understanding of drug MOA at phenotypic and pathway levels for making correct diagnostic and prognostic decisions.

4. Screening for genotoxic compounds

Genotoxicity in cancer cells can be induced by the treatment of chemotherapeutic agents, such as chlorambucil, cyclophosphamide, cisplatin, oxaliplatin, 5-fluorouracil, anthracyclines, methotrexate, and topoisomerase inhibitors, to induce cell death.[108,109] In 2009, Ji *et al.* developed a DNA repair pathways-deficient chicken DT40 cell lines for high-throughput genotoxicity screening that have effective gene targets, stable phenotype, and karyotype and are easy to maintain in suspension culture.[110-113] However, there are several other phenotypic assays for screening out genotoxic compounds, including GreenScreen HC GADD45a-green fluorescent protein (GFP) (BlueScreen HC, CellCiphr p53, and CellSensor p53-bla).[114-116] These systems utilize p53 or DNA damage-associated genes due to their role in a genotoxic stress causing the arrest of cell cycle at the G1/S phase until repair is effective. Gentronix 'GreenScreen HC' assay utilizes the fact of genotoxin-induced transcription of *GADD45a* (growth arrest and DNA damage) gene in human lymphoblastoid TK6, a karyotypically stable cell line.[114] This assay measures the cell's response to genotoxic stress, which is linked to the GFP reporter with p53 regulatory elements that ensure specific and dose-dependent response from the gene reporter.[116] The cellular systems biology (CSB™) approach (Cellumen "CellCiphr" profile) is used to measure DNA damage-induced cytotoxicity in human cellular hepatic cell line HepG2 by activating p53 via a fluorescent anti-p53 antibody.[117] Another p53-dependent beta-lactamase reporter assay is the Invitrogen 'CellSensor' assay to measure cytotoxicity in HCT-116 cells.[118,119] The lack of metabolic activation and the removal of genotoxic lesions by the DNA repair system could lead to high false negative.[115] ATAD5-luciferase assay developed by Fox *et al.* is based on the ATAD5 protein expression levels on DNA damage.[120,121] *ATAD5* is a suppressor of direct repeat recombination.[122] Using this assay, 22 antioxidant-compounds have been identified including potential chemotherapeutic agents (resveratrol, genistein, and baicalein) that offer improvements over conventional cancer drugs.[120] In 2018, Sykora *et al.* developed an advanced single-cell gel electrophoresis (SCGE) assay coupled with data processing software (CometChip Platform) to identify and characterize genotoxic agents in large compound libraries.[123] This tool can be applied to determine sensitivity to genotoxic exposures in human populations for epidemiological studies.[123]

5. Application in cancer treatment

Cancer treatment encounters a major obstacle in the form of resistance to chemotherapeutic agents. Tumor cells often develop a multidrug-resistant (MDR) phenotype by altering the expression of transporter proteins, such as the ATP-binding cassette (ABC) superfamily. These proteins play a crucial role in regulating intracellular drug concentrations. In addition, resistance can arise through mechanisms like enhanced repair of drug-induced damage. The emergence of MDR phenotypes

poses a challenge in achieving effective cancer therapy and underlines the need for innovative approaches to overcome or bypass drug resistance mechanisms.[124-127] A study on *mdr1a*$^{-/-}$ mice has reported that P-glycoprotein (P-gp) hampers the oral uptake of paclitaxel.[128] There were several efforts made to generate inhibitors to reverse chemoresistance caused by overexpression of high-molecular-weight surface P-gp.[129,130] In clinical trials, third-generation modulators such as LY335979, R101933, and XR9576 have shown better accumulation of P-gp substrate Tc-99m sestamibi, an imaging agent, in a subset of patients.[131-133] However, these inhibitors did not perform well in the clinical trials due to low bioavailability, unexpected secondary physiological effects, and unanticipated drug-drug interactions.[125,134] Therefore, several assays have been designed using human MDR cell lines to aid in the discovery of novel inhibitors against efflux pump P-gp coded by the *MDR1/ABCB1* gene and other ABC transporters. Efforts have been made to prepare drug-sensitive and -resistant human myeloma cell lines, 8226/S, and 8226/Dox6 to demonstrate association of P-gp overexpression with resistance to glucocorticoid, etoposide, doxorubicin, and vincristine.[135] Collectively, studies have identified several compounds, such as mometasone furoate, NSC23925, NSC77037, pimozide, acacetin, and loxapine, as a tolerable and effective therapy to reverse MDR.[136-139] Therefore, key components such as P-gp, ABC transporters, and MDR could be potential candidates of chemoresistance, which can be targeted in cancer drug discovery.

Another challenge to cancer treatment is the stemness caused by cancer stem cell (CSC) that can differentiate into other cell types of cells in the body due to phenotypic plasticity following transcriptional reprogramming driven by an evolutionarily conserved starvation response causing cancer progression and recurrence.[140] This leads to high heterogeneity among tumor tissue environments causing drug resistance.[141] Transcriptional reprogramming helps cancer cells not only to escape from the host immune defense system but also to stimulate invasion, proliferation, and metastasis.[142,143] This heterogeneity in the tumor microenvironment creates complexity in the signaling pathways due to unstable and altered genetic and epigenetic profiles that make drug discovery processes more difficult.[144,145] Genetical modifications and several key pathways such as Wnt, phosphoinositide 3-kinase signaling pathway (PI3K) signaling, interferons (IFNs), and Erk/MAPK signaling are involved in this reprogramming.[146-149] A detailed study by Van Keymeulen *et al.* has demonstrated how tumor heterogeneity is determined by the cancer cell origin using Cre-inducible *Pik3ca*$^{H1047]R}$ knock-in mice, specifically in basal cells (BCs) using K5-CreER^{T2} mice.[146] The mice exhibited deletion of p53 and expression of Pik3ca(H1047R), which accelerated more aggressive tumor development. Furthermore, they determined its role in cancer cell fate switches depending on its expression in basal and luminal cells. Since PI3K signaling is involved in multiple cellular processes, including cell survival and cell death mechanisms, Li *et al.* developed and implemented a high-throughput paired cell-based screen composed of parental HCT116 cells and their *PTEN* gene-targeted derivatives to identify small molecules that preferentially kill cells with mutations of *PTEN*. Among 138,758 compounds tested, two hits were identified and finally, N'-[(1-benzyl-1H-indol-3-yl)methylene]benzenesulfonohydrazide (CID1340132) was determined as a novel compound that induces apoptosis preferentially in *PTEN* and *PIK3CA* mutant human cancer cells.[151]

The stemness of nasopharyngeal carcinoma (NPC) cells is not only controlled by PI3K signaling but also by Wnt signaling that promotes migration and invasion of cancer cells by upregulating expression of WNT5A in biopsy samples of metastatic NPC tissues.[152] To study Wnt signaling role in cancer treatment, specifically the inhibition of intracellular β-catenin turnover and the formation of a nuclear β-catenin/T cell factor (TCF) transcription complex, TCF/lymphoid enhancer factor family (TCF/LEF) luciferase reporter assay is highly used because Wnt/β-catenin works through either activating or repressing transcription of genes whose promoters contain binding sites for TCF-transcription factors. To search for specific inhibitors against the formation of this complex, Wan *et al.* prepared cell lines to perform cell-based assay to screen a diverse library of small molecules. They developed cell lines with constitutive Wnt signaling,[153,154] using an inducible HEK cell line, which expresses Dvl2 fusion consisting of estrogen receptor (ER), luciferase, and *GFP* genes, under the control of a minimal c-Fos promoter with TCF-binding sites and Xnr3 enhancer. This cell line helps in screening β-catenin inhibitors such as CCT031374, CCT036477, and CCT7070535 that block β-catenin induction on estradiol addition. These compounds were able to not only block the induction of β-catenin activity but also reduce the proliferation of colorectal cancer cell lines (HCT116, HT29, and SW480) and induce caspase 3 activation in HCT116 cells.

Exploring the disruption of TCF signaling, specifically TCF4 and β-catenin, to search for anticancer drugs, has been attempted by Lepourcelet *et al.*, who screened libraries of natural compounds in an HTS manner for immunoenzymatic detection of the protein-protein interaction.[155] Finally, they were able to select two fungal derivatives (PKF115-854 and CGP049090) that passed the tested predictions including disruption of Tcf/β-

catenin complexes *in vitro*, inhibition of colon cancer cell proliferation, β-catenin-regulated transcription, and β-catenin-mediated axis duplication in *Xenopus* embryos. Another study by Yu *et al.* highlighted the special AT-rich binding protein-2 (SATB2)/β-catenin/TCF-LEF pathway in transformation and carcinogenesis.[156] SATB2 is a transcription factor and epigenetic regulator that is mostly overexpressed in colorectal cancer. Silencing of SATB2 inhibits TCF/LEF activity and its targets. Hence, these studies suggest a critical role of Wnt signaling pathway in cancer development, and targeting this pathway, in combination with current available chemotherapies, might be beneficial for controlling the cancer.

Another important signaling pathway is EGFR signaling that controls cellular and molecular pathways, and any alterations to this signaling can lead to carcinogenesis. This receptor tyrosine kinase belongs the ERBB family of receptors, and its activation regulates KRAS and PI3K/PTEN pathways. Torrance *et al.* identified triphenyl tetrazolium (TPT) and a sulfinyl-to-cytidine derivative (SC-D) as novel KRAS pathways inhibitors in DLD-1 colorectal cancer cells in which key tumorigenic genes had been deleted by targeted homologous recombination and yellow fluorescent protein were expressed, while a blue fluorescent protein expression vector was introduced into an isogenic derivative (lines (HCT116/HKH) in which the mutant K-Ras allele had been deleted.[157] TPT and SC-D were identified among 30,000 compounds through large screening, which displayed selective activity *in vitro* and inhibited tumor xenografts containing mutant Ras. Similarly, another HTS study identified two series of substituted 4-anilino-3-quinolinecarbonitriles as potent mitogen-activated protein/extracellular signal-regulated kinase 1 (MEK1) inhibitors.[158] These compounds had the same cyanoquinoline cores but differed in their respective aniline groups. Both classes inhibited *in vitro* growth of human tumor cell lines while class 2 that is 3-chloro-4-(1-methylimidazol-2-sulfanyl)aniline inhibited kinase activity upstream of Raf and had dual effect on MEK and MAPK phosphorylation and inhibited growth of the human colon tumor cell line LoVo (at 50 and 100 mg/kg BID) in a nude mouse xenograft model).[158]

MEK inhibitors such as trametinib and selumetinib have been clinically approved for use in several tumor types of cancers such as melanoma, non-small cell lung cancer, and low-grade serous ovarian cancer.[159-161] Despite having promising therapeutic efficacy, these inhibitors showed limited success clinically due to the rapid development of resistance that might be caused by gain of secondary target mutations, gene amplification, and compensatory activation of prosurvival signaling pathways. A recent study by Liu *et al.* has shown that the resistance to a MEK inhibitor trametinib can be overcome through epigenetic reprogramming using histone deacetylase (HDAC) inhibitors, *for example*, trichostatin A (TSA), suberoylanilide hydroxamic acid (SAHA), LBH589, and PXD101 in advanced ovarian cancer.[162] The novelty of this study lies in the establishment of a series of patient-derived advanced ovarian cancer models that were sensitive or resistant to trametinib. This model illustrated that enhancer reprogramming led to sustained activation of the MAPK pathway, which plays a crucial role in MEK inhibitor resistance. They also performed combinatorial drug screening with a customized epigenetics compound library from Selleck Chemicals in A2780-R and SKOV3 cells. LBH589 (Panobinostat, HDAC inhibitor) in combination with trametinib maximizes the clinical benefit. They found that the combinatorial treatment retarded tumor growth in the SKOV3 xenograft model. These findings demonstrated that HDAC inhibitors overcome resistance through the suppression of ERK restoration.

IFNs such as IFN-α and IFN-β play a key role in cancer and several chronic diseases after binding to their respective receptors, IFNAR1 and IFNAR2. This receptor complex activates Janus-activated kinases (JAKs) and signal transducers and activators of transcription (STAT) pathways. HTS against type-I IFN with the secreted embryonic alkaline phosphatase (SEAP) reporter gene assay involving 32,000 compounds resulted in 25 confirmed hits. Further screening by cytotoxicity assay in neuroblastoma cell line SH-SY5Y showed two hits (CD2093-G007 and RUS0903-C006) that decreased viability to less than 50%. Finally, RUS0910-G009 exhibited inhibition of STAT1 and STAT3 phosphorylation and suppression of IRF7 mRNA transcription.[163]

Several investigations were conducted to find DNA repair factors through HTS assays to screen inhibitors targeting PARP-1, Ape1, RecA, and Rad51.[164-168] Dillon *et al.* have notably developed a novel FlashPlate scintillation proximity assay of large compound libraries for HTS to identify inhibitors of PARP-1.[164] This assay was originally developed for the 96-well FlashPlate, but the authors have transformed it into a 384-well format with sufficient sensitivity to determine accurate IC50 values and adaptability for kinetic evaluation of lead molecules. Further, Peterson *et al.* developed a robust method to screen large number of small molecules in HTS against RecA using commercial reagents (Transcreener(®) adenosine 5'-O-diphosphate [ADP]

(2) fluorescence polarization assay).[166] Therefore, identification of biomarkers of these reprogramming at the level of gene and protein could help to explain MOA of different tumor variant types in different individuals depending on the case (Figure 3).[169] Another method to measure cellular target engagement is the Cellular Thermal Shift Assay (CETSA) that measures label-free target engagement with endogenous protein. In this assay, antibody pairs to quantify thermostable target proteins are used. For example, to measure target engagement with PARP1, Shaw *et al.* utilized a triple-negative breast cancer cell line, MDA-MB-436, with homozygous deleterious mutations in *BRCA1*.[170] Treatment of these cells with the PARP inhibitors olaparib, rucaparib, or NMS-P118 led to a thermal stabilization of roughly 2°C, providing evidence of target engagement with cellular PARP1. CETSA can be used for bridging the gap between target engagement and the desired functional effect. Pharmacological inhibition of PARP1 with olaparib was also determined by another approach in a study by Howard *et al.*, where they demonstrated the application of PARPYnD, the first photoaffinity-based probe (AfBP) for profiling PARP1/2.[171] This approach was used to profile clinical PARP inhibitor olaparib and to identify off-target proteins.[171] This strategy utilizes photoaffinity labeling of compounds without altering their phenotypic properties, *that is*, multipolar spindle formation to profile the cellular interactome of a molecule with a non-covalent binding profile. PARPYnD retained its phenotypic behavior and *in vitro* PARP binding profile comparable to parent compounds AZ9482 and AZ0108, suggesting its beneficial utility in profiling novel off-target interactions of both AZ0108 and the clinical PARP inhibitor olaparib.

In addition, there are other relevant targets or pathways that can be assessed, for instance, cancer signaling pathways involving the p53, RTK–RAS signaling[172-174] or various cell-cycle regulation targets such as cyclin D, cyclin E, and the mitotic kinase Aurora 2.[175,176] Mortality rate is higher in breast cancer patients who overexpressed cyclin-dependent kinase 2/cyclin E2 (CDK2/cyclin E2) through the estrogen receptor pathway.[177,179] Another serine/threonine kinase oncogene, STK15/BTAK (approved gene symbols are *AUR2*, *ARK1*, and *AIK1*) required for the formation of the mitotic bipolar spindle, has been reported to be overexpressed in breast cancers.[177] These targets could be used in future to find more potent and selective cancer drugs. However, a study has shown that targeting Aurora proteins

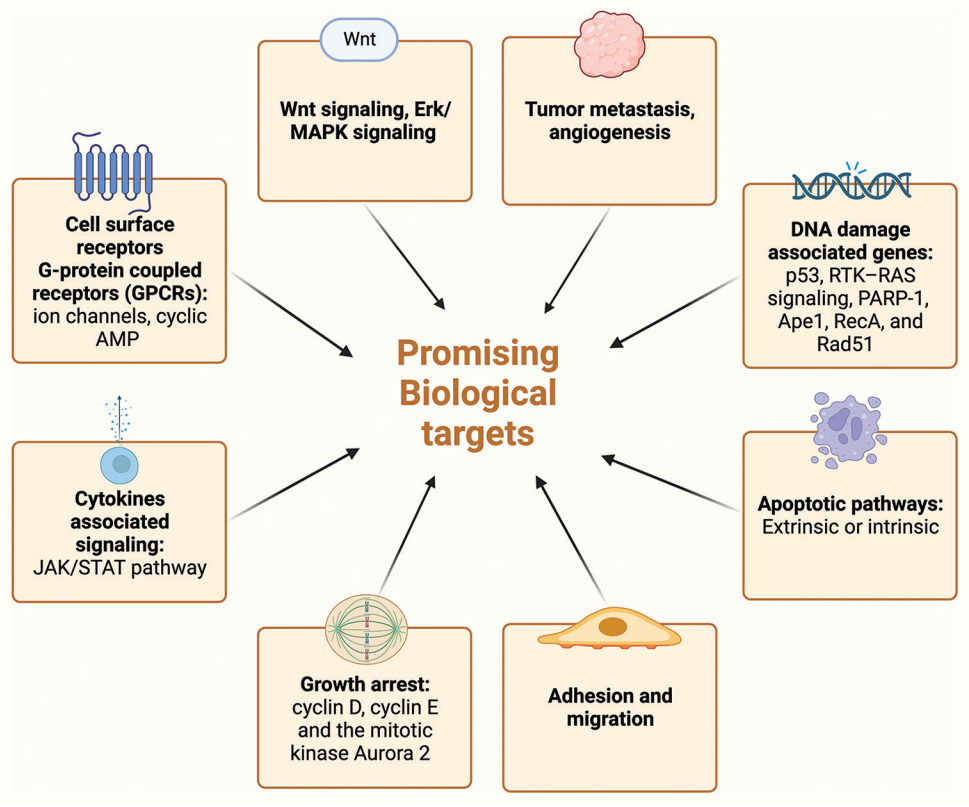

Figure 3. Promising biological targets for cancer drug screening.

subfamily members such as Aurora A and Aurora B in combination would be ineffective. Instead, each should be treated autonomously due to their distinct biological responses.[178]

Cell cycle is tightly regulated by the *p53* gene, which governs the activity of cell cycle kinases such as cyclin-dependent kinases (CDK4/6 and CDK2). Its inactivation or mutation causes dysregulation in proliferation and apoptosis, leading to cancer. Therefore, an attempt has been made in drug development to restore its activity using small molecules modulators (CP-31398, PRIMA1, and Nutlins) in p53-deficient human colon tumor xenografts (HCT116/p53$^{-/-}$ or DLD1).[179] These compounds were able to reactivate p53 reporter activity via increasing its targeted genes such as p21 (WAF1) and death receptor 5 (DR5).

Similarly, heat-shock protein 90 (HSP90) is an important molecular chaperone, which is overexpressed in patients with cancer.[180,182] HIF-1 pathway is considered to be an important signaling pathway that plays a crucial role in tumor progression and angiogenesis by upregulating kinases and hypoxia-inducible factor-1 (HIF-1).[183-185] Enzymes involved in DNA modification, such as histone acetyltransferases and histone deacetylases, play a critical role in chromatin modification. These enzymes are essential for post-translational modifications, catalyzing the acetylation and deacetylation of histones on specific lysine residues. Their possible involvement in the pathology of conditions like cancer, asthma, and viral infections highlights their significance in understanding and potentially targeting these enzymes for therapeutic interventions.[186-189]

Moreover, a genome-based strategy has successfully emphasized the use of herceptin, a humanized antibody targeting the ErbB2 receptor, for the treatment of breast cancer. This is particularly effective in cases where breast cancer patients exhibit overexpression of the receptor.[190] Another example is farnesyltransferase inhibitor R115777 that showed efficacy in the treatment of human breast cancer xenografts[191] and in patients with advanced breast cancer.[192] Hopefully, further understanding of the genetic versatility of breast cancer holds the potential to identify more druggable targets for HTS. In addition, compounds, either used in combination or alone, have demonstrated superior efficacy and tolerability compared to standard endocrine therapy, such as tamoxifen. For instance, the aromatase inhibitor Arimidex (anastrazole) has shown promising results in clinical trials for the treatment of hormone receptor-positive breast cancer in post-menopausal women.[193,194]

These studies collectively suggest that several signaling pathways can be targeted while selecting multi-target small molecules. HTS should be designed very carefully to determine effective compounds for clinical usage (Table 2).

6. Conclusion

HTS sets experiments on a more rapid mode and is applicable to a broader range of targets without necessitating prior knowledge of target and ligands or phenotypic assays. Challenges confronting the HTS practitioners are not only limited to the endpoint readouts or the quality of the biology but also the quality and quantity of compounds being tested. It requires a very broad knowledge base with expertise involving multiple areas of biology, chemistry, engineering, information technology, and logistics. All drug discovery strategies are fraught with pitfalls; therefore, practitioners need to integrate hit identification approaches to maximize success rate. Various drug screening methods in HTS have yielded numerous potent compounds currently utilized in treatment procedures. Despite these advancements, drug selection assays have not fully matured to produce endpoints directly relevant to the disease phenotype. This review underscores the importance of selecting appropriate endpoints that closely mimic the desired phenotype to identify efficacious drugs. While new technologies such as genomics and proteomics provide abundant knowledge about targets and their signaling, it is still necessary to elucidate specific signaling axes that lead to the correct clinical outcomes. Thus, continued exploration is crucial for unearthing innovative anticancer agents and maximizing patient benefits.

Acknowledgments

None.

Funding

None.

Conflict of interest

The authors declare no conflicts of interest.

Author contribution

Conceptualization: Ruchi Roy, Sunil Kumar Singh
Writing – original draft: Ruchi Roy, Sunil Kumar Singh
Writing – review and editing: All authors

Ethics approval and consent to participate

Not applicable.

Consent for publication

Not applicable.

Availability of data

Not applicable.

References

1. Macarron R, Banks MN, Bojanic D, *et al*. Impact of high-throughput screening in biomedical research. *Nat Rev Drug Discov*. 2011;10(3):188-195.

   doi: 10.1038/nrd3368

2. Wigglesworth MJ, Murray DC, Blackett CJ, Kossenjans M, Nissink JW. Increasing the delivery of next generation therapeutics from high throughput screening libraries. *Curr Opin Chem Biol*. 2015;26:104-110.

   doi: 10.1016/j.cbpa.2015.04.006

3. Pereira DA, Williams JA. Origin and evolution of high throughput screening. *Br J Pharmacol*. 2007;152(1):53-61.

   doi: 10.1038/sj.bjp.0707373

4. Shun TY, Lazo JS, Sharlow ER, Johnston PA. Identifying actives from HTS data sets: Practical approaches for the selection of an appropriate HTS data-processing method and quality control review. *J Biomol Screen*. 2011;16(1):1-14.

   doi: 10.1177/1087057110389039

5. Dreiman GHS, Bictash M, Fish PV, Griffin L, Svensson F. Changing the HTS paradigm: AI-driven iterative screening for hit finding. *SLAS Discov*. 2021;26(2):257-262.

   doi: 10.1177/2472555220949495

6. Tsoli M, Wadham C, Pinese M, *et al*. Integration of genomics, high throughput drug screening, and personalized xenograft models as a novel precision medicine paradigm for high risk pediatric cancer. *Cancer Biol Ther*. 2018;19(12):1078-1087.

   doi: 10.1080/15384047.2018.1491498

7. Mayr LM, Bojanic D. Novel trends in high-throughput screening. *Curr Opin Pharmacol*. 2009;9(5):580-588.

   doi: 10.1016/j.coph.2009.08.004

8. Szymański P, Markowicz M, Mikiciuk-Olasik E. Adaptation of high-throughput screening in drug discovery-toxicological screening tests. *Int J Mol Sci*. 2012;13(1):427-452.

   doi: 10.3390/ijms13010427

9. Milinkovic A, Martínez E. Nevirapine in the treatment of HIV. *Expert Rev Anti Infect Ther*. 2004;2(3):367-373.

   doi: 10.1586/14787210.2.3.367

10. FDA. Approved Drugs Generated from High Throughput Screening Efforts I - 20190719. Rome: FDA; 2019.

11. Coussens NP, Braisted JC, Peryea T, Sittampalam GS, Simeonov A, Hall MD. Small-molecule screens: A gateway to cancer therapeutic agents with case studies of food and drug administration-approved drugs. *Pharmacol Rev*. 2017;69(4):479-496.

    doi: 10.1124/pr.117.013755

12. Woodward AA, Urbanowicz RJ, Naj AC, Moore JH. Genetic heterogeneity: Challenges, impacts, and methods through an associative lens. *Genet Epidemiol*. 2022;46(8):555-571.

    doi: 10.1002/gepi.22497

13. Lawson ARJ, Abascal F, Coorens THH, *et al*. Extensive heterogeneity in somatic mutation and selection in the human bladder. *Science*. 2020;370(6512):75-82.

    doi: 10.1126/science.aba8347

14. Murphy N, Ward HA, Jenab M, *et al*. Heterogeneity of colorectal cancer risk factors by anatomical subsite in 10 European countries: A multinational cohort study. *Clin Gastroenterol Hepatol*. 2019;17(7):1323-1331.e6.

    doi: 10.1016/j.cgh.2018.07.030

15. Haffner MC, Zwart W, Roudier MP, *et al*. Genomic and phenotypic heterogeneity in prostate cancer. *Nat Rev Urol*. 2021;18(2):79-92.

    doi: 10.1038/s41585-020-00400-w

16. Mitelpunkt A, Galili T, Kozlovski T, *et al*. Novel Alzheimer's disease subtypes identified using a data and knowledge driven strategy. *Sci Rep*. 2020;10(1):1327.

    doi: 10.1038/s41598-020-57785-2

17. Margineanu DG. Systems biology, complexity, and the impact on antiepileptic drug discovery. *Epilepsy Behav*. 2014;38:131-142.

    doi: 10.1016/j.yebeh.2013.08.029

18. Kell DB. Finding novel pharmaceuticals in the systems biology era using multiple effective drug targets, phenotypic screening and knowledge of transporters: where drug discovery went wrong and how to fix it. *FEBS J*. 2013;280(23):5957-5980.

    doi: 10.1111/febs.12268

19. Ericson E, Gebbia M, Heisler LE, *et al*. Off-target effects of psychoactive drugs revealed by genome-wide assays in yeast. *PLoS Genet*. 2008;4(8):e1000151.

    doi: 10.1371/journal.pgen.1000151

20. Lim H, Poleksic A, Yao Y, *et al*. Large-scale off-target identification using fast and accurate dual regularized one-class collaborative filtering and its application to drug repurposing. *PLoS Comput Biol*. 2016;12(10):e1005135.

    doi: 10.1371/journal.pcbi.1005135

21. Lin A, Giuliano CJ, Palladino A, *et al*. Off-target toxicity is a common mechanism of action of cancer drugs undergoing clinical trials. *Sci Transl Med*. 2019;11(509):eaaw8412.

    doi: 10.1126/scitranslmed.aaw8412

22. Koeberle A, Werz O. Multi-target approach for natural products in inflammation. *Drug Discov Today*. 2014;19(12):1871-1882.

doi: 10.1016/j.drudis.2014.08.006

23. Konecny GE, Pegram MD, Venkatesan N, *et al*. Activity of the dual kinase inhibitor lapatinib (GW572016) against HER-2-overexpressing and trastuzumab-treated breast cancer cells. *Cancer Res*. 2006;66(3):1630-1639.

doi: 10.1158/0008-5472.Can-05-1182

24. Flinn IW, O'Brien S, Kahl B, *et al*. Duvelisib, a novel oral dual inhibitor of PI3K-δ,γ, is clinically active in advanced hematologic malignancies. *Blood*. 2018;131(8):877-887.

doi: 10.1182/blood-2017-05-786566

25. Murai R, Yoshida Y, Muraguchi T, *et al*. A novel screen using the Reck tumor suppressor gene promoter detects both conventional and metastasis-suppressing anticancer drugs. *Oncotarget*. 2010;1(4):252-264.

26. Herrmann IK, Wood MJA, Fuhrmann G. Extracellular vesicles as a next-generation drug delivery platform. *Nat Nanotechnol*. 2021;16(7):748-759.

doi: 10.1038/s41565-021-00931-2

27. Ohtaka H, Velázquez-Campoy A, Xie D, Freire E. Overcoming drug resistance in HIV-1 chemotherapy: The binding thermodynamics of Amprenavir and TMC-126 to wild-type and drug-resistant mutants of the HIV-1 protease. *Protein Sci*. 2002;11(8):1908-1916.

doi: 10.1110/ps.0206402

28. Wei F, Wang S, Gou X. A review for cell-based screening methods in drug discovery. *Biophys Rep*. 2021;7(6):504-516.

doi: 10.52601/bpr.2021.210042

29. Pathe-Neuschäfer-Rube A, Neuschäfer-Rube F, Püschel GP. Cell-based reporter release assay to determine the activity of calcium-dependent neurotoxins and neuroactive pharmaceuticals. *Toxins* (*Basel*). 2021;13(4):247.

doi: 10.3390/toxins13040247

30. Sanookpan K, Nonpanya N, Sritularak B, Chanvorachote P. Ovalitenone inhibits the migration of lung cancer cells via the suppression of AKT/mTOR and epithelial-to-mesenchymal transition. *Molecules*. 2021;26(3):638.

doi: 10.3390/molecules26030638

31. An WF, Tolliday N. Cell-based assays for high-throughput screening. *Mol Biotechnol*. 2010;45(2):180-186.

doi: 10.1007/s12033-010-9251-z

32. Takenaka T. Classical vs reverse pharmacology in drug discovery. *BJU Int*. 2001;88 Suppl 2:7-10; discussion 49-50.

doi: 10.1111/j.1464-410x.2001.00112.x

33. Lage OM, Ramos MC, Calisto R, Almeida E, Vasconcelos V, Vicente F. Current screening methodologies in drug discovery for selected human diseases. *Mar Drugs*. 2018;16(8):279.

doi: 10.3390/md16080279

34. Sriram K, Insel PA. G Protein-coupled receptors as targets for approved drugs: How many targets and how many drugs? *Mol Pharmacol*. 2018;93(4):251-258.

doi: 10.1124/mol.117.111062

35. Kenny CH, Ding W, Kelleher K, *et al*. Development of a fluorescence polarization assay to screen for inhibitors of the FtsZ/ZipA interaction. *Anal Biochem*. 2003;323(2):224-233.

doi: 10.1016/j.ab.2003.08.033

36. Burns S, Travers J, Collins I, *et al*. Identification of small-molecule inhibitors of protein kinase B (PKB/AKT) in an AlphaScreen™ high-throughput screen. *SLAS Discov*. 2006;11(7):822-827.

doi: 10.1177/1087057106290992

37. Sudo K, Yamaji K, Kawamura K, *et al*. High-throughput screening of low molecular weight NS3-NS4A protease inhibitors using a fluorescence resonance energy transfer substrate. *Antivir Chem Chemother*. 2005;16(6):385-392.

doi: 10.1177/095632020501600605

38. Swaney S, McCroskey M, Shinabarger D, Wang Z, Turner BA, Parker CN. Characterization of a high-throughput screening assay for inhibitors of elongation factor P and ribosomal peptidyl transferase activity. *J Biomol Screen*. 2006;11(7):736-742.

doi: 10.1177/1087057106291634

39. Allen M, Reeves J, Mellor G. High throughput fluorescence polarization: A homogeneous alternative to radioligand binding for cell surface receptors. *J Biomol Screen*. 2000;5(2):63-69.

doi: 10.1177/108705710000500202

40. Xu J, Wang X, Ensign B, *et al*. Ion-channel assay technologies: Quo vadis? *Drug Discov Today*. 2001;6(24):1278-1287.

doi: 10.1016/s1359-6446(01)02095-5

41. Parker GJ, Law TL, Lenoch FJ, Bolger RE. Development of high throughput screening assays using fluorescence polarization: Nuclear receptor-ligand-binding and kinase/phosphatase assays. *J Biomol Screen*. 2000;5(2):77-88.

doi: 10.1177/108705710000500204

42. Bagal SK, Brown AD, Cox PJ, *et al*. Ion channels as therapeutic targets: A drug discovery perspective. *J Med Chem*. 2013;56(3):593-624.

doi: 10.1021/jm3011433

43. Morachis JM, Huang R, Emerson BM. Identification of kinase inhibitors that target transcription initiation by RNA polymerase II. *Oncotarget*. 2011;2(1-2):18-28.

doi: 10.18632/oncotarget.212

44. Blay V, Tolani B, Ho SP, Arkin MR. High-throughput screening: Today's biochemical and cell-based approaches. *Drug Discov Today*. 2020;25(10):1807-1821.

doi: 10.1016/j.drudis.2020.07.024

45. Glickman JF. Assay development for protein kinase enzymes. In: Markossian S, Grossman A, Brimacombe K, *et al*, editors. *Assay Guidance Manual*. United States: Eli Lilly & Company and the National Center for Advancing Translational Sciences; 2004.

46. Harner MJ, Frank AO, Fesik SW. Fragment-based drug discovery using NMR spectroscopy. *J Biomol NMR*. 2013;56(2):65-75.

doi: 10.1007/s10858-013-9740-z

47. Bollag G, Hirth P, Tsai J, *et al*. Clinical efficacy of a RAF inhibitor needs broad target blockade in BRAF-mutant melanoma. *Nature*. 2010;467(7315):596-599.

doi: 10.1038/nature09454

48. Jadhav GP, Prathipati PK, Chauhan H. Surface plasmon resonance, Orbitrap mass spectrometry and Raman advancements: Exciting new techniques in drug discovery. *Expert Opin Drug Discov*. 2020;15(7):739-743.

doi: 10.1080/17460441.2020.1745771

49. Imaduwage KP, Lakbub J, Go EP, Desaire H. Rapid LC-MS based high-throughput screening method, affording no false positives or false negatives, identifies a new inhibitor for carbonic anhydrase. *Sci Rep*. 2017;7(1):10324.

doi: 10.1038/s41598-017-08602-w

50. McLaren DG, Shah V, Wisniewski T, *et al*. High-throughput mass spectrometry for hit identification: Current landscape and future perspectives. *SLAS Discov*. 2021;26(2):168-191.

doi: 10.1177/2472555220980696

51. Lu Y, Qin S, Zhang B, *et al*. Accelerating the throughput of affinity mass spectrometry-based ligand screening toward a G protein-coupled receptor. *Anal Chem*. 2019;91(13):8162-8169.

doi: 10.1021/acs.analchem.9b00477

52. Gilbert IH. Drug discovery for neglected diseases: Molecular target-based and phenotypic approaches. *J Med Chem*. 2013;56(20):7719-7726.

doi: 10.1021/jm400362b

53. Chen GQ, Xu Y, Shen SM, Zhang J. Phenotype and target-based chemical biology investigations in cancers. *Natl Sci Rev*. 2019;6(6):1111-1127.

doi: 10.1093/nsr/nwy124

54. Iqbal N, Iqbal N. Imatinib: A breakthrough of targeted therapy in cancer. *Chemother Res Pract*. 2014;2014:357027.

doi: 10.1155/2014/357027

55. Rossari F, Minutolo F, Orciuolo E. Past, present, and future of Bcr-Abl inhibitors: From chemical development to clinical efficacy. *J Hematol Oncol*. 2018;11(1):84.

doi: 10.1186/s13045-018-0624-2

56. Dong B, Liang Z, Chen Z, *et al*. Cryptotanshinone suppresses key onco-proliferative and drug-resistant pathways of chronic myeloid leukemia by targeting STAT5 and STAT3 phosphorylation. *Sci China Life Sci*. 2018;61(9):999-1009.

doi: 10.1007/s11427-018-9324-y

57. Liu C, Nie D, Li J, *et al*. Antitumor effects of blocking protein neddylation in T315I-BCR-ABL leukemia cells and leukemia stem cells. *Cancer Res*. 2018;78(6):1522-1536.

doi: 10.1158/0008-5472.Can-17-1733

58. Misra S, Zhang X, Wani NA, Sizemore S, Ray A. Both BRCA1-wild type and -mutant triple-negative breast cancers show sensitivity to the NAE inhibitor MLN4924 which is enhanced upon MLN4924 and cisplatin combination treatment. *Oncotarget*. 2020;11(8):784-800.

doi: 10.18632/oncotarget.27485

59. Swinney DC, Lee JA. Recent advances in phenotypic drug discovery. *F1000Res*. 2020;9:F1000.

doi: 10.12688/f1000research.25813.1

60. McKinney JD, Richard A, Waller C, Newman MC, Gerberick F. The practice of structure activity relationships (SAR) in toxicology. *Toxicol Sci*. 2000;56(1):8-17.

doi: 10.1093/toxsci/56.1.8

61. Newman DJ, Cragg GM. Natural products as sources of new drugs over the nearly four decades from 01/1981 to 09/2019. *J Nat Prod*. 2020;83(3):770-803.

doi: 10.1021/acs.jnatprod.9b01285

62. Krejci P, Pejchalova K, Wilcox WR. Simple, mammalian cell-based assay for identification of inhibitors of the Erk MAP kinase pathway. *Invest New Drugs*. 2007;25(4):391-395.

doi: 10.1007/s10637-007-9054-7

63. Chambers C, Smith F, Williams C, *et al*. Measuring intracellular calcium fluxes in high throughput mode. *Comb Chem High Throughput Screen*. 2003;6(4):355-362.

doi: 10.2174/138620703106298446

64. Kariv I, Stevens ME, Behrens DL, Oldenburg KR. High throughput quantitation of cAMP production mediated by activation of seven transmembrane domain receptors. *J Biomol Screen*. 1999;4(1):27-32.

doi: 10.1177/108705719900400105

65. Eggert US, Kiger AA, Richter C, *et al*. Parallel chemical genetic and genome-wide RNAi screens identify cytokinesis inhibitors and targets. *PLoS Biol*. 2004;2(12):e379.

doi: 10.1371/journal.pbio.0020379

66. Beck V, Pfitscher A, Jungbauer A. GFP-reporter for a high throughput assay to monitor estrogenic compounds. *J Biochem Biophys Methods*. 2005;64(1):19-37.

doi: 10.1016/j.jbbm.2005.05.001

67. Yarrow JC, Totsukawa G, Charras GT, Mitchison TJ. Screening for cell migration inhibitors via automated microscopy reveals a Rho-kinase inhibitor. *Chem Biol*. 2005;12(3):385-395.

doi: 10.1016/j.chembiol.2005.01.015

68. Vincent F, Loria P, Pregel M, *et al*. Developing predictive assays: The phenotypic screening "rule of 3". *Sci Transl Med*. 2015;7(293):293ps15.

doi: 10.1126/scitranslmed.aab1201

69. Engle SJ, Vincent F. Small molecule screening in human induced pluripotent stem cell-derived terminal cell types. *J Biol Chem*. 2014;289(8):4562-4570.

doi: 10.1074/jbc.R113.529156

70. McNeish J, Roach M, Hambor J, *et al*. High-throughput screening in embryonic stem cell-derived neurons identifies potentiators of α-amino-3-hydroxyl-5-methyl-4-isoxazolepropionate-type glutamate receptors. *J Biol Chem*. 2010;285(22):17209-17217.

doi: 10.1074/jbc.M109.098814

71. Ashlock MA, Olson ER. Therapeutics development for cystic fibrosis: A successful model for a multisystem genetic disease. *Annu Rev Med*. 2011;62:107-125.

doi: 10.1146/annurev-med-061509-131034

72. Van Goor F, Hadida S, Grootenhuis PDJ, *et al*. Correction of the F508del-CFTR protein processing defect *in vitro* by the investigational drug VX-809. *Proc Natl Acad Sci U S A*. 2011;108(46):18843-18848.

doi: 10.1073/pnas.1105787108

73. Lee G, Ramirez CN, Kim H, *et al*. Large-scale screening using familial dysautonomia induced pluripotent stem cells identifies compounds that rescue IKBKAP expression. *Nat Biotechnol*. 2012;30(12):1244-1248.

doi: 10.1038/nbt.2435

74. Barberis A, Gunde T, Berset C, Audetat S, Lüthi U. Yeast as a screening tool. *Drug Discov Today Technol*. 2005;2(2):187-192.

doi: 10.1016/j.ddtec.2005.05.022

75. Balgi AD, Roberge M. Screening for chemical inhibitors of heterologous proteins expressed in yeast using a simple growth-restoration assay. *Methods Mol Biol*. 2009;486:125-137.

doi: 10.1007/978-1-60327-545-3_9

76. Puri AW, Bogyo M. Using small molecules to dissect mechanisms of microbial pathogenesis. *ACS Chem Biol*. 2009;4(8):603-616.

doi: 10.1021/cb9001409

77. Zlitni S, Blanchard JE, Brown ED. High-throughput screening of model bacteria. *Methods Mol Biol*. 2009;486:13-27.

78. Hong CC. Large-scale small-molecule screen using zebrafish embryos. *Methods Mol Biol*. 2009;486:43-55.

doi: 10.1007/978-1-60327-545-3_4

79. Zon LI, Peterson RT. *In vivo* drug discovery in the zebrafish. *Nat Rev Drug Discov*. 2005;4(1):35-44.

doi: 10.1038/nrd1606

80. O'Rourke EJ, Conery AL, Moy TI. Whole-animal high-throughput screens: The *C. elegans* model. *Methods Mol Biol*. 2009;486:57-75.

doi: 10.1007/978-1-60327-545-3_5

81. Agee A, Carter D. Whole-organism screening: Plants. *Methods Mol Biol*. 2009;486:77-95.

doi: 10.1007/978-1-60327-545-3_6

82. Norambuena L, Raikhel NV, Hicks GR. Chemical genomics approaches in plant biology. *Plant Syst Biol*. 2009;553:345-354.

doi: 10.1007/978-1-60327-563-7_18

83. Stern HM, Murphey RD, Shepard JL, *et al*. Small molecules that delay S phase suppress a zebrafish bmyb mutant. *Nat Chem Biol*. 2005;1(7):366-370.

doi: 10.1038/nchembio749

84. Hong CC, Peterson QP, Hong JY, Peterson RT. Artery/vein specification is governed by opposing phosphatidylinositol-3 kinase and MAP kinase/ERK signaling. *Curr Biol*. 2006;16(13):1366-1372.

doi: 10.1016/j.cub.2006.05.046

85. Swinney DC. The value of translational biomarkers to phenotypic assays. *Front Pharmacol*. 2014;5:171.

doi: 10.3389/fphar.2014.00171

86. Ioannidis JP. Biomarker failures. *Clin Chem*. 2013;59(1):202-204.

doi: 10.1373/clinchem.2012.185801

87. Chau CH, Rixe O, McLeod H, Figg WD. Validation of analytic methods for biomarkers used in drug development. *Clin Cancer Res*. 2008;14(19):5967-5976.

doi: 10.1158/1078-0432.Ccr-07-4535

88. Spreafico R, Soriaga LB, Grosse J, Virgin HW, Telenti A. Advances in genomics for drug development. *Genes* (*Basel*). 2020;11(8):942.

doi:10.3390/genes11080942

89. Guo JB, Li XJ. Impacts of modern biology on drug discovery. *Sheng Li Ke Xue Jin Zhan*. 2007;38(1):25-31.

90. Hong AL, Tseng YY, Cowley GS, *et al*. Integrated genetic and pharmacologic interrogation of rare cancers. *Nat Commun*. 2016;7:11987.

doi: 10.1038/ncomms11987

91. Lin X, Huang XP, Chen G, *et al*. Life beyond kinases: Structure-based discovery of sorafenib as nanomolar antagonist of 5-HT receptors. *J Med Chem*. 2012;55(12):5749-5759.

doi: 10.1021/jm300338m

92. Schneidewind T, Brause A, Pahl A, *et al*. Morphological profiling identifies a common mode of action for small molecules with different targets. *Chembiochem*. 2020;21(22):3197-3207.

doi: 10.1002/cbic.202000381

93. Han X, Zhou C, Jiang M, *et al*. Discovery of RG7834: The first-in-class selective and orally available small molecule hepatitis B virus expression inhibitor with novel mechanism of action. *J Med Chem*. 2018;61(23):10619-10634.

doi: 10.1021/acs.jmedchem.8b01245

94. Moffat JG, Vincent F, Lee JA, Eder J, Prunotto M. Opportunities and challenges in phenotypic drug discovery: An industry perspective. *Nat Rev Drug Discov*. 2017;16(8):531-543.

doi: 10.1038/nrd.2017.111

95. Vincent F, Loria PM, Weston AD, *et al*. Hit triage and validation in phenotypic screening: Considerations and strategies. *Cell Chem Biol*. 2020;27(11):1332-1346.

doi: 10.1016/j.chembiol.2020.08.009

96. Warchal SJ, Unciti-Broceta A, Carragher NO. Next-generation phenotypic screening. *Future Med Chem*. 2016;8(11):1331-1347.

doi: 10.4155/fmc-2016-0025

97. Comess KM, McLoughlin SM, Oyer JA, *et al*. Emerging approaches for the identification of protein targets of small molecules-a practitioners' perspective. *J Med Chem*. 2018;61(19):8504-8535.

doi: 10.1021/acs.jmedchem.7b01921

98. Lee J, Bogyo M. Target deconvolution techniques in modern phenotypic profiling. *Curr Opin Chem Biol*. 2013;17(1):118-126.

doi: 10.1016/j.cbpa.2012.12.022

99. Lu JJ, Pan W, Hu YJ, Wang YT. Multi-target drugs: the trend of drug research and development. *PLoS One*. 2012;7(6):e40262.

doi: 10.1371/journal.pone.0040262

100. Rena G, Hardie DG, Pearson ER. The mechanisms of action of metformin. Diabetologia. 2017;60(9):1577-1585.

doi: 10.1007/s00125-017-4342-z

101. Keller MP, Attie AD. Physiological insights gained from gene expression analysis in obesity and diabetes. Annu Rev Nutr. 2010;30:341-364.

doi: 10.1146/annurev.nutr.012809.104747

102. Van't Veer LJ, Bernards R. Enabling personalized cancer medicine through analysis of gene-expression patterns. Nature. 2008;452(7187):564-570.

doi: 10.1038/nature06915

103. Bertos NR, Park M. Breast cancer-one term, many entities? J Clin Invest. 2011;121(10):3789-3796.

doi: 10.1172/JCI57100

104. Huang E, Ishida S, Pittman J, et al. Gene expression phenotypic models that predict the activity of oncogenic pathways. Nat Genet. 2003;34(2):226-230.

doi: 10.1038/ng1167

105. Loboda A, Nebozhyn M, Klinghoffer R, et al. A gene expression signature of RAS pathway dependence predicts response to PI3K and RAS pathway inhibitors and expands the population of RAS pathway activated tumors. BMC Med Genomics. 2010;3(1):26.

doi: 10.1186/1755-8794-3-26

106. Loboda A, Nebozhyn MV, Watters JW, et al. EMT is the dominant program in human colon cancer. BMC Med Genomics. 2011;4(1):9.

doi: 10.1186/1755-8794-4-9

107. Méndez-Lucio O, Naveja JJ, Vite-Caritino H, Prieto-Martínez FD, Medina-Franco JL. One drug for multiple targets: A computational perspective. J Mex Chem Soc. 2016;60(3):168-181.

doi: 10.29356/jmcs.v60i3.100

108. Hsieh JH, Smith-Roe SL, Huang R, et al. Identifying compounds with genotoxicity potential using Tox21 high-throughput screening assays. Chem Res Toxicol. 2019;32(7):1384-1401.

doi: 10.1021/acs.chemrestox.9b00053

109. Michod D, Widmann C. DNA-damage sensitizers: Potential new therapeutical tools to improve chemotherapy. Crit Rev Oncol Hematol. 2007;63(2):160-171.

doi: 10.1016/j.critrevonc.2007.04.003

110. Evans TJ, Yamamoto KN, Hirota K, Takeda S. Mutant cells defective in DNA repair pathways provide a sensitive high-throughput assay for genotoxicity. DNA Repair (Amst). 2010;9(12):1292-1298.

doi: 10.1016/j.dnarep.2010.09.017

111. Ji K, Kogame T, Choi K, et al. A novel approach using DNA-repair-deficient chicken DT40 cell lines for screening and characterizing the genotoxicity of environmental contaminants. Environ Health Perspect. 2009;117(11):1737-1744.

doi: 10.1289/ehp.0900842

112. Buerstedde JM, Takeda S. Increased ratio of targeted to

random integration after transfection of chicken B cell lines. Cell. 1991;67(1):179-188.

doi: 10.1016/0092-8674(91)90581-i

113. Yamazoe M, Sonoda E, Hochegger H, Takeda S. Reverse genetic studies of the DNA damage response in the chicken B lymphocyte line DT40. DNA Repair (Amst). 2004;3(8-9):1175-1185.

doi: 10.1016/j.dnarep.2004.03.039

114. Walmsley RM, Tate M. The GADD45a-GFP greenscreen HC assay. Methods Mol Biol. 2012;817:231-250.

doi: 10.1007/978-1-61779-421-6_12

115. Knight AW, Little S, Houck K, et al. Evaluation of high-throughput genotoxicity assays used in profiling the US EPA ToxCast™ chemicals. Regul Toxicol Pharmacol. 2009;55(2):188-199.

doi: 10.1016/j.yrtph.2009.07.004

116. Hastwell PW, Chai LL, Roberts KJ, et al. High-specificity and high-sensitivity genotoxicity assessment in a human cell line: Validation of the GreenScreen HC GADD45a-GFP genotoxicity assay. Mutat Res. 2006;607(2):160-175.

doi: 10.1016/j.mrgentox.2006.04.011

117. Giuliano KA, Gough AH, Taylor DL, Vernetti LA, Johnston PA. Early safety assessment using cellular systems biology yields insights into mechanisms of action. J Biomol Screen. 2010;15(7):783-797.

doi: 10.1177/1087057110376413

118. Brattain MG, Fine WD, Khaled FM, Thompson J, Brattain DE. Heterogeneity of malignant cells from a human colonic carcinoma. Cancer Res. 1981;41(5):1751-1756.

119. Xing JZ, Zhu L, Gabos S, Xie L. Microelectronic cell sensor assay for detection of cytotoxicity and prediction of acute toxicity. Toxicol In Vitro. 2006;20(6):995-1004.

doi: 10.1016/j.tiv.2005.12.008

120. Fox JT, Sakamuru S, Huang R, et al. High-throughput genotoxicity assay identifies antioxidants as inducers of DNA damage response and cell death. Proc Natl Acad Sci. 2012;109(14):5423-5428.

doi: 10.1073/pnas.1114278109

121. Sikdar N, Banerjee S, Lee KY, et al. DNA damage responses by human ELG1 in S phase are important to maintain genomic integrity. Cell Cycle. 2009;8(19):3199-3207.

doi: 10.4161/cc.8.19.9752

122. Scholes DT, Banerjee M, Bowen B, Curcio MJ. Multiple regulators of Ty1 transposition in Saccharomyces cerevisiae have conserved roles in genome maintenance. Genetics. 2001;159(4):1449-1465.

doi: 10.1093/genetics/159.4.1449

123. Sykora P, Witt KL, Revanna P, et al. Next generation high throughput DNA damage detection platform for genotoxic compound screening. Sci Rep. 2018;8(1):2771.

doi: 10.1038/s41598-018-20995-w

124. Gatti L, Zunino F. Overview of tumor cell chemoresistance mechanisms. Methods Mol Med. 2005;111:127-148.

doi: 10.1385/1-59259-889-7:127

125. Gottesman MM, Fojo T, Bates SE. Multidrug resistance in cancer: Role of ATP-dependent transporters. Nat Rev Cancer. 2002;2(1):48-58.

doi: 10.1038/nrc706

126. Gottesman MM, Ling V. The molecular basis of multidrug resistance in cancer: The early years of P-glycoprotein research. FEBS Lett. 2006;580(4):998-1009.

doi: 10.1016/j.febslet.2005.12.060

127. Sharom FJ. ABC multidrug transporters: Structure, function and role in chemoresistance. Pharmacogenomics. 2008;9(1):105-127.

doi: 10.2217/14622416.9.1.105

128. Sparreboom A, van Asperen J, Mayer U, et al. Limited oral bioavailability and active epithelial excretion of paclitaxel (Taxol) caused by P-glycoprotein in the intestine. Proc Natl Acad Sci U S A. 1997;94(5):2031-2035.

doi: 10.1073/pnas.94.5.2031

129. Kartner N, Riordan JR, Ling V. Cell surface P-glycoprotein associated with multidrug resistance in mammalian cell lines. Science. 1983;221(4617):1285-1288.

doi: 10.1126/science.6137059

130. Shen DW, Cardarelli C, Hwang J, et al. Multiple drug-resistant human KB carcinoma cells independently selected for high-level resistance to colchicine, adriamycin, or vinblastine show changes in expression of specific proteins. J Biol Chem. 1986;261(17):7762-7770.

131. Roe M, Folkes A, Ashworth P, et al. Reversal of P-glycoprotein mediated multidrug resistance by novel anthranilamide derivatives. Bioorg Med Chem Lett. 1999;9(4):595-600.

doi: 10.1016/s0960-894x(99)00030-x

132. Dantzig AH, Shepard RL, Law KL, et al. Selectivity of the multidrug resistance modulator, LY335979, for P-glycoprotein and effect on cytochrome P-450 activities. J Pharmacol Exp Ther. 1999;290(2):854-862.

133. Mistry P, Stewart AJ, Dangerfield W, et al. In vitro and in vivo reversal of P-glycoprotein-mediated multidrug resistance by a novel potent modulator, XR9576. Cancer Res. 2001;61(2):749-758.

134. Bates SF, Chen C, Robey R, Kang M, Figg WD, Fojo T. Reversal of multidrug resistance: Lessons from clinical oncology. Novartis Found Symp. 2002;243:83-96; discussion 96-102, 180-185.

135. Dalton W. Detection of multidrug resistance gene expression in multiple myeloma. Leukemia. 1997;11(7):1166-1169.

doi: 10.1038/sj.leu.2400724

136. Susa M, Choy E, Yang C, et al. Multidrug resistance reversal agent, NSC77037, identified with a cell-based screening assay. J Biomol Screen. 2010;15(3):287-296.

doi: 10.1177/1087057109359422

137. Winter SS, Lovato DM, Khawaja HM, et al. High-throughput screening for daunorubicin-mediated drug resistance identifies mometasone furoate as a novel ABCB1-reversal agent. J Biomol Screen. 2008;13(3):185-193.

doi: 10.1177/1087057108314610

138. Duan Z, Choy E, Hornicek FJ. NSC23925, identified in a high-throughput cell-based screen, reverses multidrug resistance. PLoS One. 2009;4(10):e7415.

doi: 10.1371/journal.pone.0007415

139. Ivnitski-Steele I, Larson RS, Lovato DM, et al. High-throughput flow cytometry to detect selective inhibitors of ABCB1, ABCC1, and ABCG2 transporters. Assay Drug Dev Technol. 2008;6(2):263-276.

doi: 10.1089/adt.2007.107

140. Gurdon JB, Elsdale TR, Fischberg M. Sexually mature individuals of Xenopus laevis from the transplantation of single somatic nuclei. Nature. 1958;182(4627):64-65.

doi: 10.1038/182064a0

141. Hass R, von der Ohe J, Ungefroren H. The intimate relationship among EMT, MET and TME: AT (ransdifferentiation) E (nhancing) M (ix) to be exploited for therapeutic purposes. Cancers. 2020;12(12):3674.

doi: 10.3390/cancers12123674

142. Saito S, Lin YC, Nakamura Y, et al. Potential application of cell reprogramming techniques for cancer research. Cell Mol Life Sci. 2019;76:45-65.

doi: 10.1007/s00018-018-2924-7

143. Welch DR. Tumor heterogeneity-a "contemporary concept" founded on historical insights and predictions. Cancer Res. 2016;76(1):4-6.

doi: 10.1158/0008-5472.CAN-15-3024

144. Denny SK, Yang D, Chuang CH, et al. Nfib promotes metastasis through a widespread increase in chromatin accessibility. Cell. 2016;166(2):328-342.

doi: 10.1016/j.cell.2016.05.052

145. Teng S, Li YE, Yang M, et al. Tissue-specific transcription reprogramming promotes liver metastasis of colorectal cancer. Cell Res. 2020;30(1):34-49.

doi: 10.1038/s41422-019-0259-z

146. Van Keymeulen A, Lee MY, Ousset M, et al. Reactivation of multipotency by oncogenic PIK3CA induces breast tumour heterogeneity. Nature. 2015;525(7567):119-123.

doi: 10.1038/nature14665

147. Katoh M. Canonical and non-canonical WNT signaling in cancer stem cells and their niches: Cellular heterogeneity, omics reprogramming, targeted therapy and tumor plasticity (Review). Int J Oncol. 2017;51(5):1357-1369.

doi: 10.3892/ijo.2017.4129

148. Zheng YW, Nie YZ, Taniguchi H. Cellular reprogramming and hepatocellular carcinoma development. World J Gastroenterol. 2013;19(47):8850-8860.

doi: 10.3748/wjg.v19.i47.8850

149. Jones PA, Laird PW. Cancer epigenetics comes of age. Nat Genet. 1999;21(2):163-167.

doi: 10.1038/5947

150. Wang D, Garcia-Bassets I, Benner C, et al. Reprogramming transcription by distinct classes of enhancers functionally defined by eRNA. Nature. 2011;474(7351):390-394.

doi: 10.1038/nature10006

151. Li HF, Keeton A, Vitolo M, et al. A high-throughput screen with isogenic PTEN+/+ and PTEN-/- cells identifies CID1340132 as a novel compound that induces apoptosis in PTEN and PIK3CA mutant human cancer cells. J Biomol Screen. 2011;16(4):383-393.

doi: 10.1177/1087057110397357

152. Qin L, Yin YT, Zheng FJ, et al. WNT5A promotes stemness characteristics in nasopharyngeal carcinoma cells leading to metastasis and tumorigenesis. Oncotarget. 2015;6(12):10239-10252.

doi: 10.18632/oncotarget.3518

153. Ewan K, Pajak B, Stubbs M, et al. A useful approach to identify novel small-molecule inhibitors of Wnt-dependent transcription. Cancer Res. 2010;70(14):5963-5973.

doi: 10.1158/0008-5472.Can-10-1028

154. Bialkowska AB, Yang VW. High-throughput screening strategies for targeted identification of therapeutic compounds in colorectal cancer. Future Oncol. 2012;8(3):259-272.

doi: 10.2217/fon.12.19

155. Lepourcelet M, Chen YNP, France DS, et al. Small-molecule antagonists of the oncogenic Tcf/β-catenin protein complex. Cancer Cell. 2004;5(1):91-102.

doi: 10.1016/S1535-6108(03)00334-9

156. Yu W, Ma Y, Shankar S, Srivastava RK. SATB2/β-catenin/TCF-LEF pathway induces cellular transformation by generating cancer stem cells in colorectal cancer. Sci Rep. 2017;7(1):10939.

doi: 10.1038/s41598-017-05458-y

157. Torrance CJ, Agrawal V, Vogelstein B, Kinzler KW. Use of isogenic human cancer cells for high-throughput screening and drug discovery. Nat Biotechnol. 2001;19(10):940-945.

doi: 10.1038/nbt1001-940

158. Mallon R, Feldberg L, Kim S, et al. Identification of 4-anilino-3-quinolinecarbonitrile inhibitors of mitogen-activated protein/extracellular signal-regulated kinase 1 kinase. Mol Cancer Ther. 2004;3(6):755-762.

159. Rissmann R, Hessel MH, Cohen AF. Vemurafenib/dabrafenib and trametinib. Br J Clin Pharmacol. 2015;80(4):765-767.

doi: 10.1111/bcp.12651

160. Fu H, Gao H, Qi X, et al. Aldolase A promotes proliferation and G 1/S transition via the EGFR/MAPK pathway in non-small cell lung cancer. Cancer Commun (Lond). 2018;38:18.

doi: 10.1186/s40880-018-0290-3

161. Champer M, Miller D, Kuo DYS. Response to trametinib in recurrent low-grade serous ovarian cancer with NRAS mutation: A case report. Gynecol Oncol Rep. 2019;28:26-28.

doi: 10.1016/j.gore.2019.01.007

162. Liu S, Zou Q, Chen JP, et al. Targeting enhancer reprogramming to mitigate MEK inhibitor resistance in preclinical models of advanced ovarian cancer. J Clin Invest. 2021;131(20):e145035.

doi: 10.1172/jci145035

163. Yuliantie E, Dai X, Yang D, Crack PJ, Wang MW. High-throughput screening for small molecule inhibitors of the type-I interferon signaling pathway. Acta Pharm Sin B. 2018;8(6):889-899.

doi: 10.1016/j.apsb.2018.07.005

164. Dillon KJ, Smith GC, Martin NM. A FlashPlate assay for the identification of PARP-1 inhibitors. J Biomol Screen. 2003;8(3):347-352.

doi: 10.1177/1087057103008003013

165. Bapat A, Glass LS, Luo M, et al. Novel small-molecule inhibitor of apurinic/apyrimidinic endonuclease 1 blocks proliferation and reduces viability of glioblastoma cells. J Pharmacol Exp Ther. 2010;334(3):988-998.

doi: 10.1124/jpet.110.169128

166. Peterson EJ, Janzen WP, Kireev D, Singleton SF. High-throughput screening for RecA inhibitors using a transcreener adenosine 5'-O-diphosphate assay. Assay Drug Dev Technol. 2012;10(3):260-268.

doi: 10.1089/adt.2011.0409

167. Sexton JZ, Wigle TJ, He Q, et al. Novel inhibitors of E. coli RecA ATPase activity. Curr Chem Genomics. 2010;4:34-42.

doi: 10.2174/1875397301004010034

168. Huang F, Motlekar NA, Burgwin CM, Napper AD, Diamond SL, Mazin AV. Identification of specific inhibitors of human RAD51 recombinase using high-throughput screening. ACS Chem Biol. 2011;6(6):628-635.

doi: 10.1021/cb100428c

169. Huang L, Yi X, Yu X, et al. High-throughput strategies for the discovery of anticancer drugs by targeting transcriptional reprogramming. Front Oncol. 2021;11:762023.

doi: 10.3389/fonc.2021.762023

170. Shaw J, Dale I, Hemsley P, et al. Positioning high-throughput CETSA in early drug discovery through screening against B-Raf and PARP1. SLAS Discov. 2019;24(2):121-132.

doi: 10.1177/2472555218813332

171. Howard RT, Hemsley P, Petteruti P, et al. Structure-guided design and in-cell target profiling of a cell-active target engagement probe for PARP inhibitors. ACS Chem Biol. 2020;15(2):325-333.

doi: 10.1021/acschembio.9b00963

172. Cancer Genome Atlas Research Network. Comprehensive genomic characterization defines human glioblastoma genes and core pathways. Nature. 2008;455(7216):1061-1068.

doi: 10.1038/nature07385

173. Ding L, Getz G, Wheeler DA, et al. Somatic mutations affect key pathways in lung adenocarcinoma. Nature. 2008;455(7216):1069-1075.

doi: 10.1038/nature07423

174. Jones S, Zhang X, Parsons DW, et al. Core signaling pathways in human pancreatic cancers revealed by global genomic analyses. Science. 2008;321(5897):1801-1806.

doi: 10.1126/science.1164368

175. Steeg PS, Zhou Q. Cyclins and breast cancer. Breast Cancer Res Treat. 1998;52(1-3):17-28.

doi: 10.1023/a:1006102916060

176. Miyoshi Y, Iwao K, Egawa C, Noguchi S. Association of centrosomal kinase STK15/BTAK mRNA expression with chromosomal instability in human breast cancers. Int J Cancer. 2001;92(3):370-373.

doi: 10.1002/ijc.1200

177. Dhillon NK, Mudryj M. Cyclin E overexpression enhances cytokine-mediated apoptosis in MCF7 breast cancer cells. Genes Immun. 2003;4(5):336-342.

doi: 10.1038/sj.gene.6363973

178. Niu D, Wang G, Wang X. Up-regulation of cyclin E in breast cancer via estrogen receptor pathway. Int J Clin Exp Med. 2015;8(1):910-915.

179. Warner SL, Munoz RM, Stafford P, et al. Comparing

Aurora A and Aurora B as molecular targets for growth inhibition of pancreatic cancer cells. Mol Cancer Ther. 2006;5(10):2450-2458.

doi: 10.1158/1535-7163.Mct-06-0202

180. Wang W, Kim SH, El-Deiry WS. Small-molecule modulators of p53 family signaling and antitumor effects in p53-deficient human colon tumor xenografts. Proc Natl Acad Sci U S A. 2006;103(29):11003-11008.

doi: 10.1073/pnas.0604507103

181. Maloney A, Workman P. HSP90 as a new therapeutic target for cancer therapy: The story unfolds. Expert Opin Biol Ther. 2002;2(1):3-24.

doi: 10.1517/14712598.2.1.3

182. Magwenyane AM, Ugbaja SC, Amoako DG, Somboro AM, Khan RB, Kumalo HM. Heat shock protein 90 (HSP90) inhibitors as anticancer medicines: A review on the computer-aided drug discovery approaches over the past five years. Comput Math Methods Med. 2022;2022:2147763.

doi: 10.1155/2022/2147763

183. Bos R, Zhong H, Hanrahan CF, et al. Levels of hypoxia-inducible factor-1 alpha during breast carcinogenesis. J Natl Cancer Inst. 2001;93(4):309-314.

doi: 10.1093/jnci/93.4.309

184. Semenza GL. HIF-1 and tumor progression: Pathophysiology and therapeutics. Trends Mol Med. 2002;8(4 Suppl):S62-S67.

doi: 10.1016/s1471-4914(02)02317-1

185. Masoud GN, Li W. HIF-1α pathway: Role, regulation and intervention for cancer therapy. Acta Pharm Sin B. 2015;5(5):378-389.

doi: 10.1016/j.apsb.2015.05.007

186. Workman P. Scoring a bull's-eye against cancer genome targets. Curr Opin Pharmacol. 2001;1(4):342-352.

doi: 10.1016/s1471-4892(01)00060-1

187. Mahlknecht U, Hoelzer D. Histone acetylation modifiers in the pathogenesis of malignant disease. Mol Med. 2000;6(8):623-644.

188. Turlais F, Hardcastle A, Rowlands M, et al. High-throughput screening for identification of small molecule inhibitors of histone acetyltransferases using scintillating microplates (FlashPlate). Anal Biochem. 2001;298(1):62-68.

doi: 10.1006/abio.2001.5340

189. Dekker FJ, Haisma HJ. Histone acetyl transferases as emerging drug targets. Drug Discov Today. 2009;14(19-20):942-948.

doi: 10.1016/j.drudis.2009.06.008

190. Miles DW. Update on HER-2 as a target for cancer therapy: Herceptin in the clinical setting. Breast Cancer Res. 2001;3(6):380-384.

doi: 10.1186/bcr326

191. Kelland LR, Smith V, Valenti M, et al. Preclinical antitumor activity and pharmacodynamic studies with the farnesyl protein transferase inhibitor R115777 in human breast cancer. Clin Cancer Res. 2001;7(11):3544-3550.

192. Johnston SR. Farnesyl transferase inhibitors: A novel targeted tnerapy for cancer. Lancet Oncol. 2001;2(1):18-26.

doi: 10.1016/s1470-2045(00)00191-1

193. Nicholls H. Aromatase inhibitors continue their ATAC on tamoxifen. Trends Mol Med. 2002;8(4 Suppl):S12-S13.

doi: 10.1016/s1471-4914(02)02304-3

194. Buzdar AU. Anastrozole (Arimidex)--an aromatase inhibitor for the adjuvant setting? Br J Cancer. 2001;85 Suppl 2(Suppl 2):6-10.

doi: 10.1054/bjoc.2001.1983

195. Chen B, Dodge ME, Tang W, et al. Small molecule-mediated disruption of Wnt-dependent signaling in tissue regeneration and cancer. Nat Chem Biol. 2009;5(2):100-107.

doi: 10.1038/nchembio.137

196. Zhang N, Wu B, Powell D, et al. Synthesis and structure-activity relationships of 3-cyano-4-(phenoxyanilino) quinolines as MEK (MAPKK) inhibitors. Bioorg Med Chem Lett. 2000;10(24):2825-2828.

doi: 10.1016/S0960-894X(00)00580-1

197. Berger D, Dutia M, Powell D, et al. Synthesis and evaluation of 4-anilino-6,7-dialkoxy-3-quinolinecarbonitriles as inhibitors of kinases of the Ras-MAPK signaling cascade. Bioorg Med Chem Lett. 2003;13(18):3031-3034.

doi: 10.1016/s0960-894x(03)00640-1

198. Fry DW, Kraker AJ, McMichael A, et al. A specific inhibitor of the epidermal growth factor receptor tyrosine kinase. Science. 1994;265(5175):1093-1095.

doi: 10.1126/science.8066447

ACCSCIENCE PUBLISHING

Global Translational Medicine

REVIEW ARTICLE

Comparative analysis of immune responses in humans infected with Alpha, Delta, and Omicron strains of SARS-CoV-2

Mihieka Bose[1,2] and Chayan Munshi[1]*

[1]Ethophilia Research Foundation, Santiniketan, India

[2]Department of Zoology, Visva Bharati University, Santiniketan, India

Abstract

The COVID-19 pandemic outbreak has profoundly challenged global public health over the last couple of years. Throughout this period, numerous mutant strains of SARS-CoV-2 have emerged, presenting diverse pathophysiology and immune response challenges for infected individuals. Among these, variant of concern strains, including Alpha (B.1.1.7), Delta (B.1.617.2), and Omicron (B.1.1.529), has garnered the most significant attention for their role in causing epidemiological dynamics, ultimately leading to elevated infectivity and significant mortality rates. This review aims to provide a comparative analysis of the immune-pathophysiological mechanisms associated with these aforementioned strains of SARS-CoV-2.

Keywords: SARS-CoV-2; Immune response; Pandemic

***Corresponding author:**
Chayan Munshi
(chayanbio@gmail.com)

Citation: Bose M, Munshi C. Comparative analysis of immune responses in humans infected with Alpha, Delta, and Omicron strains of SARS-CoV-2. *Global Transl Med.* 2024;3(1):2228.
https://doi.org/10.36922/gtm.2228

Received: November 10, 2023
Accepted: December 25, 2023
Published Online: March 19, 2023

1. Introduction

Over the past 3 years, the global SARS-CoV-2 epidemic has imposed significant strain on human immunity, resulting in numerous viral outbreaks that have claimed many lives and negatively impacted public health. Across several virologically distinct waves, SARS-CoV-2 has employed mutation mechanisms that changed its interaction with the host body. Correspondingly, the human immune response has also been modified as the viral strains evolved. The World Health Organization has identified several variants of concern (VOC) during the COVID-19 pandemic, including Alpha, Beta, Gamma, Delta, and Omicron.[1] Although these strains have diversified into additional subtypes over time, our focus remains primarily on the Alpha, Delta, and Omicron variants due to their significant influence. Throughout the pandemic, these three strains have exhibited significantly higher degrees of pathogenicity and transmissibility in comparison with other circulating strains, affecting a vast population around the globe. The characteristic route of invasion or biomarking remains consistent across all these strains. As a member of the coronavirus family, SARS-CoV-2 spreads through the air, gaining entry into the human respirational tract. Subsequently, it gains access to various cell types by utilizing its viral spike protein, leading to severe respiratory distress and other clinical symptoms. In comparison with its predecessors, the Middle East respiratory syndrome, and severe acute respiratory syndrome-1 (SARS-CoV-1), this virus has a far greater impact on public health due to its high disease spread and pathogenicity, which is tightly controlled

by tissue tropism in the host. In cases of SARS-CoV-2 infection, the main route by which the coronavirus enters the host body is through the angiotensin-converting enzyme-2 (ACE-2) receptor, which is present on the surfaces of enterocytic, epithelial, and goblet cells in the body.[2] Since the spike protein is essential for host evasion, mutations in these regions can significantly change the evasion process, influencing the pathogen's localization, mode of infection, and degree of host defense evasion.[3] As a result, the spread of the virus alters the pattern of the disease in the population, including its clinical severity.

However, there exists a distinct subset of patients who have been infected without exhibiting any symptoms or experiencing only very mild pathological outcomes. Asymptomatic infections have emerged as a potential problem in efforts to eradicate the pandemic, as these cases represent critical points of transmission that often go unnoticed. Recent reports have shedded light on host, viral, and environmental factors suspected to contribute to this phenomenon. During asymptomatic infection, a robust adaptive immune response is generated, which may differ from the attributes of T cell response and antibody action observed in symptomatic cases.[4,5]

In this review, we aim to elucidate a comparative analysis of the infection pathways in the Alpha, Delta, and Omicron strains, accompanied by exploring the epidemiological aspects of their pathogenicity and transmissibility, as well as their corresponding human immune responses.

2. Infection and pathogenicity of SARS-CoV-2

As mentioned earlier, SARS-CoV-2 gains entry into the human respiration tract through airborne transmission and subsequently infiltrates host cells through the key gateway ACE-2 receptor. The receptor binding domain (RBD) of the S1 subunit of spike protein binds to the ACE-2 receptor, adopting a trimeric conformation and triggering the formation of an endosome with a low pH level. ACE-2-S1 binding is followed by the cleavage of the S1 and S2 subunits, promoting viral fusion within the endosome. Host proteases such as transmembrane protease serine 2 (TMPRSS2) cleave multiple furin cleavage sites on the spike proteins. Endosomal fusion is further facilitated by extensive protein folding modifications of the spike HR1 and HR2 domains of S2 by forming a six-helical structure that physically reduces the distance between the host and virus, allowing fusion of both membranes. Subsequently, endosomal fusion grants the virus access to the host's cellular machinery, allowing for viral proliferation and the budding off of newly synthesized and packaged virions from the infected cell.[6]

3. Immune response against SARS-CoV-2 variants

3.1. Immune response during the Alpha wave

The VOC, Alpha, or the B.1.1.7 was initially recorded in Kent, UK, in September 2020, following the global spread of the original Wuhan strain in March 2020.[7] This particular strain follows the general pathway of invasion as discussed earlier.[8,9] Infection with the Alpha strain severely undermines the host's translational machinery through the action of a non-structural protein (NSP), NSP14.[10] Hijacking of this process disrupts the host's cellular translation, allowing the virus to amplify its own genome within the host body. Inhibition of host translation subsequently suppresses the synthesis of antiviral compounds by the host, thus compromising the first line of defense—innate immunity. Interferon (IFN)-1 has been identified as a key factor in producing an effective reaction against viral attack, inducing certain subsets of IFN-stimulated gene (ISG) to inhibit viral replication.[11] Upregulation of ISGs potentiates the functionality of immune effector cells such as B and T cells, macrophages, and dendritic cells.[12] NSP14 targets and disrupts the antiviral response by forming the NSP14-NSP10 complex as a translation inhibitor, leading to the impairment of innate immunity function against the SARS-CoV-2 infection.[10] The undermining of innate immunity also affects the adaptive immune response.

The adaptive defense against viral attack is enacted through immune cell-mediated and humoral immunity, particularly involving antibodies. However, the contagion exhibits a carefully designed pathway to escape from antibody-mediated neutralization, especially through mutations of the spike protein. Neutralizing antibodies are highly specific to the viral epitope of the spike's RBD. Mutations in this area notably modify the affinity of antibodies for the viral epitope, reducing the epitope-binding affinity and allowing the virus to escape from antibody-mediated neutralization. The N501Y mutation in the Alpha strain has been identified as the culprit behind a moderately increased escape from neutralizing antibodies compared to the ancestral strain.[13,14]

Humoral immunity is extensively intertwined with cell-mediated immunity. Following the pathogen attack, heavy production of immunoglobulin IgM and IgG occurs from B cells in response to antigen presentation, typically within 3 – 6 days. IgM serves as the primary antibody response against viral invasion, while high-affinity IgG constitutes the secondary response crucial for long-term immunological memory.[15] The release of these immunoglobulins eventually leads to an increase in inflammatory cytokine levels to combat the pathogen.

Secretion of inflammatory cytokines such as tumor necrosis factor-alpha (TNF-α), interleukin (IL)-1, and IL-6 triggers T cells. Consequently, cell-mediated immunity, controlled by helper ($CD4^+$) and killer ($CD8^+$) T cells, is activated. The cascade of stimulations initiated by helper T cells further activates and synchronizes the functions of other immune effector cells, such as macrophages and B cells.[15,16] However, the release of pro-inflammatory cytokines can, on the contrary, be accountable for T cell exhaustion. Interaction of TNF-α with tumor necrosis factor receptor 1 (TNFR1) receptor on T cells can direct T cells to undergo apoptosis. In addition, dysregulated secretion of IL-10 and IL-6 can also be responsible for a significant reduction of T cell numbers.[17] A study reveals that over-secretion of TNF-α is also associated with substantial inhibition of $Bcl\text{-}6^+$Tfh (follicular helper T lymphocytes) differentiation. This phenomenon can render the outcomes of T cell-mediated B cell activation largely ineffective due to a significant loss of germinal center B cell formation. However, non-germinal B cells can thrive in this condition; yet, they are not efficient in providing long-term immunological memory or high-affinity B cells.[18] Consequently, COVID-19 potentially compromises both cell-mediated immunity and humoral immunity, thereby hindering effective IgG production as well.[15]

3.2. Immune response during the Delta wave

The VOC B.1.617.2, first identified in India toward the end of 2020, was designated the Delta variant. By 2021, Delta had claimed a significant number of lives.[19] This strain proved to be far more contagious than its predecessor, with a transmission rate estimated at around 40–60%, posing a heightened risk to the populations with partial or no vaccination.[20] Statistics revealed approximately 400,000 cases and 4000 mortalities within the 1st weeks of May 2021 in India alone, with subsequent spread to over 40 countries across various continents.[21] The major mutation in the spike protein contributing to its increased transmissibility and evasion of antibody neutralization was D614G. In contrast to Delta, the Alpha and Beta strains exhibited an N501Y substitution.[22]

Previous variants mutations had mutations clustered in the N-terminal domain (NTD), which proved to be sensitive targets for human monoclonal antibodies (mAbs). These mAbs were highly effective in neutralizing the virus, inhibiting the cell-cell fusion method of infection, and stimulating the host's effector functions, making them promising targets for therapeutic interventions.[23] However, a critical study has elucidated the ineffectiveness of monoclonal antibodies against the Delta strain. Both anti-NTD and anti-RBD mAbs classes failed to bind effectively to the Delta spike protein and were unable to neutralize this VOC. Serum antibodies from convalescent individuals (recovered from previous COVID-19 infection) were also found futile, being four-fold less effective against Delta compared to the Alpha variant. In addition, along with the D614G and D950N mutations regulating S protein dynamics, the L452R mutation on the RBD also plays a vital part in antibody escape. The precise location of this mutation on the peripheral surface of the ACE-2 binding area allows the virus to escape from antibodies while also enhancing its attachment to the ACE-2 receptor. This strategy of accumulating mutations in the peripheral region has significantly enhanced this variant's ability to evade host immunity.[24]

The disruption in host immunity is attributed to multiple factors. Viral NSP1 and NSP14 accomplish the translational shutdown of antiviral proteins. NSP8 and NSP9 interfere with the Sec61-regulated pathway to enter the endoplasmic reticulum, disrupting the whole process of host translation necessary for survival.[21] Virus-associated proteins also impede the secretion of IFN-I and IFN-III. Proteins such as M protein, open reading frame (ORF) 3b, ORF6, and NSP13 inhibit the RIG-I/MDA-5–MAVS pathway of cytosolic double-stranded RNA sensing, directly antagonizing IFN secretion.[25]

One of the key attributes of COVID-19 infection is the cytokine storm, characterized by severe dysregulation of cytokine response. This phenomenon has been associated with an elevated degree of pathogenicity in patients and has posed a serious challenge for clinicians and researchers alike. The release of pro-inflammatory cytokines such as IL-1β, IL-2, IL-6, IL-10, TNF-α, IFN-γ, and granulocyte macrophage-colony stimulating factor is commonly observed in this scenario.

According to studies, discord in the timing of appropriate immune responses is implicated in the development of a cytokine storm in a patient. During the early phases of infection, the host body fails to produce potent IFNs (I and III) effectively to combat the pathogen while simultaneously continuing to secrete IL-6 and other chemokines. This failure to produce IFNs and continued secretion of IL-6 and other chemokines creates a conducive environment for a pro-inflammatory response.[26] The role of IL-6 remains relevant during the Delta wave, as reports indicate elevated levels of IL-6 correlating with disease severity.[27] This phenomenon facilitates viral replication and the progression of infection. As the infection progresses, by the time the body regains its ability to mount a defense, the infection load has already heightened, prompting an exaggerated and uncontrolled immune response.[28]

A balanced response of Th1 and Th2 cytokines is desirable. Immune exaggeration is a consequence of the

upregulation of Th2 activity, while polarization toward Th1 activity can tactfully perform viral clearance.[29-31] The Th2 cytokine IL-10 potentially impedes the functionality of the Th1 subset and results in poor convalescence in patients.[21,29] However, some studies found that, as an anti-inflammatory cytokine, deficiency of IL-10 led to increased disease severity in patients. Thus, the role of IL-10 in the orchestration of the cytokine storm remains fuzzy due to contradictory reports, and comprehensive quantification of other cytokines involved could help clinicians better understand the disease.[32] Both IL-10 and IL-4 allow the degranulation and aggregation of eosinophils and basophils in the lungs, causing severe impairment of the alveoli.[8,21,31,33] The final outcome of alveolar congestion and capillary hemorrhage becomes consolidation of the lungs.[34]

Focusing on the damage of cell-mediated immunity, it is crucial to shed light on antigen presentation and immune surveillance. Viral infection signals or presents itself to $CD8^+$ T cells through major histocompatibility complex-I (MHC-I) molecules. On recognition of the antigenic peptides, the infected host cell is targeted for destruction using perforins, granzymes, and Fas ligand (FasL), which are released by the $CD8^+$ T cells.[35] As this pathway is vital for precise viral eradication, the downregulation of antigen presentation remains an attractive target for SARS-CoV-2 infection. Studies have discovered that fighting against COVID-19 becomes even more challenging in the presence of dampened MHC-I regulation, which occurs under the effect of ORF8 viral protein through autophagy pathways. Cells exposed to ORF8 become more resistant to cytotoxic lysis, while cells with knocked-down ORF8 become sensitive to cytotoxicity. ORF8 selectively targets MHC-I for lysosomal degradation in an autophagy-mediated pathway, where ORF8 attaches to MHC-I molecules and directs them toward autophagosomes or lysosomes.[36] However, a report has been published stating the failure of ORF8 to downregulate MHC-I in the case of the Delta variant. Deletion mutations such as Asp119 and Phe120 in the Delta variant impair ORF8 dimer formation and structural instability, leading to poor affinity toward MHC-I molecules. The presence of these mutations indicates better host adaptation in presenting the SARS-CoV-2 antigen.[37] *In silico* studies also support this phenomenon by surmising the impact of the Delta variant on allele-specific-HLA-peptide-binding affinity, which has occurred in a diminished manner due to a heavy load of mutations.[38]

3.3. Immune response during the Omicron wave

The Omicron variant (B.1.1.529) has become a significant global concern in the later stages of the pandemic. Despite the presence of five sub-lineages (BA.1, BA.2, BA.3, BA.4, and BA.5) circulating within the population, the Omicron variant, in general, is associated with the highest degree of neutralizing antibody escape due to a heavy load of mutations on its spike protein.[1,39] Omicron was first recorded in Botswana, Southern Africa, and it exhibited 32 amino acid mutations in the spike protein. Reports observed that BA.1 and BA.2 display the highest level of escape from neutralization by host antibodies compared to any other sarbecoviruses, with mutations such as G339D, S371L/F, S373P, S375F, R408S, and D406N.[1]

The emergence of this variant marks a significant turning point in the immunological scenario of the pandemic. The genomic changes associated with this variant are deeply related to evolutionary circumstances, and the manifestation of these alterations has been responsible for a significant shift in the host-virus paradigm. Taking note of the evolutionary point, bats serve as the reservoir host for many sarbecoviruses. As reservoirs, bats develop an appropriate IFN-rich environment to defend themselves against sarbecovirus infection, which primes sarbecoviruses for IFN attack. Since humans lack such constitutive immune environments, infection with bat sarbecoviruses can overwhelm the human host's IFN response.[40] This environmental discrepancy in the human host has facilitated the evolution of the Omicron variant in a manner distinct from its ancestral sarbecoviruses, acquiring a significant degree of neutralizing antibody escape.[1]

The Omicron variant, in addition to its adeptness in evading immune responses, exhibits very high transmissibility, which is considered a vital evolutionary event during the pandemic.[41] The evasion pathway of Omicron differs significantly from that of Delta and Alpha variants, suggesting the possibility of a host-jumping event occurring amidst the pandemic. Initially, it was hypothesized that Omicron either spread cryptically within the human population or might have evolved in patients with compromised immune systems. However, a recent study dismisses other hypotheses and reveals that the mutations observed in the progenitor of Omicron most likely occurred in a cell of a mouse rather than humans. This phenomenon suggests a scenario where the progenitor of Omicron infected a mouse, acquired significant mutations, and then jumped back to human hosts, evolving into the Omicron variant. Thus, interspecific evolution has affected the mode of invasion of human host cells.[42] In contrast to prevailing strains where the virus targets the ACE-2 receptor as a key to access host cells, Omicron adopts an endosomal mode of entry, neglecting the function of TMPRSS2 protease. The pathway of endosomal fusion is probably facilitated by a geometric restructuring of

the S1-S2 protein cleavage site of the viral spike protein. Moreover, in addition to its infectivity, the modification of this route of infection further reduces the pathogenicity of the contagion.[43]

Summarizing the evolutionary changes, it is evident that the antibody-mediated immune response during Omicron variant infection has been rendered ineffective.[44] However, cell-mediated immune response plays a crucial role in fighting Omicron infection, with T cells being considered the primary warriors in this aspect of immunity. Notably, disease severity is significantly reduced when T cells are activated, as most of the mutations are in the spike protein, which is expected to be incapable of disrupting cell-mediated immunity.[45] In individuals previously exposed to SARS-CoV-2 infection, 70 – 80% of T cells were found to be highly cross-reactive to the Omicron variant despite its significant evasion from antibody neutralization. The distribution of SARS-CoV-2 specific T cell epitopes throughout the spike region suggests a response predominantly directed toward conserved regions, potentially limiting viral evasion from T cells.[46] However, it must not be overlooked that the Omicron variant possesses 20 additional mutations in other proteins, which may evade T cell immunity to some extent.[47] Nevertheless, the role of $CD8^+$ T cells appears promising, although studies have revealed the abolishment of $CD8^+$ recognition in 15% of individuals under Omicron infection, possibly indicating elevated clinical severity in some patients.[48] The predictions suggest that Omicron's 29 protein mutations alter human leukocyte antigen (HLA) binding and antigen presentation, resulting in changes in the affinity of 143 peptide-HLA class I pairs and 85 peptide-HLA class II pairs. Strikingly, compared to Delta, Omicron has a much greater impact on HLA-peptide binding.[38] Other reports provide data that elucidates a significant reduction in both $CD4^+$ and $CD8^+$ T cell responses, with the former showing a reduction of 14–30% and the latter showing a median reduction of 17 – 25%.[46]

Omicron presents a challenge in terms of B-cell immunity escape.[49] However, certain roles of B cells remain to be fully understood, as they may play a role in obstructing the contagion. Long before the pandemic, sequential seasonal coronavirus infections were common among the human population. Exposure to seasonal coronavirus infections led to the development of two sets of cross-reactive, resting switched memory B cells ($CD27^-$ and $CD27^+$), which existed even before Omicron infection. These memory B cells demonstrated cross-reactivity to non-RBD regions of both Omicron and the wild-type SARS-CoV-2 (Wuhan strain). Given the greater homology between the spike protein of seasonal coronaviruses and the non-RBD region of Omicron and the Wuhan strain, these compartments harbor abundant anti-spike B cells due to pre-pandemic exposure.[50]

4. Comparison of invasion mechanisms and corresponding pathological outcomes in SARS-CoV-2 variants

Over the course of the pandemic, immune response patterns have shifted in tandem with the fast evolutionary waves of new variants. Understanding the interplay between viral pathogenicity and transmissibility has been paramount for global public health. Hospitalization rates, closely correlated with pathogenicity, have served as a key epidemiological metric for tracking the trajectory of clinical severity. Communities with higher hospitalization rates often exhibit elevated levels of pathogenicity. Notably, amino acid changes in the spike protein have been associated with varying degrees of pathogenicity across different variants, with the Delta strain exhibiting maximal pathogenicity and the Omicron variant demonstrating the lowest. As previously noted, mutations in the spike protein efficiently regulate the pathogenicity and transmissibility of a variant. A study of epidemiological research carried out in Spain revealed a comprehensive comparative statistical analysis of COVID-19 waves. In comparison with the Delta variant, which peaked in clinical severity due to mutations such as L452R, T478K, and K417N, the Alpha variant demonstrated a 43% drop in hospitalization likelihood, while the Omicron variant demonstrated an even more significant 72% decrease.[51,52] From a virological standpoint, greater attention should be paid to comparing the structures of the spike proteins of each variant to better understand the pathological implications.[53,54] The viral genome of the Alpha strain contained 23 mutations, seven of which were deemed critical for the variant's phenotype,[55,56] while the spike genes of the Delta strain contained approximately 13 mutations.

On the other hand, the Omicron variant's spike protein exhibits an abnormally high number of mutations (about 32 mutations).[57,58] These mutations contribute to the increased transmissibility of the variant. Reports indicate that mutations such as D614G, H655Y, N679K, P681H, G339D, S371L, S373P, S375F, E484A, T951, and G142D are particularly responsible for enhancing the Omicron variant's transmissibility. Moreover, these mutations collectively change the Omicron variant's evasion route, rendering it more resistant to antibody neutralization than its ancestors.[41,52]

Figure 1 describes the mechanistic process of Omicron evasion, contrasting it with the approaches employed by other common VOCs. The endosomal entry pathway

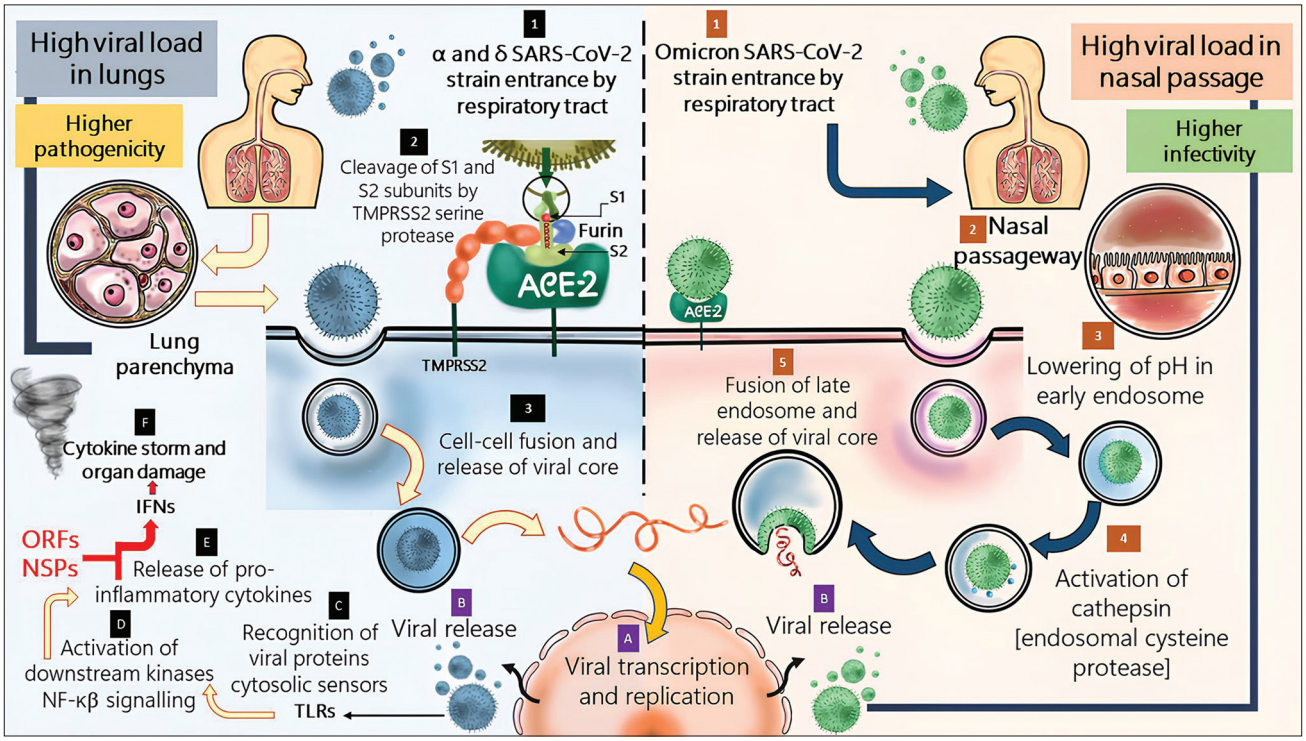

Figure 1. A comparison between the two pathways of infection by different strains of SARS-CoV-2. (1) The Alpha and Delta variants enter the body through the respiratory tract. (2) When the virus arrives at the lung parenchyma, the transmembrane protease serine 2 (TMPRSS2)-mediated entry process begins. The spike protein of the virus consists of S1 and S2 subunits, which bind to the angiotensin-converting enzyme 2 (ACE-2) receptor on the surface of the host cells. Once S2 binds to ACE-2, furin facilitates the cleavage of the S1 and S2 subunits through the activity of the cellular serine protease TMPRSS2. This pathway allows the SARS-CoV-2 virus to enter the cytosol of lung parenchyma cells. It must be noted that TMPRSS2 is a temperature-sensitive protease and is unable to function effectively in tissues with a high-temperature environment, such as the nasal passageway, which is why TMPRSS2-mediated entry is more efficient in the lung parenchyma compared to a high-temperature zone like the nasal passage, particularly for the Alpha and Delta variants of SARS-CoV-2. (3) TMPRSS2-mediated entry clears the way for cell-cell fusion, syncytium formation, and (A) viral propagation. (B) After viral propagation, (C) cytosolic toll-like receptors (TLR7/8) detect viral ribonucleic acid (RNA) and activate the (D) nuclear factor kappa B (NF-κβ) signaling pathway, activating downstream kinases. This prompts the release of (E) pro-inflammatory cytokines to combat the viral outbreak. However, SARS-CoV-2 employs a tactful strategy to inhibit the release of pro-inflammatory cytokines through viral open reading frames (ORFs) and non-structural proteins (NSPs). (F) This blockade in the release of inflammatory cytokines leads to elevated levels of interferons (IFNs) in tissues, contributing to the onset of a devastating cytokine storm that leads to severe organ damage. In contrast, in the (1) Omicron strain, the nasal passage is affected by the SARS-CoV-2 entry. (2) Upon entering nasal passage cells, the virus forms an endosome. (3) In the early endosome, the pH becomes highly acidic, contributing to (4) the activation of cathepsins, which are endosomal lysosomal cysteine proteases. (5) Cathepsins in late endosomes lead to the release of viral core into the cell and similarly lead to (A) viral propagation. (B) The propagating virus is subsequently released from the cell, causing SARS-CoV-2 infection. Figure adapted with modifications from Biswas *et al.*,[21] AbdelMassih *et al.*,[63] Willett *et al.*,[64] Pišlar *et al.*,[65] Kubo *et al.*,[66] Gomes *et al.*,[67] Hui *et al.*[61]

has replaced the ACE-2-TMPRSS2-mediated pathway, significantly altering the pathogen's mode of infection. In the earlier strains, the ACE-2 receptor, abundantly expressed in several essential human organs, allowed the virus to enter the lung parenchyma.[59] Syncytial pneumocyte development is frequently linked to severe SARS-CoV-2 infection. Cellular syncytia arise when a SARS-CoV-2-infected cell has spike protein on its surface and begins interacting with neighboring cells' ACE-2. The creation of these cellular syncytia enables the virus to initiate a new life cycle and replicate more efficiently, contributing to increased pathogenicity. Compared to the original strain, the Alpha variant produces more large-sized syncytia with higher fusogenicity, resulting in severe COVID-19 infections.[60] However, in the case of Omicron, TMPRSS2's S1-S2 cleavage is severely compromised, and entry predominantly occurs through the cellular endosomal route, which relies more on cathepsins.[61,62] Moreover, TMPRSS2 inactivity compromises the development of cellular syncytia, thereby greatly reducing the pathogenicity of the virion.[62] It is noteworthy that the site of infection can influence the severity of COVID-19. Studies suggest that the bronchi are more conducive to Omicron replication than lung parenchyma tissue. In addition, human nasal epithelial cultures exhibit higher Omicron replication rates than other common strains.[61] The lower temperature in the upper respiratory tract is crucial for maintaining the ideal acidic endolysosomal

pH. This mechanism renders the Omicron endosomal entry route temperature-sensitive, enabling more effective operation in the upper respiratory tract than the lung parenchyma, in contrast to the temperature-insensitive TMPRSS2 pathway.[63] As Omicron infection predominantly affects the upper respiratory tract, it reduces the pathogenicity of SARS-CoV-2 at this stage of the pandemic by limiting viral dissemination to other essential organs. However, despite decreased virulence, Omicron remains highly transmissible.[64] Reportedly, Omicron replication in the bronchi is 70 times higher than that of the Delta variant. It is hypothesized that increased viral replication in conducting airways might result in increased viral shedding during speaking or breathing through the nose and oral passageways, playing a major role in the airborne transmission of SARS-CoV-2.[61]

5. Conclusion

The evolutionary interplay of viral variants has extensively modified the development of corresponding immune responses in humans since the onset of the pandemic. Accumulating mutations and hypervariability in spike proteins during initial waves were associated with increased virulence and infectivity. However, as the pandemic progressed, the increasing mutations tended to decrease pathogenicity while compensating with significantly high transmissibility. This shift has enabled the human population to better manage severe clinical manifestations caused by SARS-CoV-2, leading to a normalization of social protocols globally that were disrupted by the pandemic. Therefore, a deep-rooted understanding of the evolutionary paradigms of both host and parasite systems is significant for designing effective clinical measures that address global health perspectives.

Acknowledgments

None.

Funding

None.

Conflict of interest

The authors declare no conflicts of interest.

Author contributions

Conceptualization: Chayan Munshi
Writing – original draft: Mihieka Bose
Writing – review & editing: All authors

Ethics approval and consent to participate

Not applicable.

Consent for publication

Not applicable.

Availability of data

Not applicable.

References

1. Tan CW, Chia WN, Zhu F, *et al.* SARS-CoV-2 Omicron variant emerged under immune selection. *Nat Microbiol*. 2022;7(11):1756-1761.

   doi: 10.1038/s41564-022-01246-1

2. Hou Y, Zhao J, Martin W, *et al.* New insights into genetic susceptibility of COVID-19: An ACE2 and TMPRSS2 polymorphism analysis. *BMC Med*. 2020;18(1):216.

   doi: 10.1186/s12916-020-01673-z

3. Bakhshandeh B, Jahanafrooz Z, Abbasi A, *et al.* Mutations in SARS-CoV-2; Consequences in structure, function, and pathogenicity of the virus. *Microb Pathog*. 2021;154:104831.

   doi: 10.1016/j.micpath.2021.104831

4. Mouliou DS, Gourgoulianis KI. COVID-19 'asymptomatic'patients: An old wives' tale. *Expert Rev Respir Med*. 2022;16(4):399-407.

   doi: 10.1080/17476348.2022.2030224

5. Boyton RJ, Altmann DM. The immunology of asymptomatic SARS-CoV-2 infection: What are the key questions? *Nat Rev Immunol*. 2021;21(12):762-768.

   doi: 10.1038/s41577-021-00631-x

6. Huang Y, Yang C, Xu XF, Xu W, Liu SW. Structural and functional properties of SARS-CoV-2 spike protein: Potential antivirus drug development for COVID-19. *Acta Pharmacol Sin*. 2020;41(9):1141-1149.

   doi: 10.1038/s41401-020-0485-4

7. Williams H, Hutchinson D, Stone H. Watching brief: The evolution and impact of COVID-19 variants B.1.1.7, B.1.351, P.1 and B.1.617. *Glob Biosecur*. 2021;3(1).

   doi: 10.31646/gbio.112

8. Huang C, Wang Y, Li X, *et al.* Clinical features of patients infected with 2019 novel coronavirus in Wuhan, China. *Lancet*. 2020;395(10223):497-506.

   doi: 10.1016/S0140-6736(20)30183-5

9. Acharya D, Liu G, Gack MU. Dysregulation of type I interferon responses in COVID-19. *Nat Rev Immunol*. 2020;20(7):397-398.

   doi: 10.1038/s41577-020-0346-x

10. Hsu JCC, Laurent-Rolle M, Pawlak JB, Wilen CB, Cresswell P. Translational shutdown and evasion of the innate immune response by SARS-CoV-2 NSP14 protein. *Proc Natl Acad Sci*

U S A. 2021;118(24):e2101161118.

doi: 10.1073/pnas.2101161118

11. Schoggins JW, Rice CM. Interferon-stimulated genes and their antiviral effector functions. *Curr Opin Virol*. 2011;1(6):519-525.

doi: 10.1016/j.coviro.2011.10.008

12. Murira A, Lamarre A. Type-I interferon responses: From friend to foe in the battle against chronic viral infection. *Front Immunol*. 2016;7:609.

doi: 10.3389/fimmu.2016.00609

13. Supasa P, Zhou D, Dejnirattisai W, *et al.* Reduced neutralization of SARS-CoV-2 B.1.1.7 variant by convalescent and vaccine sera. *Cell*. 2021;184(8):2201-2211.e7.

doi: 10.1016/j.cell.2021.02.033

14. Torbati E, Krause KL, Ussher JE. The immune response to SARS-CoV-2 and variants of concern. *Viruses*. 2021;13(10):1911.

doi: 10.3390/v13101911

15. Low ZY, Yip AJW, Sharma A, Lal SK. SARS coronavirus outbreaks past and present-a comparative analysis of SARS-CoV-2 and its predecessors. *Virus Genes*. 2021;57(4):307-317.

doi: 10.1007/s11262-021-01846-9

16. Kim JE, Heo JH, Kim HO, *et al.* Neurological complications during treatment of Middle East respiratory syndrome. *J Clin Neurol*. 2017;13(3):227-233.

doi: 10.3988/jcn.2017.13.3.227

17. Diao B, Wang C, Tan Y, *et al.* Reduction and functional exhaustion of T cells in patients with coronavirus disease 2019 (COVID-19). *Front Immunol*. 2020;11:827.

doi: 10.3389/fimmu.2020.00827

18. Kaneko N, Kuo HH, Boucau J, *et al.* Loss of Bcl-6-expressing T follicular helper cells and germinal centers in COVID-19. *Cell*. 2020;183(1):143-157.e13.

doi: 10.1016/j.cell.2020.08.025

19. Kumar S, Thambiraja TS, Karuppanan K, Subramaniam G. Omicron and Delta variant of SARS-CoV-2: A comparative computational study of spike protein. *J Med Virol*. 2022;94(4):1641-1649.

doi: 10.1002/jmv.27526

20. Bian L, Gao Q, Gao F, *et al.* Impact of the Delta variant on vaccine efficacy and response strategies. *Expert Rev Vaccines*. 2021;20(10):1201-1209.

doi: 10.1080/14760584.2021.1976153

21. Biswas B, Chattopadhyay S, Hazra S, Hansda AK, Goswami R. COVID-19 pandemic: The delta variant, T-cell responses, and the efficacy of developing vaccines. *Inflamm Res*. 2022;71(4):377-396.

doi: 10.1007/s00011-022-01555-5

22. Lee KS, Wong TY, Russ BP, *et al.* SARS-CoV-2 Delta variant induces enhanced pathology and inflammatory responses in K18-hACE2 mice. *PLoS one*. 2022;17(8):e0273430.

doi: 10.1371/journal.pone.0273430

23. McCallum M, De Marco A, Lempp FA, *et al.* N-terminal domain antigenic mapping reveals a site of vulnerability for SARS-CoV-2. *Cell*. 2021;184(9):2332-2347.e16.

doi: 10.1016/j.cell.2021.03.028

24. Planas D, Veyer D, Baidaliuk A, *et al.* Reduced sensitivity of SARS-CoV-2 variant Delta to antibody neutralization. *Nature*. 2021;596(7871):276-280.

doi: 10.1038/s41586-021-03777-9

25. Zheng Y, Zhuang MW, Han L, *et al.* Severe acute respiratory syndrome coronavirus 2 (SARS-CoV-2) membrane (M) protein inhibits type I and III interferon production by targeting RIG-I/MDA-5 signaling. *Signal Transduct Target Ther*. 2020;5(1):299.

doi: 10.1038/s41392-020-00438-7

26. Blanco-Melo D, Nilsson-Payant BE, Liu WC, *et al.* Imbalanced host response to SARS-CoV-2 drives development of COVID-19. *Cell*. 2020;181(5):1036-1045.e9.

doi: 10.1016/j.cell.2020.04.026

27. Hong MZ, Qiu R, Chen W, *et al.* Different clinical features of children and adults in regional outbreak of Delta COVID-19. *BMC Infect Dis*. 2022;22(1):728.

doi: 10.1186/s12879-022-07707-6

28. Zanza C, Romenskaya T, Manetti AC, *et al.* Cytokine storm in COVID-19: Immunopathogenesis and therapy. *Medicina (Kaunas)*. 2022;58(2):144.

doi: 10.3390/medicina58020144

29. Gil-Etayo FJ, Suàrez-Fernández P, Cabrera-Marante O, *et al.* T-helper cell subset response is a determining factor in COVID-19 progression. *Front Cell Infect Microbiol*. 2021;11:624483.

doi: 10.3389/fcimb.2021.624483

30. Neidleman J, Luo X, Frouard J, *et al.* SARS-CoV-2-specific T cells exhibit phenotypic features of helper function, lack of terminal differentiation, and high proliferation potential. *Cell Rep Med*. 2020;1(6):100081.

doi: 10.1016/j.xcrm.2020.100081

31. Roncati L, Nasillo V, Lusenti B, Riva G. Signals of T_h2 immune response from COVID-19 patients requiring intensive care. *Ann Hematol*. 2020;99(6):1419-1420.

doi: 10.1007/s00277-020-04066-7

32. Elbadawy HM, Khattab A, El-Agamy DS, *et al.* IL-6 at the center of cytokine storm: Circulating inflammation mediators as biomarkers in hospitalized COVID-19 patients.

J Clin Lab Anal. 2023;37(7):e24881.

doi: 10.1002/jcla.24881

33. Weiskopf D, Schmitz KS, Raadsen MP, *et al.* Phenotype and kinetics of SARS-CoV-2-specific T cells in COVID-19 patients with acute respiratory distress syndrome. *Sci Immunol*. 2020;5(48):eabd2071.

doi: 10.1126/sciimmunol.abd2071

34. Geng J, Chen L, Yuan Y, *et al.* CD147 antibody specifically and effectively inhibits infection and cytokine storm of SARS-CoV-2 and its variants Delta, Alpha, Beta, and Gamma. *Signal Transduct Target Ther*. 2021;6(1):347.

doi: 10.1038/s41392-021-00760-8

35. Berke G. The CTL's kiss of death. *Cell*. 1995;81(1):9-12.

doi: 10.1016/0092-8674(95)90365-8

36. Zhang Y, Chen Y, Li Y, *et al.* The ORF8 protein of SARS-CoV-2 mediates immune evasion through down-regulating MHC-I. *Proc Natl Acad Sci U S A*. 2021;118(23):e2024202118.

doi: 10.1073/pnas.2024202118

37. Chaudhari AM, Singh I, Joshi M, Patel A, Joshi C. Defective ORF8 dimerization in SARS-CoV-2 delta variant leads to a better adaptive immune response due to abrogation of ORF8-MHC1 interaction. *Mol Divers*. 2023;27(1):45-57.

doi: 10.1007/s11030-022-10405-9

38. Augusto DG, Hollenbach JA. HLA variation and antigen presentation in COVID-19 and SARS-CoV-2 infection. *Curr Opin Immunol*. 2022;76:102178.

doi: 10.1016/j.coi.2022.102178

39. Dhawan M, Saied AA, Emran TB, Choudhary OP. Emergence of Omicron variant's sublineages BA.4 and BA.5: Risks assessment and possible countermeasures. *New Microbes New Infect*. 2022;48:100997.

doi: 10.1016/j.nmni.2022.100997

40. Schountz T, Baker ML, Butler J, Munster V. Immunological control of viral infections in bats and the emergence of viruses highly pathogenic to humans. *Front Immunol*. 2017;8:1098.

doi: 10.3389/fimmu.2017.01098

41. Dhawan M, Saied AA, Mitra S, Alhumaydhi FA, Emran TB, Wilairatana P. Omicron variant (B.1.1.529) and its sublineages: What do we know so far amid the emergence of recombinant variants of SARS-CoV-2? *Biomed Pharmacother*. 2022;154:113522.

doi: 10.1016/j.biopha.2022.113522

42. Wei C, Shan KJ, Wang W, Zhang S, Huan Q, Qian W. Evidence for a mouse origin of the SARS-CoV-2 Omicron variant. *J Genet Genomics*. 2021;48(12):1111-1121.

doi: 10.1016/j.jgg.2021.12.003

43. Fantini J, Yahi N, Colson P, Chahinian H, La Scola B, Raoult D. The puzzling mutational landscape of the SARS-2-variant Omicron. *J Med Virol*. 2022;94(5):2019-2025.

doi: 10.1002/jmv.27577

44. Goutam Mukherjee A, Ramesh Wanjari U, Murali R, *et al.* Omicron variant infection and the associated immunological scenario. *Immunobiology*. 2022;227(3):152222.

doi: 10.1016/j.imbio.2022.152222

45. May DH, Rubin BE, Dalai SC, *et al.* Immunosequencing and epitope mapping reveal substantial preservation of the T cell immune response to Omicron generated by SARS-CoV-2 vaccines. *medRxiv*. 2021.

doi: 10.1101/2021.12.20.21267877

46. Keeton R, Tincho MB, Ngomti A, *et al.* T cell responses to SARS-CoV-2 spike cross-recognize Omicron. *Nature*. 2022;603(7901):488-492.

doi: 10.1038/s41586-022-04460-3

47. Grifoni A, Sidney J, Vita R, *et al.* SARS-CoV-2 human T cell epitopes: Adaptive immune response against COVID-19. *Cell Host Microbe*. 2021;29(7):1076-1092.

doi: 10.1016/j.chom.2021.05.010

48. Naranbhai V, Nathan A, Kaseke C, *et al.* T cell reactivity to the SARS-CoV-2 Omicron variant is preserved in most but not all individuals. *Cell*. 2022;185(6):1041-1051.e6.

doi: 10.1016/j.cell.2022.01.029

49. Barros-Martins J, Hammerschmidt SI, Morillas Ramos G, *et al.* Omicron infection-associated T-and B-cell immunity in antigen-naive and triple-COVID-19-vaccinated individuals. *Front Immunol*. 2023;14:1166589.

doi: 10.3389/fimmu.2023.1166589

50. Perugino CA, Liu H, Feldman J, *et al.* Preferential expansion upon boosting of cross-reactive "pre-existing" switched memory B cells that recognize the SARS-CoV-2 Omicron variant Spike protein. *medRxiv*. 2022.

doi: 10.1101/2021.12.30.21268554

51. Varea-Jiménez E, Cano EA, Vega-Piris L, *et al.* Comparative severity of COVID-19 cases caused by Alpha, Delta or Omicron SARS-CoV-2 variants and its association with vaccination. *Enferm Infecc Microbiol Clín (Engl Ed)*. 2022:S2529-993X(23)00039-4.

doi: 10.1016/j.eimce.2022.11.021

52. Dhawan M, Sharma A, Priyanka N, Thakur N, Rajkhowa TK, Choudhary OP. Delta variant (B.1.617.2) of SARS-CoV-2: Mutations, impact, challenges and possible solutions. *Hum Vaccin Immunother*. 2022;18(5):2068883.

doi: 10.1080/21645515.2022.2068883

53. Meng B, Kemp SA, Papa G, *et al.* Recurrent emergence of SARS-CoV-2 spike deletion H69/V70 and its role in the

Alpha variant B.1.1.7. *Cell Rep.* 2021;35(13):109292.

doi: 10.1016/j.celrep.2021.109292

54. Zhang J, Xiao T, Cai Y, *et al.* Membrane fusion and immune evasion by the spike protein of SARS-CoV-2 Delta variant. *Science*. 2021;374(6573):1353-1360.

doi: 10.1126/science.abl9463

55. Sanches PRS, Charlie-Silva I, Braz HLB, *et al.* Recent advances in SARS-CoV-2 Spike protein and RBD mutations comparison between new variants Alpha (B.1.1.7, United Kingdom), Beta (B.1.351, South Africa), Gamma (P.1, Brazil) and Delta (B.1.617.2, India). *J Virus Erad*. 2021;7(3):100054.

doi: 10.1016/j.jve.2021.100054

56. Lubinski B, Fernandes MHV, Frazier L, *et al.* Functional evaluation of the P681H mutation on the proteolytic activation of the SARS-CoV-2 variant B.1.1.7 (Alpha) spike. *iScience*. 2022;25(1):103589.

doi: 10.1016/j.isci.2021.103589

57. Gupta AM, Chakrabarti J, Mandal S. Non-synonymous mutations of SARS-CoV-2 leads epitope loss and segregates its variants. *Microbes Infect*. 2020;22(10):598-607.

doi: 10.1016/j.micinf.2020.10.004

58. Vitiello A, Ferrara F, Auti AM, Di Domenico M, Boccellino M. Advances in the Omicron variant development. *J Intern Med*. 2022;292(1):81-90.

doi: 10.1111/joim.13478

59. Li MY, Li L, Zhang Y, Wang XS. Expression of the SARS-CoV-2 cell receptor gene ACE2 in a wide variety of human tissues. *Infect Dis Poverty*. 2020;9(1):45.

doi: 10.1186/s40249-020-00662-x

60. Rajah MM, Hubert M, Bishop E, *et al.* SARS-CoV-2 Alpha, Beta, and Delta variants display enhanced Spike-mediated syncytia formation. *EMBO J*. 2021;40(24):e108944.

doi: 10.15252/embj.2021108944

61. Hui KPY, Ho JCW, Cheung MC, *et al.* SARS-CoV-2 Omicron variant replication in human bronchus and lung *ex vi*vo. *Nature*. 2022;603(7902):715-720.

doi: 10.1038/s41586-022-04479-6

62. Meng B, Abdullahi A, Ferreira IAT, *et al.* Altered TMPRSS2 usage by SARS-CoV-2 Omicron impacts infectivity and fusogenicity. *Nature*. 2022;603(7902):706-714.

doi: 10.1038/s41586-022-04474-x

63. AbdelMassih A, Sedky A, Shalaby A, *et al.* From HIV to COVID-19, molecular mechanisms of pathogens' trade-off and persistence in the community, potential targets for new drug development. *Bull Natl Res Cent*. 2022;46(1):194.

doi: 10.1186/s42269-022-00879-w

64. Willett BJ, Grove J, MacLean OA, *et al.* SARS-CoV-2 Omicron is an immune escape variant with an altered cell entry pathway. *Nat Microbiol*. 2022;7(8):1161-1179.

doi: 10.1038/s41564-022-01143-7

65. Pišlar A, Mitrović A, Sabotič J, *et al.* The role of cysteine peptidases in coronavirus cell entry and replication: The therapeutic potential of cathepsin inhibitors. *PLoS Pathog*. 2020;16(11):e1009013.

doi: 10.1371/journal.ppat.1009013

66. Kubo Y, Hayashi H, Matsuyama T, Sato H, Yamamoto N. Retrovirus entry by endocytosis and cathepsin proteases. *Adv Virol*. 2012;2012:640894.

doi: 10.1155/2012/640894

67. Gomes CP, Fernandes DE, Casimiro F, *et al.* Cathepsin L in COVID-19: From pharmacological evidences to genetics. *Front Cell Infect Microbiol*. 2020;10:589505.

doi: 10.3389/fcimb.2020.589505

ACCSCIENCE PUBLISHING

Global Translational Medicine

REVIEW ARTICLE

The dawn of personalized multi-omics: Detecting disease before you know it

Filip Mundt Madsen[1,2]*

[1]Novo Nordisk A/S, Novo Nordisk Park, DK-2760 Måløv, Denmark

[2]Novo Nordisk Foundation Center for Protein Research, Faculty of Health and Medical Sciences, University of Copenhagen, Copenhagen, Denmark

Abstract

Recent advancements in omics techniques have enabled deep profiling of an individual's molecular makeup. The wealth of data produced offers insights into genetic predispositions, early disease markers, and personalized treatment strategies. However, the full potential of omics data emerges when combined into longitudinal and personal multi-omics space. Another interesting venue is the inclusion of continuous monitoring of physiological parameters through wearable technology. Wearable health devices, including smartwatches and biosensors, provide real-time data on heart rate, oxygen saturation, sleep patterns, activity levels, and much more. By integrating with omics data, wearables offer a comprehensive view of an individual's health, allowing for early detection of deviations from normalcy. This convergence allows for the prediction and prevention of diseases at the individual level and provides a powerful monitoring tool in clinical and drug developmental settings. This review explores the fusion of omics and wearable technology, envisioning their synergy as a catalyst for a transformative shift in modern healthcare. Their merging enables predictive and personalized medicine. As these technologies continue to evolve, their translation into routine clinical practice holds the promise of a healthier future for all. Provided herein is a step-by-step vision for how longitudinal personalized multi-omics, combined with wearable devices, will guide proactive healthcare and transform drug discovery in translational medicine.

Keywords: Genomics; Proteomics; Metabolomics; Multi-omics; Wearable health technology; Precision medicine; Personalized medicine; Translational medicine

***Corresponding author:**
Filip Mundt Madsen
(FPMN@novonordisk.com)

Citation: Madsen FM. The dawn of personalized multi-omics: Detecting disease before you know it. *Global Transl Med.* 2024;3(1):2357. https://doi.org/10.36922/gtm.2357

Received: December 2, 2023
Accepted: January 31, 2024
Published Online: March 25, 2024

1. Introduction

Precision medicine, a medical field that encompasses personalized medicine, is gaining substantial attention today. It aims to provide tailored health-care solutions based on an individual's unique molecular makeup, lifestyle, and environment. Since its inception, the approach has been revolutionizing medical research, leading to more effective treatments, drug discovery, and better health outcomes for patients.

In this paper, the potential for how personalized multi-omics and wearable health technologies could further develop precision medicine is reviewed. Omics and multi-omics are first introduced, followed by a section regarding wearable health trackers. A vision will be presented on how the integration of these two technologies could lead

to a new era of personalized medicine. The vision will be exemplified through the involvement of an imaginary participant in a randomized clinical trial, seamlessly monitored with wearable technologies, and the analysis with longitudinal, personal multi-omics.

2. Omics and multi-omics

Despite the impressive advancements, the modern molecular medicine approach has been utilized to study only a small fraction of human genes, leaving many understudied proteins in the "dark proteome."[1] However, omics-like technologies constitute a paradigm shift by providing a more comprehensive molecular picture of biological systems.

The first draft of the Human Genome Project in the early 2000s marked a transformative moment in genomics and systems biology as a whole. Spearheaded by the Human Genome Organization, it provided a comprehensive catalog of human genes and laid the foundation for large-scale omics investigations.[2] Subsequent initiatives such as The Cancer Genome Atlas leveraged the same genomic technologies to explore the underpinnings of cancer, demonstrating the feasibility of clinical omics research.[3-5] The TCGA project has significantly advanced our understanding of cancer, and TCGA's comprehensive cancer genomic maps have accelerated precision medicine in cancer research and treatment. These successes foreshadowed a multitude of other initiatives aimed at unraveling the omics landscape of diverse diseases and conditions. Initiatives such as the Genotype-Tissue Expression (GTEx) project[6] and the International Human Epigenome Consortium (IHEC)[7] further expanded the scope of omics research. GTEx, focusing on diverse tissue gene expressions, uncovered general principles of gene regulation and splicing across tissues. Complementarily, IHEC provided epigenetic profiles across diverse cell types, elucidating how DNA methylation and histone marks influence gene regulation. Current trends are pushing our methodologies towards single-cell analyses in all divisions of systems biology.[8]

In parallel, the emergence of the Clinical Proteomic Tumor Analysis Consortium (CPTAC), which was built upon the foundational work of TCGA, exemplifies the cooperative spirit and strength of multi-omics and systems biology. CPTAC, heavily based on mass spectrometry-based proteomics, has added layers of molecular information on top of genomic and transcriptomic profiles. This has led to unique proteomic (and proteogenomic) signatures of colorectal,[9] breast[10] and ovarian cancers,[11] identified novel therapeutic targets in lung adenocarcinoma,[12] and revealed phosphoproteome-based mechanisms of drug resistance in breast cancer,[13] and novel targets in medulloblastoma,[14] ultimately enhancing precision medicine approaches in cancer treatment. There are many proteomics groups globally that have pioneered and driven the advent of mass spectrometry-based proteomics and the characterization of post-translational modifications.[15-20] The inclusion of proteomics, post-translational modifications, and metabolomics[21-23] are slowly bridging the gap between the genotype and the phenotype, providing invaluable insights into the dynamic molecular processes underlying health and diseases.

Recent translational initiatives have utilized quantitative proteomics to pinpoint candidate serum biomarkers for drug-induced liver injury in humans. These efforts have successfully identified highly discriminative biomarkers, boasting area under the curves ranging from 0.94 to 0.99, underscoring their capacity to efficiently distinguish drug-induced liver injury from healthy samples.[24] Similar machine learning models have effectively identified noninvasive proteomics biomarker panels, surpassing the accuracy of current clinical assays in staging alcohol-related liver disease.[25] There have also been monumental efforts made, where more than 50,000 individual biosamples were analyzed with genomics and proteomics to unravel novel genetic variants influencing plasma protein abundance, providing a rich resource for drug discovery and for understanding proteogenomic mechanisms.[26-28] Other studies have used modified-aptamer proteomics, an alternative proteomic technology, to identify diagnostic signatures of non-alcoholic fatty liver disease in serum samples. The models developed could be used to test treatment response and identify novel targets for evaluation in the pathogenesis of non-alcoholic fatty liver disease.[29] These examples are just the tip of the proverbial iceberg, and the literature of novel clinical signatures based on omics techniques is vast, with new applications continually accumulating.

3. The maturation of omics techniques

The maturation of omics techniques over the past few decades has been nothing short of remarkable. This evolution has been characterized by significant advancements in several key aspects, including robustness, increased resolution, high throughput, the development of sophisticated statistical tools, and a substantial reduction in costs. These collective improvements have not only enhanced our ability to generate comprehensive molecular data but have also, to some extent, democratized access to these powerful tools, opening doors to a wider range of research and applications.[30] One of the foremost achievements in the maturation of many omics techniques is the substantial increase in robustness. Early iterations of

these technologies were often plagued by issues such as low reproducibility and sensitivity. Today, robust experimental protocols, standardized workflows, and improved instrumentation have mitigated many of these challenges. Researchers can now generate reliable and consistent data, enabling meaningful comparisons across experiments and laboratories.[31]

The depth of omics analysis has expanded exponentially. In genomics, for instance, the advent of next-generation sequencing platforms has facilitated the sequencing of entire genomes, including regions previously considered "dark matter" due to their inaccessibility. Similarly, advancements in proteomics, metabolomics, lipidomics and other omics domains have enabled the detection and quantification of a broader range of molecules with greater sensitivity. As an illustrative example, the profiling of the plasma proteome has advanced from the determination of a few hundred proteins to the quantification of several thousands of proteins in less than a decade.[26,32,33] An increase in depth is also an increase in sensitivity, and the evolution of omics techniques has also made them increasingly adaptable to low-input material samples, conserving priceless clinical materials and allowing analyses previously impossible due to limited sample materials.[34,35] This evolution has, for example, opened up for the utilization of dried blood spots, which is a minimally invasive sample collection method only involving a few drops of blood applied onto filter paper and then dried.[36] This approach allows for the analysis of nucleic acids, proteins, metabolites and other biomolecules from small, easily obtainable blood samples. The ability to work with modest input material has far-reaching implications, facilitating studies in remote or resource-limited settings, pediatric research and population-scale omics investigations, ultimately making the benefits of personalized medicine more accessible to diverse populations. Like the increased depth, a current increase in throughput now allows for tens of thousands of samples for a genomics study and even a thousand samples for metabolomics and proteomics. These numbers will soon be surpassed – indeed if they have not been already.[26,28,37]

Generating impressive data are a lot less impressive if they are beyond our comprehension. Therefore, continued development of statistical techniques is required to process and analyze the tidal wave of data points generated from each experiment. Bioinformatics and data science have long since become indispensable players in omics research. Within this dynamic landscape, innovative techniques such as machine learning[38] and artificial intelligence (AI) have risen to prominence in the way we interpret and utilize omics data. Specifically, large language models used in natural language processing, such as BERT and GPT, have the potential to be applied to bioinformatics problems, including genomics, transcriptomics, proteomics, drug discovery, and single-cell analysis.[39] New bioinformatics tools continue to emerge and evolve to deepen our understanding of the omics landscape,[40,41] showcasing the dynamic of this field.

Perhaps one of the most transformative aspects of omics techniques maturation has been the significant reduction in costs. What were once prohibitively expensive endeavors have become increasingly accessible to researchers and clinicians alike. Economies of scale, competition among technology providers and advancements in automation have all contributed to making omics analyses more affordable. This cost-efficiency has democratized access to these techniques and has kick-started their integration into research, routine healthcare, and personalized medicine.

As omics techniques continue to mature, their impact on science, medicine, and society at large is poised to also grow. The convergence of robustness, increased depth, high throughput, advanced statistical tools, and cost-efficiency has set the stage for personalized omics-based approaches that have the potential to revolutionize healthcare, diagnosis, treatment, and our understanding of the molecular underpinnings of health and disease.

4. Wearable health trackers: Pioneering predictive and diagnostic healthcare

Another emerging area of modern medicine is the inclusion of wearable medical devices that offer a novel potential for health research, a niche that has been gaining popularity due to their noninvasive nature, affordability, and improved accuracy.[42-44] They provide insights into many health fields since they can measure diverse health parameters, including gastrointestinal activity for predicting diseases such as ileus,[45] ultraviolet (sun) exposure for skin health,[46] and electrolyte levels for conditions such as cystic fibrosis;[47] and allow early detection of atrial fibrillation and other heart conditions,[48] continuous electrocardiogram monitoring,[49] determination of noninvasive blood glucose levels,[50] smart inhaler usage for asthma management,[51] activity tracking for fitness, sleep patterns profiling, assessment of environmental exposures, and more.[52] Wearable health trackers have, in their own right, also ushered in a new era of personalized healthcare, offering continuous monitoring and the potential to predict and diagnose a range of conditions. Health-care providers can remotely monitor patient data, allowing for timely interventions and reducing the need for frequent in-person visits. These devices, which encompass smartwatches, fitness trackers, smart rings, hearables, smart clothing and more, have transcended their

initial roles as fitness companions to become valuable tools in the early detection and management of various health issues. Innovatively, proteomics techniques show promise when connected to biosensors for monitoring the efficacy of skin graft transplantation.[53]

By leveraging advanced sensors and AI algorithms, these devices can identify subtle deviations from established baselines, often before symptoms manifest. Many wearable technologies incorporate machine learning and AI-based algorithms to interpret and report the collected data. To date, the U.S. Food and Drug Administration (FDA) has approved several hundred AI-enabled medical devices, including wearable health trackers.[54]

These novel measuring techniques are here to stay, and a canopy of interesting examples of where wearable devices aid in diagnosis are being presented – whether for monitoring post-stroke patients' activity in different environments and providing valuable insights for care plans[55] or for augmenting type 1 diabetes sensing,[56] some devices incorporate skin temperature sensors that can be used to detect fever, a potential sign of infection.[57] Cardiac functions can also be measured with similar accuracy to electrocardiography (ECG) with in-ear wearables using infrasonic hemodynography.[58] Another well-tested system is remote photoplethysmography (PPG), which is a noninvasive technique that uses a camera to measure changes in blood volume in the skin, providing an indirect measurement of heart rate and other physiological parameters.[48,59] This technology has numerous applications, including telemedicine, sports and fitness monitoring, as well as sleep tracking. Using machine learning coupled with cloud computing allowed the detection of cardiovascular disease (CVD) based on PPG signals with an accuracy of 99.5%,[60] and there is already a company using remote PPG (rPPG) for telemedicine, working together with the National Health Service in the United Kingdom.[61]

As of now, one of the most prominent wearable monitoring technology is a continuous glucose monitor (CGM), a device that measures glucose levels in real time. CGM devices are minimally invasive, with a short needle inserted in the arm, constituting a glucose sampler connected to a battery and transmitter that communicates with a smart device to provide diabetes sufferers with a more comprehensive understanding of their blood sugar fluctuations. Time in range has gradually emerged as a key blood glucose metric, providing an additional layer of information that is "beyond HbA1c" for a deeper insight into glycemic control in diabetic individuals.[62] CGMs can help individuals make informed decisions about their diet, exercise, and insulin dosing, contributing to better diabetes management and improved health outcomes. In addition, CGMs can alert users to dangerous blood sugar levels, allowing for prompt intervention and potentially preventing serious complications.[50,63] In theory, the technique on which CGM is based could be tailored to measure any biomarker of interest or sets of biomarkers, adding a deeper clinical depth to wearable devices. Serum lactate has been identified as a marker of hypoxia and can also serve as a potential biomarker for diagnosis of NAFLD stage,[64] and a glucose-lactate analyzer has been developed.[65] Another expansive and important area being investigated is the ECG functionality in smartwatches, which can provide valuable insights into heart health, aiding the early detection of arrhythmias and other cardiac conditions. Apple's Series 4 watch received clearance from the FDA in 2018 for its ECG app[66] and enables users to monitor their heart rhythm and detect any irregularities, a feature that is now included in all Apple's smartwatches. Samsung, Garmin, and Withing's ScanWatch have all followed suit with the FDA.[67] Omron, a well-known blood pressure monitor provider, has now developed an innovative wearable blood pressure monitor wristwatch, which is clinically accurate and is registered with the FDA as a medical device.[68]

One of the most promising aspects of wearable trackers is their ability to predict health events. By analyzing data trends, machine learning models can identify patterns associated with specific conditions. Irregular heart rate patterns may signal the onset of cardiac arrhythmias, while changes in sleep duration and quality can hint at sleep disorders or compose early signs of neurodegeneration. This predictive power enables individuals and healthcare providers to take proactive measures to mitigate health risks. In a notable application of smart rings, the technology demonstrated its potential by accurately detecting early signs of COVID-19 infection almost 3 days before a positive test result in a large cohort of more than 60,000 participants.[69] In fact, a scoping review described more than 20 different types of wearable technology that can be used to detect COVID-19 infections early, with reported accuracy values ranging from 75% to 94.4%.[70] However, further research is needed to validate the effectiveness and clinical dependability of wearable technology before it can be used widely for remote surveillance. This underscores the instrumental role of participant-co-designed digital tools in healthcare advancement, particularly in early detection and proactive health monitoring. In addition, recent advancements in proteomics allowed for the analysis of 180 samples/day, and the stratification of COVID severity on a protein level.[71] One cannot help to think about the implications for COVID research if wearable technology was augmented by ultra-rapid proteomic analyses for precision medicine.

The integration of wearable technology into clinical settings is currently being discussed for its potential scalability. In fact, clinical trials have a long history of incorporating wearable technology, even before the advent of modern wearables. Devices such as continuous heart monitors, oxygen saturation monitors, and other traditional health tools have been essential for data collection. They enable the seamless tracking of vital signs, activity levels, medication adherence, and symptom progression, significantly enhancing the quality and efficiency of clinical trials. Wearable tech furthermore minimizes the need for frequent in-person visits, reducing the burden on participants and making trials more accessible to diverse populations. The expanded use of digital tools available to measure and monitor health parameters is one key enabler to decentralized clinical trials, where those tools are used for recruitment, for example, screening, to safety monitoring and outcome measures.[72] Wearable devices offer the potential in early detection of adverse events, which aids in improving patient safety and enhancing accuracy of trial results, thereby enriching the clinical trial experience.

5. Challenges and future directions

While the promise of true personalized medicine is tantalizing, several challenges remain. Patient compliance over time, data privacy, ethical considerations, data integrity and ownership, robust data generation, and the need for robust data integration platforms are among the key hurdles to overcome. Accidental findings are a palpable risk that needs to be handled upfront and ahead of time.[30,73] When undergoing the comprehensive evaluation outlined herein, there is a possibility that previously unknown health risks, such as cancer, as well as other variables such as pregnancy or illicit drug use may be, detected. It is important to note that the participant may not have requested nor wish to know such information and certainly may not want others to be privy to it. We also need to be able to understand the complex data that is generated to achieve robustness, precision, and interpretability—by no means a simple or trivial feat, and we are still a long way from standardized bioinformatic solutions. This ties into data FAIRification (making data Findable, Accessible, Interoperable, and Reusable),[74] which is another challenge to overcome. The generation of extensive multi-omics data yields limited benefits if such datasets lack standardization, comparability, thorough annotation, and easy accessibility, hindering their integration and reuse.[75] Furthermore, integrating such rich and complex data into routine clinical practice necessitates a shift in medical education, research, and health-care infrastructure, not to mention the validation and the development of robust guidelines. The teaching of these novel techniques to health care providers is underway, but there is still a long way to go. It is crucial to consider integrating omics analysis and interpretation into medical education, as it is becoming increasingly important to align curricula with evolving technologies. This highlights the need to recognize the essential role of data science and AI in healthcare and incorporate these disciplines into academic portfolios. By doing so, we can ensure a comprehensive and future-ready approach to medical training.

In addition, these technologies come with an upfront price tag that might seem unsurmountable for many strained health-care systems. However, as has already been mentioned, these techniques are becoming more economically sustainable with their advancements. Furthermore, an upfront investment might save a large sum of money downstream, exemplified by many prophylactic measures implemented in public health and screening programs.[76] With that being said, and as just one illustrative example, fewer than one in four individuals with or at risk of CVD in the U.S. use wearable devices, with older age, lower educational attainment and lower household income associated with lower likelihoods of use. Strategies are needed to ensure equitable adoption to avoid exacerbating disparities.[77]

It is important to highlight that we will probably resolve the technical challenges in the near future, but addressing the ethical and societal challenges will require further considerations of multiple stakeholders from research, governments, health-care providers, private sector, patients, *etc.* and dedicated funding and development of solutions that limit the risks and protect the individuals.

Extending beyond diagnostics and monitoring, in true personalized medicine, therapies are meticulously crafted based on an individual's personal and longitudinal data. For example, cancer treatments can be customized to target specific genetic mutations[78] or protein signatures that change during progression of the disease,[79,80] maximizing efficacy while minimizing side effects. Similarly, medications for chronic conditions can be optimized to match an individual's metabolism and response, ensuring the best possible outcomes. Going beyond diagnosis to predicting treatments is a huge leap, which needs considerable effort from medical research fields.

In summary, the era of personalized diagnostics and treatments represents a transformative shift in healthcare. While challenges in data privacy, ethical considerations and integration persist, the prospect of tailoring therapies to an individual's molecular blueprint holds promise. Overcoming hurdles in education, infrastructure and cost will be crucial for realizing the full potential of personalized

medicine, offering a paradigm shift toward more effective and efficient healthcare.

6. Envisioned future in healthcare: a convergence of multi-omics characterization and wearable technology

Here, in the last part of this review, I would like to preface with a summary of some existing pioneering work merging personalized multi-omics and wearable health technologies. Afterward, I will conclude by envisioning the inclusion of these technologies into clinical trials for improved outcomes.

Personalized medicine is at the forefront of the current medical revolution. Rather than relying on population-based reference ranges, diagnostics has the potential to now consider an individual's baseline profile. This enables the detection of deviations from one's unique molecular profile, flagging potential health issues long before clinical symptoms manifest. This is all exemplified by the integrated Personal Omics Profiling (iPOP) studies where researchers at Stanford University conducted a comprehensive and longitudinal analysis on individuals. Their proof-of-principle study involved a single, relatively healthy individual who was analyzed with whole-genome sequencing, transcriptomics, proteomics, metabolomics, and autoantibody profiles over time. The analyses revealed the individuals' medical risks, such as type 2 diabetes and dynamic molecular changes across health and disease states (during two viral infections), emphasizing the importance of combining genomic information with continuous physiological monitoring for personalized medicine, and the significance of personal baseline characterization.[81] In a follow-up study, the researchers explored the use of portable biosensors to monitor human physiology during different activities. The biosensors measured three physiological parameters (heart rate, skin temperature, and peripheral capillary oxygen saturation), six activity-related parameters (sleep, steps, walking, biking, running, and calories), weight, and total gamma and X-ray radiation exposure. By collecting over 250,000 daily measurements from the biosensors of multiple individuals, it uncovered personalized circadian variations and significant physiological changes in specific environments, such as airline flights. These biosensors also helped in identifying early signs of diseases like Lyme disease and distinguishing between insulin-sensitive and -resistant individuals, indicating their potential for managing health and improving healthcare access.[82] In yet another follow-up iPOP study, they monitored approximately 100 individuals at risk for diabetes mellitus and aimed to establish a foundation for precision personalized medicine by deeply profiling biochemical and physiological data in both healthy and ill states. The study encompasses whole genomics, transcriptomics, proteomics, methylomics and metabolomics as well as microbiome information. It also considers lifestyle factors, such as diet, stress and activity levels, along with wearable device (including CGM) data for tracking physiology and activity. The research aimed to characterize normal health at a molecular level, detect early disease indicators and potentially enable early disease prediction and prevention. The study discovered more than 67 clinically actionable health deviations, developed prediction models for insulin resistance and identified multiple molecular pathways associated with metabolic, cardiovascular and even oncologic pathophysiology. Interestingly, the predictive models to assess insulin resistance were built on omics measurements and demonstrate the possibility of replacing some clinical tests that today are rather laborious.[83] However, since current healthcare practices can be limited in collecting clinical material in a longitudinal fashion, the team adopted a Mitra device, a micro-sampler that conveniently collected capillary fingerpick blood. This enabled frequent and dense multi-omics micro-sampling in 10 μL of blood alongside physiological information from wearable sensors. From these restrictive biosamples, the team analyzed shallow proteomes, lipidomes and metabolomes. In this study, they investigated the effect of a complex nutritional shake on metabolic profiles, and performed a dense 24/7 profiling (98 microsamples) over 7 days. In the first part, after data cleaning and annotation, 769 analytes were detected from microsamples, including 560 metabolites, 155 lipids and 54 cytokines/hormones. The metabolic response to the shake was seen across all classes of molecules and each participant had a unique molecular profile, indicating high inter-individual variability in the metabolism of nutrients. In the second part of the study, a single participant collected blood microsamples every 1 – 2 h over 7 days, along with wearable data from a smartwatch, a CGM, and food logging using an app. Ninety-eight microsamples were collected from the individual and used for multi-omics profiling, which generated outcomes for 2,213 analytes and 214,661 biochemical measurements, along with wearable physiological data, providing comprehensive data on human physiome and lifestyle. In this part of the study, they found that high-frequency internal multi-omics data can monitor and reflect the participant's health status and that wearable data can predict internal molecular changes on an hourly scale at an individual level, including building predictive models. The study also identified circadian rhythms of internal molecules in human blood and revealed rhythmic molecules and demonstrated that lipids related to energy metabolism have distinct circadian patterns. Figure 1 provides an overview of the iPOP study.[84]

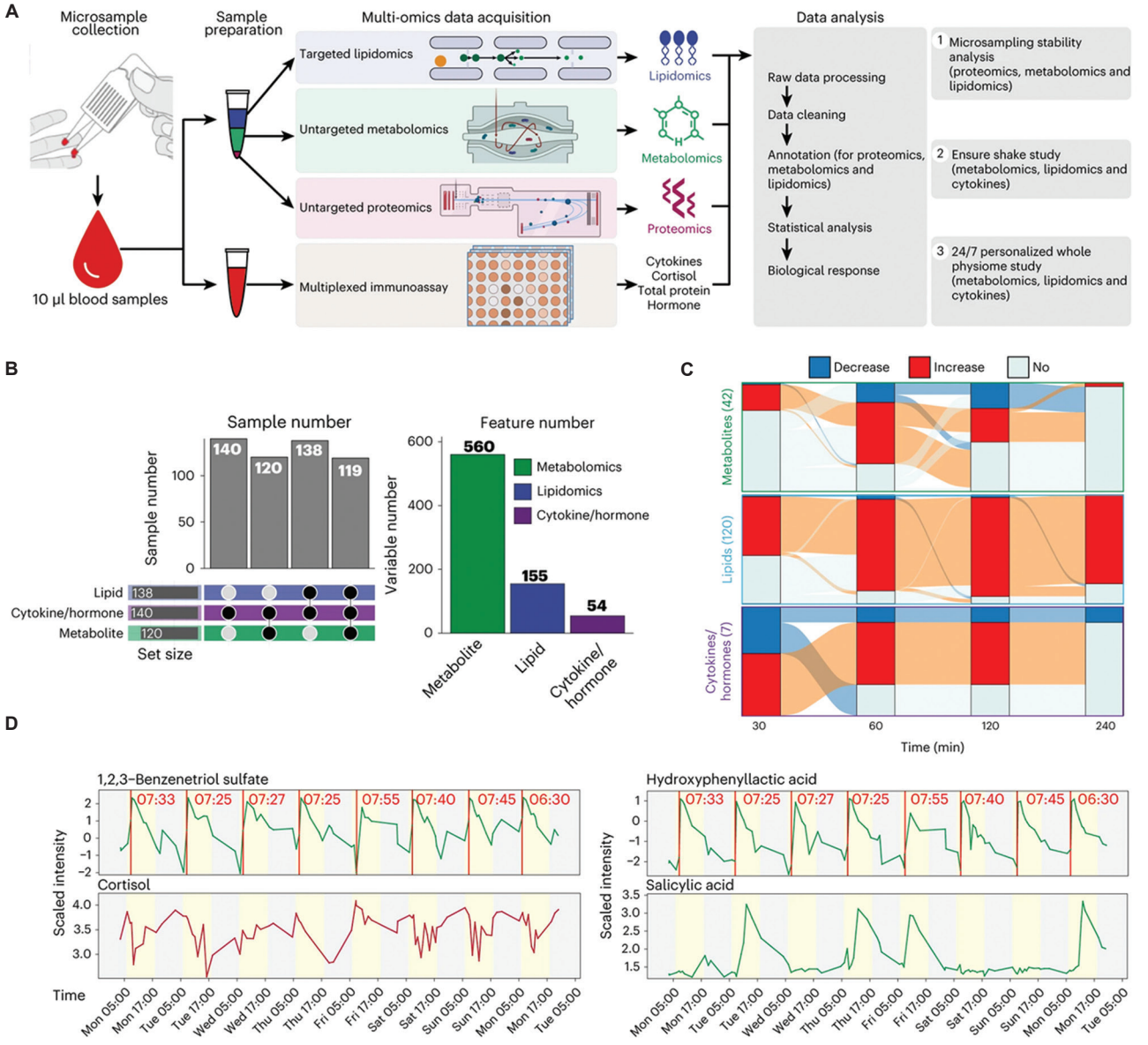

Figure 1. Outline of the iPOP microsampling multi-omics workflow, the molecular changes that occur in response to the consumption of a shake, and insight into an individual's physiological status and circadian rhythm. (A) Microsampling devices were used to collect the samples, which were then subjected to multi-omics analysis involving proteomics, metabolomics, lipidomics, cytokine profiling and other techniques. (B) The multi-omics data obtained from the microsamples are summarized. (C) The metabolites, lipids and cytokines/hormones were analyzed to determine their response to the consumption of an Ensure shake, using a two-sided Wilcoxon rank test. (D) Four molecules that are indicative of the participant's lifestyle and circadian rhythm are shown. This figure has been modified from Shen *et al.*,[84] which is licensed under a Creative Commons Attribution 4.0 International License.

7. Vision

In the envisioned future of healthcare, the fusion of wearable technology and multi-omics characterization promises to revolutionize how we monitor and manage health at every stage of the healthcare journey. Whether for a healthy individual seeking proactive health insights, a participant in a clinical trial or a patient in a hospital, this transformative approach aims to provide personalized, real-time health assessments and interventions. The following sections present an expanded vision built on the visions of the iPOP studies, demonstrated with the multiple stages a patient enrolled in a phase 3 clinical trial for a new sickle cell disease treatment will undergo, in which the patient is required to self-administer medication while at home. This vision is summarized and generalized in Figure 2.

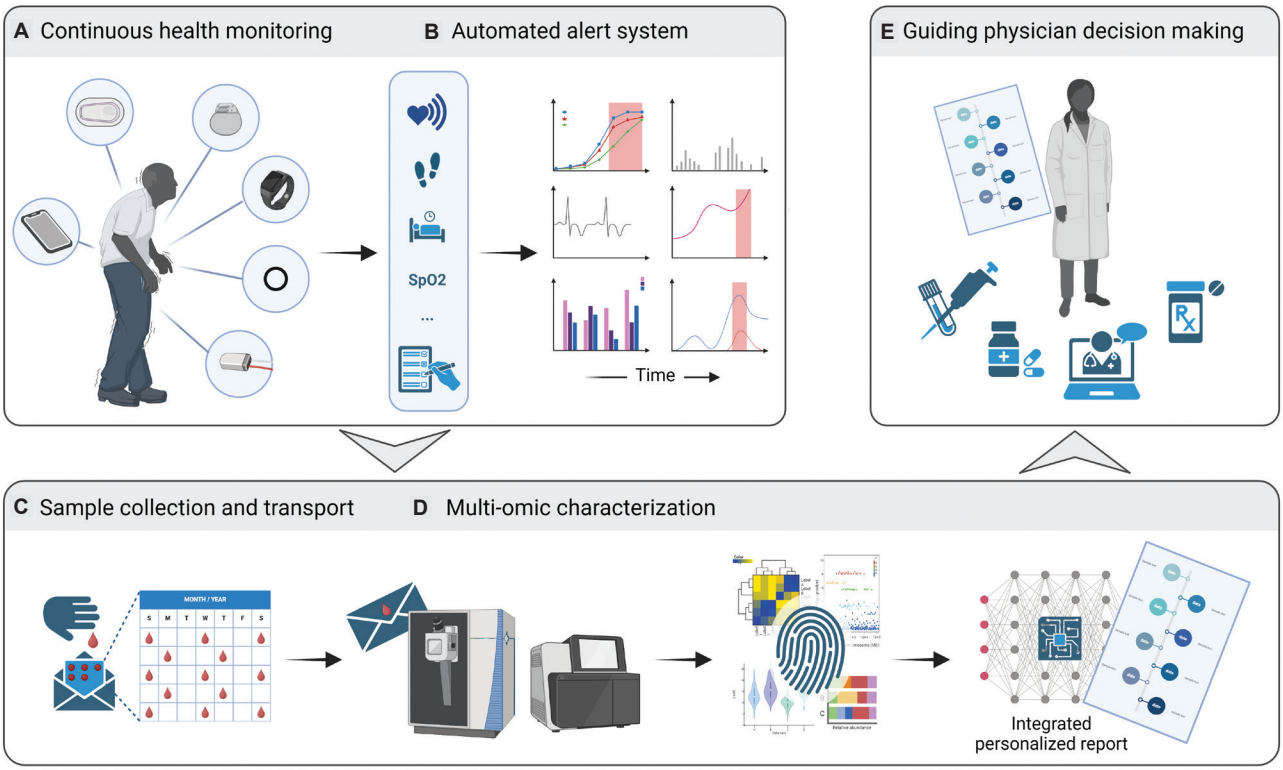

Figure 2. A schematic representation of the envisioned future of healthcare and drug discovery, where wearable technology and multi-omics characterization are fused to provide personalized, real-time health assessments and interventions. (A) The patient is monitored by wearable devices that unobtrusively track vital signs and physiological parameters. (B) An automated alert system triggers a response when significant deviations occur, and (C) biosamples, which have been sampled continuously and regularly from the beginning, are collected for (D) multi-omics characterization, which provides a unique molecular profile of the patient. All data is summarized in a legible integrated personalized report. (E) The insights gleaned from the multi-omics characterization serve as a powerful tool for healthcare providers, triggering additional measures, enabling early detection and tailored therapeutic interventions. The illustration was created with BioRender.com.

7.1. Continuous health monitoring

The patient is seamlessly monitored by wearable devices that unobtrusively monitor his vital signs (such as heart rate, blood pressure, oxygenation levels, blood glucose, nitrogen levels, or others of relevance) and physiological parameters (such as motion and sleep patterns). Supplementing the wearable tech data are an electronic diary[85] where the patient logs food and supplements, intake of other drugs (such as prescribed, over-the-counter, or recreational) and any self-reported ailments (e.g., the common cold or a sprained ankle). These wearables are equipped with advanced sensors and machine learning algorithms that establish personalized health baselines. They continuously track the participant's health metrics and generate alerts when significant deviations occur.

7.2. Automated alert system

When a deviation from the established baseline is detected, an automated alert is sent to a central computer program, which assesses the data. For a sickle cell disease patient, this could include, but not be limited to, heart rate and heart rate variability, body temperature, oxygen saturation or even sleep disturbances.[86] The deviation could also constitute a general health decline, possibly due to drug-induced liver toxicity or other adverse side effects, particularly those that are unexpected. If the deviation is substantial and cannot be explained by dietary choices or any other self-reported incidents from the electronic diary, the system would trigger a response.

7.3. Sample collection and transport

In response to these alerts, a courier will be dispatched to the individual's location to collect stored biosamples, such as dried blood spots, which have been routinely collected on a daily or weekly basis by the participant themself. Alternatively, a micro sampler device of the type used in iPOP research could be adapted for this purpose. These samples serve as a snapshot of the individual's physiology and molecular composition during the period of deviation as well as for the baseline prior to the deviation. Dried blood spots can be easily obtained with a finger prick by the patient and stored on a piece of paper at room temperature. Of course, pre- and post-assessment of analyte stability are pivotal.

7.4. Longitudinal and personal multi-omics characterization

Once collected, these biosamples are transported to a central laboratory and subjected to comprehensive multi-omics characterization. State-of-the-art mass spectrometry and other suitable sequencers are employed to analyze the genetic, transcriptomic, proteomic, metabolomic and other omics profiles, as well as the targeting of specific immune markers in the samples. A suite of automatic bioinformatic analyses is triggered as soon as the data is generated. Albeit shallow, this detailed multi-omics data provides a rich understanding of the molecular underpinnings of the health deviation and provides a personal fingerprint of molecular data.

7.5. Guiding physician decision making

The insights gleaned from multi-omics characterization serve as a powerful tool for healthcare providers. Armed with this data, physicians can make informed decisions regarding the most appropriate course of action. This may involve closer monitoring, additional in-clinic analyses, tailored therapeutic interventions, or, in cases where the deviation is a transient anomaly, reassurance for the patient. Importantly, the turnaround time from the triggering of the automatic alarms system from the wearable technology to the generation of an analyzed, personal multi-omics profile should only be a few days for the doctor's convenience. This approach facilitates preemptive identification of adverse side effects, enabling early detection, possibly even in advance of symptomatic manifestation in the patient.

8. Concluding remarks

Wearable devices have the potential to significantly benefit clinical trials by detecting side effects, correcting dosages, improving understanding of the mechanism of action, identifying drug-drug interactions and complementing other data-driven interventions. Moreover, if implemented correctly, this approach could reveal drug efficacy. With a likely future's increases in sensitivity and depth, it could even be applied to healthy subjects in a phase 1 clinical trial, where downstream pharmacodynamic effects may be evident from a multi-omics data set, depending on the drug and dosage being studied.

However, it is important to consider the additional costs associated with implementing this system. Comparing the cost increase to that of a failed clinical trial phase can help evaluate the feasibility of this approach. Despite the potential costs, incorporating wearable devices into clinical trials can lead to more accurate drug development and improved patient outcomes, and ultimately retained value of investments.

This envisioned future in health-care represents a profound shift from the reactive model of treating diseases to a proactive, preventative and highly personalized approach to maintaining health and managing illnesses. It enables early detection of health deviations, rapid intervention and precise treatment strategies. Ultimately, this convergence of wearable technology and multi-omics characterization empowers individuals, researchers, and health-care professionals alike to unlock the full potential of personalized medicine, advancing the goal of optimal health and wellbeing for all. Global implementation might be unattainable in our lifetimes, but this new, unified approach can be first attempted in clinical trials conducted by the medical industry, where many of the mentioned techniques are already enlisted in one shape or form. Identify relevant patient groups is another factor that needs to be considered. Patient populations with certain chronic diseases and with a clear and vital treatment intervention might be a first target subject group for testing the feasibility of the proposed approach.

In the ever-evolving healthcare landscape, personalized multi-omics characterization emerges as the future of medicine. Integrating multiple omics technologies provides a holistic understanding of individuals, enabling precise, and data-driven health-care decisions. This explosion of omics research further exemplifies how collaborative efforts continue to drive innovations in translational research and expand our understanding of complex diseases. As wearable technology merges with multi-omics analysis, we are on the cusp of a new era, where proactive, personalized healthcare becomes the norm – where we could detect untold ailments days before the patient is even aware of their predicament. The transformation we see currently in medicine marks the dawn of a truly personalized era and, if implemented correctly, we could detect disease before we know it.

Acknowledgments

I would like to thank Alberto Santos Delgado and Fabrice Chimienti for their valuable contributions to this review. Their expertise in omics-bioinformatics and wearables, respectively, and their insightful feedback helped shape the analyses. Furthermore, I would like to thank Edward Handyside for his valuable input and expertise in editing this manuscript. His assistance was very helpful in improving the clarity and readability of this paper. I am grateful for all my colleagues support, and positive attitude throughout the process. Finally, I would like to acknowledge the application ChatGPT in improving the clarity and coherence of my work.

Funding

None.

Conflict of interest

The author is an employee of Novo Nordisk A/S, but the views expressed in this review are solely those of the author and do not represent the views of Novo Nordisk A/S. This work was conducted independently and without any influence from Novo Nordisk A/S. Novo Nordisk A/S did not provide any financial support for this research. There are no other potential conflicts of interest related to this research.

Author contributions

This is a single-authored article.

Ethics approval and consent to participate

Not applicable.

Consent for publication

Not applicable.

Availability of data

Not applicable.

References

1. Carter AJ, Kraemer O, Zwick M, Mueller-Fahrnow A, Arrowsmith CH, Edwards AM. Target 2035: Probing the human proteome. *Drug Discov Today*. 2019;24(11):2111-2115.

   doi: 10.1016/j.drudis.2019.06.020

2. Nurk S, Koren S, Rhie A, *et al*. The complete sequence of a human genome. *Science*. 2022;376(6588):44-53.

   doi: 10.1126/science.abj6987

3. Cancer Genome Atlas Research Network. Comprehensive genomic characterization defines human glioblastoma genes and core pathways. *Nature*. 2008;455(7216):1061-1068.

   doi: 10.1038/nature07385

4. Cancer Genome Atlas Research Network. Integrated genomic analyses of ovarian carcinoma. *Nature*. 2011;474(7353):609-615.

   doi: 10.1038/nature10166

5. Cancer Genome Atlas Network. Comprehensive molecular portraits of human breast tumours. *Nature*. 2012;490(7418):61-70.

   doi: 10.1038/nature11412

6. GTEx Consortium. The genotype-tissue expression (GTEx) project. *Nat Genet*. 2013;45(6):580-585.

   doi: 10.1038/ng.2653

7. Stunnenberg HG, International Human Epigenome Consortium, Hirst M. The international human epigenome consortium: A blueprint for scientific collaboration and discovery. *Cell*. 2016;167(5):1145-1149.

   doi: 10.1016/j.cell.2016.11.007

8. Regev A, Teichmann SA, Lander ES, *et al*. The human cell atlas. *Elife*. 2017;6:e27041.

   doi: 10.7554/eLife.27041

9. Zhang B, Wang J, Wang X, *et al*. Proteogenomic characterization of human colon and rectal cancer. *Nature*. 2014;513(7518):382-387.

   doi: 10.1038/nature13438

10. Mertins P, Mani DR, Ruggles KV, *et al*. Proteogenomics connects somatic mutations to signalling in breast cancer. *Nature*. 2016;534(7605):55-62.

    doi: 10.1038/nature18003

11. Zhang H, Liu T, Zhang Z, *et al*. Integrated proteogenomic characterization of human high-grade serous ovarian cancer. *Cell*. 2016;166(3):755-765.

    doi: 10.1016/j.cell.2016.05.069

12. Gillette MA, Satpathy S, Cao S, *et al*. Proteogenomic characterization reveals therapeutic vulnerabilities in lung adenocarcinoma. *Cell*. 2020;182(1):200-225.e35.

    doi: 10.1016/j.cell.2020.06.013

13. Mundt F, Rajput S, Li S, *et al*. Mass spectrometry-based proteomics reveals potential roles of NEK9 and MAP2K4 in resistance to PI3K inhibition in triple-negative breast cancers. *Cancer Res*. 2018;78(10):2732-2746.

    doi: 10.1158/0008-5472.CAN-17-1990

14. Archer TC, Ehrenberger T, Mundt F, *et al*. Proteomics, post-translational modifications, and integrative analyses reveal molecular heterogeneity within medulloblastoma subgroups. *Cancer Cell*. 2018;34(3):396-410.e8.

    doi: 10.1016/j.ccell.2018.08.004

15. Heck AJ, Krijgsveld J. Mass spectrometry-based quantitative proteomics. *Expert Rev Proteomics*. 2004;1(3):317-326.

    doi: 10.1586/14789450.1.3.317

16. Pernemalm M, Lehtio J. Mass spectrometry-based plasma proteomics: State of the art and future outlook. *Expert Rev Proteomics*. 2014;11(4):431-448.

    doi: 10.1586/14789450.2014.901157

17. Aebersold R, Mann M. Mass-spectrometric exploration of proteome structure and function. *Nature*. 2016;537(7620):347-355.

    doi: 10.1038/nature19949

18. Invergo BM, Beltrao P. Reconstructing phosphorylation signalling networks from quantitative phosphoproteomic data. *Essays Biochem*. 2018;62(4):525-534.

    doi: 10.1042/EBC20180019

19. Orre LM, Vesterlund M, Pan Y, *et al*. SubCellBarCode: Proteome-wide mapping of protein localization and

relocalization. *Mol Cell*. 2019;73(1):166-182.e7.

doi: 10.1016/j.molcel.2018.11.035

20. Lehtio J, Arslan T, Siavelis I, *et al*. Proteogenomics of non-small cell lung cancer reveals molecular subtypes associated with specific therapeutic targets and immune evasion mechanisms. *Nat Cancer*. 2021;2(11):1224-1242.

doi: 10.1038/s43018-021-00259-9

21. Clish CB. Metabolomics: An emerging but powerful tool for precision medicine. *Cold Spring Harb Mol Case Stud*. 2015;1(1):a000588.

doi: 10.1101/mcs.a000588

22. Lu Z, Priya Rajan SA, Song Q, *et al*. 3D scaffold-free microlivers with drug metabolic function generated by lineage-reprogrammed hepatocytes from human fibroblasts. *Biomaterials*. 2021;269:120668.

doi: 10.1016/j.biomaterials.2021.120668

23. Triozzi PL, Stirling ER, Song Q, *et al*. Circulating immune bioenergetic, metabolic, and genetic signatures predict melanoma patients' response to Anti-PD-1 immune checkpoint blockade. *Clin Cancer Res*. 2022;28(6):1192-1202.

doi: 10.1158/1078-0432.CCR-21-3114

24. Ravindra KC, Vaidya VS, Wang Z, *et al*. Tandem mass tag-based quantitative proteomic profiling identifies candidate serum biomarkers of drug-induced liver injury in humans. *Nat Commun*. 2023;14(1):1215.

doi: 10.1038/s41467-023-36858-6

25. Niu L, Thiele M, Geyer PE, *et al*. Noninvasive proteomic biomarkers for alcohol-related liver disease. *Nat Med*. 2022;28(6):1277-1287.

doi: 10.1038/s41591-022-01850-y

26. Eldjarn GH, Ferkingstad E, Lund SH, *et al*. Large-scale plasma proteomics comparisons through genetics and disease associations. *Nature*. 2023;622(7982):348-358.

doi: 10.1038/s41586-023-06563-x

27. Sun BB, Chiou J, Traylor M, *et al*. Plasma proteomic associations with genetics and health in the UK Biobank. *Nature*. 2023;622(7982):329-338.

doi: 10.1038/s41586-023-06592-6

28. Dhindsa RS, Burren OS, Sun BB, *et al*. Rare variant associations with plasma protein levels in the UK Biobank. *Nature*. 2023;622(7982):339-347.

doi: 10.1038/s41586-023-06547-x

29. Sanyal AJ, Williams SA, Lavine JE, *et al*. Defining the serum proteomic signature of hepatic steatosis, inflammation, ballooning and fibrosis in non-alcoholic fatty liver disease. *J Hepatol*. 2023;78(4):693-703.

doi: 10.1016/j.jhep.2022.11.029

30. Mundt F, Albrechtsen NJW, Mann SP, *et al*. Foresight in clinical proteomics: current status, ethical considerations, and future perspectives. *Open Res Eur*. 2023;3:59.

doi: 10.12688/openreseurope.15810.1

31. Mertins P, Tang LC, Krug K, *et al*. Reproducible workflow for multiplexed deep-scale proteome and phosphoproteome analysis of tumor tissues by liquid chromatography-mass spectrometry. *Nat Protoc*. 2018;13(7):1632-1661.

doi: 10.1038/s41596-018-0006-9

32. Candia J, Daya GN, Tanaka T, Ferrucci L, Walker KA. Assessment of variability in the plasma 7k SomaScan proteomics assay. *Sci Rep*. 2022;12(1):17147.

doi: 10.1038/s41598-022-22116-0

33. Huang T, Wang J, Stukalov A, *et al*. Protein coronas on functionalized nanoparticles enable quantitative and precise large-scale deep plasma proteomics. *bioRxiv* [*Preprint*]. 2023.

doi: 10.1101/2023.08.28.555225

34. Mund A, Coscia F, Kriston A, *et al*. Deep visual proteomics defines single-cell identity and heterogeneity. *Nat Biotechnol*. 2022;40(8):1231-1240.

doi: 10.1038/s41587-022-01302-5

35. Eckert MA, Coscia F, Chryplewicz A, *et al*. Proteomics reveals NNMT as a master metabolic regulator of cancer-associated fibroblasts. *Nature*. 2019;569(7758):723-728.

doi: 10.1038/s41586-019-1173-8

36. Zhuang YJ, Mangwiro Y, Wake M, Saffery R, Greaves RF. Multi-omics analysis from archival neonatal dried blood spots: Limitations and opportunities. *Clin Chem Lab Med*. 2022;60(9):1318-1341.

doi: 10.1515/cclm-2022-0311

37. Omenn GS, Lane L, Overall CM, *et al*. The 2022 Report on the human proteome from the HUPO human proteome project. *J Proteome Res*. 2023;22(4):1024-1042.

doi: 10.1021/acs.jproteome.2c00498

38. Webel H, Niu L, Nielsen BA, *et al*. Imputation of label-free quantitative mass spectrometry-based proteomics data using self supervised deep learning. *bioRxiv* [*Preprint*]. 2023.

doi: 10.1101/2023.01.12.523792

39. Liu J, Yang M, Yu Y, Xu H, Li K, Zhou X. Large language models in bioinformatics: applications and perspectives. *ArXiv* [*Preprint*]. 2024.

40. Mani DR, Krug K, Zhang B, *et al*. Cancer proteogenomics: current impact and future prospects. *Nat Rev Cancer*. 2022;22(5):298-313.

doi: 10.1038/s41568-022-00446-5

41. Santos A, Colaço AR, Nielsen AB, *et al*. A knowledge graph to interpret clinical proteomics data. *Nat Biotechnol*. 2022;40(5):692-702.

doi: 10.1038/s41587-021-01145-6

42. Smith AA, Li R, Tse ZTH. Reshaping healthcare with wearable biosensors. *Sci Rep.* 2023;13(1):4998.

doi: 10.1038/s41598-022-26951-z

43. Huhn S, Axt M, Gunga HC, *et al*. The impact of wearable technologies in health research: Scoping review. *JMIR Mhealth Uhealth*. 2022;10(1):e34384.

doi: 10.2196/34384

44. Lu L, Zhang J, Xie Y, *et al*. Wearable health devices in health care: Narrative systematic review. *JMIR Mhealth Uhealth*. 2020;8(11):e18907.

doi: 10.2196/18907

45. Wells CI, Xu W, Penfold JA, *et al*. Wearable devices to monitor recovery after abdominal surgery: Scoping review. *BJS Open*. 2022;6(2):zrac031.

doi: 10.1093/bjsopen/zrac031

46. Horsham C, Antrobus J, Olsen CM, Ford H, Abernethy D, Hacker E. Testing wearable UV Sensors to improve sun protection in young adults at an outdoor festival: Field study. *JMIR Mhealth Uhealth*. 2020;8(9):e21243.

doi: 10.2196/21243

47. Salusky IB, Holloway M, Kuizon BD. Peritoneal dialysis in children: Issues for the 21st century. *Perit Dial Int*. 1999;19(Suppl 2):S484-S488.

48. Al Younis SM, Hadjileontiadis LJ, Stefanini C, Khandoker AH. Non-invasive technologies for heart failure, systolic and diastolic dysfunction modeling: A scoping review. *Front Bioeng Biotechnol*. 2023;11:1261022.

doi: 10.3389/fbioe.2023.1261022

49. Prieto-Avalos G, Cruz-Ramos NA, Alor-Hernandez G, Sanchez-Cervantes JL, Rodriguez-Mazahua L, Guarneros-Nolasco LR. Wearable devices for physical monitoring of heart: A review. *Biosensors (Basel)*. 2022;12(5):292.

doi: 10.3390/bios12050292

50. Handy C, Chaudhry MS, Qureshi MRA, *et al*. Noninvasive continuous glucose monitoring with a novel wearable dial resonating sensor: A clinical proof-of-concept study. *J Diabetes Sci Technol*. 2023.

doi: 10.1177/19322968231170242

51. Van de Hei SJ, Poot CC, van den Berg LN, *et al*. Effectiveness, usability and acceptability of a smart inhaler programme in patients with asthma: Protocol of the multicentre, pragmatic, open-label, cluster randomised controlled ACCEPTANCE trial. *BMJ Open Respir Res*. 2022;9(1):e001400.

doi:10.1136/bmjresp-2022-001400

52. Iqbal SMA, Mahgoub I, Du E, Leavitt MA, Asghar W. Advances in healthcare wearable devices. *NPJ Flex Electron*. 2021;5(1):9.

doi: 10.1038/s41528-021-00107-x

53. Özsoylu D, Janus KA, Achtsnicht S, Wagner T, Keusgen M, Schöning MJ. (Bio-)Sensors for skin grafts and skin flaps monitoring. *Sens Actuators Rep*. 2023;6:100163.

doi: 10.1016/j.snr.2023.100163

54. (FDA) USFaDA. *Artificial Intelligence and Machine Learning (AI/ML)-Enabled Medical Devices*. Available from: https://www.fda.gov/medical-devices/software-medical-device-samd/artificial-intelligence-and-machine-learning-aiml-enabled-medical-devices [Last accessed on 2023 Nov 30].

55. Peters DM, O'Brien ES, Kamrud KE, *et al*. Utilization of wearable technology to assess gait and mobility post-stroke: A systematic review. *J Neuroeng Rehabil*. 2021;18(1):67.

doi: 10.1186/s12984-021-00863-x

56. Daskalaki E, Parkinson A, Brew-Sam N, *et al*. The potential of current noninvasive wearable technology for the monitoring of physiological signals in the management of type 1 diabetes: Literature survey. *J Med Internet Res*. 2022;24(4):e28901.

doi: 10.2196/28901

57. Smarr BL, Aschbacher K, Fisher SM, *et al*. Feasibility of continuous fever monitoring using wearable devices. *Sci Rep*. 2020;10(1):21640.

doi: 10.1038/s41598-020-78355-6

58. Gilliam FR, 3rd, Ciesielski R, Shahinyan K, *et al*. In-ear infrasonic hemodynography with a digital health device for cardiovascular monitoring using the human audiome. *NPJ Digit Med*. 2022;5(1):189.

doi: 10.1038/s41746-022-00725-3

59. Cheng CH, Wong KL, Chin JW, Chan TT, So RHY. Deep learning methods for remote heart rate measurement: A review and future research agenda. *Sensors (Basel)*. 2021;21(18):6296.

doi: 10.3390/s21186296

60. Sadad T, Bukhari SAC, Munir A, Ghani A, El-Sherbeeny AM, Rauf HT. Detection of cardiovascular disease based on ppg signals using machine learning with cloud computing. *Comput Intell Neurosci*. 2022;2022:1672677.

doi: 10.1155/2022/1672677

61. Heiden E, Jones T, Brogaard Maczka A, *et al*. Measurement of vital signs using lifelight remote photoplethysmography: Results of the VISION-D and VISION-V observational studies. *JMIR Form Res*. 2022;6(11):e36340.

doi: 10.2196/36340

62. Saboo B, Kesavadev J, Shankar A, *et al*. Time-in-range as a target in type 2 diabetes: An urgent need. *Heliyon*. 2021;7(1):e05967.

doi: 10.1016/j.heliyon.2021.e05967

63. Zou Y, Chu Z, Guo J, Liu S, Ma X, Guo J. Minimally invasive electrochemical continuous glucose monitoring sensors: Recent progress and perspective. *Biosens Bioelectron*. 2023;225:115103.

doi: 10.1016/j.bios.2023.115103

64. Ma YL, Ke JF, Wang JW, Wang YJ, Xu MR, Li LX. Blood lactate levels are associated with an increased risk of metabolic dysfunction-associated fatty liver disease in type 2 diabetes: A real-world study. *Front Endocrinol (Lausanne)*. 2023;14:1133991.

doi: 10.3389/fendo.2023.1133991

65. Liu F, Lu JX, Tang JL, *et al*. Relationship of plasma creatinine and lactic acid in type 2 diabetic patients without renal dysfunction. *Chin Med J (Engl)*. 2009;122(21):2547-2553.

66. (FDA) USFaDA. *ECG App Classified into Class II-FDA*. Cupertino: Apple Inc.; 2018. Available from: https://www.accessdata.fda.gov/cdrh_docs/pdf18/den180044.pdf [Last accessed on 2024 Mar 20].

67. Smith S. *Which Smartwatch is FDA Approved?*; 2023. Available from: https://isp.page/news/which-smartwatch-is-fda-approved/#gsc.tab=0 [Last accessed on 2023 Nov 30].

68. FDA.Report. *Omron Heart Guide Wrist Blood Pressure Monitor, Large BP8000-L*. Available from: https://fda.report/GUDID/20073796268026 [Last accessed on 2024 Mar 20].

69. Mason AE, Hecht FM, Davis SK, *et al*. Detection of COVID-19 using multimodal data from a wearable device: Results from the first TemPredict Study. *Sci Rep*. 2022;12(1):3463.

doi: 10.1038/s41598-022-07314-0

70. Cheong SHR, Ng YJX, Lau Y, Lau ST. Wearable technology for early detection of COVID-19: A systematic scoping review. *Prev Med*. 2022;162:107170.

doi: 10.1016/j.ypmed.2022.107170

71. Messner CB, Demichev V, Wendisch D, *et al*. Ultra-high-throughput clinical proteomics reveals classifiers of COVID-19 infection. *Cell Syst*. 2020;11(1):11-24.e4.

doi: 10.1016/j.cels.2020.05.012

72. Vayena E, Blasimme A, Sugarman J. Decentralised clinical trials: Ethical opportunities and challenges. *Lancet Digit Health*. 2023;5(6):e390-e394.

doi: 10.1016/S2589-7500(23)00052-3

73. Porsdam Mann S, Treit PV, Geyer PE, Omenn GS, Mann M. Ethical principles, opportunities and constraints in clinical proteomics. *Mol Cell Proteomics*. 2021;20:100046.

doi: 10.1074/mcp.RA120.002435

74. Caufield JH, Fu J, Wang D, Guevara-Gonzalez V, Wang W, Ping P. A Second look at FAIR in proteomic investigations. *J Proteome Res*. 2021;20(5):2182-2186.

doi: 10.1021/acs.jproteome.1c00177

75. Giannattasio S, Heil KF, Hermjakob H, *et al*. The next challenge: Data management, submission and FAIRness in multi-omics experiments. *F1000Res*. 2023;12:1379.

doi: 10.7490/f1000research.1119646.1

76. Medicine IoMURoE-B. 6, Missed Prevention Opportunities. In: Yong PL, Olsen LA, editors. *The Healthcare Imperative: Lowering Costs and Improving Outcomes: Workshop Series Summary*. Washington, D.C: National Academies Press; 2010.

77. Dhingra LS, Aminorroaya A, Oikonomou EK, *et al*. Use of wearable devices in individuals with or at risk for cardiovascular disease in the US, 2019 to 2020. *JAMA Netw Open*. 2023;6(6):e2316634.

doi: 10.1001/jamanetworkopen.2023.16634

78. Roche. *Technical Specifications-FoundationOne®CDx (F1CDx)*; 2023. Available from: https://assets.ctfassets.net/w98cd481qyp0/yqqkhaqqmfeqc5ueqk48w/d12f19680205941ea3fee417f08e9524/f1cdx_technical_specifications.pdf [Last accessed on 2024 Mar 20].

79. Mundt F. Nielsen, AB, Duel JK, *et al*. In depth profiling of the cancer proteome from the flowthrough of standard RNA-preparation kits for precision oncology. *bioRxiv [Perprint]*. 2023.

doi: 10.1101/2023.05.12.540582

80. Doll S, Kriegmair MC, Santos A, *et al*. Rapid proteomic analysis for solid tumors reveals LSD1 as a drug target in an end-stage cancer patient. *Mol Oncol*. 2018;12(8):1296-1307.

doi: 10.1002/1878-0261.12326

81. Chen R, Mias GI, Li-Pook-Than J, *et al*. Personal omics profiling reveals dynamic molecular and medical phenotypes. *Cell*. 2012;148(6):1293-1307.

doi: 10.1016/j.cell.2012.02.009

82. Li X, Dunn J, Salins D, *et al*. Digital health: Tracking physiomes and activity using wearable biosensors reveals useful health-related information. *PLoS Biol*. 2017;15(1):e2001402.

doi: 10.1371/journal.pbio.2001402

83. Schussler-Fiorenza Rose SM, Contrepois K, Moneghetti KJ, *et al*. A longitudinal big data approach for precision health. *Nat Med*. 2019;25(5):792-804.

doi: 10.1038/s41591-019-0414-6

84. Shen X, Kellogg R, Panyard DJ, *et al*. Multi-omics microsampling for the profiling of lifestyle-associated changes in health. *Nat Biomed Eng*. 2023;8:11-29.

doi: 10.1038/s41551-022-00999-8

85. (FDA) USFaDA. *Use of Electronic Informed Consent in Clinical Investigations–Questions and Answers*; 2023. Available from: https://www.fda.gov/regulatory-information/search-fda-guidance-documents/use-electronic-informed-consent-clinical-investigations-questions-and-answers [Last accessed on 2024 Mar 20].

86. Sharma S, Efird JT, Knupp C, *et al*. Sleep disorders in adult sickle cell patients. *J Clin Sleep Med*. 2015;11(3):219-223.

doi: 10.5664/jcsm.4530

ACCSCIENCE PUBLISHING

Global Translational Medicine

PERSPECTIVE ARTICLE

Pixels to precision: Remote thoracic and pediatric cardiac surgery mentorship with Rods&Cones® Technology in Kigali, Rwanda

Jessica D. Blum[1]*, Yayehyirad Mekonnen Ejigu[2], Girma Tefera[3], and James D. Maloney[4]

[1]Department of Surgery, Division of Plastic Surgery, University of Wisconsin Madison, Madison, Wisconsin, United States of America

[2]Department of Cardiothoracic Surgery, King Faisal Hospital, Kigali, Rwanda

[3]Department of Surgery, Division of Vascular Surgery, University of Wisconsin Madison, Madison, Wisconsin, United States of America

[4]Department of Surgery, Division of Cardiothoracic Surgery, University of Wisconsin Madison, Madison, Wisconsin, United States of America

Abstract

Surgery is the final frontier in global medicine; yet, access to essential surgical services in low- and middle-income countries remains a significant barrier to equitable care. With a rise in non-communicable diseases and a shortage of skilled surgeons, the need for mentorship becomes crucial to capacity building. The COVID-19 pandemic acted as a catalyst for remote mentorship, leading to the development of innovative solutions such as Rods&Cones®. Herein, we describe one example of remote mentorship conducted across a distance of more than 7,700 miles between King Faisal Hospital in Rwanda and the University of Wisconsin Hospital in the US. This paper aims to demonstrate how advances in remote mentorship technology can overcome existing barriers and aid in expanding the global surgical workforce in thoracic surgery.

Keywords: Global health; Global surgery; Remote mentorship; Mentorship; Thoracic surgery; Cardiothoracic surgery

***Corresponding author:**
Jessica D. Blum
(jblum2@uwhealth.org)

Citation: Blum JD, Ejigu YM, Tefera G, Maloney JD. Pixels to precision: Remote thoracic and pediatric cardiac surgery mentorship with Rods&Cones® Technology in Kigali, Rwanda. *Global Transl Med*. 2024;3(1):2795. https://doi.org/10.36922/gtm.2795

Received: January 21, 2024
Accepted: February 22, 2024
Published Online: March 26, 2024

1. Brain drain and capacity building

In the global health landscape, surgery has long been considered the "final frontier;" yet, challenges persist in delivering essential surgical services to low- and middle-income countries (LMICs).[1] The World Health Organization estimates that provision of essential surgical services could prevent 6–7% of all avertable deaths in LMICs.[2] Yet, issues with a low-density skilled workforce and barriers to timely care lead to increased morbidity and mortality, further stressing existing systems. The greatest burden of surgically treatable diseases falls on people in LMICs, but the poorest third of people receive only 3.5% of operations and have the lowest numbers of surgeons per capita.[3]

With a decreased global incidence of communicable diseases, an increase in non-communicable diseases (NCDs) is the logical result of a larger, aging population. A study

published by Gouda and colleagues in *The Lancet Global Health* revealed a 67% increase in disability-adjusted life-years (DALYs) due to NCDs in sub-Saharan Africa, from 90.6 million in 1990 – 151.3 million in 2017.[4] In 2017, the leading causes of NCD burden were cardiovascular disease (22.9 million) and neoplasms (16.9 million), both of which include surgical intervention as an integral part of their management. Specifically, lack of access to thoracic surgery in sub-Saharan Africa is an urgent problem. In 2019, Africa had 124 thoracic surgeons, which translates to 1.2 thoracic surgeons per 10 million population.[5]

When educational demand and available resources are incongruent, bright young people interested in pursuing medicine or surgery are forced to seek training outside of their home country. This cyclic process fuels existing issues of "brain drain," which is the emigration of highly trained individuals from their home country. As a result, newly trained providers do not return home to serve their communities. Efforts in capacity building and retention of local physicians are essential to combat existing issues of brain drain, and providing access to highly specialized education is critical to this effort. If this problem is not addressed and current educational methods are not updated, it is estimated that there will be a global deficit of about 12.9 million skilled health professionals by 2035.[6]

2. The rise of remote mentorship

As the volume and complexity of surgical needs increases, the global surgical community must develop strategies to support individual surgeons, hospitals, and training programs as they take on the challenge of expanding the surgical workforce. Mentorship is the foundation of surgical training and stands as a paramount focus for research and resource allocation when attempting to build surgical capacity.

The COVID-19 pandemic served as an unexpected catalyst for remote mentorship. As traditional avenues for in-person mentorship faced abrupt limitations, necessity forced innovation in surgical education and training. This unforeseen shift forced the rapid development and adoption of telepresence technology, transforming operating rooms (ORs) into classrooms accessible across the globe. Surgeons worldwide swiftly embraced virtual platforms such as Zoom, Microsoft Teams, and Facetime to bridge geographical gaps and connect with mentees remotely. During this age of unparalleled advancement in remote mentorship, obstacles such as technological limitations and infrastructural inadequacies came to light. Herein, the authors describe one example of how advances in remote mentorship technology can overcome existing barriers and aid in expanding the global surgical workforce in thoracic surgery. The primary objective of this endeavor was to investigate the feasibility of establishing a remote mentorship program in hopes of expanding bi-directional learning between Rwanda and the United States.

3. Feasibility: Implementing Rods&Cones® in Rwanda

Rods&Cones® is a health-care technology company based out of the Netherlands that offers a remote telepresence solution for medical environments that is adaptable to global surgical support and is HIPAA- and GDPR-compliant.[7] It incorporates "smart glasses" and a digital remote assistance platform to allow users to connect safely with an assisting surgeon, product specialist, or other medical professional anywhere in the world, in real-time. What is especially noteworthy about Rods&Cones'® technology is its capacity to access and integrate multiple views for the Remote Expert to view from the comfort of home: (i) a direct surgeon view through the "smart glasses" worn by the operating surgeon (visOR), (ii) a Remote Expert-controlled live camera feed situated in the OR that provides a broader perspective of the operating theater (panOR), and (iii) direct minimally invasive surgery tower input (mirrOR). Moreover, the Rods&Cones® audio system provides detailed auditory input and output, enhancing the mentor's ability to provide live feedback through audio and chat capabilities. It is a lean, portable machine that does not require downtime for OR construction or remodeling. Rods&Cones® is currently active at more than 1500 hospitals in over 100 countries and has a robust live support network that is available to users around the clock.

With the goal of establishing feasibility of use of the Rods&Cones® technology for remote thoracic surgery mentorship, the senior author brought the technology on a surgical trip to King Faisal Hospital in Kigali, Rwanda in August 2022 (Figure 1). Using a Stupnik Video Assisted Thoracopic Surgery (VATS) Simulator, the team was able to ensure sufficient internet bandwidth and troubleshoot technological snags in an artificial setting (Figure 2). This

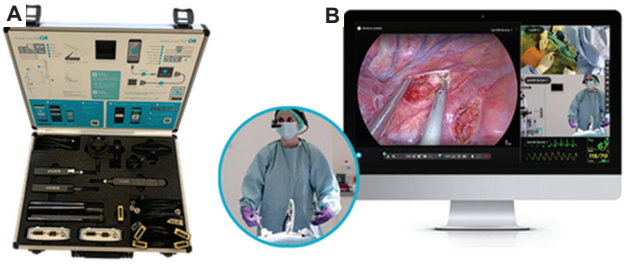

Figure 1. Rods and cones hardware and software. (A) The Rods&Cones® MIS Kit for minimally invasive surgeries. (B) The smart glasses in-use and associated Remote Expert interface. The images were used with permission (Source: https://rods-cones.com/mis-kit/).

involved having the operating surgeon manipulate the VATS simulator under the guidance of a "Remote Expert" who could assist in troubleshooting. The Remote Expert was initially in the same room with the operator but eventually transitioned to providing live technical feedback from a separate part of the hospital. The surgical team spent 2 days using the VATS simulator to troubleshoot issues both immediately related to Rods&Cones® devices as well as internet connectivity issues.

After simulation, the Rods&Cones® technology was progressed to intraoperative testing, initially within King Faisal Hospital, subsequently from a remote site in Kigali, and ultimately, from across the Atlantic Ocean. The Remote Expert was able to tune in at 4 am central standard time from the US to view the procedure in real-time and interact with the team performing pediatric cardiac surgery being conducted in Kigali, Rwanda, manipulating multiple views of the operative field to facilitate complete visualization without drawing attention from surgical proceedings (Figure 3). The benefits of having a remote surgeon mentor

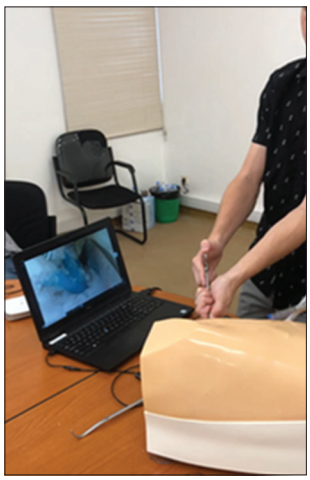

Figure 2. Rods&Cones® feasibility trial using Stupnik VATS simulator.

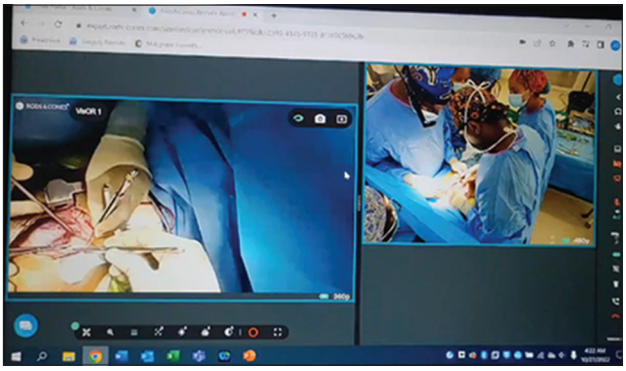

Figure 3. Example of Remote Expert user interface showing a pediatric cardiac surgery conducted in Kigali, Rwanda with remote guidance from Madison, Wisconsin.

that can interact in real-time are manifold, including but not limited to identification of key structures, modification of surgical technique, and indication of device and suture placement. When asked for direct feedback, one learner, who is also a local pediatric cardiac surgeon, provided the following:

> "Using the Rods&Cones® technology while performing pediatric cardiac surgery, we managed to interact with a remote mentor without interrupting the flow of surgery nor compromising the safety for the patient. With a mentor surgeon clearly seeing the operating field and guiding the mentee, we demonstrated that in cases when the two surgeons can't be in the same operating room together it's possible to learn and consult. I personally look forward to using the technology in the future when I have cases that I have not performed or are challenging without someone experienced around."

The surgical team performed four procedures with the Rods&Cones® technology while in-country and two additional procedures with transatlantic live interaction. One of the two remote procedures was more successful due to issues maintaining robust internet connectivity. King Faisal Hospital's internet technology team was intimately involved with testing in the OR suites and with establishing WiFi boosting devices to increase signal strength.

Challenges associated with the implementation of this technology at King Faisal Hospital were non-negligible. The primary concern was difficulty in establishing and maintaining adequate hospital internet connectivity. This was overcome by boosting Wi-Fi signal, as previously mentioned, to meet internet upload and download requirements of 24 Mbps and 7 Mbps, respectively. Having a Rods&Cones® on-site expert, such as a scrub nurse or other supportive staff, is essential as they can champion its use and provide in-person technologic support, demonstrating the value added relative to the effort required and promoting buy-in from the surgical teams. Concerns related to headset comfort also arose as one of the surgeons had to remove the headset intraoperatively while wearing it for a longer time. In addition, the cost of implementing Rods&Cones® technology could render it prohibitive without the support of government funding, charitable aid, or private sector investments.

For those considering implementation of a remote mentorship technology, it is also worth mentioning that additional education was required for staff to be comfortable with transmission of in-line feeds from the laparoscopy tower and echo machine to the Rods&Cones® system. Moreover, on the first day the team was attempting to set-up the technology, they were not allowed to start until

they had received a memo from the Hospital President and Chief of Staff, highlighting the importance of buy-in from local stakeholders.

4. Comparative analysis of remote mentorship technologies

Although the literature on remote thoracic surgery mentorship is not extensive, alternate technologies have been employed for surgical training, each with their own advantages and disadvantages. A study by Ponsky *et al.* describes their experience trialing two different remote "telemonitoring" technologies between Akron, Ohio, and Seattle, Washington. Their study compares the use of store-bought equipment that connects the laparoscope to a Skype™ connection to a proprietary telementoring robot, Karl Storz Endoscopy-America, Inc. VisitOR1®. The technologies were then compared in various pediatric surgical procedures, including a VATS lower lobectomy, among others. Ultimately, they found the less expensive Skype™ technology to be inferior in its security and telestrator abilities.[8]

Another alternative technology, Google Glass™ (Google, Inc, Mountain View, Calif.), was first introduced in 2012 and costs approximately US$1,000. This technology uses a peripherally positioned camera and prism. The camera can take photographs or videos to live-stream for teaching purposes, while the prism provides a semitransparent overlay on the wearer's visual field by projecting a computer-generated image directly onto the wearer's retina. Sound is recorded and transmitted by means of a mastoid bone conductor and earpiece, allowing dialogue between wearer and the remote viewer. Use of the Google Glass™ for surgical education has been demonstrated in LMICs; however, its primary drawback is the potential for distraction.[9] Google Glass™ can be distracting for the surgeon, particularly if they are not used to wearing the device. This can increase the risk of errors and complications during surgery. Additionally, certain editions of Google Glass™ technology (*e.g.*, Google Glass™ Enterprise) are no longer being sold or supported by Google. Lastly, concerns regarding patient confidentiality with transmission of audio and video content remain pertinent.

The Microsoft® HoloLens 2 has also been applied in a surgical context in the form of augmented reality for surgical navigation.[10] It is largely used as a surgical aid aimed at the visualization of medical data, blood vessel search, and targeting support for precise positioning of mechanical elements, rather than for remote mentorship. Moreover, despite improvement from its predecessor, the HoloLens 1, the headset remains relatively heavy (566 g), has a limited field of view (52°), and a battery life of only 3 h, precluding its use in most complex thoracic procedures. Apple© released the Vision Pro in the United States in February 2024 for the price of US$3,499, with limited availability. This mixed-reality technology has the potential to allow the surgeon to visualize key imaging intraoperatively without having to turn their head to look at a monitor, but applications for remote learning remain to be explored and are seemingly limited based on the current capabilities of the Vision Pro. Finally, none of the aforementioned technologies, aside from VisitOR1®, were designed for remote surgical training, unlike Rods&Cones®.

There has been a longstanding model of a visiting surgical expert or team traveling to a hospital site that wishes to develop a program or advance their surgical capabilities, but this is often for a limited period or does not provide sufficient consistent. The described technology does not require embedded equipment or structural remodeling, allowing for deployment for relatively brief periods, such as during the initiation process of a new surgical program. Once expertise and mentorship are available locally, the technology could be used in additional scopes of practice.[11] Intraoperative mentorship is just one component of a multifaceted effort to educate the next generation of thoracic surgeons. This technology can be transported by a single person for use in the clinic, the OR, or even the inpatient ward, spanning the entirety of perioperative care. Other initiatives include classroom or conference-based learning, visitation to other facilities for case observation, and expansion of access to primary literature. As technologies for remote mentorship continue to evolve, we are presented with an opportunity to transcend the limitations of traditional models, fostering interactive, bi-directional learning that is essential to establish and sustain comprehensive thoracic surgery globally.

Acknowledgments

None.

Funding

None.

Conflict of interest

James Maloney is a consultant for Ethicon, part of the Johnson & Johnson company. He has no relevant material or financial interests that relate to the research described in this paper. The other authors declare no conflict of interest.

Author contributions

Conceptualization: James D. Maloney
Writing – original draft: Jessica D. Blum
Writing – review & editing: Yayehyirad Mekonnen Ejigu, Girma Tefera, James D. Maloney

Ethics approval and consent to participate

Not applicable.

Consent for publication

Not applicable.

Availability of data

Not applicable.

References

1. Global surgery--the final frontier? *Lancet*. 2012;379:194.

   doi: 10.1016/S0140-6736(12)60083-X

2. World Health Organization. Ensuring Safe and Affordable Surgery. Switzerland: World Health Organization. Available from: https://www.who.int/westernpacific/activities/ensuring-safe-and-affordable-surgery [Last accessed 2023 Nov 18].

3. Weiser TG, Regenbogen SE, Thompson KD, *et al.* An estimation of the global volume of surgery: A modelling strategy based on available data. *Lancet*. 2008;372(9633):139-144.

   doi: 10.1016/S0140-6736(08)60878-8

4. Gouda HN, Charlson F, Sorsdahl K, *et al.* Burden of non-communicable diseases in sub-Saharan Africa, 1990-2017: Results from the Global Burden of Disease Study 2017. *Lancet Glob Health*. 2019;7(10):e1375-e1387.

   doi: 10.1016/S2214-109X(19)30374-2

5. *Quantifying International Access to Cardiac, Thoracic and Vascular Surgery: The American Association for Thoracic Surgery*. AATS; 2022. Available from: https://www.aats.org/resources/quantifying-international-access-to-cardiac-thoracic-vascular-surgery [Last accessed on 18 Nov 2023].

6. World Health Organization. (n.d.). *A Universal Truth: No Health without a Workforce*. World Health Organization. Available from: https://www.who.int/publications/m/item/hrh_universal_truth [Last accessed on 2023 Nov 26].

7. *Our Story in Remote Surgical Assistance-Rods and Cones*. Rods and Cones; 2023. Available from: https://rods-cones.com/about-us [Last accessed on 2023 Nov 26].

8. Ponsky TA, Bobanga ID, Schwachter M, *et al.* Transcontinental telementoring with pediatric surgeons: Proof of concept and technical considerations. *J Laparoendosc Adv Surg Tech A*. 2014;24(12):892-896.

   doi: 10.1089/lap.2014.0363

9. McCullough MC, Kulber L, Sammons P, Santos P, Kulber DA. Google glass for remote surgical tele-proctoring in low- and middle-income countries: A feasibility study from Mozambique. *Plast Reconstr Surg Glob Open*. 2018;6(12):e1999.

   doi: 10.1097/GOX.0000000000001999

10. Palumbo A. Microsoft HoloLens 2 in medical and healthcare context: State of the art and future prospects. *Sensors* (*Basel*). 2022;22(20):7709.

    doi: 10.3390/s22207709

11. Bui DT, Barnett T, Hoang H, Chinthammit W. Development of a framework to support situational tele-mentorship of rural and remote practice. *Med Teach*. 2023;45(6):642-649.

    doi: 10.1080/0142159X.2022.2150607

ACCSCIENCE PUBLISHING

Global Translational Medicine

ORIGINAL RESEARCH ARTICLE

Effects of high-calorie diet-induced visceral obesity on reproductive hormones and muscle tissues in male and female Wistar rats

Tatyana A. Mityukova*, Anastasia A. Basalai*, Olga Y. Poluliakh, and Tatyana E. Kuznetsova

Department of Laboratory of Biomedical Technologies and Medical Rehabilitation, Institute of Physiology, National Academy of Sciences of Belarus, Minsk, Republic of Belarus

Abstract

Overweight and obesity are associated with alterations in the reproductive system, which affect the anabolic supply to peripheral muscle tissues. The study aimed to investigate the effects of a high-calorie diet (HCD) on the development of obesity, reproductive hormone levels, and morphofunctional characteristics of muscle tissues in Wistar rats (i.e., 54 sexually mature male and female Wistar rats) for 16 weeks. Male rats fed with an HCD displayed (i) visceral obesity and hypogonadism, (ii) a decrease in the mass of the musculus triceps surae, (iii) increased levels of total protein, cholesterol, glucose, lactate, lactate dehydrogenase, and malonic dialdehyde (MDA) and superoxide dismutase (SOD) activities, and (iv) stable concentrations of estradiol and testosterone in the muscle tissues. In contrast, female rats fed with HCD displayed (i) visceral obesity, (ii) alterations in reproductive hormones toward hyperandrogenism, (iii) decreased metabolism in the muscle tissues, and (iv) increased levels of estradiol and MDA (without SOD activation). The cross-sectional area of the muscle fiber was significantly reduced by 20% in male and 44% in female rats on HCD. In addition, the total muscle edema was reportedly increased by twofold in both male and female rats. In summation, obese male and female rats developed an imbalance of reproductive hormones and alterations in muscle tissue metabolism.

Keywords: Visceral obesity; High-calorie diet; Reproductive hormones; Muscle metabolism; Male and female Wistar rats

***Corresponding authors:**
Tatyana A. Mityukova (mityukovat@gmail.com)
Anastasia A. Basalai (anastasiya.basalay@gmail.com)

Citation: Mityukova TA, Basalai AA, Poluliakh OY, Kuznetsova TE. Effects of high-calorie diet-induced visceral obesity on reproductive hormones and muscle tissues in male and female Wistar rats. *Global Transl Med*. 2024;3(1):2321. https://doi.org/10.36922/gtm.2321

Received: November 27, 2023
Accepted: March 6, 2024
Published Online: March 21, 2024

1. Introduction

Obesity is an escalating global epidemic due to the availability of high-calorie diets (HCDs) and decreased physical activity in the general population. Obesity is a complex multifactorial disease that leads to the development of several comorbidities (e.g., metabolic syndrome [MS], type 2 diabetes mellitus, and fatty hepatosis).[1] In addition, obesity affects the reproductive system and, consequently, the other systems of the body, as reproductive hormones are involved not only in the development and function of the reproductive system but also in the peripheral tissues and central nervous system.[2] The prevalence of overweight and obesity among men and women varies by country and region. Hypogonadism has been reported in obese men and is characterized

by decreased levels of testosterone, luteinizing hormone (LH), and sex hormone-binding globulin.[2] In contrast, obesity affects the health and metabolism of females and their offspring.[3] Along with reproductive hormones, corticosterone plays an important role in the pathogenesis of obesity and MS.[4] Notably, obesity also affects the condition of muscle tissues and can lead to progressive skeletal muscle atrophy and sarcopenia, as well as decreased muscle mass and strength.[5,6] MS may be caused by decreased levels of anabolic hormones and increased oxidative stress, correlating to MS and mitochondrial dysfunction in obesity.[5] Mitochondrial dysfunction by oxidative stress results in excessive reactive oxygen species (ROS) generation, and the overproduction of ROS (exceeding the cellular antioxidant defense) damages the cellular macromolecules and affects cellular functions and viability.[7] Given the multifaceted effects of obesity, it is of particular interest to further investigate these effects in relation to gender, reproductive hormone levels, muscle tissue condition, and their combined association.[8]

Therefore, this study aimed to investigate the effects of HCD on the development and progression of obesity, reproductive hormone levels, and morphofunctional characteristics in the muscle tissues of both male and female Wistar rats.

2. Methods

2.1. Animals and diets

The study was conducted on 2-month-old sexually mature male and female Wistar rats. These rats were bred in-house in a certified vivarium at the Institute of Physiology of the National Academy of Sciences of Belarus. The rats were kept under a 12/12 h light/dark cycle at a temperature of 22 ± 2°C and humidity of 60–65%. The male (n = 27) and female (n = 27) Wistar rats were randomly divided into two experimental groups: control and HCD. The control group, consisting of 13 male and 14 female Wistar rats, received the standard diet (StD). The HCD group, comprising 14 male and 13 female Wistar rats, was given an HCD for 16 weeks.

The HCD consisted of StD supplemented with animal fats (lard) (45% daily caloric content) and 10% fructose solution (instead of water) *ad libitum*.[9] The caloric content of StD for each rat was 150 kcal/day (i.e., the normal diet at the vivarium of the Institute of Physiology of the National Academy of Sciences of Belarus). In contrast, the caloric content of HCD for each rat was 228 kcal/day.

This study was approved by the Bioethics Committee of the Institute of Physiology of the National Academy of Sciences of Belarus (protocols No.:1 on January 22, 2021, and No:2 on February 2, 2022) and was conducted in accordance with the guidelines set forth by the European Convention for the Protection of Vertebrate Animals (ETS No. 123).

The rats were euthanized through decapitation with prior anesthesia (sodium thiopental). Female rats were euthanized in the diestrus phase of the estrous cycle, determined by the type of cells present in the rat vaginal swab.[10]

The body weight of the rats was measured on a weighing scale (Saturn ST-KS7230, China). After euthanasia, the blood and tissues (i.e., visceral fat and musculus triceps surae) of the rats were collected and weighed on a laboratory weighing scale (Scout Pro, China). For the male rats, the visceral fat mass included the paranephral and epididymal fat deposits. For the female rats, the visceral fat mass included the paranephral and periovarian fat deposits. Mass coefficients (MCs) of the organs and tissues were calculated using the following formula:

$$MC = (\text{Organ mass/body weight}) \times 100\% \quad (I)$$

2.2. Biochemical and hormonal parameters

Biochemical parameters were measured from the serum and muscle tissue homogenates of rats (1/10 dilution in 0.1 M sodium phosphate buffer, pH 7.4) on a biochemical automatic analyzer BS-200 (SHENZHEN MINDRAY Bio-Medical Electronics Co., LTD., China) and with commercial kits, including DiaSens (Production unitary enterprise "Diasens," Republic of Belarus) and Lactat-Vital (Vital Development Corporation, Russia). Quality control was maintained using commercial control sera (Randox Laboratories Ltd., UK). Testosterone, estradiol, corticosterone, and LH levels were determined from the serum using Hema commercial kits (Xema Co., Russia). Testosterone, estradiol, and malondialdehyde (MDA) levels were also determined from muscle tissue homogenates (1/10 dilution in 0.1 M sodium phosphate buffer, pH 7.4). MDA and superoxide dismutase (SOD) activities were determined spectrophotometrically through reaction with thiobarbituric acid[11] and the inhibition of adrenaline autooxidation,[12] respectively.

2.3. Morphological analysis

For morphological analysis, fragments of the musculus triceps surae were subjected to rapid freezing in a cryostat. Several 7 μm thick slices were made using the HM525 Cryostat (MICROM International GmbH, Germany) and stained with hematoxylin and eosin. The slides were examined using the LUM-1 light microscope equipped with a digital camera (Altami LLC, Russia). The ImageJ software was used for morphometric analysis. On the digitized images, eight to ten transversely cut fibers were

traced in each field of view in the Image J program using the "Freehand selection" tool. Measurements were made in ten fields of view at ×400 magnification. The pixels were converted into metric units (μm) using the coefficient obtained during calibration of the measuring system. On the digitized images, areas of edema were also traced using the "Freehand selection" tool in the Image J program and presented as a percentage of the field of view. Measurements were performed at ×400 magnification in ten fields of view.

2.4. Statistical analysis

Statistical analysis was performed using Statistica 10.0. Normality was defined with the Shapiro-Wilk test. Parametric variables were expressed as mean ± standard deviation (M ± SD) and analyzed with Student's *t*-test. The non-parametric variables were expressed as median and the 25th and 75th percentiles (Me [25; 75]), and the variables were analyzed using the Mann–Whitney U-test. For all statistical tests, $P < 0.05$ was considered significant.

3. Results

3.1. Mass-metric parameters

We observed that the body weight of male and female rats in the HCD group did not significantly differ from those in the control group (Table 1). The mass and MC of visceral adipose tissues were significantly increased in male and female rats in the HCD group, indicating visceral obesity in the rats (Table 1). Notably, the increase in body weight was less pronounced in the obese female rats than in the obese male rats. However, the proportion of visceral adipose tissue per total body weight was comparable in obese male and female rats.

3.2. Biochemical and hormonal parameters of blood

Biochemical analysis of the serum from male and female rats with HCD-induced obesity revealed biochemical alterations associated with liver and pancreatic dysfunction (Table 2), of which the findings were consistent with the previous studies.[13,14] After prolonged HCD, alterations in lipid metabolism were detected in the male rats and not in the female rats.

Obese male rats reported a significant decrease in the serum levels of testosterone and estradiol by 3 and 1.5 times, respectively, compared to the control group ($P = 0.047$ and $P = 0.031$, respectively). In addition, the testosterone/estradiol ratio decreased by approximately twofold (Table 2). In contrast, obese female rats exhibited a significant increase in testosterone of approximately 60 times higher than the female rats in the control group ($P = 0.016$). Notably, obese female rats displayed hormonal imbalance toward hyperandrogenism (Table 2). Blood corticosterone levels were reportedly unchanged in obese male rats but were significantly increased in obese female rats. The increase in blood corticosterone levels in the obese female rats was approximately 1.5 times higher than reported in the female rats of the control group ($P = 0.026$) (Table 2).

3.3. Morphological and metabolic parameters of the musculus triceps surae

Male rats in the HCD group displayed a significant decrease in the mass and MC of the musculus triceps surae compared to the control group. In contrast, female rats in the HCD group displayed a slight decrease in the mass and MC of musculus triceps surae compared to the control group (Table 1).

The histostructure of the musculus triceps surae of male and female rats in the control group corresponded to the structure of a normal musculus triceps surae[15] (Figures 1A and B & 2A and B for male and female rats, respectively).

Table 1. Mass and mass coefficients (MC) of organs and tissues of the experimental animals

Index	Male rats		Female rats	
	Control (n = 13)	HCD (n = 14)	Control (n = 14)	HCD (n = 13)
Body mass before the experiment (g)	230.69 ± 19.71	229.43 ± 25.54	224.79 ± 14.82	228.31 ± 6.52
Body mass after 8 weeks of experiment (g)	358.69 ± 44.27	384.36 ± 73.72	289.86 ± 16.07	281.31 ± 43.07
Body mass after 16 weeks of experiment (g)	433.46 ± 48.38	471.14 ± 94.11	310.93 ± 25.43	316.31 ± 72.07
Mass of visceral adipose tissue (g)	7.99 ± 2.64	22.99 ± 11.97***	8.86 ± 4.86	17.22 ± 9.07##
MC of the visceral adipose tissue (%)	1.82 ± 0.49	4.64 ± 1.67****	2.78 ± 1.31	5.15 ± 2.11##
Mass of the musculus triceps surae (g)	2.64 ± 0.33	2.34 ± 0.35 *	1.93 ± 0.17	1.81 ± 0.45
MC of the musculus triceps surae (%)	0.61 ± 0.05	0.51 ± 0.07****	0.62 ± 0.07	0.58 ± 0.11

Notes: Data are presented as mean±standard deviation; statistically significant differences between the male HCD and male control groups at *$P < 0.05$, **$P < 0.01$, ***$P < 0.001$, and ****$P < 0.0001$; statistically significant difference between the female HCD and female control groups at ##$P < 0.01$.
Abbreviation: HCD: High-calorie diet.

Table 2. Biochemical and hormonal parameters of serum of the experimental animals

Index	Male rats		Female rats	
	Control (n = 13)	HCD (n = 14)	Control (n = 14)	HCD (n = 13)
Total bilirubin (μmol/l)	1.40 (1.20; 1.60)	2.40 (1.60; 3.00)**	2.30 (2.10; 2.90)	3.60 (2.40; 4.20)$^{\#}$
Aspartate aminotransferase (U/l)	196.00 (181.00; 217.00)	172.00 (146.00; 189.00)*	162.00 (144.00; 185.00)	159.00 (129.00; 164.00)
Alanine aminotransferase (U/l)	65.00 (62.00; 74.00)	57.50 (51.00; 68.00)	54.00 (43.00; 67.00)	36.00 (33.00; 41.00)$^{\#\#}$
Alkaline phosphatase (U/l)	373.00 (333.00; 423.00)	674.50 (371.00; 850.00)**	276.50 (219.00; 392.00)	496.00 (365.00; 661.00)$^{\#\#\#}$
Urea (mmol/l)	6.83 (6.45; 8.40)	4.35 (3.45; 4.77)****	6.35 (5.83; 6.73)	3.66 (3.37; 4.21)$^{\#\#\#\#}$
Glucose (mmol/l)	5.81 (5.61; 7.37)	7.54 (7.10; 8.21)**	6.88 (6.07; 7.21)	7.80 (7.24; 8.03)$^{\#}$
Alpha amylase (U/l)	1508 (1426; 1712)	1940 (1788; 2124)***	1556 (1418; 1748)	1758 (1580; 1860)$^{\#}$
Cholesterol (mmol/l)	1.43 (1.23; 1.61)	1.88 (1.50; 1.95)**	1.62 (1.47; 1.77)	1.67 (1.36; 1.90)
Triglycerides (mmol/l)	0.88 (0.63; 1.18)	1.18 (0.94; 2.21)*	1.37 (0.84; 1.80)	0.96 (0.66; 2.47)
Estradiol (nmol/l)	0.65 (0.50; 0.76)	0.43 (0.19; 0.62)*	0.39 (0.35; 0.43)	0.41 (0.39; 0.45)
Testosterone (nmol/l)	7.78 (5.35; 24.70)	2.73 (2.11; 5.22)*	0.01 (0.00; 0.28)	0.62 (0.10; 1.36)$^{\#}$
Testosterone/estradiol ratio	12.61 (8.44; 31.95)	7.30 (4.03; 23.25)	0.03 (0.03; 0.64)	1.46 (0.18; 4.61)$^{\#}$
Luteinizing hormone (IU/l)	0.30 (0.09; 0.73)	0.70 (0.27; 4.15)	0.81 (0.17; 2.08)	0.55 (0.40; 1.06)
Corticosterone (nmol/l)	727.60 (489.70; 1013.80)	817.20 (565.50; 1027.60)	655.10 (264.20; 741.30)	1020.30 (898.50; 1050.70)$^{\#}$

Note: Data are presented as median (25th percentile; 75th percentile); statistically significant differences between the male HCD and male control groups at *P < 0.05, **P < 0.01, ***P < 0.001, and ****P < 0.0001; statistically significant differences between the female HCD and female control groups at $^{\#}P$ < 0.05,$^{\#\#}P$ < 0.01, $^{\#\#\#}P$ < 0.001, and $^{\#\#\#\#}P$ < 0.0001.
Abbreviation: HCD: High-calorie diet.

Male rats in the HCD group exhibited pronounced changes in the structure of the musculus triceps surae, as observed from the mosaic pattern in Figure 1C and D. Moreover, edema was observed predominantly in the muscle fiber itself, causing it to acquire a cellular or ring-like shape. Lysis of contractile elements was detected in some muscle fibers, and moderate inflammatory infiltration was observed in the epimysium. Lipid inclusions were also detected in the perimysium (Figure 1D). In contrast to the male rats in the HCD, the structure of the musculus triceps surae of female rats in the HCD group had more pronounced interstitial edema and inflammatory infiltration, indicating significant trophic disturbances in the myocytes (Figure 2C and D).

There was a significant decrease in median muscle fiber area in obese male rats by 20% and in obese female rats by 44% compared with the control rats, while the total edema area increased in both obese male and female rats by approximately twofold (Table 3).

Biochemical parameters measured from the muscle tissue homogenates of the rats are presented in Table 4. Obese male rats had a significant increase in total protein (TP) (P = 0.020), cholesterol (P = 0.031), glucose (P = 0.003), lactate (P = 0.006), and lactate dehydrogenase (LDH) activity (P = 0.002) in the musculus triceps surae compared to the control group, indicating an increase in energy substrates and glycolysis. In contrast, obese female rats had a significant decrease in TP (P = 0.021), cholesterol

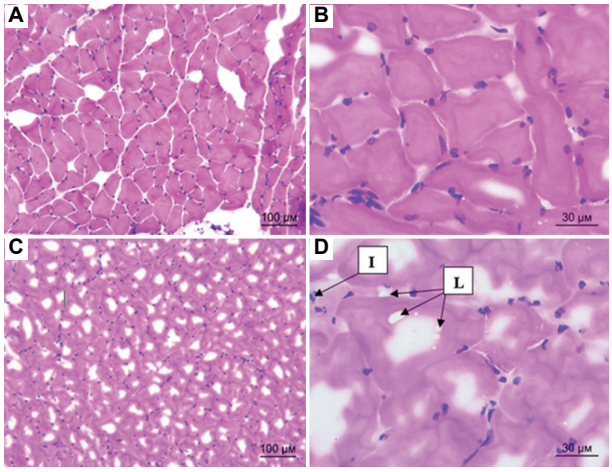

Figure 1. Histostructure of the hematoxylin-eosin-stained musculus triceps surae of male rats from the (A and B) control and (C and D) HCD groups. Magnification: (A and C) ×100 and (B and D) ×400.
Abbreviation: HCD: High-calorie diet; I: Inflammatory infiltration; L: Lipid inclusions.

(P = 0.048), lactate (P = 0.046), and creatine kinase (CK) activity (P = 0.004) in the musculus triceps surae compared to the control group. Despite the absence of sarcopenia, the results indicated a slight decrease in metabolic processes for obese female rats (Table 4).

Obese male rats also displayed an increase in MDA levels by 25%, whereas obese female rats displayed an increase

Table 3. The cross-sectional area of muscle fibers and total edema area in rat muscle tissues based on morphological analysis

Index	Male rats		Female rats	
	Control (n = 13)	HCD (n = 14)	Control (n = 14)	HCD (n = 13)
Muscle fiber area (μm^2)	1547 (1198; 2074)	1249 (859; 1694)****	1878 (1397; 2544)	1060 (851; 1420)####
Total edema area (%)	4.03 (3.12; 4.95)	11.13 (9.42; 12.07)****	4.40 (3.00; 7.77)	10.68 (8.02; 13.16)####

Note: Data are presented as median (25th percentile; 75th percentile); statistically significant difference between the male HCD and male control groups at ****P<0.0001; statistically significant difference between the female HCD and female control groups at ####P<0.0001.
Abbreviation: HCD: High-calorie diet.

Table 4. Biochemical parameters in the musculus triceps surae tissues of the experimental animals

Index	Male rats		Female rats	
	Control (n = 13)	HCD (n = 14)	Control (n = 14)	HCD (n = 13)
Total protein (mg/g tissue)	46.20 (41.00; 48.60)	51.10 (47.40; 53.80)*	62.60 (61.90; 62.80)	60.30 (54.80; 61.40)#
Cholesterol (μmol/g tissue)	1.00 (0.90; 1.10)	1.10 (1.00; 1.20)*	0.77 (0.69; 0.84)	0.62 (0.61; 0.79)#
Triglycerides (μmol/g tissue)	12.90 (9.30; 17.70)	14.95 (13.30; 16.10)	9.30 (7.70; 12.60)	11.90 (8.70; 14.10)
Glucose (μmol/g tissue)	1.70 (1.60; 2.00)	2.30 (1.90; 2.50)**	2.79 (2.61; 2.97)	2.85 (2.72; 2.99)
Lactate (μmol/g tissue)	30.49 (26.62; 33.80)	38.94 (34.67; 48.02)**	45.30 (39.80; 51.90)	41.20 (31.90; 45.20)#
Lactate dehydrogenase (U/g tissue)	619.00 (584.00; 688.00)	808.50 (748.00; 922.00)**	772.00 (746.00; 834.00)	685.00 (655.00; 765.00)
Creatine kinase (U/g tissue × 10^3)	7.80 (6.19; 8.72)	7.89 (7.39; 8.77)	5.25 (4.72; 7.05)	4.28 (3.57; 4.41)##
Malonic dialdehyde (μmol/g tissue)	18.88 (17.21; 20.51)	23.69 (20.54; 28.73)**	23.79 (6.39; 46.01)	40.76 (34.00; 63.97)#
Superoxide dismutase (U/ml)	36.21 (31.49; 42.30)	46.93 (42.67; 49.89)**	36.57 (32.14; 40.25)	33.82 (32.39; 37.64)

Note: Data are presented as median (25th percentile; 75th percentile); statistically significant differences between the male HCD and male control groups at *P < 0.05 and **P < 0.01; statistically significant differences between the female HCD and female control groups at #P < 0.05 and ##P < 0.01.
Abbreviation: HCD: High-calorie diet.

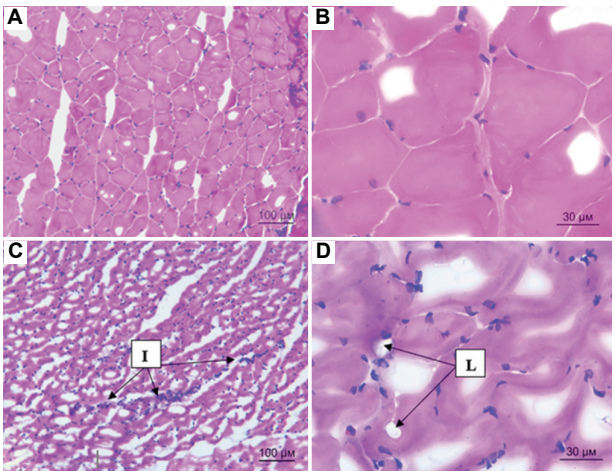

Figure 2. Histostructures of the hematoxylin-eosin-stained musculus triceps surae of female rats from the (A and B) control and (C and D) HCD groups. Magnification: (A and C) ×100 and (B and D) ×400.
Abbreviation: HCD: High-calorie diet; I: Inflammatory infiltration; L: Lipid inclusions.

in MDA levels by approximately twofold compared to the control group (P = 0.029). SOD activity was significantly increased in male rats of the HCD group but remained unchanged in female rats of the HCD group (Table 4).

It has been reported that changes in metabolic processes in the muscle tissue can be associated with anabolic hormones in the blood and muscle tissues (from extragonadal synthesis).[8] Based on this information, estradiol and testosterone were determined in muscle tissue homogenates from male and female rats. The level of testosterone and estradiol in the muscle tissue of male rats did not change regardless of the type of diet (Table 5). However, there was a significant increase in the concentration of estradiol in the musculus triceps surae of obese female rats (P = 0.003), and the estradiol level in the musculus triceps surae of female rats from both groups was higher than in the male rats. The testosterone levels in the musculus triceps surae of male and female rats of all experimental groups were comparable.

4. Discussion

The HCD used in this study included excessive amounts of fats and carbohydrates to mimic overnutrition in a human diet that promotes obesity and MS.[16] Obesity studies were often performed on male rats, leading to a lack of information on the sexual dimorphism exhibited in diet-induced obesity. Maric *et al.* indicated that female rats, compared to male rats, would gain body weight

Table 5. Testosterone and estradiol levels in the musculus triceps surae tissues of the experimental animals

Index	Male rats		Female rats	
	Control (n = 13)	HCD (n = 14)	Control (n = 14)	HCD (n = 13)
Testosterone (nmol/g tissue)	72.19 ± 15.95	68.91 ± 13.44	74.51 ± 9.96	71.47 ± 9.54
Estradiol (nmol/g tissue)	40.60 ± 10.52	41.18 ± 9.24	133.55 ± 11.82	146.83 ± 8.13$^{\#\#}$

Note: Data are presented as mean±standard deviation; statistically significant difference between the female HCD and female control groups at $^{\#\#}P < 0.01$.
Abbreviation: HCD: High-calorie diet.

more slowly and have fewer metabolic complications with overnutrition.[17] Taraschenko *et al.* reported that males were more prone to obesity than females when given HCD.[18] Besides that, Chukijrungroat *et al.*[19] and several other studies[20] validated the hepatoprotective role of female reproductive hormones. Notably, our study demonstrated that lipid metabolism was not impaired in obese female rats.

It is known that obesity can lead to male hypogonadism, but the underlying mechanism remains unclear. Diet-induced obesity could reportedly reduce sperm motility, relative testicular and testicular appendage mass ratios, and plasma levels of testosterone and LH in mice.[20] In addition, obese rodents often display a significant decrease in the expression of *GnRH, Kiss1, GpR54*, and *Ob-R* genes in the hypothalamus, potentially contributing to the development of male hypogonadism.[21,22] The results of our study indicated a significant decrease in testosterone levels and testosterone/estradiol ratio in obese male Wistar rats, the finding of which is consistent with the previous clinical observations and experimental studies.

The female reproductive health is known to be markedly impaired in obesity. A high-fat diet can significantly increase the body weight and earlier onset of puberty in female rats. Likewise, estrus cycling is commonly impaired due to a significant decrease in the expression of ovulation-related genes.[23] Our data indicated a pronounced increase in the level of testosterone in the blood of female rats, significantly altering the natural estrogen-androgen balance. Polycystic ovary syndrome is often observed in obese female rats and is characterized by elevated blood testosterone levels.[24] Moreover, androgenic-anabolic steroids can significantly increase body weight and lipid peroxidation[25] and decrease the antioxidant levels in female rats.[26] Nonetheless, a significant increase in serum testosterone levels in females consuming HCD can significantly exacerbate the effects of diet-induced obesity.

Insulin-mediated glucose uptake in skeletal muscle *in vivo* and *in vitro* is reduced in obesity.[27] For lipid metabolism, there is an increased uptake and accumulation of fatty acids and decreased intensity of lipolysis. In addition, fatty acid oxidation may increase until complete oxidation as β-oxidation is enhanced in obesity, indicating mitochondrial dysfunction.[27] Our findings demonstrated that obese male rats had an increase in TP, cholesterol, glucose, lactate, and LDH activity, implying the increased flow of lipids and glucose from the bloodstream into the muscle tissues, as well as the activation of glucose metabolism. This finding was consistent with the results of recent studies that indicated signs of impaired metabolic flexibility in skeletal muscle in obesity.[27]

There is currently a lack of reports on the biochemical changes in the muscle tissues of obese female rats. Interestingly, obese female rats displayed a significant decrease in TP, cholesterol, lactate, and CK activity in the muscle tissues, indicating a reduction in metabolic processes. Our morphological analysis demonstrated the development of intracellular edema and inflammatory infiltration in the muscle tissue of obese male and female rats. In the obese rats, the cross-sectional area of muscle fibers was significantly reduced, while the total edema area increased. There was a significant increase in lipid peroxidation in obese female rats, but not in the obese male rats that displayed SOD activation, providing them with antioxidant protection. According to a study, mice lacking Cu-Zn-SOD exhibited oxidative stress and loss of muscle mass.[28]

The functional importance of sex steroid hormones (androgens and estrogens) synthesized in extragonadal tissues is widely recognized.[8] The circulating dehydroepiandrosterone (DHEA) in the bloodstream can be taken up by tissues and converted to testosterone when appropriate enzymes, such as 3-beta-hydroxysteroid dehydrogenase (HSD) and 17-beta-HSD, are present. Testosterone is then irreversibly converted to estrogens by cytochrome P-450 aromatase (P450arom).[8] This mechanism increases the production of anabolic hormones in the skeletal muscle of rats during exercise.[29,30] Our findings confirmed the presence of locally synthesized hormones (i.e., testosterone and estradiol) in the muscle tissue of male and female rats. The local synthesis of androgens and estrogens in the muscle tissue of male rats presumably provides a compensatory anabolic effect

against obesity-related hypogonadism. Moreover, the localized hormonal synthesis in female rats compensates for the low serum testosterone concentrations in the blood under normal conditions. Taken together, the localized hormonal synthesis stimulates functional muscle activity in both male and female rats.

In obese male rats, we hypothesized several factors that could decrease muscle mass and muscle fiber area, including insulin resistance, inability to adapt to excessive energy substrates, and decreased serum testosterone levels. In contrast, the decrease in muscle mass and muscle fiber area in female rats could be affected by increasing interstitial edema, decreased metabolic processes, and more pronounced oxidative stress associated with insufficient SOD activity.[28]

5. Conclusion

A 16-week HCD leads to visceral obesity in male and female rats. Blood biochemical analyses demonstrated biochemical changes associated with liver and pancreatic dysfunction in obese male and female rats. Obese male rats displayed a significant decrease in serum testosterone levels, whereas obese female rats displayed hormonal imbalance toward hyperandrogenism and increased blood corticosterone levels.

In addition, the decrease in musculus triceps surae mass was most pronounced in obese male rats. The structure of the musculus triceps surae revealed changes in the form of edema, lysis of contractile elements, inflammatory infiltration, and lipid inclusions in obese male and female rats, but the effects were more pronounced in obese female rats. Likewise, the cross-sectional area of the muscle fibers was reduced and the total edema area was increased in both obese male and female rats.

In obese male rats, an increase in energy substrates and glycolysis in muscle tissue were observed. In comparison, obese female rats reported a decrease in metabolic processes and a significant increase in oxidative stress in the muscle tissue.

Our findings also reported unchanged levels of testosterone and estradiol in muscle tissue of male rats regardless of the diet, whereas the level of estradiol in muscle tissue of obese female rats significantly increased compared to the female rats of the control group.

Taken together, this study evaluated the relationship between reproductive hormones and muscle condition in obese male and female rats, and the findings demonstrated that the changes in the muscle tissues of obese male and female rats were more closely associated with metabolic disorders and increased lipid peroxidation in the muscle tissues instead of anabolic hormones.

Acknowledgments

None.

Funding

The work was supported by the State Program for Scientific Research (No.:4.1.1.5) of the National Academy of Sciences of Belarus.

Conflict of interest

The authors declare that they have no competing interests.

Author contributions

Conceptualization: Tatyana A. Mityukova
Formal analysis: Anastasia A. Basalai, Olga Y. Poluliakh, Tatyana E. Kuznetsova
Investigation: Anastasia A. Basalai, Olga Y. Poluliakh, Tatyana E. Kuznetsova
Methodology: All authors
Writing – original draft: Tatyana A. Mityukova
Writing – review & editing: All authors

Ethics approval and consent to participate

This study was approved by the Bioethics Committee of the Institute of Physiology of the National Academy of Sciences of Belarus (protocols No.:1 on January 22, 2021, and No.:2 on February 2, 2022) and conducted in accordance with the guidelines set forth by the European Convention for the Protection of Vertebrate Animals (ETS No. 123).

Consent for publication

Not applicable.

Availability of data

The datasets used and/or analyzed during the present study are available from the Institute of Physiology of the National Academy of Sciences of Belarus, upon reasonable and justifiable request in accordance with the rules and procedures of the Institute of Physiology of the National Academy of Sciences of Belarus (https://physiology.by/or biblio@fizio.bas-net.by).

References

1. WHO. *Report Highlights the Dangers of Obesity*. Available from: https://www.hps.scot.nhs.uk/publications/hps-weekly-report/volume-56/issue-18/who-report-highlights-the-dangers-of-obesity [Last accessed on 2023 Sep 05].
2. Lainez NM, Coss D. Obesity, neuroinflammation, and reproductive function. *Endocrinology*. 2019;60:2719-2736. doi: 10.1210/en.2019-00487

3. Brion MJA, Ness AR, Rogers I, *et al.* Maternal macronutrient and energy intakes in pregnancy and offspring intake at 10 y: Exploring parental comparisons and prenatal effects. *Am J Clin Nutr*. 2010;91:748-756.

doi: 10.3945/ajcn.2009.28623

4. Akalestou E, Genser L, Rutter GA. Glucocorticoid metabolism in obesity and following weight loss. *Front Endocrinol (Lausanne)*. 2020;11:59.

doi: 10.3389/fendo.2020.00059

5. Tomlinson DJ, Erskine RM, Morse CI, *et al.* The impact of obesity on skeletal muscle strength and structure through adolescence to old age. *Biogerontology*. 2016;17:467-483.

doi: 10.1007/s10522-015-9626-4

6. Godoy-Matos AF, Silva Junior WS, Valerio CM. NAFLD as a continuum: From obesity to metabolic syndrome and diabetes. *Diabetol Metab Syndr*. 2020;12:60.

doi: 10.1186/s1309802000570y

7. Prasun P. Mitochondrial dysfunction in metabolic syndrome. *Biochim Biophys Acta*. 2020;1866(10):165838.

doi: 10.1016/j.bbadis.2020.165838

8. Aizawa K, Iemitsu M, Maeda S. Expression of steroidogenic enzymes and synthesis of sex steroid hormones from DHEA in skeletal muscle of rats. *Am J Physiol Endocrinol Metab.* 2007;292(2):E577-E584.

doi: 10.1152/ajpendo.00367.2006

9. Gancheva S, Zhelyazkova-Savova M, Galunska B, *et al.* Experimental models of metabolic syndrome in rats. *Scr Sci Medica*. 2015;47(2):14-21.

doi: 10.14748/ssm.v47i2.1145

10. Marcondes FK, Bianchi FJ, Tanno AP. Determination of the estrous cycle phases of rats: Some helpful considerations. *Braz J Biol*. 2002;62(4A):609-614.

doi: 10.1590/S1519-69842002000400008

11. Стальная ИД, Гаришвили ТГ. Метод определения малонового диальдегида с помощью тиобарбитуровой кислоты. Современные методы биохимии. Москва : Медицина. 1977;66-68. Stalnaya ID, Garishvili TG. Method for the determination of malondialdehyde using thiobarbituric acid. Mod Methods Biochem. Moscow : Medicine. 1977; 66-68. [In Russ].

12. Сирота ТВ. Новый подход в исследовании процесса аутоокисления адреналина и использование его для измерения активности супероксиддисмутазы. *Вопросы медицинской химии*. 1999;3:263-272. Sirota TV. A new approach to the study of the process of autoxidation of adrenaline and its use to measure the activity of superoxide dismutase. *Quest Med Chem*. 1999;3:263-272. [In Russ].

13. *Liver Disorders and Gallstones. Functions of the Liver.* Available from: https://uomustansiriyah.edu.iq/media/lectures/4/4_2019_04_09!05_38_02_PM.pdf [Last accessed on 2023 Sep 07].

14. Matull WR, Pereira SP, O'Donohue JW. Biochemical markers of acute pancreatitis. *J Clin Pathol*. 2006;59(4):340-344.

doi: 10.1136/jcp.2002.002923

15. Mescher AL. *Junqueira's Basic Histology: Text and Atlas*. 12th ed. United States: McGraw-Hill Medical; 2010. p. 480.

16. Parker R. The role of adipose tissue in fatty liver diseases. *Liver Res*. 2018;2(1):35-42.

doi: 10.1016/j.livres.2018.02.002

17. Maric I, Krieger JP, Van der Velden P, *et al.* Sex and species differences in the development of diet-induced obesity and metabolic disturbances in rodents. *Front Nutr*. 2022;9:828522.

doi: 10.3389/fnut.2022.828522

18. Taraschenko OD, Maisonneuve IM, Glick SD. Sex differences in high fat-induced obesity in rats: Effects of 18-methoxycoronaridine. *Physiol Behav*. 2011;103(3-4):308-314.

doi: 10.1016/j.physbeh.2011.02.011

19. Chukijrungroat N, Khamphaya T, Weerachayaphorn J, *et al.* Hepatic FGF21 mediates sex differences in high-fat high-fructose diet-induced fatty liver. *Am J Physiol Endocrinol Metab*. 2017;313(2):E203-E212.

doi: 10.1152/ajpendo.00076.2017

20. Leeners B, Geary N, Tobler PN, *et al.* Ovarian hormones and obesity. *Hum Reprod Update*. 2017;23(3):300-321.

doi: 10.1093/humupd/dmw045

21. Zhai L, Zhao J, Zhu Y, *et al.* Downregulation of leptin receptor and kisspeptin/GPR54 in the murine hypothalamus contributes to male hypogonadism caused by high-fat diet-induced obesity. *Endocrine*. 2018;62(1):195-206.

doi: 10.1007/s12020-018-1646-9

22. Feng J, Xu R, Li Y, *et al.* The effect of high-fat diet and exercise on KISS-1/GPR54 expression in testis of growing rats. *Nutr Metab* (*Lond*). 2021;18(1):1.

doi: 10.1186/s12986-020-00517-0

23. Zhou Q, Chen H, Yang S, *et al.* High-fat diet decreases the expression of Kiss1 mRNA and kisspeptin in the ovary, and increases ovulatory dysfunction in postpubertal female rats. *Reprod Biol Endocrinol*. 2014;12:127.

doi: 10.1186/1477-7827-12-127

24. Khodabandeh S, Hosseini A, Khazali H, *et al.* Interplay between polycystic ovary syndrome and hypothyroidism on serum testosterone, oxidative stress and StAR gene expression in female rats. *Endocrinol Diabetes Metab*. 2022;5(5):e359.

doi: 10.1002/edm2.359

25. Alrabadi N, Al-Rabadi GJ, Maraqa R, *et al*. Androgen effect on body weight and behaviour of male and female rats: Novel insight on the clinical value. *Andrologia*. 2020;52(10):e13730.

doi: 10.1111/and.13730

26. Memudu AE, Dongo GA. A study to demonstrate the potential of anabolic androgen steroid to activate oxidative tissue damage, nephrotoxicity and decline endogenous antioxidant system in renal tissue of Adult Wistar Rats. *Toxicol Rep.* 2023;10:320-326.

doi: 10.1016/j.toxrep.2023.02.010

27. Mengeste AM, Rustan AC, Lund J. Skeletal muscle energy metabolism in obesity. *Obesity (Silver Spring)*. 2021;29:1582-1595.

doi: 10.1002/oby.23227

28. Muller FL, Song W, Liu Y, *et al*. Absence of CuZn superoxide dismutase leads to elevated oxidative stress and acceleration of age-dependent skeletal muscle atrophy. *Free Radic Biol Med*. 2006;40(11):1993-2004.

doi: 10.1016/j.freeradbiomed.2006.01.036

29. Aizawa K, Iemitsu M, Maeda S, *et al*. Acute exercise activates local bioactive androgen metabolism in skeletal muscle. *Steroids*. 2010;75(3):219-223.

doi: 10.1016/j.steroids.2009.12.002

30. Aizawa K, Iemitsu M, Maeda S, *et al*. Endurance exercise training enhances local sex steroidogenesis in skeletal muscle. *Med Sci Sports Exerc*. 2011;43(11):2072-2080.

doi: 10.1249/MSS.0b013e31821e9d74

ACCSCIENCE PUBLISHING

Global Translational Medicine

ORIGINAL RESEARCH ARTICLE

Evaluating machine learning models for prediction of coronary artery disease

Rejath Jose, Anvin Thomas, Jennifer Guo, Robert Steinberg, and Milan Toma*

Department of Osteopathic Manipulative Medicine, College of Osteopathic Medicine, New York Institute of Technology, Old Westbury, New York, United States of America

Abstract

Coronary artery disease (CAD) is a prevailing global health issue and a leading cause of death worldwide. Its accurate and timely diagnosis is crucial for effectively managing the disease and improving patient outcomes. In this study, we conducted a comparative analysis of machine learning (ML)-based approaches to detect and diagnose CAD. A dataset of 918 instances from the UCI ML repository, comprising 11 typical risk factors and CAD predictors, was used for this investigation. The study deployed ML models in Google Colaboratory and PyCaret, testing their efficacy in diagnosing CAD. Our study provides a detailed overview of these ML methodologies, their strengths, and limitations, underscoring the potential of these algorithms to revolutionize CAD diagnosis and treatment. The overall goal of the study is to create a model that can predict the presence or chance of presence of CAD based on different parameters of the patient's history. Findings include the showcased logistic regression model, which was proven to be particularly effective, with an area under curve of 0.88, indicating a high ability to differentiate between patients with and without CAD, and a successful ability to identify clinically key features of CAD such as the presence of exertional angina and chest pain. This study emphasizes the importance of further research in this field to establish ML as a cornerstone of modern healthcare diagnostics.

Keywords: Machine learning; Coronary artery disease; Diagnosis; Predictive modeling; Health informatics; Medical data analysis

***Corresponding author:**
Milan Toma
(tomamil@tomamil.com)

Citation: Jose R, Thomas A, Guo J, Steinberg R, Toma M. Evaluating machine learning models for prediction of coronary artery disease. *Global Transl Med*. 2024;3(1):2669.
https://doi.org/10.36922/gtm.2669

Received: January 8, 2024
Accepted: March 12, 2024
Published Online: March 22, 2024

1. Introduction

Cardiovascular disease (CVD) is the leading cause of morbidity and mortality worldwide and in the United States.[1] In 2019, coronary artery disease (CAD), a complex medical subtype of CVD characterized by plaque buildup in the arteries that supply blood to the heart, accounted for 8.9 million deaths, or 16% of the world's total deaths.[1] In 2021, CAD was responsible for almost 400,000 deaths in the United States and exacted a financial burden of over $200 billion in health-care costs.[2,3] Such statistics maintain the importance of early detection and accurate diagnosis in improving patient prognoses and outcomes.

Coronary angiography is currently the gold standard for the definitive diagnosis of CAD, which uses computed tomography (CT) to visualize the extent of blockage in the coronary arteries. For this procedure, patients are asked to avoid oral intake of food

and water several hours before the scan, and contrast dye is administered to enhance the visibility of coronary vasculature. Administration of angiographic dye has been proven to worsen renal function in patients with underlying kidney disease, which can lead to oliguria and a need for hemodialysis.[4] Other complications associated with CT angiography include arterial dissection, arrhythmia, stroke, and death, on top of the generalized risk of radiation exposure.[5,6] Researchers have started to rely on risk assessment models to overcome the various inconveniences and complications associated with current diagnostic modalities.

The traditional method of CVD risk assessment predicts the likelihood of CVD events over a 10-year period or a lifetime, and it relies on nine modifiable and non-modifiable risk factors such as age, sex, race, blood pressure, cholesterol levels, and smoking behavior to generate a quantitative estimation.[7] Other regression-based tools (Framingham risk score, GRACE score, TIMI score, *etc.*) utilize similar readily retrievable population samples to stratify risk and guide the course and intensity of therapies. While the new 2013 ACC/AHA Pooled Cohort Equations Risk Calculator has made major advancements in providing specific estimates for atherosclerotic CVD (ASCVD),[7] such tools are inherently limited by their reliance on conventional statistical methods. These methods rely on a small subset of risk factors to generalize predictions for much larger and more diverse populations and require manual recalibration with every additional data set. This inevitably leads to both over- and under-estimation of CVD events in certain demographics.[8]

The rapidly emerging field of machine learning (ML) in healthcare has created a new avenue to overcome the limitations of current clinical diagnostic and prediction models.[9,10] ML uses computer algorithms to process large amounts of data to identify patterns not only between the variables and possible outcomes but also relationships between the different variables themselves.[11,12] IBM's Watson has recently been receiving a significant amount of media attention for its focus on precision medicine regarding cancer diagnosis and treatment utilizing combinations of ML and natural language processing capabilities.[13] ML also has a wide range of applications in the advancement of clinical trial research. Through the use of predictive analytics, researchers can determine optimal sample sizes to optimize efficacy and reduce data errors, along with evaluating broader ranges of data.[14] In regards to CAD, ML could account for the multifactorial nature of the pathology by analyzing a variety of populations and novel risk factors, ultimately improving risk calculations at the level of the individual patient.[12,15,16]

Previous literature regarding ML and CAD has shown promising results, especially when compared to traditional risk assessment tools. One study developed an ML Risk Calculator using the same factors as the 2013 ACC/AHA Pooled Cohort Equations Risk Calculator which outperformed the latter by recommending less statin therapy and missing fewer CVD events.[17] ML models developed for both clinical and imaging parameters such as a coronary artery calcium score also increased the predictive power of obstructive CAD.[18,19] Quite impressively, one study utilizing a databank of over 400,000 participants and 450 discrete variables retrospectively discovered new predictors of CVD in the diabetic population where traditional risk calculation tools have been unreliable.[20]

ML has been used to identify the most important features to arrive at a diagnosis of CAD. Studies have agreed that age, male sex, smoking, and number of calcified segments as most useful within their respective models.[20,21] Using these tools, ML can provide a different perspective – it can help identify evidence of CAD in patients without a formal clinical diagnosis.[22] Its utility extends to informing pertinent clinical management, wherein it facilitates the precise categorization of patients necessitating blood pressure-lowering or lipid-lowering interventions,[23] as well as enhances screening efficacy through the incorporation of treadmill exercise test characteristics.[24] An inventive non-invasive technique utilizing iris imaging has shown promise for the early detection of CAD.[25] This approach integrates iridology with digital image processing to analyze features of the iris corresponding to heart health. Involving 198 volunteers, researchers successfully distinguished individuals with CAD from those without, using algorithms to process iris patterns. Their findings suggest that analyzing iris images with a support vector machine classifier can predict CAD with a 93% accuracy rate, presenting a potential alternative to conventional diagnostic methods and paving the way for its application in telemedicine. In addition, recent advances in cardiovascular CT technology, such as multi-slice imaging and photon-counting CT, have significantly improved image resolution and diagnostic capabilities in CVD. Techniques like CT-derived fractional flow reserve offer better detection of myocardial ischemia than standard CT scans. In addition, 3D-printed models and visualization tools like virtual reality are enhancing surgical planning and patient communication. The integration of AI is further boosting the diagnostic accuracy of cardiovascular CT, making it a powerful tool for both diagnosing and predicting cardiovascular conditions.[26,27]

Early detection of CAD is crucial to limit the progression and severity of this pathology, but image-based detection

has many risks and limitations regarding screening large populations. Due to these reasons, along with the recent advancements in artificial intelligence, researchers have been turning to ML prediction models to aid in the early detection of CAD. In our study, we have utilized a vast amount of data, incorporating 918 datasets and evaluated the performance of 14 ML models in accurately detecting and predicting CAD based on 11 factors. By doing so, we aim to contribute to the continuously growing pool of research on artificial intelligence in healthcare and provide insights into the effectiveness of ML models in early CAD detection.

Hence, in this study, the PyCaret Classification Module, a tool for supervised ML, was used to compare various classification models for predicting the presence of CAD. After setting up the data, transforming it, and separating it into training and test sets, the "Compare Models" function in PyCaret trained and evaluated the performance of all available estimators using cross-validation. This process included a scoring grid with average cross-validated scores based on metrics pertinent to classification model evaluation. Out of 14 ML classification models assessed, the logistic regressor model emerged as the most effective, yielding the highest overall performance. The logistic regression model's effectiveness has been appraised against standard metrics such as accuracy, sensitivity, specificity, and the area under the receiver operating characteristic (ROC) curve, indicative of its capability to differentiate the presence or absence of CAD.

2. Materials and methods

2.1. Data collection and processing

A combination of open-source online databases was used to train and test the ML models. Datasets were derived from the UC Irvine ML Repository[5,6,28,29] and were externally curated through "fedesoriano" on Kaggle.com and by the authors. The first dataset comprises information from five discrete heart-related datasets: Cleveland (n = 303), Hungarian (n = 294), Switzerland (n = 123), Long Beach, VA (n = 200), and Stalog (Heart) Data Set (n = 270). This combined dataset included 11 common features and predictors of CAD: age, sex, chest pain type, resting systolic blood pressure, serum cholesterol, fasting blood sugar, resting electrocardiogram (ECG) reading, maximum heart rate, presence of angina during exercise, oldpeak (ST depression induced by exercise relative to rest), and ST sloping. To improve the generalizability of the model, another dataset called "Z-Alizadeh Sani" and its extension were added (n = 303),[5,6] and extraneous variables were removed to form the final dataset comprising variables such as sex, chest pain type, resting blood pressure, cholesterol, fasting blood sugar, resting ECG, and presence of angina during exercise, with the presence or absence of a diagnosis of heart disease as the target variable (Table 1). Age, sex, cholesterol, and exercise angina were represented as binary variables. Age was delineated as above or below the age of 55, sex was categorized based on sex assigned at birth (male or female), cholesterol was stratified with

Table 1. Example of dataset setup

Age	Sex	Chest pain type	Resting BP	Cholesterol	Fasting BS	Resting ECG	Exercise angina	HeartDZ
0	M	ATA	140	1	0	Normal	N	0
0	F	NAP	160	0	0	Normal	N	1
0	M	ATA	130	1	0	ST	N	0
0	F	ASY	138	1	0	Normal	Y	1
0	M	NAP	150	0	0	Normal	N	0
0	M	NAP	120	1	0	Normal	N	0
0	F	ATA	130	1	0	Normal	N	0
0	M	ATA	110	1	0	Normal	N	0
0	M	ASY	140	1	0	Normal	Y	1
0	F	ATA	120	1	0	Normal	N	0
0	F	NAP	130	1	0	Normal	N	0
1	M	ATA	136	0	0	ST	Y	1
0	M	ATA	120	1	0	Normal	N	0
0	M	ASY	140	1	0	Normal	Y	1
0	F	NAP	115	1	0	ST	N	0
0	F	ATA	120	1	0	Normal	N	0

Abbreviations: ASY: Asymptomatic, ATA: Atypical angina, BP: Blood pressure, BS: Blood sugar, ECG: Electrocardiogram, F: Female, M: Male, N: No, NAP: Non-anginal pain, ST: ST segment abnormality, Y: Yes.

a cutoff of 200 mg/dL, and exercise-induced angina was categorized as either "yes" or "no," depending on the presence or absence of chest pain during exertion.

Chest pain type and resting ECG were categorical variables with multiple choices. Chest pain type was categorized as typical (TA), atypical (ATA), non-anginal pain (NAP), and asymptomatic (ASY). Resting ECG was categorized as normal, ST for having ST-T wave abnormalities (T wave inversions and/or ST elevation or depression of >0.05 mV), and left ventricular hypertrophy if patients showed probable or definite left ventricular hypertrophy by Estes' criteria. Some variables from the separate datasets were excluded due to variations in data collection and if they differed between datasets. The nine variables mentioned above were common across all three datasets.

2.2. PyCaret setup

PyCaret Classification Module is a supervised ML tool for predicting categorical class labels, particularly discrete and unordered ones. It handles binary and multiclass problems adeptly, finding applications in diverse scenarios. The standard PyCaret classification workflow involves five key steps: set up, compare models, analyze model, save model, and predict. The initial step, "set up," establishes the training environment and constructs a transformation pipeline. This stage requires two essential parameters, "data" and "target," with additional optional parameters for customization. The user organizes the data cohesively, ensuring that the target variable is appropriately labeled. The data, supplied in comma-separated values (CSV) format, conforms to a binary classification model, where the target is numerically represented (0 for no diagnosis of heart disease, and 1 for the presence of heart disease).

Experiment-level details for the ML classification model are displayed in Table 2**.** The session ID is a pseudo-random number (000 in this case) used as a seed for reproducibility in all functions throughout the PyCaret pipeline. It ensures that the same results can be obtained when running the same code with the same session ID. The target refers to the column in the dataset (the CSV file) that will be predicted. In this case, the target is named "HeartDZ." The target type specifies the nature of the target variable, which, in this case, is "Binary;" this means that the target variable has an output of either 1 (presence of heart disease) or 0 (absence of heart disease). The original data shape shows the dimensions of the dataset before any transformations, with 1049 rows and eight columns, meaning that there were 1049 individual patients, and there were nine parameters (age, sex, chest pain type, resting blood pressure, cholesterol, fasting blood sugar, resting ECG, exercise angina, and HeartDZ). The transformed data shape has 1049 rows and 14 columns as the categorical variables (chest pain type and resting ECG) were converted to binary outputs depending on the number of categories present. For example, chest pain was converted from one column to four columns, and resting ECG was converted from one column to three columns; altogether, there are 14 columns (age, sex, chest pain type ASY, chest pain type NAP, chest pain type ATA, chest pain type TA, resting blood pressure, cholesterol, fasting blood sugar, resting ECG of left ventricular hypertrophy, resting ECG Normal, resting ECG ST, exercise angina, and HeartDZ). The transformed train set shape indicates that the training dataset contains 734 observations after preprocessing (~70% of the total dataset) used to train the ML models. The transformed test set shape indicates that the test dataset contains 315 observations after preprocessing (~30% of the total dataset) used to evaluate the performance of the trained models.

Table 2. Experiment setup details

Description	Value
Session ID	000
Target	HeartDZ
Target type	Binary
Original data shape	1049,9
Transformed data shape	1049,14
Transformed train set shape	734,14
Transformed test set shape	315,14
Preprocess	True

The original dataset was transformed through the addition of several preprocessing steps, including simple imputer (1st step), simple imputer (2nd step), ordinal encoder, and one-hot encoder. The simple imputer (1st and 2nd steps) is employed to address missing values in the dataset. The ordinal encoder transforms categorical variables with an ordinal relationship into numerical values by replacing categories with integers. Finally, the one-hot encoder converts categorical variables into binary vectors. Figure 1 illustrates the dataset's progression before undergoing training with the classification models in PyCaret.

The "Compare Models" function trains and evaluates the performance of all available estimators using cross-validation, providing a scoring grid with average cross-validated scores. For analyzing the performance of a trained model on the test set, the "plot_model" function can be used. It offers different plot types, such as confusion matrix and area under the ROC curve (AUC), for assessing model performance. In some cases, re-training the model may be required for plotting specific visualizations. Figure 2 shows a summary of the workflow for this study.

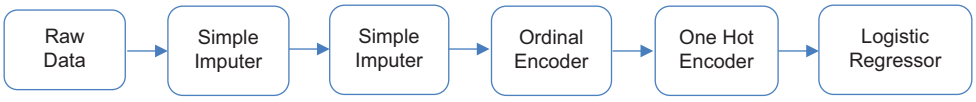

Figure 1. Preprocessing pipeline for logistic regressor model.

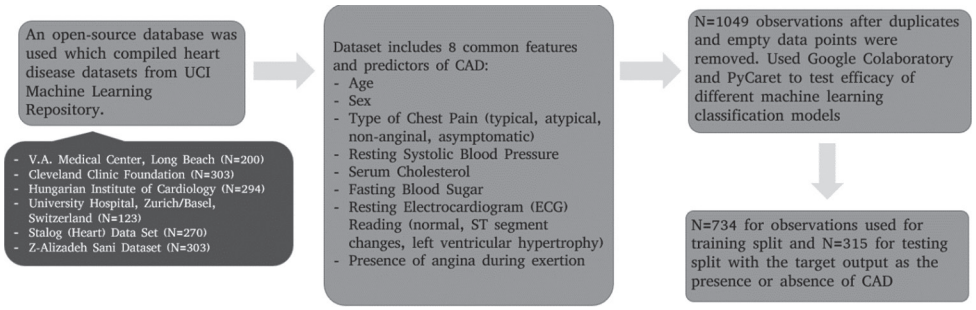

Figure 2. Flowchart demonstrating workflow for Pycaret.

3. Results

Overall, 14 ML classification models were assessed with the current dataset. The logistic regressor (LR) model had the best outcome with the highest overall performance. LR had an accuracy of 0.79, recall of 0.80, precision of 0.80, F1 score of 0.80, Cohen's Kappa (κ) of 0.57, and Matthews correlation coefficient (MCC) of 0.57. The linear discriminant analysis (LDA) had a comparable outcome to the LR model with slightly lower metrics. The overall performance metrics of all 14 ML models are outlined in Table 3.

Since the LR had the highest overall performance metrics, further analysis was performed on this model and its learning process. The confusion matrix (Figure 3) indicated a true positive (TP) value of 139 out of 315 record (44.12%), true negative (TN) value of 116 (36.83%), false-negative value of 33 (10.48%), and false-positive value of 27 (8.57%). Hence, 116 instances were correctly identified as TP, indicating patients with CAD, while 139 were TN, correctly identifying patients without the disease. Clinically, these numbers are significant as they ensure that patients with the disease are identified for treatment and those without are not subjected to unnecessary procedures. However, the model also produced 27 false positives, where the disease was incorrectly predicted, potentially leading to undue stress and unwarranted further testing for those individuals. Of greater clinical concern are the 33 false negatives, where the disease was present but went undiagnosed, potentially resulting in delayed treatment with serious health implications. The model's sensitivity, or its ability to correctly identify those with the disease, is calculated as 116/(116 + 33), which equals approximately 0.78, while the specificity, or the ability to correctly rule out disease, is 139/(27 + 139), which equals roughly 0.84. These figures suggest that the logistic regression model has a reasonable balance of sensitivity and specificity, making it a potentially viable tool for assisting in the diagnosis of CAD.

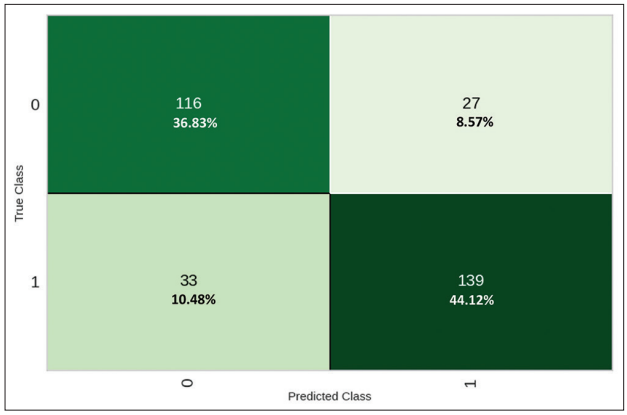

Figure 3. Confusion matrix for logistic regressor model.

The ROC curve (Figure 4) is a graphical plot that illustrates the diagnostic ability of a binary classifier system as its discrimination threshold is varied. It is created by plotting the TP rate against the false-positive rate at various threshold settings. The AUC represents the degree of separability achieved by the model; it tells us how well the model is capable of distinguishing between classes. In the context of the study, the ROC curves and their respective AUC values for class 0 and class 1 being equal to 0.88 suggest that the logistic regression model has a high level of discrimination for both identifying patients with CAD (class 1) and for identifying those without the disease (class 0). The same AUC of 0.88 for both the micro-average and macro-average ROC curves indicates that the model is consistently accurate across both classes. Clinically, this means that the model is very effective at distinguishing between patients with and without the disease, which is crucial for a diagnostic tool where the cost of misdiagnosis

Table 3. Performance of all machine learning classification models

Model	Accuracy	Recall	Precision	F1-Score	Kappa	MCC
Logistic regression (LR)	0.7861	0.8075	0.8025	0.8030	0.5687	0.5719
Linear discriminant analysis (LDA)	0.7834	0.7950	0.8059	0.7984	0.5641	0.5674
Ridge classifier (RIDGE)	0.7820	0.7950	0.8040	0.7974	0.5612	0.5646
AdaBoost classifier (ADA)	0.7793	0.8000	0.7975	0.7967	0.5550	0.5584
Gradient Boost classifier (GBC)	0.7765	0.8075	0.7897	0.7968	0.5481	0.5516
Naive Bayes (NB)	0.7725	0.8000	0.7866	0.7923	0.5405	0.5423
Light Gradient Boosting Machine (LGBM)	0.7628	0.7950	0.7761	0.7851	0.5205	0.5214
Extreme Gradient Boosting (XGBOOST)	0.7559	0.7725	0.7815	0.7753	0.5077	0.5103
Random Forest classifier (RF)	0.7491	0.7675	0.7739	0.7683	0.4944	0.4980
Extra Trees classifier (ET)	0.7383	0.7350	0.7753	0.7530	0.4748	0.4776
K-nearest neighbor classifier (KNN)	0.7315	0.7575	0.7559	0.7551	0.4575	0.4597
Decision Tree classifier (DT)	0.7260	0.6975	0.7827	0.7347	0.4526	0.4592
Quadratic discriminant analysis (QDA)	0.6920	0.7550	0.7038	0.7215	0.3751	0.3886
Support vector machines–linear kernel (SVM-LK)	0.5670	0.5050	0.5095	0.4355	0.1401	0.1713

Abbreviation: MCC: Matthews correlation coefficient.

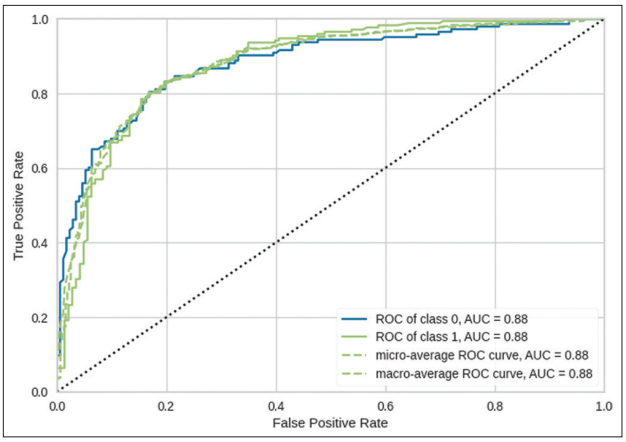

Figure 4. Area under the ROC curves for logistic regressor model.

can be high – in terms of both health outcomes for the patient and resource allocation in health-care settings. An AUC of 0.88 is considered to be very good, suggesting that the logistic regression model can be trusted to make accurate predictions about the presence or absence of CAD, though it should typically be used in conjunction with other diagnostic information and clinical judgment.

Through LR, a feature importance plot was created to categorize the impact of each variable in diagnosing CAD (Figure 5). The feature importance plot in ML is used to identify which variables have the most influence on the predictions made by the model. In the context of the study, exercise angina had the highest variable importance, followed very closely by chest pain type TA. Additional variables with high importance were age, chest pain type NAP, and chest pain type ATA, which are arranged in descending order of importance. Variables with lower importance in the context of this model included sex, fasting blood sugar, chest pain type ASY, resting ECG ST, and cholesterol, which are listed in order of decreasing impact on the model's predictions. These findings imply that the occurrence of exercise-induced angina (chest pain) and the type of chest pain categorized as TA angina are the strongest predictors for CAD in this logistic regression model. Age and other types of chest pain, such as NAP and ATA angina, are also important considerations, although they have less influence compared to exercise angina and chest pain type TA. The factors of lesser importance, such as patient's gender, fasting blood sugar levels, presence of asymptomatic chest pain, certain ECG changes denoted as resting ECG ST, and cholesterol levels, still contribute to the predictive power of the model, but to a smaller extent. Clinically, this information can be valuable for risk stratification and tailoring diagnostic evaluations. For example, the prominence of exercise-induced angina suggests a significant association with CAD and could be a strong indicator for further diagnostic testing. Similarly, the type and characteristics of chest pain can influence clinical decision-making. While the other variables may have less importance in the model's predictions, they might still contribute to a comprehensive risk profile and should not be disregarded in clinical evaluation.

The learning curve for LR reveals a training score that stays consistent between a score of 0.78 to 0.80, and the cross-validation score exhibits a rising trend as it reaches a point of intersection with the training score within the 0.78 to 0.80 range (Figure 6). The learning curve

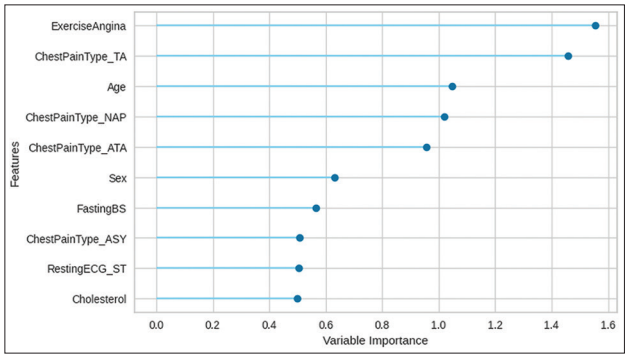

Figure 5. Feature importance plot.

Figure 6. Learning curve for logistic regression.

of the LR model described indicates that the training score is consistently high across different sizes of the training dataset, suggesting that the model was able to fit the training data well from an early stage and did not significantly improve in accuracy with the addition of more training instances. The cross-validation score, representing the model's performance on unseen data, initially starts lower, which is common as models tend to perform better on the data on which they were trained than on new data. However, as more data points are added, the cross-validation score increases steadily, indicating that the model is generalizing better with more data. On reaching approximately 500 training instances, the cross-validation score plateaus, aligning closely with the training score, implying that adding more data beyond this point does not yield improvements in the model's performance. Technically, this learning curve suggests that the logistic regression model has likely reached its learning capacity with the given features and model complexity – further learning with additional data is subject to diminishing returns. It is also indicative of a well-fitting model, as the curves converge, meaning there is a good balance between bias and variance; that is, the model neither underfits nor overfits the data. Clinically, the stabilization of model performance with more data suggests that the model has a stable predictive capability that can be deemed reliable for its intended purpose of predicting the presence of CAD. However, this also suggests a plateau in performance, indicating that any further collection of training data of the same type may not lead to improved predictive accuracy. This is a useful insight for resource allocation in clinical settings, as it can help in making informed decisions about when to prioritize model refinement and when to consider the model sufficiently trained for deployment in a clinical environment.

4. Discussion

The present study aimed to develop a robust ML model for predicting CAD based on a comprehensive dataset, encompassing various aspects of a patient's medical history and laboratory findings. The aim of the study is to compare how well the model performs in executing the binary task of predicting the presence or absence of CAD in patients with certain comorbidities, as outlined in section 2.2. The overall goal of the study is to create a model that can predict the presence or chance of presence of CAD based on different parameters of the patient's history, and this study represents the first step in creating such a model. For the present study, the LR model had the highest metrics; therefore, further analysis on performance was focused on the LR model (Table 3).

The confusion matrix generated by PyCaret demonstrated moderate success in distinguishing TPs (44.12%) and TNs (36.83%) of CAD (80.95%); however, the model encountered some difficulties in distinguishing false negatives (10.48%) and false positive (8.57%) cases (19.05%) (Figure 3). The model's effectiveness is reinforced by the LR model achieving an accuracy of 78.61% (Table 3). In addition, LR had a recall of 80.75%. Recall is also known as sensitivity, and a high recall score signifies that the model is successfully recognizing a greater number of real positive examples.[30] LR had a precision of 80.25%, and a high precision indicates that the model is making fewer false-positive predictions.[30] Finally, the F-1 score for LR is 80.30%. The F-1 score is calculated using both the precision and recall as it is calculated as the harmonic mean of precision and recall; the harmonic mean penalizes extreme values of both the precision and recall.[30]

In addition, LR had $\kappa = 0.5687$ and MCC = 0.5719. Both κ and MCC provide nuanced performance evaluation of ML models. κ measures the agreement between predicted and actual classifiers while also considering the possibility of this agreement occurring purely by chance, whereas MCC considers both correct and incorrect predictions

made by the model using the counts of TPs, TNs, false positives, and false negatives.[31] Both κ and MCC range from a scale between -1 and 1, where 1 means that the model is making perfect predictions (perfect agreement between model's predictions and actual outcomes), 0 indicates that the model's predictions are equivalent to what is expected from chance alone, and -1 indicates that the predictions are worse than chance.[31,32] A κ value of 0.57 indicates a weak level of agreement between the model's predictions and actual outcomes (κ of 0.40–0.59 = weak, and 0.60–0.79 = moderate).[33] Little information can be obtained from interpreting the actual score for MCC; however, prior research has shown that the MCC is a special case of the Pearson's correlation coefficient between the observed and predicted binary classification.[34,35] Therefore, the MCC can be crudely interpreted with similar cutoff values as the Pearson's correlation coefficient, so for a MCC of 0.57, there is a moderate agreement between the model's predictions and actual outcomes (Pearson's correlation coefficient of 0.40–0.69 = moderate correlation, and 0.70–0.89 = strong correlation).[35,36] Prior studies has also shown that MCC is a better metric than κ, especially if the dataset is unbalanced such as the current dataset (+CAD = 572 and -CAD = 477) because an unbalanced dataset could affect the hypothetical probability of chance agreement, which is part of the κ formula; however, for the current study, the κ and MCC are the same number.[31]

The ROC curve shows the performance of a binary ML model as it evaluates the trade-off between the TP rate (sensitivity) on the Y-axis and false-positive rate (1-specificity) on the X-axis.[37] The TP rate is the proportion of actual positive instances correctly identified by the model, and the false-positive rate is the proportion of actual negative instances incorrectly classified as positive by the model. The AUC is used to quantify the performance of the model from the ROC curve. If there is a one-to-one relationship between the TP rate and false-positive rate (meaning that the ROC curve is a straight diagonal line), then the model's ability to discriminate between the positive and negative classes is no better than random chance, and thus, the AUC will be 0.5.[37] The perfect ROC curve has a value of 1.0 where the model achieves a TP rate of 1 and false-positive rate of 0, meaning that model makes no errors in distinguishing between positive and negative cases (presence or absence of CAD in the current study). The LR model had an AUC of 0.88 (Figure 4), outperforming other models in this metric. Comparing similar literature, this AUC matches the performance of other chosen models.[18] This also indicates a positive performance, given the sensitivity to certain imbalances in the data set (572 +CAD compared to 477 -CAD).

The feature importance plot revealed that exercise-induced angina, TA chest pain, and age stood out as the most significant factors in influencing the model's predictions; however, more known factors in CAD diagnosis, including male sex and cholesterol, held less impact in our model (Figure 5). Variability in the dataset in terms of abundance of certain parameters (*i.e.*, more male records as compared to female records) could skew the feature importance plot in that the model focuses on the features that are most different between positive and negative CAD cases. In addition, the present study had a relatively low number of records (1049), so this could also explain the differences between the feature importance plot generated by the model and the actual risk factors that lead to CAD. To further analyze the performance of the model, and to assess whether the model can be improved with more data points, a learning curve for LR was assessed (Figure 6).

Learning curves are plots that demonstrate an ML model's performance (prediction accuracy, F1 score, error) over time with more experience and with more training instances. Learning curves usually consist of two lines, one for the model performance using the training dataset (data that was used to train the model) and validation dataset (data that the model has never seen).[38] The learning study in the present study has an X-axis that consists of training iterations and a Y-axis that consists of the model's F-1 score with the blue line representing the training dataset and the green line representing the validation dataset. As the training interactions increase, the training score starts off high and remains constant while the cross-validation score starts lower and increases until there is a small gap between the training and cross-validation scores. The small gap between the two scores could indicate that the model is not overfitting. However, since the training score remained constant throughout the training iterations, it could have been memorizing the information provided by the dataset or it has simply learned all it can from the dataset. In addition, since the training score and cross-validation scores are converging, the addition of more patient records would most likely yield minimal improvements in model metrics.[39]

The three ML models that provided the best results in predicting CAD included LR, linear discriminant analysis (LDA), and Ridge classifier (RIDGE). As a statistical method for binary classification, logistic regression is applied when there are only two possible outcomes for the target variable. Logistic regression accomplishes binary classification by modeling the probability that a given input belongs to a certain class.[40] For instance, in the medical field, logistic regression can be used to determine the relationship between variables such as weight and exercise

to predict whether a person will suffer from a heart attack or other medical complication. Such a model is set up through training and testing. Throughout the training phase, the logistic regression model's parameters are learned.[41] The model identifies patterns in the input data and associates them with some form of output. As such, after training, the model can forecast the likelihood that an input will belong to a specific class. This makes logistic regression a valuable algorithm for linearly separable datasets where two classes are separated by a line on a graph. Due to its simplicity, logistic regression often serves as the baseline for more complex classification models.

LDA is a classification algorithm used in ML that is employed to solve multi-class classification equations.[42] LDA utilizes a linear combination of features to separate classes to ultimately determine whether an input set belongs to an output. It accomplishes this task through dimensionality reduction in which the separation between classes is prioritized while the dimensionality of classes is aimed to be reduced.[43] For instance, in the realm of medicine, an LDA algorithm would aim to maximize class separability, such as separating disease categories from one another. Within each class, the algorithm identifies key patterns to simplify the information to appropriately make predictions based on how the data were reduced.

RIDGE is an important tool used in ML that utilizes examples to learn to classify new inputs into different categories. RIDGE is a linear classifier that extends the concept of logistic regression and LDA by incorporating regularization to mitigate overfitting, a situation that occurs when a machine classification algorithm performs exceptionally well on the training data but poorly in the testing phase.[44] This allows for more accurate predictions. As a model used for multi-class classification tasks, RIDGE learns from examples in the training set to categorize variables into different classes. Once trained, the RIDGE calculates a decision function based on the learned coefficients.[45]

Known hurdles in previous literature of ML datasets and CAD are that most investigated datasets have a limited number of features and small sample sizes.[18] The limitations of the present study also mostly involve the dataset. Since the dataset is a combination of different resources, institutional differences in collecting data could have an impact on the quality of the dataset. In addition, even though the learning curve suggests that addition of more data would yield minimal improvement, the present study still has a relatively low number of patient records. In addition, the training score of the learning curve staying constant (Figure 6) could also indicate the model learned everything it can early on due to the lack of complexity in the dataset. Some continuous variables such as age and fasting blood sugar were converted to binary outcomes, and the final outcome of presence of heart disease is also a binary outcome.

There have been a multitude of studies that provide a non-invasive method of predicting CAD using ML. Özbilgin *et al.* proposed a method of early diagnosis of CAD using iris images.[25] The study used images from 198 volunteers: 94 with CAD and 104 without CAD. Features of the iris images were extracted using wavelength transform, first-order statistical analysis, gray level co-occurrence matrix, and a gray level run length matrix based on the ReliefF feature selection method. Similar to the present study, a number of different classifiers were employed, and their efficacy was compared. The support vector machine model provided the highest accuracy at 93%.[25] Another study by Akella and Akella had a similar design to the current study where data from the UCI Center for ML and Intelligent Systems were used to train six different ML algorithms to predict the presence of CAD. The ML models included linear model, decision tree, random forest, support vector machine, neural network, and k-nearest neighbor.[46] Neural network achieved the highest accuracy of 93.03% and a sensitivity of 93.80 as well as the highest AUC.[46] The present study is different in that PyCaret was used with the same dataset to automatically train a total of 14 different ML models.

Hence, the results demonstrate that among the various ML models tested, LR exhibited superior performance with an AUC of 0.88, reflecting a high degree of discriminative ability. Clinically, the importance attributed to features such as exercise angina, chest pain type TA, age, and other chest pain types indicates that the model aligns well with known clinical predictors of CAD, reinforcing its potential utility in a clinical setting. However, it is crucial to acknowledge the plateau observed in the learning curve, suggesting that further expansion of the dataset beyond the 500-instance mark may not significantly enhance model performance unless new varieties of data or features are introduced. Therefore, future work should focus on refining the logistic regression model with more diverse and complex data, as well as on external validation of the model to ensure its generalizability and applicability across different patient populations.

Future studies for the present study would involve improving the quality and quantity of the dataset as well as making the dataset more complex. In addition to the LR model, it is also important to note that the LDA, RIDGE, AdaBoost classifier (ADA), Gradient Boosting classifier (GBC), and Naive Bayes (NB), all had comparable results to the LR classifier; therefore, further research should also

focus on comparing and understanding the metrics of these other comparable classifiers, and developing an ML model based on the above models. Finally, external validity of the model can also be tested by collecting patient information on patients with and without CAD diagnosis and seeing if the model can predict whether the patients have CAD or not.

The study demonstrates important strengths and limitations in its approach to applying ML for the prediction of CAD.

(i) Strengths

- The logistic regression model showcased in the study has proven to be particularly effective, with an AUC of 0.88, indicating a high ability to differentiate between patients with and without CAD.
- The model successfully identified clinical features of significant importance, such as exercise angina and chest pain type, as central to predicting CAD, aligning with existing clinical knowledge and practices.
- The use of cross-validation techniques and a well-performing training curve suggests that the model has good generalizability while avoiding overfitting.

(ii) Limitations

- The dataset used for training the models was relatively small and combined from different resources, which could impact the overall data quality and the model's predictive power due to institutional differences in data collection methods.
- A flat learning curve for the training score indicates that the logistic regression model may not benefit from additional data under its current configuration, suggesting potential limitations in dataset complexity or model capacity.
- Continuous variables in the dataset were converted into binary outcomes, which may oversimplify clinical nuances and reduce the subtlety with which the model can identify patterns.
- The end result of predicting the presence of CAD is also binary, without accounting for the disease's severity or progression, limiting the clinical applicability of the model's outputs.
- External validity is yet to be tested; the results observed are potentially specific to the dataset and may not generalize to different populations without further validation.

Moving forward, it would be beneficial to address these limitations by expanding and diversifying the dataset to include more patient records and a broader set of features, including continuous variables and clinical modalities such as imaging results and detailed smoking histories. By increasing the complexity and volume of the dataset, the robustness and sensitivity of the model could be improved, which may reveal more intricate patterns and relationships that are clinically relevant. In addition, it is imperative to explore the possibility of using a more granular output than a binary classification to capture the severity or stages of CAD. The study should also focus on testing the external validity of the model by applying it to independent datasets from varied demographical and geographical backgrounds to ensure the model's predictions hold true across different populations. Moreover, comparing other ML models such as the ADA, GBC, and NB, which showed comparable results to logistic regression, could provide insights into the optimal approach for predicting CAD. In the clinical context, model outputs should be integrated with clinical decision-making processes to evaluate their real-world effectiveness. It involves assessing not just the model's predictive accuracy but also its impact on patient outcomes, cost-effectiveness, and user-friendliness for healthcare providers. By addressing these limitations, future research can enhance the model's predictive accuracy and increase confidence in its clinical usefulness. Further research is also essential to understand how such predictive models could be deployed in clinical workflows, balancing the benefits of ML assistance with the expertise of health-care professionals to optimize patient care outcomes.

5. Conclusion

The present study offers significant insights into the application of ML for predicting CAD, with logistic regression emerging as a leading model featuring high discriminative capacity. The strength of logistic regression, underscored by an AUC of 0.88, lies in its ability to harness key clinical features effectively, which is indicative of its potential to support diagnostic decisions.

This model also demonstrated a high overall accuracy in predicting true CAD and distinguishing between TPs and TNs. The most important features in the prediction of CAD included the presence of exertional angina, asymptomatic chest pain, and systolic blood pressure; however, this could be explained by imbalances in the dataset itself that erroneously make the above factors seem more important. The study can be improved with more robust data and the addition of other clinical modalities and risk factors, such as imaging and smoking histories. Expanding the dataset to include more robust data and adding other clinical factors such as imaging results and smoking histories may help improve the model's predictive power. Future research could focus on refining and comparing other models such as the LDA, RIDGE, ADA, GBC, and NB, which had similar performance to the LR model. Validation on external datasets is also suggested to test the model's external validity, which is necessary to ensure that the model can predict CAD accurately

in different patient populations. Overall, this study's conclusion emphasizes the promise of ML in enhancing the prediction and detection of CAD and recommends further research to build upon the initial findings, improve the dataset, and validate the model externally.

Hence, the limitations uncovered, such as the dataset's relatively limited size and the simplicity of the binary outcomes, highlight the need for further research. To enhance the model's predictive power and clinical applicability, future efforts should concentrate on enriching the dataset's complexity, incorporating more nuanced clinical parameters, and conducting external validations across diverse patient cohorts. This progression work is vital to ensure the model's robustness, relevance, and generalizability to different demographic and clinical settings, striving to integrate advanced ML tools into everyday clinical practice to the benefit of patient care and outcomes.

Acknowledgments

None.

Funding

None.

Conflict of interest

The authors declare that they have no competing interests.

Author contributions

Conceptualization: All authors
Formal analysis: All authors
Investigation: All authors
Methodology: All authors
Writing – original draft: All authors
Writing – review & editing: All authors

Ethics approval and consent to participate

Not applicable.

Consent for publication

Not applicable.

Availability of data

All data are included in the manuscript.

References

1. World Health Organization. *The Top 10 Causes of Death*. Available from: https://www.who.int/news-room/fact-sheets/detail/the-top-10-causes-of-death [Last accessed on 2023 Dec 22].
2. Ralapanawa U, Sivakanesan R. Epidemiology and the magnitude of coronary artery disease and acute coronary syndrome: A narrative review. *J Epidemiol Glob Health*. 2021;11(2):169-177.
   doi: 10.2991/jegh.k.201217.001
3. Tsao CW, Aday AW, Almarzooq ZI, *et al*. Heart disease and stroke statistics-2023 update: A report from the American heart association. *Circulation*. 2023;147:e93-e621.
   doi: 10.1161/CIR.0000000000001123.
4. Moriguchi JD, Kobashigawa JA, Ro TK, *et al*. At what creatinine level is angiographic dye safe for coronary angiography in cardiac transplant recipients? *Transplantation*. 1998;65(12):S160.
5. Alizadehsani R, Abdar M, Roshanzamir M, *et al*. Machine learning-based coronary artery disease diagnosis: A comprehensive review. *Comput Biol Med*. 2019;111:103346.
   doi: 10.1016/j.compbiomed.2019.103346
6. Alizadehsani R, Habibi J, Hosseini MJ, *et al*. A data mining approach for diagnosis of coronary artery disease. *Comput Methods Programs Biomed*. 2013;111(1):52-61.
   doi: 10.1016/j.cmpb.2013.03.004
7. Goff DC Jr., Lloyd-Jones DM, Bennett G, *et al*. 2013 ACC/AHA guideline on the assessment of cardiovascular risk: A report of the American College of Cardiology/American Heart Association Task Force on Practice Guidelines. *Circulation*. 2014;129(25_suppl_2):S49-S73.
   doi: 10.1161/01.cir.0000437741.48606.98
8. DeFilippis AP, Young R, Carrubba CJ, *et al*. An analysis of calibration and discrimination among multiple cardiovascular risk scores in a modern multiethnic cohort. *Ann Intern Med*. 2015;162(4):266-275.
   doi: 10.7326/M14-1281
9. Toma M, Wei OC. Predictive modeling in medicine. *Encyclopedia*. 2023;3(2):590-601.
   doi: 10.3390/encyclopedia3020042
10. Bekbolatova M, Mayer J, Ong CW, Toma M. Transformative potential of AI in healthcare: Definitions, applications, and navigating the ethical landscape and public perspectives. *Healthcare* (*Basel*). 2024;12(2):125.
    doi: 10.3390/healthcare12020125
11. Abraham A, Jose R, Ahmad J, *et al*. Comparative analysis of machine learning models for image detection of colonic polyps vs. Resected polyps. *J Imaging*. 2023;9(10):215.
    doi: 10.3390/jimaging9100215
12. Gautam N, Saluja P, Malkawi A, *et al*. Current and future applications of artificial intelligence in coronary artery disease. *Healthcare* (*Basel*). 2022;10(2):232.
    doi: 10.3390/healthcare10020232
13. Davenport T, Kalakota R. The potential for artificial

intelligence in healthcare. *Future Healthc J*. 2019;6(2):94-98.

doi: 10.7861/futurehosp.6-2-94

14. Javaid M, Haleem A, Pratap Singh R, Suman R, Rab S. Significance of machine learning in healthcare: Features, pillars and applications. *Int J Intell Netw*. 2022;3:58-73.

doi: 10.1016/j.ijin.2022.05.002

15. Srinivasan S, Gunasekaran S, Mathivanan SK, Malar MB, Jayagopal P, Dalu GT. An active learning machine technique based prediction of cardiovascular heart disease from UCI-repository database. *Sci Rep*. 2023;13:13588.

doi: 10.1038/s41598-023-40717-1

16. Garavand A, Behmanesh A, Aslani N, Sadeghsalehi H, Ghaderzadeh M. Towards diagnostic aided systems in coronary artery disease detection: A comprehensive multiview survey of the state of the art. *Int J Intell Syst*. 2023;2023:6442756.

doi: 10.1155/2023/6442756

17. Kakadiaris IA, Vrigkas M, Yen AA, Kuznetsova T, Budoff M, Naghavi M. Machine learning outperforms ACC/AHA CVD risk calculator in MESA. *J Am Heart Assoc*. 2018;7(22):e009476.

doi: 10.1161/JAHA.118.009476

18. Baskaran L, Ying X, Xu Z, *et al*. Machine learning insight into the role of imaging and clinical variables for the prediction of obstructive coronary artery disease and revascularization: An exploratory analysis of the CONSERVE study. *PLoS One*. 2020;15:e0233791.

doi: 10.1371/journal.pone.0233791

19. Al'Aref SJ, Maliakal G, Singh G, *et al*. Machine learning of clinical variables and coronary artery calcium scoring for the prediction of obstructive coronary artery disease on coronary computed tomography angiography: Analysis from the CONFIRM registry. *Eur Heart J*. 2020;41:359-367.

doi: 10.1093/eurheartj/ehz565

20. Alaa AM, Bolton T, Di Angelantonio E, Rudd JHF, van der Schaar M. Cardiovascular disease risk prediction using automated machine learning: A prospective study of 423,604 UK Biobank participants. *PLoS One*. 2019;14(5):e0213653.

doi: 10.1371/journal.pone.0213653

21. Motwani M, Dey D, Berman DS, *et al*. Machine learning for prediction of all-cause mortality in patients with suspected coronary artery disease: A 5-year multicentre prospective registry analysis. *Eur Heart J*. 2017;38(7):500-507.

doi: 10.1093/eurheartj/ehw188

22. Forrest IS, Petrazzini BO, Duffy Á, *et al*. Machine learning-based marker for coronary artery disease: Derivation and validation in two longitudinal cohorts. *Lancet*. 2023;401(10372):215-225.

doi: 10.1016/S0140-6736(22)02079-7

23. Cho SY, Kim SH, Kang SH, *et al*. Pre-existing and machine learning-based models for cardiovascular risk prediction. *Sci Rep*. 2021;11(1):8886.

doi: 10.1038/s41598-021-88257-w

24. Lee YH, Tsai TH, Chen JH, *et al*. Machine learning of treadmill exercise test to improve selection for testing for coronary artery disease. *Atherosclerosis*. 2022;340:23-27.

doi: 10.1016/j.atherosclerosis.2021.11.028

25. Özbilgin F, Kurnaz Ç, Aydın, E. Prediction of coronary artery disease using machine learning techniques with iris analysis. *Diagnostics*. 2023;13(6):1081.

doi: 10.3390/diagnostics13061081

26. Sun Z, Silberstein J, Vaccarezza M. Cardiovascular computed tomography in the diagnosis of cardiovascular disease: Beyond lumen assessment. *J Cardiovasc Dev Dis*. 2024;11(1):22.

doi: 10.3390/jcdd11010022

27. Ahsan MM, Siddique Z. Machine learning-based heart disease diagnosis: A systematic literature review. *Artif Intell Med*. 2022;128:102289.

doi: 10.1016/j.artmed.2022.102289

28. Janosi A, Steinbrunn W, Pfisterer M, Detrano R. *Heart Disease*. UCI Machine Learning Repositoryl; 1988.

doi: 10.24432/C52P4X

29. Unknown. (n.d.). Statlog (Heart) [Dataset]. UCI Machine Learning Repository.

doi: 10.24432/C57303

30. Hicks SA, Strümke I, Thambawita V, *et al*. On evaluation metrics for medical applications of artificial intelligence. *Sci Rep*. 2022;12(1):5979.

doi: 10.1038/s41598-022-09954-8

31. Delgado R, Tibau XA. Why Cohen's Kappa should be avoided as performance measure in classification. *PLoS One*. 2019;14(9):e0222916.

doi: 10.1371/journal.pone.0222916

32. Chicco D, Jurman G. The Matthews correlation coefficient (MCC) should replace the ROC AUC as the standard metric for assessing binary classification. *BioData Min*. 2023;16(1):4.

doi: 10.1186/s13040-023-00322-4

33. McHugh ML. Interrater reliability: The kappa statistic. *Biochem Med (Zagreb)*. 2012;22(3):276-282.

34. Xia Y. Correlation and association analyses in microbiome study integrating multiomics in health and disease. *Prog Mol Biol Transl Sci*. 2020;171:309-491.

doi: 10.1016/bs.pmbts.2020.04.003

35. Mao L. *Matthews Correlation Coefficient*; 2019. Available from: https://leimao.github.io/blog/matthews-correlation-coefficient [Last accessed on 2024 Jan 03].

36. Schober P, Boer C, Schwarte LA. Correlation coefficients: Appropriate use and interpretation. *Anesth Analg*. 2018;126(5):1763-1768.

doi: 10.1213/ANE.0000000000002864

37. Nahm FS. Receiver operating characteristic curve: Overview and practical use for clinicians. *Korean J Anesthesiol*. 2022;75(1):25-36.

doi: 10.4097/kja.21209

38. Viering T, Loog M. The shape of learning curves: A review. *IEEE Trans Pattern Anal Mach Intell*. 2023;45(6):7799-7819.

doi: 10.1109/TPAMI.2022.3220744

39. Bengfort B, Gray L, Bilbro R, *et al*. *Yellowbrick v1.5*. Zenodo; 2022. Available from: https://www.scikit-yb.org/en/latest/api/model_selection/learning_curve.html [Last accessed on 2024 Jan 04].

40. Kanade VA. *Logistic Regression: Equation, Assumptions, Types, and Best Practices*. Austin: Spiceworks. Available from: https://www.spiceworks.com/tech/artificial-intelligence/articles/what-is-logistic-regression [Last accessed on 2022 Apr 18].

41. Rymarczyk T, Kozłowski E, Kłosowski G, Niderla K. Logistic regression for machine learning in process tomography. *Sensors*. 2019;19(15):3400.

doi: 10.3390/s19153400

42. Tharwat A, Gaber T, Ibrahim A, Hassanien AE. Linear discriminant analysis: A detailed tutorial. *AI Commun*. 2017;30:169-190.

doi: 10.3233/AIC-170729

43. Xanthopoulos P, Pardalos PM, Trafalis TB. Linear discriminant analysis. In: *Robust Data Mining. SpringerBriefs in Optimization*. New York: Springer; 2013.

doi: 10.1007/978-1-4419-9878-1_4

44. Peng C, Cheng Q. Discriminative ridge machine: A classifier for high-dimensional data or imbalanced data. *IEEE Trans Neural Netw Learn Syst*. 2021;32(6):2595-2609.

doi: 10.1109/TNNLS.2020.3006877

45. Singh A, Prakash BS, Chandrasekaran K. A Comparison of Linear Discriminant Analysis and Ridge Classifier on Twitter Data. In: *2016 International Conference on Computing, Communication and Automation (ICCCA)*. Greater Noida, India: IEEE; 2016. p. 133-138.

doi: 10.1109/CCAA.2016.7813704

46. Akella A, Akella S. Machine learning algorithms for predicting coronary artery disease: Efforts toward an open source solution. *Future Science OA*. 2021;7(6):FSO698.

doi: 10.2144/fsoa-2020-0206

ACCSCIENCE PUBLISHING

Global Translational Medicine

ORIGINAL RESEARCH ARTICLE

Ineffective voluntary motor improvement through non-invasive BCI-FES with static magnetic field in complete spinal cord injury: A pilot study

Larissa Gomes Sartori[1]*, Roger Burgo de Souza[2], Daniel Prado Campos[1,3], Paulo Broniera Júnior[1,4], José J. A. Mendes Junior[5], and Eddy Krueger[1]

[1]Neural Engineering and Rehabilitation Laboratory, State University of Londrina, Londrina, Brazil

[2]Department of Physiotherapy, State University of Londrina, Londrina, Londrina, Brazil

[3]Department of Computer Engineering, Federal Technological University of Paraná, Apucarana, Brazil

[4]Electronic Systems Laboratory - Embedded and Power, IoT and Manufacturing 4.0, Instituto Senai de Tecnologia da Informação e Comunicação (ISTIC), Londrina, Brazil

[5]Department of Computer and Electronic Engineering, Federal Technological University of Paraná, Curitiba, Brazil

Abstract

In response to the challenge of spinal cord injury (SCI) rehabilitation, this study aimed to investigate the effect of applying a non-invasive interface of surface neuroelectrical signals and functional electrical stimulation (sNES-sFES) with a static magnetic field on the motor outcome of the quadriceps femoris muscle in an individual with a complete SCI. The participant, who had a complete SCI in the chronic stage, was evaluated before (pre) and after nine (post) interventions using surface electromyography (sEMG). In addition, spasticity (modified Ashworth scale [MAS]) was observed in all sessions. Moreover, the user learning curve process (classifier percentage and correct success of the sFES hits) was evaluated. In general, we observed: (i) No voluntary muscle contraction (pre- and post-root mean square of sEMG = 0%) improvement; (ii) spasticity decrease (average one point in MAS); (iii) gradual improvement in the user learning effect on the interface, reaching 84% in classifier accuracy and a maximum percentage of correct sFES activation of 53%. In conclusion, no improvement in voluntary muscular contraction was observed within 9 weeks of the intervention (1 session/day; 1 h/week). However, our study demonstrates the safety and feasibility of our methodology for future research involving continuous physical rehabilitation training and the implementation of assistive technology.

Keywords: Brain-machine interface; Motor imagery; Neuroscience; Paraplegic; Rehabilitation

***Corresponding author:**
Larissa Gomes Sartori
(llarissa.sartori@uel.br)

Citation: Sartori LG, de Souza RB, Campos DP, Júnior PB, Junior JJAM, Krueger E. Ineffective voluntary motor improvement through non-invasive BCI-FES with static magnetic field in complete spinal cord injury: A pilot study. *Global Transl Med*. 2024;3(1):2285. https://doi.org/10.36922/gtm.2285

Received: November 21, 2023
Accepted: February 27, 2024
Published Online: March 22, 2024

1. Introduction

Spinal cord injury (SCI) is a neurological condition that partially or completely impairs sensorimotor and autonomic function below the lesion segment.[1] SCI recovery remains an unsolved challenge in biomedical engineering and related fields.[2] Non-invasive techniques such as brain-machine interfaces (BCI)[3] function as technological bridges,

connecting the brain to the paralyzed muscles through surface functional electrical stimulation (sFES).[4] Following a SCI, the body undergoes molecular changes.[5] Therefore, the implementation of physical rehabilitation techniques is essential to facilitate neuroplasticity, leading to clinical improvement in the individual.[6]

The quadriceps femoris muscle is located in the anterior thigh region. It is innervated by the femoral nerve (lumbar plexus/L2 – L4), with hip flexion functions, mainly knee extension.[7] Knee extension is essential to remaining upright, allowing greater autonomy and independence in activities of daily living. Injuries to the spinal cord at or above the lumbar level compromise activation of the quadriceps femoris muscle, negatively impacting the individual's level of independence.

Functional electrical stimulation has demonstrated widespread success in treating several clinical cases, especially SCI, with a significant incidence in the world population.[4] This therapy contributes to improving muscular trophism and the autonomic system, such as the intestinal, vesical, and sexual systems, in SCI patients. Facts that enhance the quality of life of people with SCI include functional independence, improved self-esteem, and social inclusion.[8]

Conventionally, sFES is applied using commercial equipment, which allows pre-setting of the stimulation current, duty cycle, and frequency; however, they have a manual trigger. Recently, the scientific community has been interested in developing research that proposes sFES triggered by surface myoelectric signals (sMES) acquired through non-invasive electromyography sensors (EMG) or surface neuroelectric signals (sNES) acquired through non-invasive electroencephalography (EEG) sensors. Implementation of this approach reduces spasticity, contributing to the physical rehabilitation of affected limb movements.[9]

Similar to sMES, sNES detects the motor action intention of the individual and triggers the sFES to perform electrically evoked movements.[10] An efficient strategy for using sNES is event-related desynchronization/synchronization detection (ERD/ERS). These are sensorimotor oscillatory rhythms associated with motor imagery (MI), i.e., a mental process by which an individual rehearses or simulates a certain motor action.[11]

Integrated approaches, such as combining stem cells with intraspinal electrical stimulation, are being evaluated in animal models.[12] This can be performed using a current intensity below the sensory level to facilitate direct neural growth.[13] SCI causes changes in the organization of the somatosensory cortex due to the non-use of the affected region.[14] This cortical reorganization causes a disconnection from the body representation,[15] turning a command such as "extend your leg" into a challenging activity as the individual is unable to comprehend the process and lacks the neural circuit necessary for it. This integrated neuromodulation technique, such as sFES and transcutaneous spinal cord stimulation in a pool, has shown initial motor results.[16]

Scientific evidence suggests that the motor imagery process activates sensorimotor regions similar to actual task performance and that repeated practice of motor imagery can induce plasticity changes in the brain. Some researchers reiterate the potential of this technology, suggesting that it can promote neuroplasticity and motor recovery by applying Hebb's law, rewarding cortical activity associated with sensorimotor rhythms through the use of a variety of self-guided or assistive modalities.[17] Osuagwu *et al.*[18] compared NES-FES and sFES interfaces in the motor rehabilitation of quadriplegic volunteers. The patients were divided into two groups. The participants of the first group received sessions of FES controlled by a brain-computer interface (BCI), while the participants of the second group received a manually commanded sFES intervention. Neurological assessment measures were: (i) event-related desynchronization (ERD) during attempted movement and (ii) the somatosensory evoked potential (PEEP) of the ulnar and median nerves. Limb function was evaluated using a range of motion (ROM) and manual muscle testing. The muscle strength of volunteers in the first group improved significantly, whereas those in the second group showed minor improvements in specific tasks. Neuromuscular fatigue during the tasks was disregarded in both groups, and small increments were made in the intensity of the sFES (in the open loop) to compensate for the reduction in force due to fatigue. The study concluded that combination therapy with the sNES-sFES interface resulted in better neurological and muscle strength recovery than sFES alone. For people with SCI, the sNES-sFES interface should be considered a therapeutic tool for restoring lost function in individuals with SCI rather than solely a long-term assistive device.

Magnetic field (MF) can be applied to the nervous system with a wide range of intensities (4.35 μT – 8 T). Neurites have been proven to grow parallel to the applied MF.[19] Another study investigated the intrathecal application of $CD133^+$ (derived from human blood) in rats associated with the use of a static magnetic field (SMF) with an intensity of 0.6 T for 30 min.[20] As a result, the group treated with CM and $CD133^+$ showed functional improvements after 14 days compared to the group with $CD133^+$ without SMF and the group with SMF and the application of the phosphate-

buffered saline solution. The spinal cord contains stem cells that can be activated during neuroplasticity.[21] Thus, it is expected that the combination of SMF and NES-FES will promote sufficient neuroplasticity for motor recovery after SCI.

Although the feasibility of using human-machine interfaces in the motor improvement of individuals with SCI has been proven,[10] one of the challenges in this area is to understand the mechanisms that can provide neuroplasticity, which remains uncertain. Thus, this work aimed to investigate the feasibility of applying sNES-sFES with SMF to the response of the quadriceps femoris muscle group in a volunteer with a complete SCI. As a primary hypothesis, an improvement in voluntary muscle contraction is expected in the quadriceps femoris, which has the function of knee extension and is important for daily activities such as standing and walking. An increase in local vascularization is expected to improve sexual, intestinal, and urinary functions. The secondary hypothesis suggests that training and intervention have a gradual learning effect, resulting in greater mastery of the sNES-sFES interface.

2. Methods

The ethics committee at the State University of Londrina (CEP-UEL) approved the research involving human participants (no. 4.060.700). The study was conducted in 2021 at the Neural Engineering and Rehabilitation Laboratory (LENeR), located in the Department of Anatomy at UEL. The initial contact with the participant was through a brief telephone interview, during which information regarding his injury was collected. In addition, we briefly explained the project objectives and outlined how the interventions would be carried out. Subsequently, the participant was invited to visit the laboratory to provide informed consent, marking the initiation of the research protocols. The laboratory administration covered the transportation costs of the participants. During the interventions, strict adherence to the current health standards and recommendations of the World Health Organization was maintained due to the COVID-19 pandemic.

2.1. Participant

The participant was a 46-year-old male who was a victim of a car accident in November 2002. Magnetic resonance imaging revealed lesions in the posterior lamina and ligaments and an altered signal on T2 in the cervical cord at C6 – C7. Computed tomography revealed complete bilateral lesions of the C6 lamina and C7 vertebral bodies. Consequently, surgical intervention was required to stabilize the cervical spine, which involved the fixation of screws in the fifth and sixth cervical vertebrae, a sublaminar hook in the first thoracic vertebra, and the extraction of a loose blade from the sixth cervical vertebra. The participant's kinetic-functional diagnosis was spastic quadriplegia with a neurological level at C6 (sensory-C6, motor-T1)—classified as "A" on the Disability Scale (AIS1). He experienced urinary, intestinal, and sexual dysfunctions, requiring the permanent use of an indwelling urinary catheter due to a lack of bladder control. Bowel control was absent, and stool evacuation was achieved every two days through an abdominal pressure maneuver, digit-anal touch, and manual stool extraction. Furthermore, the participant had erectile dysfunction and was unable to report an ejaculation, even if it was retrograde.

2.2. Neuromuscular assessment

Neuromuscular assessment was performed using surface electromyography (sEMG) before the first intervention (pre) and after the ninth session (post).

2.2.1. Surface electromyography acquisition

The neuromuscular assessment was performed using sEMG (Figure 1) with a Bitalino® electromyograph and MuscleBIT model. The board operates using Bluetooth technology, with a resolution of 10 bits per channel for the analog-to-digital converter and OpenSignals® for signal acquisition, controlled by a smartphone with an Android operating system. The participant was instructed to remain in his wheelchair, and asepsis with 70% ethyl alcohol was performed in the evaluated region (previously shaved by the participant). Then, four channels (3M® Ag/AgCl electrodes) were positioned bilaterally over the rectus femoris and vastus lateralis muscles, and a reference electrode was positioned on the right iliac crest. The

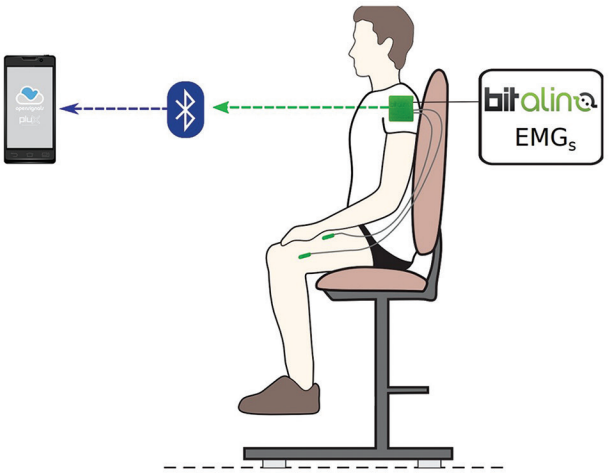

Figure 1. Illustration of neuromuscular assessment equipment. Equipment representing Bitalino® reproduced from https://bitalino.com/products/musclebit-bt.

acquisition frequency was 1 kHz. The instructor gave a voice command to the participant, saying, "Extend as much as possible" to perform knee joint extension movement for approximately 5s and giving an interval of approximately 10s before repeating the activity. Concurrently with the knee extension movement request, a digital output was activated using the OpenSignals® program. This allowed for the evaluation of spasticity simultaneously with the activation of the digital output in the OpenSignals® program to avoid any interference in the evaluation of voluntary contraction in the knee extensor muscle group. The same evaluation was performed on the bilateral biceps brachii (dominant) muscle as a normalization criterion (Section 2.2.3), before the first intervention (pre) and after the ninth session (post).

2.2.2. Surface electromyography processing

Signal processing was performed using a custom routine in the program Octave®2, and from the 5 s registered, a 2 s intermediate was selected for processing. The signals were filtered with a fourth-order bandpass Butterworth filter with a passband of 10 – 450 Hz, reducing the effect of the electrical network, mainly the 60, 120, 180, 240, 300, 360, and 420 Hz components. The descriptors were extracted from the temporal and spectral domains. For temporal features, we selected the root mean squared (RMS) value (sEMG-RMS), whereas for spectral characteristics, the median frequency (sEMG-MDF) was calculated.

2.2.3. Signals normalization

The maximum voluntary isometric contraction is one of the most recurrent methods for evaluating sEMG signals. However, people with spinal cord injuries often lack voluntary contractions. Unlike other neurological conditions, such as after a stroke, where the affected side can be compared with the healthy side, in SCI, this is not possible. However, in a study conducted by Fukuda *et al.*,[22] sEMG signals of 24 young, physically active female participants (20 ± 6 years old) with a body mass index between 18.5 kg/m^2 and 25 kg/m^2, were acquired. In that study, the rectus femoris and biceps brachii were analyzed using sEMG-RMS. Activities were performed during (i) maximum voluntary isometric contraction and holding dumbbells of (ii) 2, (iii) 4, (iv) 6, and (v) 8 kg, respectively. Normalization was achieved by calculating the mean values along the activities of the rectus femoris with the biceps brachii, resulting in a value of 0.54. Thus, the average value during rectus femoris muscle contraction is approximately 54% of that of the biceps brachii muscle. In this sense, the signals were normalized by the biceps brachii muscle on the right side (or left when the right side was not accessible), as shown in Equation I:

$$Mus_{av}^{NORM} = \left(\frac{Mus_{av}}{BB_{Pre}} \right) \times 100 = \%BB_{Pre} \quad \text{(I)}$$

where *Mus* is the rectus femoris or vastus lateralis muscle. The superscript *NORM* indicates normalization with a percentage value of the biceps brachii muscle in the pre-assessment period (BB_{Pre}). The subscript *av* indicates whether the assessment is conducted before (pre) or after (post).

2.3. Spasticity assessment

In all sessions, the participant underwent assessment using the modified Ashworth scale (MAS) for knee extension and bilateral ankle dorsiflexion movements, evaluated through passive mobilization of these joints, and was conducted pre- and post-interventions (conducted intraday for both).

2.4. Interventions

In the sessions following the initial evaluation (pre), nine interventions were carried out (once a week for 9 consecutive weeks), with which the participant was already familiar, having performed three sessions before the evaluation. During each session, the participant was instructed to remain seated in his wheelchair while the static magnetic field was positioned, and the electrodes of the sNES (Section 2.4.2) and sFES (Section 2.4.3) were fixed accordingly, as described in the subsequent sections. The learning curve of the sNES-sFES interface by the user was evaluated by classifier accuracy and the number of misses and hits to the sFES trigger.

2.4.1. Static magnetic field

The static magnetic field (SMF) was obtained using a neodymium magnet (measuring 2 cm × 3 cm × 4 cm) positioned at the level of the affected spinal cord segment (C7) of the participant. The value of magnetic induction to determine the exact position of the SMF was approximately 0.1 T, measured using a Tunkia® portable digital gaussmeter, and the intervention period with the SMF lasted approximately 1 h, applied during the intervention with the NES-FES interface.

2.4.2. Surface neuroelectric signals

In all sessions, brain activity was recorded using gold electrodes (Maxxi Gold®) distributed in a 10-10 system pattern on the scalp with conductive paste (Carbofix®) and conductive gel (Electro Ultra-gel®). The channels (unipolar) were positioned in the Cz, C1, FCz, and CPz regions[23] and fixed with the aid of a customized EEG cap.[24] Reference channels A1 and A2 were fixed using Ag/AgCl electrodes on the mastoid processes of the temporal bones bilaterally. EEG data were acquired using commercial Cyton OpenBCI

Board® hardware. The OpenVibe® software platform is used for the acquisition of signals and consists of an open-source tool in C++ that can be customized for different purposes. The EEG acquisition, pre-, and processing methods were based on those described by Broniera Junior *et al.*[24] After the EEG electrodes are properly positioned, the training of the sNES begins, which is divided into two phases: the calibration phase, in which the acquisition of the sNES and adjustment of the classifier (common spatial pattern [CSP] filter and linear discriminant analysis [LDA]) are carried out, and the feedback phase. In the calibration phase, the participant was instructed to perform knee extension motor imagery or remain inactive. The testing procedure was adapted from Abdalsalam *et al.*,[11] where participants looked at a reference while simultaneously receiving instructions to perform motor imagery. In this study, an instructor was introduced to observe the movement guidelines provided by the software and reproduce them physically. The instructor was seated in front of the participant, giving the voice command to imagine the extension movement and perform the movement simultaneously, or the instructor could provide both voice and motor commands for the participant to remain inactive. Five to ten repetitions were performed with an average duration of 8s for two different classes: (i) Motor imagery and (ii) rest. The sequence of motor imagery classes presented to the individual was random to avoid bias. In the feedback phase of the sNES, participants were again instructed to imagine the movement indicated by the instructor. At each motor imagery test, new data acquisition from the sNES channels was performed, and simultaneously, the classifier produced a real value, quantifying the class probability associated with the participant brainwave response. Once calculated, the probability of class association (actual value from 0 to 100 %) was transferred from the OpenVibe® software to a network-based interface (VRPN: Virtual-Reality Peripheral Network) developed in C++ in the Microsoft Visual Studio® environment.[25] The sNES received by the VRPN were processed and sent in binary form through Bluetooth to the electrical stimulator.

2.4.3. Surface functional electrical stimulation

For artificial muscle activation,[26] an electrical stimulator was customized exclusively for this work, following the criteria outlined in the IEC 60601-2-10 standard.[27] Two self-adhesive electrodes, sized 5 × 9 cm, were placed in the anterior region of the volunteer's right thigh according to the methodology described by Krueger *et al.*[28] One of the electrodes was positioned at the lower edge, 3 cm from the base of the patella, and the other over the femoral triangle[29] to stimulate the quadriceps muscle group through the femoral nerve.[30] According to Krueger *et al.*,[28] after fixing the electrodes, an interval of 10 min was used to stabilize the electrode-skin impedance. The frequency parameters of the electrical stimulation were: 1 kHz carrier frequency (positive: 200 μs + negative: 200 μs + off: 800 μs); 20 – 40 Hz modulated frequency (24 ms active period) to rise and decay pulse trains. The amplitude was modulated based on the instant of maximum electrically stimulated extension.[28] During the feedback phase, communication took place through Bluetooth with an electrical stimulator, which initiated activation. The activation condition of sFES occurs when the probability of similarity of the classifier output signal is ≥72%. The equipment assembly for the participant is illustrated in Figure 2.

2.5. Data analysis

The analyses conducted in this pilot study were inherently descriptive and did not involve the application of statistical tests.

3. Results

The present study analyzed the feasibility of applying the sNES-sFES interface with a static magnetic field to a person with a complete SCI.

3.1. Neuromuscular assessment

During the neuromuscular evaluation, the participants did not experience simultaneous muscle spasms. In both the pre- and post-evaluations, the sEMG-RMS values were 0% (about the biceps brachii muscle in the pre-evaluation [Section 2.2.3]) for the evaluated muscles, rectus femoris, and vastus lateralis, bilaterally. Owing to the low value (indicating only electrical noise), sEMG-MDF analysis was unfeasible.

3.2. Spasticity

The results of assessing the muscle tone of the knee extensors and plantiflexors ranged from 1 (increased tone at the beginning or end of the range of motion) to 1+ (increased tone in less than half of the range of motion, manifested by abrupt tension followed by minimum resistance). In most sessions, the pre-intervention (intraday) muscle tone assessment was 1+. The exceptions were the third from the last and last sessions, with the pre-outcome being 1. In the post-intervention (intraday) assessment, there was a reduction in muscle tone in most sessions.

3.3. Interventions

3.3.1. Static magnetic field

In the present study, the SMF was used in association with NES-FES, with a total duration of approximately 1 h. We did not identify an improvement in the neuromuscular condition, possibly due to factors related to the severity of a complete and chronic SCI in returning muscle contractions.

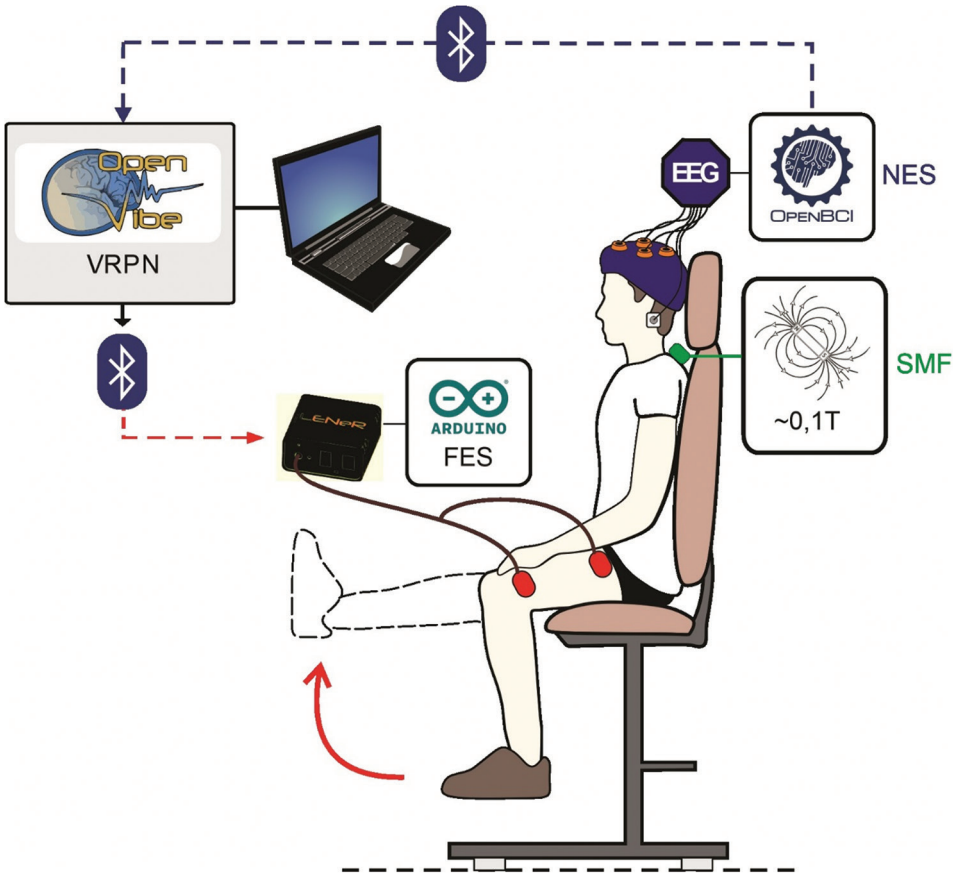

Figure 2. Illustration of participants during the interventions.
Abbreviations: sFESs: Surface functional electrical stimulation; sNES: Surface neuroelectric signal; SMF: Static magnetic field; VRPN: Virtual-Reality Peripheral Network.

However, Beros *et al.*[31] investigated the effects of SMF application (6 and 48 h, 0.5 T) on the structural plasticity of the axon initial segment in primary cortical neurons. Their findings revealed that after 6 h of SMF, there was a shortening in the average length of the axon initial segment compared to the control, which persisted 24 h after stimulation. In contrast, 48 h of SMF treatment induced an immediate distal shift that persisted for 24 h after stimulation, suggesting that SMF can induce neural plasticity and last longer than the stimulation period. Although this study was carried out on primary cortical neurons, it demonstrated alterations in neural activity and the induction of neural plasticity. Further exploration is required, especially in spinal cord plasticity, to understand its effects and mechanisms.

3.3.2. Neuroelectrical signals and functional electrical stimulation interface

As indicated earlier, there was no improvement in the neuromuscular condition in the present study. Despite this limitation, the BCI can be used as an auxiliary device for the movement of paralyzed muscles in individuals with SCI. The total session duration, from the participant's arrival at the laboratory until departure, was, on average, 1 h. The actual time of the intervention alone lasted approximately 25 – 30 min. The mean (standard deviation) duration of the set of experiments for assembly and disassembly was 406.6 ± 84.86 s and 102.2 ± 20.20 s, respectively. By observing the time intervals during the performance of each stage of the intervention, the training time was gradually increased, which can be explained by the training of the intervention stage despite having received the therapist's start of the collection from the participant. During the sessions, the ease and simplicity of the physical disassembly ensure that resources are readily available. This consideration is important because the assembly/disassembly period can influence the intervention level, not only in the laboratory but also in clinical settings, mainly in public services that serve a great demand for patients and at home.

3.3.3. User learning curve

During the sessions, a gradual optimization was observed in the performance of the interventions, number of repetitions

of the training, classifier accuracy (AcCSP-LDA), and number of misses and hits for the activation of the sFES, as shown in Figure 3. Some aspects that may have impaired the learning effect of the training and the intervention with the sNES-sFES interface were to cancel out all the factors that interfered with the participant's concentration, such as maintaining absolute silence during training and intervention, keeping them in a very comfortable position, and avoiding any factors that increased muscle spasms.

It was also observed that for the success of the training, voice commands and orientations other than those mentioned above are necessary. We emphasize the importance of keeping the muscles intact, such as the relaxed upper limbs, especially when providing the command of motor imagery to perform knee extension. In addition, participants tend to close their eyes in an attempt to concentrate, which is not recommended due to the change in the sNES. In addition to the time, the amount of training per session was counted, as only one training was rarely performed owing to different situations, such as an alteration of the sNES or a low value of the cross-correlation. As a result, between one and three training sessions were performed because, despite the participant denying mental fatigue, when they passed three training sessions in the session, the values of the cross-correlation were substantially reduced.

3.3.3.1. Classifier accuracy

The classifier accuracy (AcCSP-LDA) resulting from training tended to increase gradually throughout the sessions (Figure 3), which can be explained by the participant learning effect. The average AcCSP-LDA value was 67% (a satisfactory AcCSP-LDA value was considered to be closer to 100%).

3.3.3.2. Hits and misses

Figure 3 depicts the percentage of hits, misses, and successes in the sFES activation. It was observed that

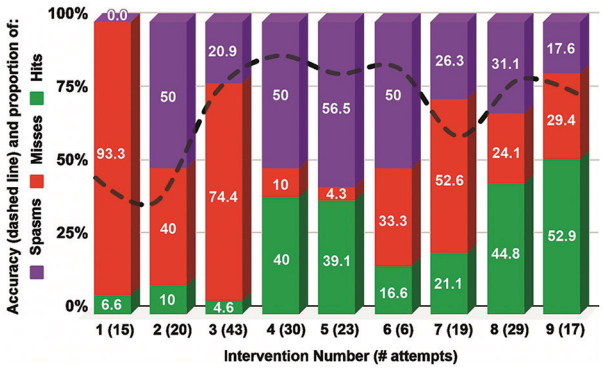

Figure 3. User's learning trend.
Note: Dashed line = Classifier accuracy.

the higher the AcCSP-LDA, the greater the tendency to reduce the percentage of errors and increase the number of correct answers. It was possible to identify that in all sessions, errors were recorded in the activation of sFES, and in most cases, the percentage of errors exceeded the percentage of correct answers. These errors occurred in two situations: (i) activation of the sFES without the therapist's command for this action, and (ii) non-activation of the sFES when the motor imagery was requested (within 4s). Regarding the activation of the sNES-sFES resulting from muscle spasms, it was not counted as an error, as it possibly did not occur due to a mental response by the participant but rather due to interference with the sNES measurement.

4. Discussion

4.1. Neuromuscular assessment

The lack of improvement in neuromuscular function can be explained by the complexity of the condition in SCI, especially in the chronic phase, and the fact that a short-term intervention protocol was carried out. In contrast to the present study, Donati *et al.*[32] conducted a study involving eight individuals with chronic SCI and paraplegics (seven complete and one incomplete) who underwent gait neurorehabilitation through a BCI in the long term (12 months). The intervention was divided into six stages, combining the integration of traditional physical rehabilitation and multiple brain-machine interface paradigms to restore locomotion. At the end of neurorehabilitation, all participants demonstrated neurological improvements in somatic sensitivity in various dermatomes. In addition, they exhibited recovery of voluntary motor control in muscles below the level of SCI (assessed by sEMG), resulting in a marked improvement in their gait index. In other words, greater intensity, frequency, and long-term training are important for recovery.

4.2. Spasticity

In this study, we observed a reduction in spasticity throughout the sessions, which is already well-established in the literature regarding the efficacy of electrical stimulation in spasticity reduction. As shown in the systematic review, Bekhet *et al.*[33] identified different stimulation parameters that can reduce spasticity after SCI, with the primary outcome being the assessment of spasticity using MAS. These authors identified that the stimulation parameters were a frequency of 20 – 30 Hz, a pulse duration of 300 – 350 μs, and a current amplitude >100 mA. The results of this review were similar to those of the present study, showing that sFESs reduced spasticity by 45 – 60%, in addition to reducing EMG activity and increasing range of motion.

4.3. Interventions

4.3.1. Static magnetic field

In this study, there was no improvement in neuromuscular condition (Section 4.1), possibly due to factors related to the severity of the injury (injury time, extent, level, and classification). The results observed in a human model (chronic condition) are different from those in animal models in the acute phase. For instance, Bhattacharyya *et al.*[34] exposed rats to a low-intensity magnetic field (17.94 μT) for 2 h/day for 3 weeks after SCI. The results suggest that short-term exposure to a magnetic field on locomotor behavior is beneficial because of the attenuation of secondary damage and calcium ion-mediated excitotoxicity.

Although the intervention in the present study was performed at the spinal cord level, studies using the SMF in the human cortex have shown that this intervention modulates cortical excitability[35] and improves the detection of somatosensory stimuli when applied to the parietal cortex.[36] Another item that should be investigated in depth is the ideal time for the application of the SMF. Despite the extended duration of SMF application in our study (approximately 1 h), a study by Oliviero *et al.*[37] showed that the application of transcranial SMF for up to 2 h is safe and does not appear to produce neural damage.

Nakagawa and Nakazawa[38] investigated the effects of trans-spinal SMF stimulation applied to the cervical spinal cord on corticospinal excitability. They used a magnet with a magnetic induction value of 0.45 T positioned on the spinal cord level C8 of 24 healthy individuals for 15 min. The motor-evoked potentials of the first digital interosseous muscle were evaluated before, during, and after trans-spinal SMF stimulation. They showed that this intervention could reduce corticospinal tract excitability. Therefore, researchers have suggested that trans-spinal SMF stimulation can be a neuromodulatory tool, and its suppressive effect can be in those with pathological hyperexcitability of the spinal neural network, similar to spasticity, a common condition in individuals with complete SCI. As in the present study, the participant presented a reduction in muscle tone, which can be explained both by the use of the NES-FES interface and also by the SMF. We cannot say whether this effect was potentiated by the combined use of these interventions, and future investigations are necessary.

4.3.2. Neuroelectrical signals and functional electrical stimulation interface

Although the participant did not exhibit improvement in his neuromuscular condition with the use of the NES-FES interface, it remains an assistive technology option. King *et al.*[39] developed a NES-FES interface to walk over the ground for a duration of 30 sessions and evaluated its performance in an individual with paraplegia due to SCI. This study investigated sessions in (i) screenings (BCI screening to determine whether one could control the BCI in a virtual reality environment—four sessions total) and (ii) training (BCI training to learn to ambulate within a virtual reality environment) using the attempt to walk and relax as a control strategy, starting in the fifth session and extending to the last. Their study concluded that the restoration of brain-controlled walking is feasible. In the current study, the participants performed only three initial sessions to get acclimated, and despite having had a relatively low performance in the training of the following sessions, interventions with the sNES-sFES interface had already started. Thus, it is essential to invest in more sessions to familiarize the participants before starting the interventions, including avoiding anxiety due to their responsibility to master the interface.

4.4. User learning curve

4.4.1. Classifier accuracy

The AcCSP-LDA value in this study increased over the training sessions, reaching an average of 67%. Comparatively, King *et al.*[39] obtained an average value of cross-correlation between the instructor's verbal commands and the response of the sNES-sFES interface of 77%, reaching 93% between sessions 20 and 21. Therefore, this study demonstrated that restoring brain-controlled walking in patients with paraplegia is feasible. Given this, although the average value of the participants in the present study was 67%, in the last sessions, the values of cross-correlation were close to the average cited by King *et al.*[39] Thus, it was found that the learning effect interferes with the brain-machine domain, and the user's performance may have been influenced by the reduced number of sessions.

4.4.2. Hits and misses

The hits (intentional response) and errors (unintentional response) of AcCSP-LDA were tallied, and any unintentional response of the device controlled by the participant was associated with the potential errors found in the sNES.[40] To avoid incorrect actions by BCI and improve performance, Liu *et al.*[41] proposed a new method based on an adaptive autoregressive model and a typical spatial pattern for extracting error-related potential features. They showed that the average precision and false positive rate for detecting error-related potential outperformed methods that use features extracted from a single domain. This new method efficiently improves the detection accuracy of error-related potentials and reduces the number of false positives.

4.5. Study implications and limitations

The implications of the present study include improving therapeutic tools and assistive technologies to enhance the functionality of individuals with SCI. Our proposal was to utilize a laboratory interface, but further research is needed to optimize it for home use. The results were limited by the small number of interventions and the severe neurological conditions of the participants. Moreover, only one participant underwent the experimental intervention.

5. Conclusion

The sNES-sFES interface and static magnetic field are non-invasive interfaces with an average duration of 1 h (equivalent to conventional therapy) and a setup and dismount time of approximately 10 min. A gradual learning effect was perceived regarding (i) training repetition up to three times per session to avoid mental fatigue, (ii) classifier accuracy reaching up to 84%, and (iii) maximum sFES activation hits of 53%. Therefore, intervention with the sNES-sFES interface and the static magnetic field is a viable therapeutic option for study participants. Studies with a larger number of participants are needed to generalize these results to the SCI population. No improvement in voluntary muscular contraction was observed as an outcome of the 9-week intervention. Nevertheless, it can be used as a complementary tool to activate movement in a paralyzed muscle and reduce spasticity, along with continuous physical rehabilitation. Future studies will include the implementation of novel machine learning algorithms based on deep learning techniques to improve classifier performance. A better accuracy model should enhance user control with SCI over the sNES-sFES interface and enable the application to be used in different positions, such as orthostasis or walking.

Acknowledgments

None.

Funding

None.

Conflict of interest

The authors declare that they have no competing interests.

Author contributions

Conceptualization: Eddy Krueger Larissa Gomes Sartori
Methodology: All authors
Writing—original draft: Larissa Gomes Sartori Eddy Krueger
Writing—review & editing: Roger Burgo de Souza, Daniel Prado Campos, Paulo Broniera Júnior, José J. A. Mendes Junior, Eddy Krueger

All authors have read and agreed to the published version of the manuscript.

Ethics approval and consent to participate

The present study was approved by the Ethics Committee and Research Involving Human Beings of the State University of Londrina (no.: 4.060.700) on June 1, 2020. The participant provided written consent.

Consent for publication

Written informed consent has been obtained from the patient(s) to publish this paper.

Availability of data

The neuroelectrical signals recorded through electroencephalography were not stored. Furthermore, all available data are presented in the images provided in the article.

References

1. Brown AR, Martinez M. From cortex to cord: Motor circuit plasticity after spinal cord injury. *Neural Regen Res*. 2019;14(12):2054-2062.

   doi: 10.4103/1673-5374.262572

2. Yang T, Dai Y, Chen G, Cui, S. Dissecting the dual role of the glial scar and scar-forming astrocytes in spinal cord injury. *Front Cell Neurosci*. 2020;14:78.

   doi: 10.3389/fncel.2020.00078

3. Aggarwal S, Chugh, N. Signal processing techniques for motor imagery brain computer interface: A review. *Array*. 2019;1-2:100003.

   doi: 10.1016/j.array.2019.100003

4. Barroso FO, Pascual-Valdunciel A, Torricelli D, *et al*. Noninvasive modalities used in spinal cord injury rehabilitation. In: *Spinal Cord Injury Therapy*. London: IntechOpen; 2019.

   doi: 10.5772/intechopen.83654

5. Chédotal A. Roles of axon guidance molecules in neuronal wiring in the developing spinal cord. *Nat Rev Neurosci*. 2019;20(7):380-396.

   doi: 10.1038/s41583-019-0168-7

6. Courtine G, Sofroniew MV. Spinal cord repair: Advances in biology and technology. *Nat Med*. 2019;25(6):898-908.

   doi: 10.1038/s41591-019-0475-6

7. Friedrich P, Waschke J. *Sobotta; Editora Guanabara Koogan LTDA*. United States: Bloomberg; 2012.

8. Krueger-Beck E, Scheeren EM, Neto GNN, Button VL, Nohama P. Effects Of Functional Electrical Stimulation In Artificial Neuromuscular Control. *Rev Neurociên*. 2011;19:530-541.

doi: 10.4181/RNC.2010.06ip.11

9. Mukhopadhyay R, Lenka PK, Biswas A, Mahadevappa M. Evaluation of functional mobility outcomes following electrical stimulation in children with spastic cerebral palsy. *J Child Neurol*. 2017;32(7):650-656.

doi: 10.1177/0883073817700604

10. Selfslagh A, Shokur S, Campos DS, *et al*. Non-invasive, Brain-controlled functional electrical stimulation for locomotion rehabilitation in individuals with Paraplegia. *Sci Rep*. 2019;9(1):6782.

doi: 10.1038/s41598-019-43041-9

11. Abdalsalam ME, Yusoff MZ, Kamel N, *et al*. Mental Task Motor Imagery Classifications for Noninvasive Brain Computer Interface. In: Proceedings of the 2014 5th International Conference on Intelligent and Advanced Systems: Technological Convergence for Sustainable Future, ICIAS 2014 (ICIAS). United States: IEEE. 2014. p. 1-5.

doi: 10.1109/ICIAS.2014.6869531

12. Hedayatzadeh M, Tehranipour M, Kobravi HR. Motor neuron recovery in rats after incomplete spinal cord injury using intra-spinal electrical stimulation and stem cell transfusion: A prelude to human applications. *Med Sci*. 2020;24:706-716.

13. Krueger E, Magri LM, Botelho AS, *et al*. Effects of low-intensity electrical stimulation and adipose derived stem cells transplantation on the time-domain analysis-based electromyographic signals in dogs with SCI. *Neurosci Lett*. 2019;696:38-45.

doi: 10.1016/j.neulet.2018.12.004

14. Farrell K, Detloff MR, Houle JD. Plastic changes after spinal cord injury. In*: Oxford Research Encyclopedia of Neuroscience*. Oxford: Oxford University Press; 2019.

doi: 10.1093/acrefore/9780190264086.013.241

15. Leemhuis E, De Gennaro L, Pazzaglia AM. Disconnected body representation: Neuroplasticity following spinal cord injury. *J Clin Med*. 2019;8(12):2144.

doi: 10.3390/jcm8122144

16. Spieker EL, Wiesener C, Niedeggen A, Wenger N Schauer T. Motor and sensor recovery in a paraplegic by transcutaneous spinal cord stimulation in water. In: *Proceedings on Automation in Medical Engineering*. Vol. 1; 2020. p. 22.

doi: 10.18416/AUTOMED.2020

17. Chaudhary U, Birbaumer N, Ramos-Murguialday, A. Brain-computer interfaces for communication and rehabilitation. *Nat Rev Neurol*. 2016;12(9):513-525.

doi: 10.1038/nrneurol.2016.113

18. Osuagwu BC, Wallace L, Fraser M, Vuckovic A. Rehabilitation of hand in subacute tetraplegic patients based on brain computer interface and functional electrical stimulation: A randomised pilot study. *J Neural Eng*. 2016;13(6):065002.

doi: 10.1088/1741-2560/13/6/065002

19. Macias MY, Battocletti JH, Sutton CH, Pintar FA, Maiman DJ. Directed and enhanced neurite growth with pulsed magnetic field stimulation. *Bioelectromagnetics*. 2000;21:272-286.

20. Fujioka Y, Tanaka N, Nakanishi K, *et al*. Magnetic field-based delivery of human CD1331 cells promotes functional recovery after rat spinal cord injury. *Spine*. 2012;7(13):E768-E777.

doi: 10.1097/BRS.0b013e318246d59c

21. Silvestro S, Bramanti P, Trubiani O, Mazzon E. Stem cells therapy for spinal cord injury: An overview of clinical trials. *Int J Mol Sci*. 2020;21:659.

doi: 10.3390/ijms21020659

22. Fukuda TY, Echeimberg JO, Pompeu JE, *et al*. Root mean square value of the electromyographic signal in the isometric torque of the quadriceps, hamstrings and brachial biceps muscles in female subjects. *J Appl Res*. 2010;10:32-39.

23. Júnior PB, Campos DP, Lazzaretti AE, *et al*. Influence of EEG channel reduction on lower limb motor imagery during electrical stimulation in healthy and paraplegic subjects. *Res Biomed Eng*. 2022;38:1-11.

doi: 10.1007/s42600-021-00189-6

24. Broniera Junior PB, Campos DP, Lazzaretti AE, *et al*. EEG-FES-Force-MMG closed-loop control systems of a volunteer with paraplegia considering motor imagery with fatigue recognition and automatic shut-off. *Biomed Signal Process Control*. 2021;68,102662.

doi: 10.1016/j.bspc.2021.102662

25. Silva CR, De Araújo RS, Albuquerque G, Moioli RC, Brasil FL. Interfacing brains to robotic devices-A VRPN communication application. In: *Proceedings of the XXVI Brazilian Congress on Biomedical Engineering*. Germany: Springer; 2019. p. 597-603.

26. Nogueira-Neto G, Scheeren E, Krueger E, *et al*. The influence of window length analysis on the time and frequency domain of mechanomyographic and electromyographic signals of submaximal fatiguing contractions. *Open J Biophys*. 2013;3(3):178-190.

doi: 0.4236/ojbiphy.2013.33021

27. International Electrotechnical Commission. *IEC 60601-2-10: 2012-Medical Electrical Equipment-Part 2-10: Particular Requirements for the Basic Safety and Essential Performance*

of Nerve and Muscle Stimulators. United Kingdom: International Electrotechnical Commission; 2012.

28. Krueger E, Scheeren EM, Nogueira-Neto GN, Nohama P. Mechanomyography energy decreases during muscular fatigue in paraplegics. In: *Proceedings of the 2014 36th Annual International Conference of the IEEE Engineering in Medicine and Biology Society*. United States: IEEE. 2014:5824-5827.

doi: 10.1109/EMBC.2014.6944952

29. Rabischong E. Surface action potentials related to torque output in paraplegics' electrically stimulated quadriceps muscle. *Med Eng Phys.* 1996;18:538-547.

doi: 10.1016/1350-4533(96)00001-x

30. Schiefer MA, Triolo RJ, Tyler DJ. A model of selective activation of the femoral nerve with a flat interface nerve electrode for a lower extremity neuroprosthesis. *IEEE Trans Neural Syst Rehabil Eng*. 2008;16(2):195-204.

doi: 10.1109/TNSRE.2008.918425

31. Beros J, King E, Clarke D, Jaeschke-Angi L, Tang AD. Static magnetic stimulation induces structural plasticity at the axon initial segment of inhibitory cortical neurons. *Sci Rep.* 2024;14(1):1479.

doi: 10.1038/s41598-024-51845-7

32. Donati AR, Shokur S, Morya E, *et al.* Long-term training with a brain-machine interface-based gait protocol induces partial neurological recovery in paraplegic patients. *Sci Rep.* 2016;6:30383.

doi: 10.1038/srep30383

33. Bekhet AH, Bochkezanian V, Saab IM, Gorgey AS. The effects of electrical stimulation parameters in managing spasticity after spinal cord injury: A systematic review. *Am J Phys Med Rehabil*. 2019;98(6):484-499.

doi: 10.1097/PHM.0000000000001064

34. Bhattacharyya S, Sahu S, Kaur S, Jain S. Effect of low intensity magnetic field stimulation on calcium-mediated cytotoxicity after mild spinal cord contusion injury in Rats. *Ann Neurosci.* 2020;27:49-56.

doi: 10.1177/0972753120950072

35. Kirimoto H, Tamaki H, Matsumoto T, *et al.* Effect of transcranial static magnetic field stimulation over the sensorimotor cortex on somatosensory evoked potentials in humans. *Brain Stimul*. 2014;7:836-840.

doi: 10.1016/j.brs.2014.09.016

36. Carrasco-López C, Soto-León V, Céspedes V, *et al.* Static magnetic field stimulation over parietal cortex enhances somatosensory detection in humans. *J Neurosci.* 2017;37:3840-3847.

doi: 10.1523/JNEUROSCI.2123-16.2017

37. Oliviero A, Carrasco-López M, Campolo M, *et al.* Safety study of transcranial static magnetic field stimulation (tSMS) of the human cortex. *Brain Stimul*. 2015;8:481-485.

doi: 10.1016/j.brs.2014.12.002

38. Nakagawa K, Nakazawa K. Static magnetic field stimulation applied over the cervical spinal cord can decrease corticospinal excitability in finger muscle. *Clin Neurophysiol Pract.* 2018;3:49-53.

doi: 10.1016/j.cnp.2018.02.001

39. King CE, Wang PT, McCrimmon CM, Chou CC, Do AH, Nenadic Z. The feasibility of a rain-computer interface functional electrical stimulation system for the restoration of overground walking after paraplegia. *J Neuroeng Rehabil.* 2015;12:1-11.

doi: 10.1186/s12984-015-0068-7

40. Schalk G, Wolpaw JR, McFarland DJ, Pfurtscheller G. EEG-based communication: Presence of an error potential. *Clin Neurophysiol.* 2000;111(12):2138-2144.

doi: 10.1016/s1388-2457(00)00457-0

41. Liu Q, Zheng W, Chen K, Ma L, Ai Q. Online detection of class-imbalanced error-related potentials evoked by motor imagery. *J Neural Eng.* 2021;18(4):046032.

doi: 10.1088/1741-2552/abf522

ACCSCIENCE PUBLISHING

Global Translational Medicine

CASE REPORT

You're a pain in my side! Abscess and microperforation as a complication of therapy from early-stage endometrial cancer: A case report

Jennifer McCall*, Jena Hall, and Elena Park

Department of Obstetrics and Gynecology, Queen's University, Kingston, Ontario, Canada

Abstract

This paper reports on a 55-year-old woman presenting with left lower quadrant and groin pain that posed a significant diagnostic challenge. She had a history of obesity and stage 1B endometrial carcinoma treated with surgery and radiation 1-year prior. Despite several unsuccessful biopsy attempts and unclear imaging findings, she was ultimately diagnosed with a pelvic sidewall abscess secondary to a bowel microperforation, a rare late complication of radiation related to adhesions, weakened bowel, and peristalsis. Her condition was successfully treated with drainage and antibiotics. It is widely known that patients with endometrial cancer and comorbid obesity often experience diagnostic delay, weight stigma, and other barriers and thus deserve careful attention and continued advocacy.

Keywords: Endometrial cancer; Obesity; Weight stigma; Radiation; Case report

***Corresponding author:**
Jennifer McCall
(jmccall@qmed.ca)

Citation: McCall J, Hall J, Park E. You're a pain in my side! Abscess and microperforation as a complication of therapy from early-stage endometrial cancer: A case report. *Global Transl Med*. 2024;3(1):2114.
https://doi.org/10.36922/gtm.2114

Received: October 26, 2023
Accepted: January 30, 2024
Published Online: March 19, 2024

1. Background

Uterine cancer is the fourth most common cancer among females in Canada and sixth most common cancer in the world.[1,2] Both the incidence and the mortality rates of uterine cancer are increasing.[1,3] Obesity is the main underlying cause for the increasing incidence globally.[3] Risk factors for endometrial cancer include advanced age, nulliparity, obesity, sedentary lifestyle, early menarche, anovulatory cycles, late menopause, unopposed systemic estrogen, tamoxifen use, diabetes, pelvic radiation, hypertension, family history, and genetic conditions.[2,4,5] The International Federation of Gynecology and Obstetrics (FIGO) staging system is the most widely used in the world, with an update published in 2023.[6] Stage I is confined to the uterine corpus and ovary, further subdivided into stage IA characterized by invasion into less than half the myometrium for non-aggressive histological types and stage IB for invasion into more than half the myometrium for non-aggressive histological types.[6] The mainstay of management is cytoreductive surgery, with minimally invasive surgery being a safe alternative with better perioperative and post-operative outcomes and comparable oncologic outcomes in affected individuals,[3,7] including obese patients.[8] However, one study found that conversions occur in 31% of laparoscopic hysterectomies for endometrial cancer in patients with obesity.[9] Many patients undergoing major gynecologic oncology surgery, including open hysterectomy, will experience early complications, including 35% with

hemorrhage requiring transfusion, 13% with ileus, and 9.7% with infection including 3.9% with abscess formation.[10] People with obesity have higher risks of complications.[11] It is unknown whether obesity impacts survival outcomes among people with endometrial cancer.[12] Recurrence of stage 1 endometrial cancer treatment after combined surgery and radiation therapy is 4%; 25% of these patients experience late complications.[13]

This case report details a rare late complication, the description of which can assist physicians in quickly reaching the correct diagnosis and treatment.

2. Case presentation

A 55-year-old woman with a history of grade 2 stage 1B endometrioid adenocarcinoma of the endometrium presented to a community emergency department following a 2-week onset of left lower quadrant and groin pain and left leg swelling (Table 1). Her cancer treatment included a total abdominal hysterectomy bilateral salpingo-oophorectomy (TAHBSO) (laparoscopic converted to open) and pelvic lymph node dissection (PLND) 1-year prior, and adjuvant external beam radiation therapy (EBRT) completed 9-month prior. The pain was a constant, severe ache associated with mild paresthesias in her left thigh. Her past medical history included morbid obesity (BMI 60), insulin-dependent type 2 diabetes with poor control, obstructive sleep apnea, hypertension, non-alcoholic fatty liver disease, hypothyroidism, and depression. She had been surgically operated with procedures such as oncology surgery and a dilation and curettage. She was nulliparous.

At the community emergency department, deep vein thrombosis was ruled out and an outpatient computed tomography (CT) was ordered (Figure 1). One day later, she presented to our tertiary care site with a complaint of increasing pain. She had normal vital signs, normal bilateral lower limb perfusion and strength, pain on hip flexion, and a soft, non-tender abdomen. She had a mild leukocytosis (white blood cells [WBC]: 16.3 × 10^9/L [4.0–11.0 ×10^9/L]), a slightly elevated lactate (2.3 mmol/L [0.5–2.2 mmol/L]), and an HbA1c of 10.7% (4.0–6.0%) (Table 2). Her hemoglobin, platelets, and creatinine levels were normal. Ca-125 was found to be 147 units/mL, reduced from 370 units/mL at her initial cancer diagnosis.

Based on the CT findings from the day prior demonstrating a pelvic sidewall mass, she was admitted for a presumed mass due to cancer recurrence, which was speculated to have compressed the left external iliac artery. Vascular surgery assessment demonstrated non-claudication pain and no ischemia, and radiation oncology-based evaluation recommended pathologic confirmation of recurrence.

Interventional radiology unit was consulted to obtain a biopsy of the mass. The biopsy was anticipated to be challenging due to its proximity to major vessels, the patient's body habitus, and her inability to lay in the optimal position for biopsy due to pain. In the initial attempt, fibroadipose tissue and skeletal muscle with focal acute and chronic inflammation as well as fibrosis were obtained, and no evidence of neoplasia was identified. A magnetic resonance imaging (MRI) test was attempted on post-admission day (PAD) 6, but the patient was too uncomfortable to lie flat.

In the ongoing consultation, the radiation oncology unit persisted in their request for pathologic confirmation before providing an opinion on treatment. On PAD 10, another biopsy was attempted but the patient was again unable to lie prone due to anxiety and respiratory difficulties. Abdominal entry was not possible due to abdominal obesity.

Due to her worsening leukocytosis, which peaked at 25.2 × 10^9/L on PAD 5, infectious work-up was performed and was negative (including urine and blood cultures and chest X-ray). General internal medicine unit was then consulted and found no indication for antibiotics for her isolated leukocytosis, which started to decline after PAD 5 without treatment.

Throughout this period of time, the patient continued to suffer from severe pain that was challenging to manage despite consultation with the Acute Pain Management Service and Palliative Care unit. Higher doses of narcotics and pregabalin are required to alleviate the intense pain; she was confronting. She also complained of increasing drowsiness beginning 1 week after admission. It was unclear if this was related to her pain management regimen or underlying pathology.

A repeat CT scan on PAD 11 showed slight measurable growth in the mass-like soft-tissue density in the left pelvis, extending into the groin muscles. This causes new mild obstruction of the left ureter at the pelvic brim and impending bladder invasion. While infection cannot be entirely excluded, the growing line of findings pointed to a highly potential malignant recurrence.

On PAD 15, she was diagnosed with cellulitis of the left foot that was treated with cephalexin. On PAD 16, she had a fever at 38.2°C, but an immediately repeated measurement was found to be normal.

On PAD 15, the patient's case was again reviewed at a multidisciplinary gynecologic oncology conference. It was determined that she was ineligible for further radiation due to the previous dose received. A decision was made to proceed with a treatment using carboplatin and paclitaxel

Table 1. Timeline of events

Admission day	Events
One year before presentation	• Diagnosis and treatment for grade 2 stage IB endometrioid adenocarcinoma of the endometrium • Hysterectomy and adjuvant radiation
One day pre-admission	• Patient presented to community emergency department with complaints of left lower quadrant pain, groin pain, and left leg swelling • DVT ruled out • Patient discharged • Outpatient CT demonstrated pelvic sidewall mass
PAD 0	• Patient presented to tertiary care center • Patient admitted for further work up and presumed cancer recurrence
PAD 1–4	• Claudication and ischemia ruled out at vascular surgery unit • Interventional radiology unit consulted for biopsy but with inconclusive initial biopsy pathology • Acute Pain Management Service and Palliative Care consulted to assist with pain management
PAD 5	• WBC peaks • Infectious work-up showing negative results • General internal medicine unit consulted, providing no indications of antibiotics
PAD 6	• MRI attempted but patient unable to lie flat due to pain
PAD 7–9	• Ongoing interdisciplinary discussion with tumor conference members
PAD 10	• Second biopsy attempt by interventional radiology unit but unable to perform
PAD 11	• Repeat CT showing mass expanding; an involvement of infection cannot be ruled out but a potential malignant recurrence was speculated, according to findings
PAD 15	• Case again reviewed at tumor conference, in which radiation oncology unit determined that additional radiation was no longer feasible due to previous doses received, and a decision to proceed with chemotherapy was made
PAD 17	• Patient given paclitaxel, which resulted in allergic-type reaction • Carboplatin was scheduled for administration on PAD 18
PAD 18	• Significant decrease in level of consciousness • Head CT was normal • Abdomen/pelvis CT showed rapid increase in pelvic mass size, consistent with abscess • Blood cultures result was positive
PAD 18–discharge	• Patient developed febrile neutropenia and initially treated with Pip-Tazo • Interventional radiology unit successfully placed a drain • Infectious disease unit re-consulted, giving a diagnosis of rare, late complication of radiation (microperforation of bowel due to adhesions) • Patient discharged home on a 4-week course of ertapenem

Abbreviations: CT: Computed tomography; DVT: Deep vein thrombosis; MRI: Magnetic resonance imaging; PAD: Post-admission day; WBC: White blood cell.

for suspected recurrence. On PAD 17, she received paclitaxel only. Due to an allergic-type reaction to paclitaxel (fleeting back pain, chest heaviness, hypertension, and flushing), the carboplatin dose was scheduled for the following day.

In the morning on PAD 18, the patient had a decreased level of consciousness that was more profound than her previously perceived drowsiness. Head CT showed no mass or infarct, and abdomen/pelvis CT demonstrated a rapid increase in pelvic mass size, consistent with the finding for an abscess. Blood cultures were positive for *Klebsiella pneumoniae* and *Citrobacter koseri*, confirming sepsis. The patient subsequently developed a fever and febrile neutropenia. She was initially treated with Pip-Tazo. Infectious disease unit was consulted and determined that it was caused by a rare late complication of radiation: Abscess from a microperforation of the bowel due to adhesions, weakened bowel, and peristalsis. A few days later, a drain was successfully placed by the interventional radiology unit, releasing more than 1 L of purulent fluid. Her cytology report showed negative results. She was discharged home on intravenous ertapenem for 4 weeks. To date, there has been no evidence of cancer (or abscess) recurrence.

3. Discussion

The current report demonstrates the challenges in unraveling a case of a post-radiation bowel microperforation and pelvic abscess in a patient with grade 2 stage 1B endometrial carcinoma treated with surgery and EBRT. Despite several unsuccessful biopsy attempts and unclear imaging findings, an ultimate diagnosis was made, i.e., a pelvic sidewall

Figure 1. Abdomen/pelvis computed tomography showing a mass along the left pelvic sidewall, which is partially encasing and narrowing the left external iliac artery and inseparable from the left psoas, iliacus, and obturator internus muscles.

Table 2. Results of clinical biomarkers on different dates

Biomarker	Date	Value/Finding
HbA1c (normal 4.0 – 6.0%)	PAD 0	10.7%
	PAD 1	10.7%
Ca-125	PAD 0	147 units/mL
	PAD 1	147 units/mL
WBC (normal 4.0 – 11.0×10^9/L)	PAD 0	16.3×10^9/L
	PAD 1	16.3×10^9/L
	PAD 5	25.2×10^9/L
Lactate (normal 0.5 – 2.2 mmol/L)	PAD 0	2.3 mmol/L
	PAD 1	2.3 mmol/L
Infectious workup	PAD 5	Negative
	PAD 18	Blood culture positive for *Klebsiella pneumonia* and *Citrobacter koseri*

Abbreviations: PAD: Post-admission day; WBC: White blood cell.

abscess secondary to a bowel microperforation, which was successfully managed with drainage and antibiotics.

Several challenges limited our ability to make a timely diagnosis in this case. A delayed presentation of infection from the initial surgery and radiation therapy made infection a less likely probability. The initially stable size of the pelvic collection and absence of other infectious symptoms did not suggest abscess. Leukocytosis was a clue that an infectious process was at play but is also a non-specific marker that can be implicated in inflammatory processes including neoplastic disease. The difficulty in obtaining an adequate sample due to multiple factors including the patient's body habitus and comorbid anxiety added to diagnostic delay. However, our persistence in determining a cause, our dedication to listen to the patient's symptoms and take them seriously, and our agility to react to changing circumstances and reinvestigate new presentations was crucial to eventually determining the correct diagnosis. Ultimately, this patient received a dose of chemotherapy that was not indicated; however, we could no longer delay taking action. For a future presentation, we would consider starting empiric antibiotic therapy for a pelvic mass and leukocytosis.

4. Conclusion

This was a challenging case of a post-radiation bowel microperforation and pelvic abscess in a patient with grade 2 stage 1B endometrial carcinoma treated with surgery and EBRT. Diagnosis was challenging due to non-specific symptoms and inability to obtain a biopsy specimen for culture and pathology due to comorbid obesity, anxiety, pain and respiratory disease. Patients with stage 1 endometrial carcinoma who receive adjuvant EBRT are known to have increased complication rates with no impact on survival.[13,14] Use of EBRT should be limited to special circumstances. Patients with pelvic mass not yet diagnosed and leukocytosis, especially those with prior radiation to the affected area, should be started on empiric antibiotics as first line therapy. Patients with endometrial cancer and comorbid obesity often experience diagnostic delay, weight stigma, and other barriers[15] and require careful case consideration and continued advocacy, as was provided in this case. We are very grateful to this patient and her spouse, who was an excellent support for her during this time.

Acknowledgments

The authors thank Jessica Pudwell for her assistance with obtaining ethics approval.

Funding

None.

Conflict of interest

The authors declare that they have no competing interests.

Author contributions

Conceptualization: Jennifer McCall, Jena Hall
Supervision: Elena Park
Writing – original draft: Jennifer McCall
Writing – review & editing: Jennifer McCall, Jena Hall

Ethics approval and consent to participate

The Queen's University Health Sciences and Affiliated Teaching Hospitals Research Ethics Board (HSREB) have granted ethics clearance for this study (No: OBGY-413-22).

Consent for publication

The participant has consented to the submission of the case report to the journal.

Availability of data

Not applicable.

References

1. Brenner DR, Weir HK, Demers AA, *et al*. Projected estimates of cancer in Canada in 2020. *CMAJ*. 2020;192(9):E199-E205.

   doi: 10.1503/cmaj.191292

2. World Cancer Research Fund International. Endometrial Cancer Statistics; 2022. Available from: https://www.wcrf.org/cancer-trends/endometrial-cancer-statistics [Last accessed on 2024 Jan 21].

3. Crosbie EJ, Kitson SJ, McAlpine JN, Mukhopadhyay A, Powell ME, Singh N. Endometrial cancer. *Lancet*. 2022;399(10333):1412-1428.

   doi: 10.1016/S0140-6736(22)00323-3

4. Renaud MC, Le T. No. 291-Epidemiology and investigations for suspected endometrial cancer. *J Obstetr Gynaecol Can*. 2018;40:e703-e711.

   doi: 10.1016/j.jogc.2018.07.005

5. Hamilton CA, Pothuri B, Arend RC, *et al*. Endometrial cancer: A society of gynecologic oncology evidence-based review and recommendations. *Gynecol Oncol*. 2021;160(3):817-826.

   doi: 10.1016/j.ygyno.2020.12.021

6. Berek JS, Matias-Guiu X, Creutzberg C, *et al*. FIGO staging of endometrial cancer: 2023. *Int J Gynecol Obstetr*. 2023;162:383-394.

   doi: 10.1002/ijgo.14923

7. Scaletta G, Dinoi G, Capozzi V, *et al*. Comparison of minimally invasive surgery with laparotomic approach in the treatment of high risk endometrial cancer: A systematic review. *Eur J Surg Oncol*. 2020;46(5):782-788.

   doi: 10.1016/j.ejso.2019.11.519

8. Gehrig PA, Cantrell LA, Shafer A, Abaid LN, Mendivil A, Boggess JF. What is the optimal minimally invasive surgical procedure for endometrial cancer staging in the obese and morbidly obese woman? *Gynecol Oncol*. 2008;111(1):41-45.

   doi: 10.1016/j.ygyno.2008.06.030

9. Cusimano MC, Simpson AN, Dossa F, *et al*. Laparoscopic and robotic hysterectomy in endometrial cancer patients with obesity: A systematic review and meta-analysis of conversions and complications. *Am J Obstetr Gynecol*. 2019;221(5):410-428.

   doi: 10.1016/j.ajog.2019.05.004

10. Fagotti A, Costantini B, Fanfani F, *et al*. Risk of postoperative pelvic abscess in major gynecologic oncology surgery: One-year single-institution experience. *Ann Surg Oncol*. 2010;17:2452-2458.

    doi: 10.1245/s10434-010-1059-3

11. Bouwman F, Smits A, Lopes A, *et al*. The impact of BMI on surgical complications and outcomes in endometrial cancer surgery--an institutional study and systematic review of the literature. *Gynecol Oncol*. 139(2):369-376.

    doi: 10.1016/j.ygyno.2015.09.020

12. Arem H, Irwin ML. Obesity and endometrial cancer survival: A systematic review. *Int J Obes* (*Lond*). 2013;37(5):634-639.

    doi: 10.1038/ijo.2012.94

13. Creutzberg CL, Van Putten WL, Koper PC, *et al*. Surgery and postoperative radiotherapy versus surgery alone for patients with stage-1 endometrial carcinoma: Multicentre randomised trial. PORTEC Study Group. Post operative radiation therapy in endometrial carcinoma. *Lancet*. 2000;355(9213):1404-1411.

    doi: 10.1016/S0140-6736(00)02139-5

14. Creutzberg CL, Van Putten WL, Koper PC, *et al*. The morbidity of treatment for patients with Stage I endometrial cancer: Results from a randomized trial. *Int J Radiat Oncol Biol Phys*. 2001;51(5):1246-1255.

    doi: 10.1016/S0360-3016(01)01765-5

15. Cusimano MC, Simpson AN, Han A, *et al*. Barriers to care for women with low-grade endometrial cancer and morbid obesity: A qualitative study. *BMJ Open*. 2019;9(6):e026872.

    doi: 10.1136/bmjopen-2018-026872

ACCSCIENCE PUBLISHING

Global Translational Medicine

CASE REPORT

Carbon monoxide poisoning manifesting with rhabdomyolysis, Takotsubo syndrome, and skin lesion: A case report

Damiano Cardinale[1†*], Edoardo Pennacchio[2†], and Marco Russo[1]

[1]Unit of Cardiology, Sacro Cuore di Gesù Hospital, Gallipoli (Lecce), Italy

[2]Emergency Medicine Unit, San Carlo Hospital, Potenza, Italy

Abstract

Carbon monoxide (CO) poisoning is characterized by non-specific and protean clinical manifestations, exhibiting a highly variable presentation. We present a case of an 83-year-old female Alzheimer's patient, a non-smoker, who was found unconscious in her wheelchair by her caregiver at home. The heating in the apartment was powered by liquefied petroleum gas. On admission to the emergency department, her vital signs were normal, but she was unconscious and slightly dyspneic. The examination revealed red-colored skin lesions in the submammary area, where the wheelchair safety belt was firmly fastened. The rest of the physical examination results were unremarkable. The carboxyhemoglobin level was 23%, and there was an increase in creatine phosphokinase and troponin I levels. On the 2nd day of hospitalization in the emergency ward, the electrocardiogram revealed negative T waves in the V1–V6 leads, while the bedside echocardiogram revealed apical ballooning of the left ventricle. The myocardial perfusion examination yielded a negative result for myocardial ischemia. In the management of patients with CO poisoning, it is important for emergency physicians to assess the presence of multiple organ and tissue disorders. Consequently, the patient was diagnosed with CO poisoning with skin, skeletal, and cardiac muscle involvement.

Keywords: Carbon monoxide poisoning; Rhabdomyolysis; Takotsubo syndrome

†*These authors contributed equally to this work*

***Corresponding author:**
Damiano Cardinale
(damiano.cardinale@asl.lecce.it)

Citation: Cardinale D, Pennacchio E, Russo M. Carbon monoxide poisoning manifesting with rhabdomyolysis, Takotsubo syndrome, and skin lesion: A case report. *Global Transl Med.* 2024;3(1):1718.
https://doi.org/10.36922/gtm.1718

Received: August 30, 2023
Accepted: January 4, 2024
Published Online: March 20, 2024

1. Background

Carbon monoxide (CO) is an odorless, colorless, and tasteless gas produced by the incomplete combustion of organic substances. More than 20,000 emergency department visits/year are related to CO poisoning; the worldwide cumulative incidence and mortality are currently estimated at 137 cases and 4.6 deaths per million, respectively. Carbon monoxide binds to hemoglobin (forming carboxyhemoglobin [COHb]) with an affinity nearly 200-fold higher than oxygen (O_2). As a result, hemoglobin becomes less efficient at delivering O_2 to the cells, ultimately causing intracellular hypoxia. Elevated COHb blood levels (over 5% in non-smokers and 10% in smokers) suggest external exposure to CO.[1,2] The brain and the myocardium are constantly involved in CO poisoning due to their high levels of O_2 consumption. The clinical symptoms of CO poisoning are non-specific and can lead to diagnostic uncertainty. The most frequently reported acute symptoms of CO poisoning are headache, dizziness, weakness,

nausea, difficulty in concentration, confusion, shortness of breath, visual changes, chest pain, loss of consciousness, abdominal pain, and muscle cramping. Severe CO poisoning can cause skin lesions (cherry-red erythema, vesicles, bullae, and cutaneous necrosis); these lesions are often misdiagnosed as burns.[3] Takotsubo cardiomyopathy is a form of non-ischemic cardiomyopathy, characterized by transient regional systolic dysfunction of the left ventricle mimicking acute myocardial infarction but with only minimal release of cardiac enzymes. The term "Takotsubo" means octopus trap in Japanese, as the shape resembles the systolic apical ballooning appearance of the left ventricle.[4]

2. Case presentation

An 83-year-old female patient, diagnosed with Alzheimer's dementia and Type 2 diabetes mellitus, was transported to the emergency department by ambulance due to impaired consciousness. Her caregiver reportedly discovered the patient unconscious, sitting in the wheelchair with vomit on her clothes, in the morning. The heating in the apartment was powered by liquefied petroleum gas. On admission to the emergency department, the reported vital signs of the patient were as follows: blood pressure, 110/67 mmHg; body temperature, 36°C; heart rate, 90 beats/min; and respiratory rate, 22 breaths/min. Physical examination revealed mild dyspnea, warm and dry skin with a cherry-red lesion in the submammary area, rhythmic heart action, a normal vesicular murmur over the entire lung area, and a Glasgow Coma Scale score of 8 (E2-V2-M4). The electrocardiogram (ECG) revealed sinus rhythm at 90 bpm, with normal ST segment and T waves. Additionally, the arterial blood gas analysis in ambient air was as follows: pH 7.32; pCO_2: 31 mmHg; pO_2: 60 mmHg; HCO_3: 16 mmol/L; COHb: 23.8%; and lactate: 10.5 mmol/L. Laboratory test results were as follows: creatinine: 1.12 mg/dL; creatine phosphokinase (CPK): 2352 U/L; myoglobin: 1141 ng/mL; and troponin I: 3276 ng/L. A head computed tomography revealed age-compatible brain atrophy. Following the diagnosis of CO poisoning, the patient was admitted to the emergency medicine ward. Subsequently, the patient was administered O_2 via continuous positive airway pressure (CPAP), with a FiO_2 of 50% and a positive pressure of 7.5 cm H_2O. Large volumes of crystalloids were administered to prevent renal damage due to rhabdomyolysis, and low-molecular-weight heparin (LMWH) was administered for antithrombotic prophylaxis. Hyperbaric O_2 therapy was deemed unnecessary by the poison control center. The CPAP rapidly reduced COHb levels (1.6% after 4 h and 0.3% after 5 h). On the following day, we found changes in the ECG, specifically the appearance of negative T waves in the precordial leads (V1–V6) (Figure 1A). The bedside echocardiogram showed akinesia and dilatation of the mid-apical segments of the left ventricle with a slightly reduced global systolic function (EF 50%); these findings were compatible with the diagnosis of Takotsubo cardiomyopathy (Figure 1B). After the initial stabilization, the patient was transferred to the geriatric department, and a week later, troponin I, CPK, lactate, and cardiac kinetics normalized (Figure 1C). The submammary cherry-red skin lesion partially healed (Figure 1D), and a skin biopsy was not performed due to a lack of consent. The myocardial perfusion imaging test (SPECT) result (Figure 1E) was negative for myocardial ischemia.

3. Discussion

Takotsubo cardiomyopathy is a syndrome characterized by transient left ventricular dysfunction (hypokinesia, akinesia, or dyskinesia), usually presenting as apical ballooning or midventricular, basal, or focal wall motion abnormalities that extend beyond a single epicardial vessel territory. New ECG abnormalities (ST-segment elevation or depression, T-wave inversion, and rate-related [or corrected] QT interval [QTc] prolongation) and mild increases in troponin levels are common. Takotsubo usually affects postmenopausal women with ischemic-like chest pain and is strongly correlated with physical and emotional stress. Although most patients present with a complete recovery, mortality is higher than previously thought.[5] According to a 2016 study by Sung *et al.*, 30% of patients affected by CO intoxication report myocardial damage; 25.6% of these patients had normal echocardiography; 51.2% presented with global changes in left ventricular kinetics; and 23.2% had Takotsubo-like cardiomyopathy.[6] The abnormalities of Takotsubo CO-related cardiomyopathy are thought to be caused by an increase in catecholamines and consequent myocardial stunning.[7] This condition is usually transient and is managed with supportive care, but some patients require intensive care due to acute complications such as cardiogenic shock or acute heart failure; in patients with severe left ventricular systolic dysfunction, the risk of left ventricular thrombosis and systemic embolization should be considered. Rhabdomyolysis is characterized by an elevation in CPK due to the damage to striated muscle fibers and the consequent release of intracellular muscular constituents into the blood circulation. This complication is reported in approximately 30% of patients with CO intoxication;[8] among non-traumatic causes of rhabdomyolysis, CO intoxication represents 3.2% of the total number of cases.[9] In CO poisoning, muscle compression, caused by the patient's own weight, increases the pressure within the muscle compartment, causing edema and ischemia. If this condition persists, COHb production increases and the O_2 supply further decreases, leading to necrosis of muscle fibers and rhabdomyolysis.[10] Numerous CO-related skin

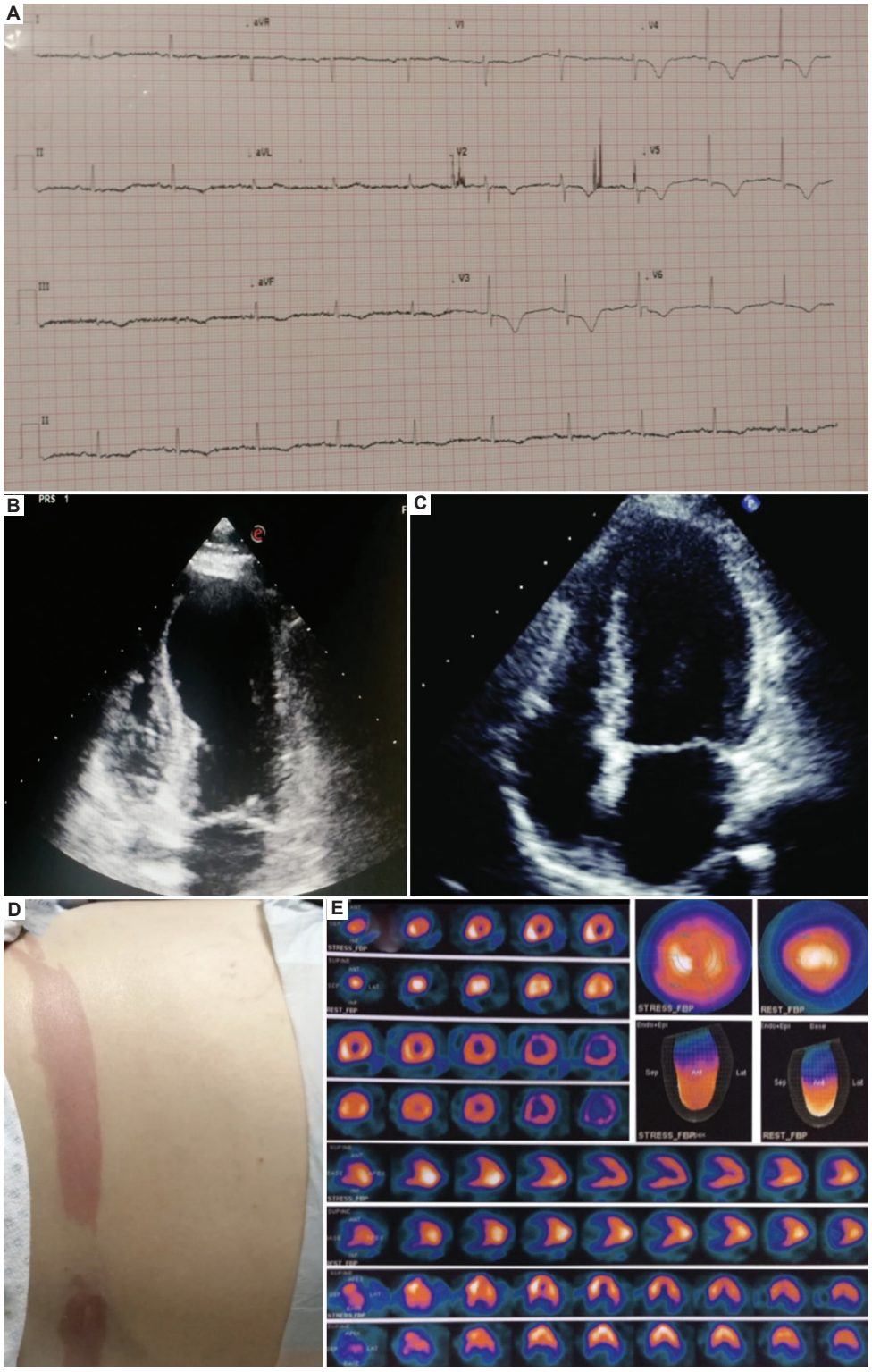

Figure 1. Clinical manifestations and diagnostic findings in the patient. (A) Electrocardiogram evolution displaying T waves inversion in precordial leads; (B) apical ballooning of left ventricle at echocardiography; (C) normal kinetics of the left ventricle on echocardiography; (D) typical well-defined red skin lesions at the sites where the comatose patient had lain; and (E) myocardial perfusion imaging test.

injury types have been reported in the literature, such as erythema, vesicles, edema, abscesses, and ulcers, which are found in approximately 30% of patients and develop mainly in skin areas subjected to pressure. The most common skin lesion is cherry-red erythema, which is often erroneously diagnosed as a burn. This type of injury is thought to be caused by pressure skin necrosis and CO-mediated inhibition of tissue oxidative enzymes.[11]

4. Conclusion

CO poisoning is a prevalent issue, with a multitude of annual emergency department admissions. A limited number of these patients may have cardiac injury as well as striated muscle (rhabdomyolysis) and skin (cherry red erythema) involvement. It is essential for emergency physicians to diagnose these complications in time, especially cardiac complications, to prevent permanent myocardial damage. Given the increasing utility of point-of-care ultrasound by emergency physicians, the detection of this disease will be more feasible if they are aware of this important correlation between CO poisoning and multiorgan damage. One must further bear in mind that Takotsubo syndrome could share multiple etiologies, such as CO poisoning as well as coronary microvascular dysfunction, coronary artery spasm, catecholamine-induced myocardial stunning, reperfusion injury following acute coronary syndrome, myocardial microinfarction, and abnormalities in cardiac fatty acid metabolism.[12]

Acknowledgments

None.

Funding

None.

Conflict of interest

The authors declare that they have no competing interests.

Author contributions

Conceptualization: Damiano Cardinale
Investigation: Damiano Cardinale, Edoardo Pennacchio
Writing – original draft: Damiano Cardinale, Marco Russo
Writing – review & editing: Damiano Cardinale, Marco Russo

Ethics approval and consent to participate

Patient gave consent to participate in the study

Consent for publication

Patient gave consent to publish data.

Availability of data

The data that support the findings of this case report are openly available at https://doi.org/10.36922/gtm.1718

References

1. Mattiuzzi C, Lippi G. Worldwide epidemiology of carbon monoxide poisoning. *Hum Exp Toxicol*. 2020;39(4):387-392.
doi: 10.1177/0960327119891214
2. Ernst A, Zibrak JD. Carbon monoxide poisoning. *N Engl J Med*. 1998;339(22):1603-1608.
doi: 10.1056/NEJM199811263392206
3. Ng PC, Long B, Koyfman A. Clinical chameleons: An emergency medicine focused review of carbon monoxide poisoning. *Intern Emerg Med*. 2018;13:223-229.
doi: 10.1007/s11739-018-1798-x
4. Ahmad SA, Brito D, Khalid N, Ibrahim MA. Takotsubo cardiomyopathy. In: *Statpearls*. Treasure Island (FL): StatPearls Publishing; 2023.
5. Boyd B, Solh T. Takotsubo cardiomyopathy: Review of broken heart syndrome. *JAAPA*. 2020;33(3):24-29.
doi: 10.1097/01.JAA.0000654368.35241.fc
6. Cha YS, Kim H, Hwang SO, *et al*. Incidence and patterns of cardiomyopathy in carbon monoxide-poisoned patients with myocardial injury. *Clin Toxicol (Phila)*. 2016;54(6):481-487.
doi: 10.3109/15563650.2016.1162310
7. Wittstein IS, Thiemann DR, Lima JA, *et al*. Neurohumoral features of myocardial stunning due to sudden emotional stress. *N Engl J Med*. 2005;352(6):539-548.
doi: 10.1056/NEJMoa043046
8. Jang SW, Jeon JC, Choi WI. Risk factors associated with complications of carbon monoxide poisoning. *J Korean Soc Clin Toxicol*. 2009;7(1):10-18.
9. Kang SW, Kim YW, Kim YH. Analysis of nontraumatic rhabdo myolysis during recent 2 years. *Korean J Med*. 2004;67:467-474.
10. Chung KJ, Chung YK, Yoo JH, Wang JS. Sciatic nerve palsy complicating gluteal compartment syndrome due to rhabdomyolysis: A case report. *J Korean Orthop Assoc*. 2005;40:103-106.
11. Myers RA, Snyder SK, Majerus TC. Cutaneous blisters and carbon monoxide poisoning. *Ann Emerg Med*. 1985;14(6):603-606.
doi: 10.1016/s0196-0644(85)80792-7
12. Komamura K, Fukui M, Iwasaku T, Hirotani S, Masuyama T. Takotsubo cardiomyopathy: Pathophysiology, diagnosis and treatment. *World J Cardiol*. 2014;6(7):602-609.
doi: 10.4330/wjc.v6.i7.602

ACCSCIENCE PUBLISHING

Global Translational Medicine

CASE REPORT

Anergy as a potential risk factor for squamous cell carcinoma in an immunocompetent patient with diffuse cutaneous leishmaniasis: A case report

Andrés Tirado-Sánchez[1]*, Alexandro Bonifaz[2], and Sebastián Hernández-Gómez[1]

[1]Department of Internal Medicine, Hospital General de Zona 30, Instituto Mexicano del Seguro Social, Mexico City, México

[2]Mycology Laboratory, Hospital General de México, Mexico City, México

Abstract

Despite the rarity, leishmaniasis may occur in tandem with malignancy. This co-occurrence contributes to a postulation that anergy to parasite antigens may predispose an infected patient to the development of diffuse cutaneous leishmaniasis and also increase the risk of developing squamous cell carcinoma due to decreased host immune response. We, herein, present a 63-year-old man suffering diffuse cutaneous leishmaniasis that was poorly responsive to treatment. Furthermore, the patient had several nodule-like, infiltrative, and coalescent lesions on his right face. The Montenegro skin test revealed signs of anergy and the biopsy test revealed squamous cell carcinoma (SCC) coexisting with *Leishmania* sp. bodies. The patient was given a treatment with amphotericin B and later with radiation therapy, but the tumors showed a poor response to the treatment, and the patient was lost on follow-up. Our observations of the current case highlight the role of a weakening host immune response as a result of diffuse cutaneous leishmaniasis in the development of SCC. Such postulation points to and corroborates the involvement of anergy, a condition probably caused by parasite-induced suppression of the immune response, linking leishmaniasis, and skin malignancy development.

Keywords: Leishmaniasis; Squamous cell carcinoma; Anergy; Immunosuppression

***Corresponding author:**
Andrés Tirado-Sánchez
(Andres.tiradosa@anahuac.mx)

Citation: Tirado-Sánchez A, Bonifaz A, Hernández-Gómez S. Anergy as a potential risk factor for squamous cell carcinoma in an immunocompetent patient with diffuse cutaneous leishmaniasis: A case report. *Global Transl Med*. 2024;3(1):2281.
https://doi.org/10.36922/gtm.2281

Received: November 20, 2023
Accepted: January 24, 2024
Published Online: March 20, 2024

1. Background

Leishmaniasis is caused by obligate intracellular parasites of the *Leishmania* genus.[1] There are more than 20 species of *Leishmania*, mainly found in animals, which can be transmitted to humans by sandflies (*Phlebotomus* spp. or *Lutzomyia* spp.).[2] Inoculation is deployed to control the replication of the parasite in the majority of cases, who would still harbor strands of the parasite despite the lack of relevant symptoms.[3] Reactivation of the parasite and re-infection can occur during immunosuppression or in the absence of overt immunosuppression, in conditions such as T-cell deficiency and delayed-type hypersensitivity reactions with parasite anergy.[4,5]

Despite the inconclusive evidence, numerous studies have linked *Leishmania* sp. to cancer.[6-8] Pathologically, the manifestations of leishmaniasis resemble those of cancer, and their appearance may precede those of cancer. A number of studies have reported the association between *Leishmania* sp. and the development of malignant lesions such as basal cell carcinoma, squamous cell carcinoma (SCC), leukemia and lymphoma, and hemangiosarcoma.[6] Cutaneous SCC is the most common skin cancer among blacks and the second most common among Whites, Asians, and Hispanics. The mortality rate due to cutaneous SCC ranges from 1.5% to 3.4%, with nodal metastases occurring in 1.9% to 5.2% of cases,[7] but early diagnosis can improve the prognosis. The risk of developing cutaneous SCC, the number of lesions, and the aggressiveness of each lesion can be augmented by congenital, acquired, and iatrogenic immunosuppression. Chronic inflammation and infectious agents are other risk factors for developing cutaneous SCC.[7]

Here, we report the case of a patient with diffuse cutaneous leishmaniasis who developed cutaneous SCC in the active lesions of leishmaniasis.

2. Case presentation

In the present case, we report a 63-year-old farmer from Comalcalco, Tabasco, Mexico, suffering from diffuse cutaneous leishmaniasis, which was diagnosed 10 years ago. The parasitic disease had been treated intermittently with 20 mg/kg intramuscular meglumine antimonate (Glucantime) for 20 days, but the patient had a record of poor compliance in adhering to the prescribed medications. No relevant comorbidity was reported in his medical history, and his HIV ELISA result was negative.

After being untreated for 6 months, several new lesions appeared on the right side of the patient's face, besides those that first appeared 4 months before the new additions. The dermatosis consisted of multiple nodular lesions measuring 5 – 12 mm with deep infiltrates and deep, non-tender plaques (Figure 1). There were also ulcers with irregular margins oozing serous exudate, which reportedly appeared 1 month before seeking medical consultation at our clinic. Bleeding was observed in two of these lesions but was generally left unattended. No actinic keratosis was detected, and cervical examination did not reveal signs of lymphadenopathy.

Several non-ulcerated and non-infiltrated nodules on the trunk and extremities measuring approximately 0.5 cm in diameter were observed. These lesions were painless and flesh-colored. Some nodules had hemorrhagic crusts on the surface, fine scaling, and hyper- and hypo-chromic macular scarring.

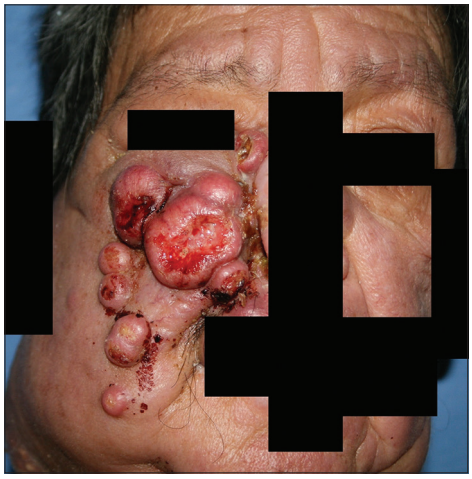

Figure 1. Multiple nodular lesions, each measuring 5 – 12 mm in size, that were deeply infiltrated and fused to the skin with purulent exudate-oozing ulcers of irregular margins.

The Montenegro skin test showed non-reactive outcome after 72 h, indicating positive anergy. Hematoxylin and eosin staining showed severe chronic histiocytic inflammation with multiple amastigotes in the tissue specimens (Figure 2). DNA amplification testing assays were not performed. A biopsy procured from an ulcerated lesion unveiled SCC with mild coexistence of *Leishmania* sp. bodies (Figure 3).

An axial computed tomography scan was performed, uncovering imaging manifestations suggestive of cervical lymph node metastasis (Figure 4), a diagnosis that was later confirmed by histopathological examination. The patient was treated with 3 mg/kg/day amphotericin B for 10 days and prescribed radiotherapy. However, the tumor exhibited poor response to radiotherapy, and the patient did not return to the hospital for follow-up medical consultations and interventions.

3. Discussion

SCC is the second most common malignancy that originates from the skin.[7] Despite its multifactorial etiology, chronic sun exposure, pre-existing lesions (actinic keratosis, unhealed wounds, or scar known as Marjolin ulcer), and chronic infections (mainly viral diseases) are some of the prominent the risk factors of SCC.[7] The occurrence of skin cancer in the previous leishmaniasis lesions is a rare but an already reported phenomenon in the literature.[8] Older men with a long history of ultraviolet exposure are particularly vulnerable to the development of skin cancer on the prior lesion sites of leishmaniasis. Most of these tumors arise from previous leishmaniasis scars, although there are reports of an association between active infection and skin cancer.[8-12] However, to the best of our knowledge and experience, such an association is rare.

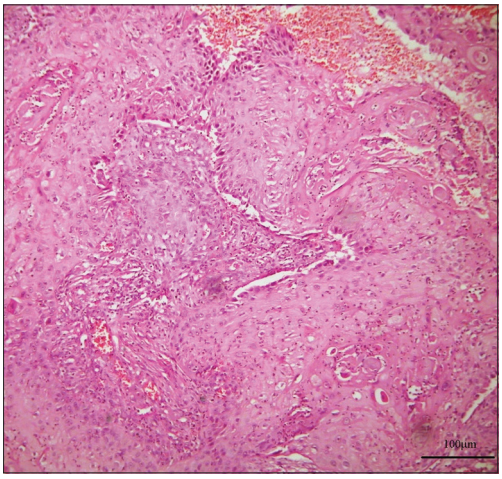

Figure 2. Malignant epithelial cells with abnormal mitoses characteristic of squamous cell carcinoma, alternating with histiocytes parasitized by *Leishmania* and abundant extracellular microorganisms (H&E, ×40). Scale bar: 100 μm.

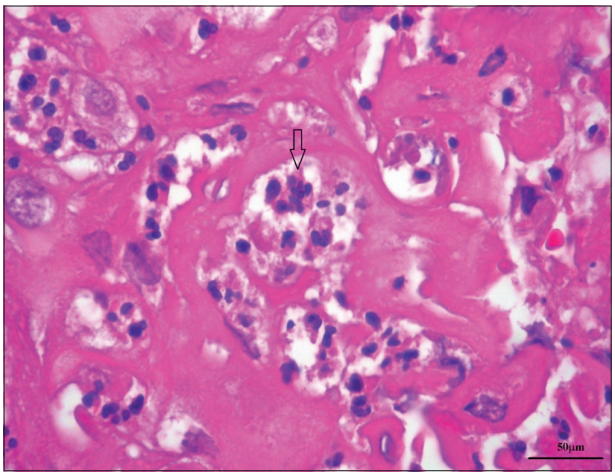

Figure 3. Histological section of the skin nodules showing numerous *Leishmania* amastigotes (arrow) infiltrating into the cytoplasm of histiocytes (H&E, ×100). Scale bar: 50 μm.

The mechanism responsible for the development of cutaneous neoplasms in patients with leishmaniasis has not yet been fully elucidated.[12] The association between these two diseases is not coincidental given the number of published cases. Chronic inflammation that occurs during active infection or during the healing process offers a plausible link between skin pathology and parasitic disease.[13] In the present case, persistent anergy stands as a potential factor influencing the development of skin cancer in active leishmaniasis lesions which had been affecting the patient for more than 10 years. Corroborating such a postulation is the increased risk of developing cancer that has been reported in immunosuppressed as well as in immunocompetent patients.[8,13-15] The previous

Figure 4. Axial computed tomography image suggesting cervical lymph node metastases, which were histopathologically confirmed.

studies have also demonstrated that patients with diffuse cutaneous leishmaniasis showed reduced or no immune response to *Leishmania* sp. antigens and no effective cellular immune response with lymphoplasmacytic infiltrates, which collectively indicate a sign of parasite-mediated immunosuppression.[9,12]

Potential association patterns between leishmaniasis and malignancies have been reported, including (1) leishmaniasis mimicking malignancies, (2) leishmaniasis coexisting with malignancies, (3) malignancies occurring in patients with leishmaniasis, and (4) leishmaniasis occurring in patients with cancer.[12] Our case fits into the description of category (3).

Failure to mount a protective cell-mediated immune response and induction of a regulatory response by the parasite are currently the two most plausible mechanisms underlying the development of diffuse cutaneous leishmaniasis.[9,16] In this case, the role of the host immune response in disease development is implicated in the development of massive SCCs during active infection.

Although the virulence factors involved are not well characterized, *Leishmania* sp. is capable of suppressing the cellular immune response, leading to anergy.[16] The exact defective state that results in anergy to the parasite is not clear, but may be attributed to the release of immunosuppressive cytokines; increased macrophage expression of transforming growth factor beta occurs when exposed to *Leishmania* sp. antigens.[16] This permissive environment shaped by the anergy may also be involved in the development and progression of SCC. Additional virulence factors include the expression of arginase I and enzymes involved in the synthesis of prostaglandins and polyamines.[17]

Chronic inflammation may be a predisposing factor for the development of human neoplastic process. In addition, risk factors for leishmaniasis (immunosuppression), such as parasite-specific anergy, may promote the development of skin cancer.[9,16] Although there is no known time interval between resolution of infection and malignant transformation,[8] both may be present simultaneously, even during active infection.

4. Conclusion

In many cases of leishmaniasis that have been satisfactorily cured, cancers may develop in the prior old, healed lesions, but can also occur in active leishmaniasis lesions in immunocompetent patients as well as in immunocompromised cases. The current case underlines the role of a weakening host immune response as a result of diffuse cutaneous leishmaniasis in the development of SCC. Such postulation points to and corroborates the involvement of anergy, a condition probably caused by parasite-induced suppression of the immune response, in the co-occurrence of leishmaniasis and skin malignancy development. The role of the host immune response in the development of the disease is highlighted by the development of SCC. Anergy, probably related to a parasite-induced suppression of the immune response, may be a common factor linking leishmaniasis and malignancy. Therefore, it is of utmost clinical significance to consider malignancy in the differential diagnosis of rapidly growing or difficult-to-treat lesions for in patients with active leishmaniasis.

Acknowledgments

None.

Funding

None.

Conflict of interest

The authors declare that they have no competing interest.

Author contributions

Conceptualization: Andrés Tirado-Sánchez, Alexandro Bonifaz
Investigation: Andrés Tirado-Sánchez, Sebastián Hernández-Gómez
Writing – original draft: Andrés Tirado-Sánchez
Writing – review & editing: Andrés Tirado-Sánchez, Alexandro Bonifaz, Sebastián Hernández-Gómez

Ethics approval and consent to participate

Written consent was obtained from the patient to participate in the study.

Consent for publication

Written consent was obtained from the patient to publish his data and images. Efforts had been made by the authors to mask any identifying information and facial features of the patient that may appear in the paper.

Availability of data

Not applicable.

References

1. Sasidharan S, Saudagar P. Leishmaniasis: Where are we and where are we heading? *Parasitol Res*. 2021;120(5):1541-1554.
doi: 10.1007/s00436-021-07139-2
2. Lopez Y, Arana B, Rizzo N, Duran E, Acosta-Serrano Á, Mendizabal-Cabrera R. A neglected among the neglected: A review of cutaneous leishmaniasis in Guatemala. *Trans R Soc Trop Med Hyg*. 2023;117(9):609-616.
doi: 10.1093/trstmh/trad024
3. Bañuls AL, Bastien P, Pomares C, Arevalo J, Fisa R, Hide M. Clinical pleiomorphism in human leishmaniases, with special mention of asymptomatic infection. *Clin Microbiol Infect*. 2011;17(10):1451-1461.
doi: 10.1111/j.1469-0691.2011.03640.x
4. Pinheiro RO, Pinto EF, Benedito AB, Lopes UG, Rossi-Bergmann B. The T-cell anergy induced by *Leishmania amazonensis* antigens is related with defective antigen presentation and apoptosis. *An Acad Bras Cienc*. 2004;76(3):519-527.
doi: 10.1590/s0001-37652004000300006
5. Saidi N, Blaizot R, Prévot G, *et al*. Clinical and immunological spectra of human cutaneous leishmaniasis in North Africa and French Guiana. *Front Immunol*. 2023;14:1134020.
doi: 10.3389/fimmu.2023.1134020
6. Rashidi S, Fernández-Rubio C, Manzano-Román R, *et al*. Potential therapeutic targets shared between leishmaniasis and cancer. *Parasitology*. 2021;148(6):655-671.
doi: 10.1017/S0031182021000160
7. Wysong A. Squamous-cell carcinoma of the skin. *N Engl J Med*. 2023;388:2262-2273.
doi: 10.1056/NEJMra2206348
8. Carrillo-Larco RM, Acevedo-Rodriguez JG, Altez-Fernandez C, Ortiz-Acha K, Ugarte-Gil C. Is there an association between cutaneous leishmaniasis and skin cancer? A systematic review. *Wellcome Open Res*. 2019;4:110.
doi: 10.12688/wellcomeopenres.15367.1
9. Morsy TA. Cutaneous leishmaniasis predisposing to human skin cancer: Forty years local and regional studies. *J Egypt Soc Parasitol*. 2013;43(3):629-648.

doi: 10.12816/0006420

10. Armengot-Carbó M, Carmena-Ramón R, Rodrigo-Nicolás B, Ferrando-Marco J. Unsuspected visceral leishmaniasis infiltrating a squamous cell carcinoma. *Actas Dermosifiliogr.* 2012;103(4):321-323.

doi: 10.1016/j.ad.2011.04.016

11. Ouattassi N, Titou A, Hammas N, Kamal D, El Amine El Alami MN. Squamous cell carcinoma associated with an active cutaneous leishmaniasis in immunocompetent patient: Case presentation of an unlikely association and literature-review. *Egypt J Otolaryngol.* 2022;38:148.

doi: 10.1186/s43163-022-00335-6

12. Kopterides P, Mourtzoukou EG, Skopelitis E, Tsavaris N, Falagas ME. Aspects of the association between leishmaniasis and malignant disorders. *Trans R Soc Trop Med Hyg.* 2007;101(12):1181-1189.

doi: 10.1016/j.trstmh.2007.08.003

13. Dalgleish AG, O'Byrne KJ. Chronic immune activation and inflammation in the pathogenesis of AIDS and cancer. *Adv Cancer Res.* 2002;84:231-276.

doi: 10.1016/s0065-230x(02)84008-8

14. Christopoulos P, Dopfer EP, Malkovsky M, *et al*. A novel thymoma-associated immunodeficiency with increased naive T cells and reduced CD247 expression. *J Immunol.* 2015;194(7):3045-3053.

doi: 10.4049/jimmunol.1402805

15. Friedman R, Hanson S, Goldberg LH. Squamous cell carcinoma arising in a *Leishmania* scar. *Dermatol Surg.* 2003;29(11):1148-1149.

doi: 10.1046/j.1524-4725.2003.29354.x

16. Sinha S, Fernández G, Kapila R, Lambert WC, Schwartz RA. Diffuse cutaneous leishmaniasis associated with the immune reconstitution inflammatory syndrome. *Int J Dermatol.* 2008;47(12):1263-1270.

doi: 10.1111/j.1365-4632.2008.03804.x

17. França-Costa J, Van Weyenbergh J, Boaventura VS, *et al*. Arginase I, polyamine, and prostaglandin E2 pathways suppress the inflammatory response and contribute to diffuse cutaneous leishmaniasis. *J Infect Dis.* 2015;211(3):426-435.

doi: 10.1093/infdis/jiu455

Our Journals

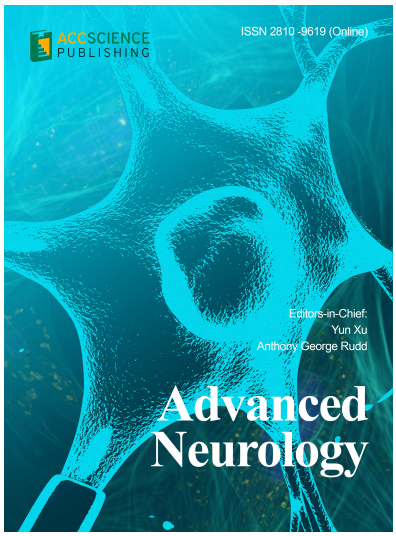

Advanced Neurology is a peer-reviewed and open-access journal that aims to publish and disseminate novel research in the breadth of neurology and neuroscience. The journal aims to advance our understanding in the nervous system and provide a platform to neuroscientists and physicians to showcase their findings in original fundamental and clinical research as well as to present new ideas that highlight the changes in the neurological clinical practice.

Advanced Neurology covers subject areas, including but not limited to the following:

- Neurological disorders
- Neurodegenerative disease
- Cerebrovascular disease
- Epilepsy and movement disorders
- Neuroimmune disease
- Neurological infections
- Muscle disease
- Molecular and cellular neuroscience
- Systems neuroscience
- Cognitive neuroscience
- Computational modeling of nervous system

Gene & Protein in Disease publishes rigorously peer-reviewed and high quality original articles and authoritative reviews that focus on the latest development in multidisciplinary areas in biology and biomedicine, with an emphasis on gene and protein research. The journal has worldwide authorship, and a broad scope in basic and translational biomedical research of genetics, biochemistry, biophysics, oncology, immunology, cell biology, molecular biology, developmental biology, microbiology, neuroscience, stem cell, protein science, structural biology, regenerative medicine and translational medicine.

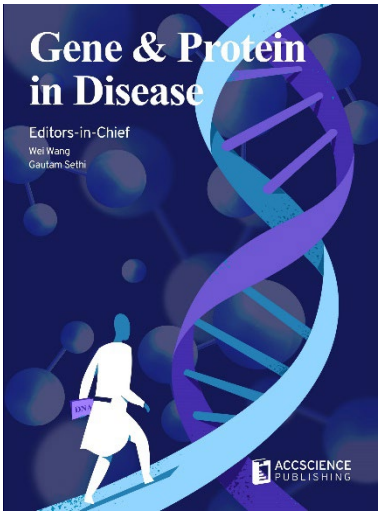

Start a new journal

Write to us via email if you are interested to start a new journal with AccScience Publishing. Please attach your CV, professional profile page and a brief pitch proposal in your email. We shall inform you of our decision whether we are interested to collaborate in starting a new journal.

Contact: info@accscience.com

https://accscience.com/journal/GTM

Contact
www.accscience.com
8 Burn Road, #15-03 Trivex, Singapore 369977
Email: editorial@accscience.com
Phone: +65 8182 1586